SANDIA REPORT

SAND97-0506 • UC-722
TTC Number 1480
Unlimited Release
Printed March 1997

Experimental Determination of the Shipboard Fire Environment for Simulated Radioactive Material Packages

J. A. Koski, J. G. Bobbe, M. Arviso, S. D. Wix, D. E. Beene, Jr., R. Byrd, J. Graupmann

Prepared by
Sandia National Laboratories
Albuquerque, New Mexico 87185 and Livermore, California 94550

Sandia is a multiprogram laboratory operated by Sandia Corporation, a Lockheed Martin Company, for the United States Department of Energy under Contract DE-AC04-94AL85000.

Sandia National Laboratories

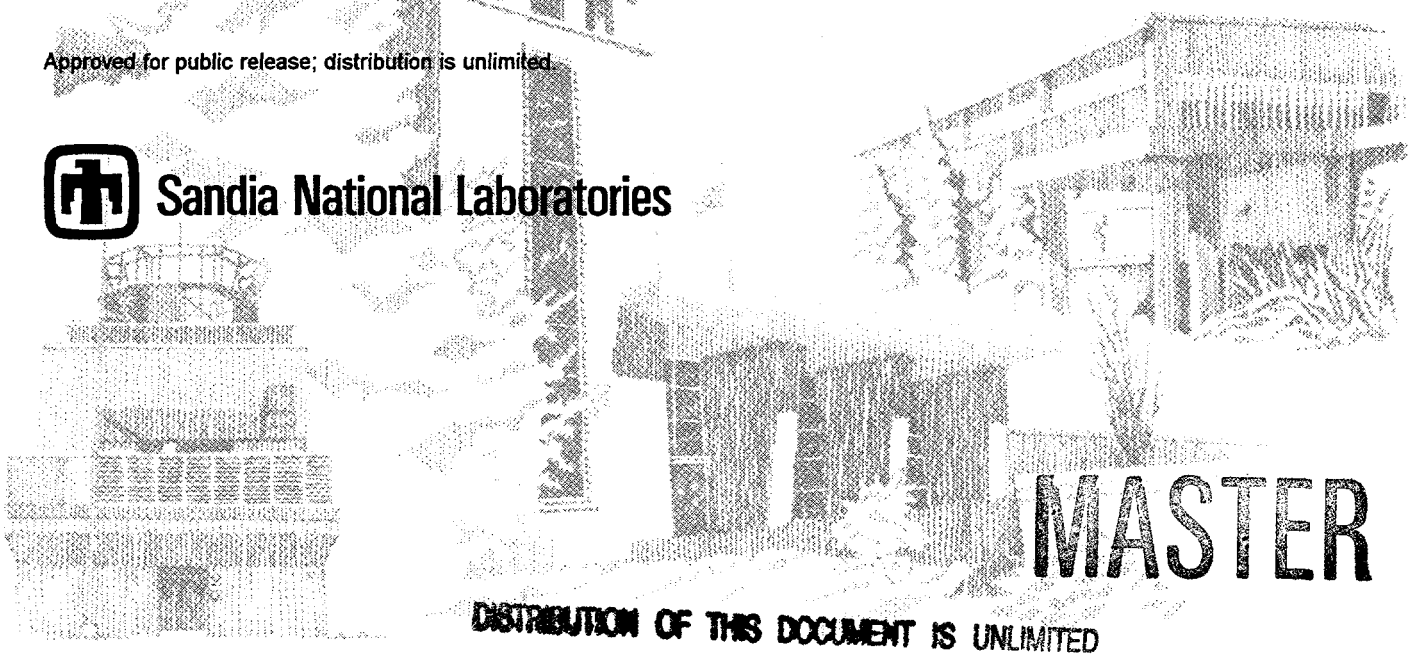

Issued by Sandia National Laboratories, operated for the United States Department of Energy by Sandia Corporation.

Available to DOE and DOE contractors from
Office of Scientific and Technical Information
P.O. Box 62
Oak Ridge, TN 37831

Prices available from (615) 576-8401, FTS 626-8401

Available to the public from
National Technical Information Service
U.S. Department of Commerce
5285 Port Royal Rd
Springfield, VA 22161

NTIS price codes
Printed copy: A08
Microfiche copy: A01

SAND 97-0506
TTC Number 1480
Unlimited Release
Printed March 1997

Distribution
Category UC-722

Experimental Determination of the Shipboard Fire Environment for Simulated Radioactive Material Packages

J. A. Koski, J. G. Bobbe, M. Arviso
Transportation Systems Department
Sandia National Laboratories
Albuquerque, NM 87185-0717

S. D. Wix
Gram, Inc.
Albuquerque, NM

D. E. Beene, Jr.
U. S. Coast Guard, Research and Development Center
Groton, CT

R. Byrd, J. Graupmann
U. S. Coast Guard, Fire and Safety Test Detachment
Mobile, AL

ABSTRACT

A series of eight fire tests with simulated radioactive material shipping containers aboard the test ship *Mayo Lykes* , a break-bulk freighter, is described. The tests simulate three basic types of fires: engine room fires, cargo fires and open pool fires. Detailed results from the tests include temperatures, heat fluxes and air flows measured during the fires. The first examination of the results indicates that shipboard fires are not significantly different from fires encountered in land transport.

CONTENTS

FIGURES

TABLES

APPENDICES

ACKNOWLEDGMENTS

We would like to thank the many individuals that contributed to this report. In particular we would wish to thank Kenny Wolverton, Lewis Glisson, Jason Leonard, Kevin Bryan, and Rita Thompson who hosted the experiments and enabled the installation at the Fire and Safety Test Detachment in Mobile. Special thanks also go to Diana Helgesen who, besides documenting the efforts photographically, helped install the experiments at Mobile, often under less than desirable conditions. In Albuquerque we would like to thank Rick Knight who converted the files from the data acquisition system and placed them on the local area network for easy access, Elizabeth Tahmoush who plotted all the thermocouple data and prepared the Appendices, and Rod Mahoney who made the total emittance measurements of the calorimeters and paint flakes from the test ship.

1.0 INTRODUCTION

With responsibilities that include the return of spent fuel from foreign research reactors, the U.S. Department of Energy (DOE) must assure the safe transport of radioactive materials by sea. For this reason, DOE awareness and interest in the safety of maritime shipments of radioactive materials continues. DOE, as part of a Cooperative Research Program with the International Atomic Energy Agency (IAEA) entitled *Fire Environment on Board Ships* is investigating accidental ship fires. The purpose of the DOE sponsored research conducted by Sandia National Laboratories and reported here is to measure the heat transfer to simulated radioactive material packages during a series of controlled ship fires, and apply these results to improve predictions of the shipboard fire environment for radioactive packages.

Several international regulations cover the transport of radioactive materials by sea. The International Maritime Dangerous Goods (IMDG) code [1] issued by the International Maritime Organization (IMO), part of the United Nations, covers the permissible stowage arrangements for hazardous materials aboard ships. The IMO has also issued the Irradiated Nuclear Fuel (INF) regulations [2] that specify the safety and design features for ships carrying nuclear materials. Safety Series 6 [3], issued by the IAEA, covers the required safety features of the protective packages that are used to transport radioactive materials by land, air and sea. Besides their main purpose of assuring safe transport, these regulations can also aid the current study by defining the typical shipboard location and surrounding environment for radioactive materials packages.

The IAEA Safety Series 6, and its equivalent regulation in the United States, Title 10, Code of Federal Regulations, Part 71 (10CFR71), considers the thermal integrity of a radioactive material package satisfactory if the package can survive exposure to a large, fully engulfing hydrocarbon pool fire for 30 minutes without releasing any contents. This fire simulates hypothetical severe land-based accidents that might occur, for example, after a transport vehicle collides with a large gasoline tanker truck. During sea transport, this type of threat is not relevant, but many other fire threats must be considered. For the break-bulk type of freighter that has normally been used for sea transport of the larger "Type B" quantities of radioactive materials, a cargo fire in the same hold could be a threat. The IMDG code forbids transport of flammable materials in the same cargo hold with radioactive materials, so common fire threats consist of ordinary combustible materials such as wood crating or pallets. Another typical threat would be from fires in adjacent ship spaces with combustible materials such as other cargo holds, engine rooms or galleys. A wide range of fire scenarios based on cargo and configuration can be suggested, but in most cases the heat transfer to the radioactive material package would likely be much less than occurs in a fully-engulfing pool fire. To date, how these scenarios compare to the heat transfer from a fully engulfing pool fire has not been experimentally investigated. A major purpose of the current program is to compare the shipboard fire environment with the current regulatory fire environment.

1.1 Test Overview

The fire tests discussed in this report were conducted aboard the *Mayo Lykes*, a *Liberty* class World War II freighter rated at 10700 deadweight tons with a length of 139 m, a beam of 22 m and a draft of 4.3 m. The ship was located at the Coast Guard Fire and Safety Test Detachment at Mobile, Alabama. The *Mayo Lykes* was operated for purposes of fire research by the Coast Guard Research and Development Center, Groton, Connecticut, and since the completion of these tests has been sent for salvage. The ship was located on Little Sand Island in Mobile Bay as shown in Figure 1. Controlled fires were set in Hold 4 of the *Lykes* (see Figure 2), with calorimeters simulating transportation casks located in both Holds 4 and 5. The tests were conducted on Level 1 of the holds, the first level below the weather deck. Three types of shipboard fire were considered: a cargo fire in the same hold as the simulated radioactive materials package, an engine room or galley fire in an adjacent hold, and, strictly for comparison purposes, fully engulfing hydrocarbon pool fires both in-hold and on deck. Figure 3 shows a schematic of the test arrangement for the cargo fires and the simulated engine room fires. For simulated cargo fires, wood cribs of Douglas fir built to UL 711 [4] were used because methods for determining heat release from such cribs has been published [5]. For simulated engine room fires, ignited heptane fuel was sprayed on the Hold 4 bulkhead with a known pattern and flow rate. Heptane fuel was chosen because it is a typical hydrocarbon fuel that is clean burning, and the Test Detachment has both the equipment and the experience to safely handle the fuel. To enhance smoke production,

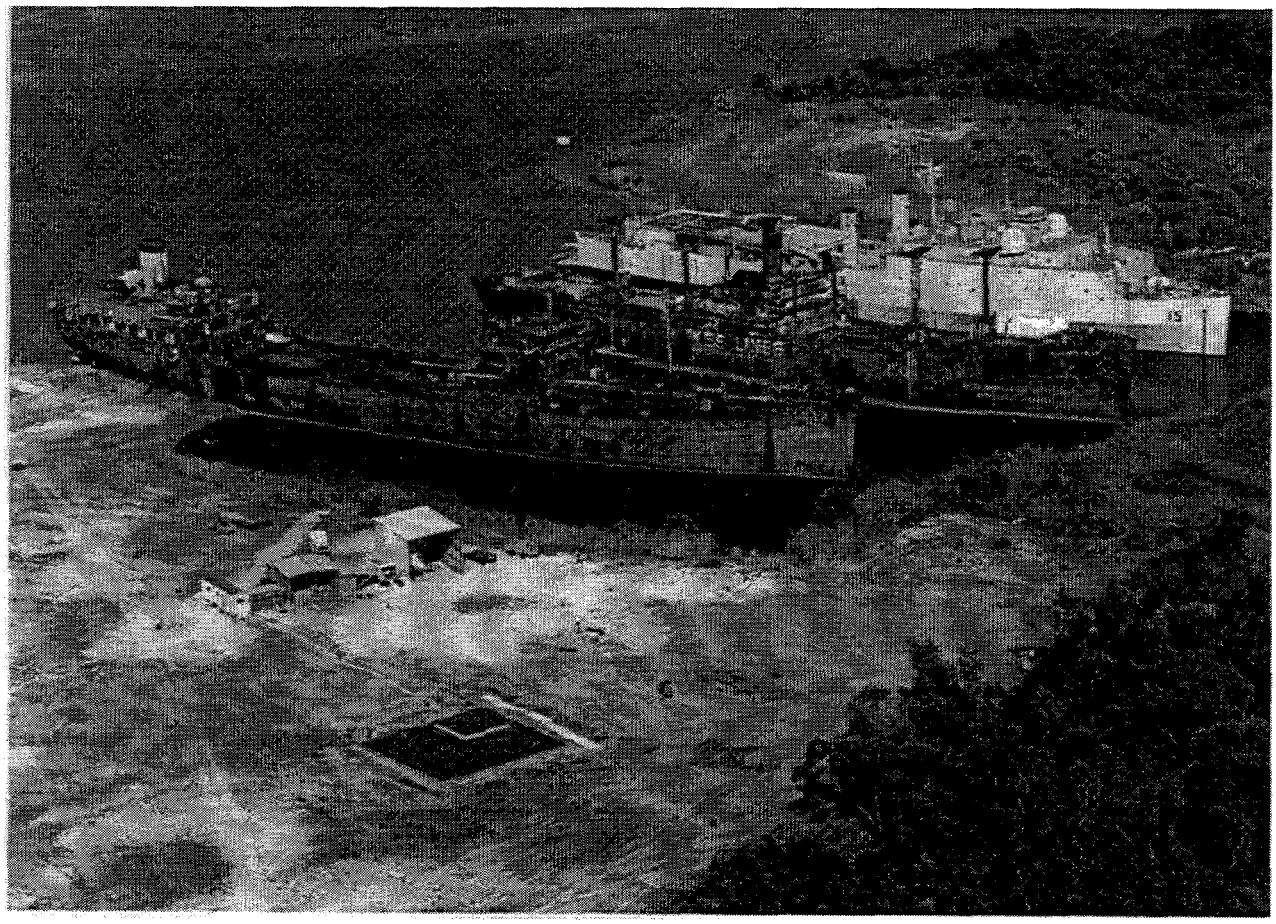

Figure 1. Little Sand Island in Mobile Bay, Alabama. The *Mayo Lykes* is the ship in the center.

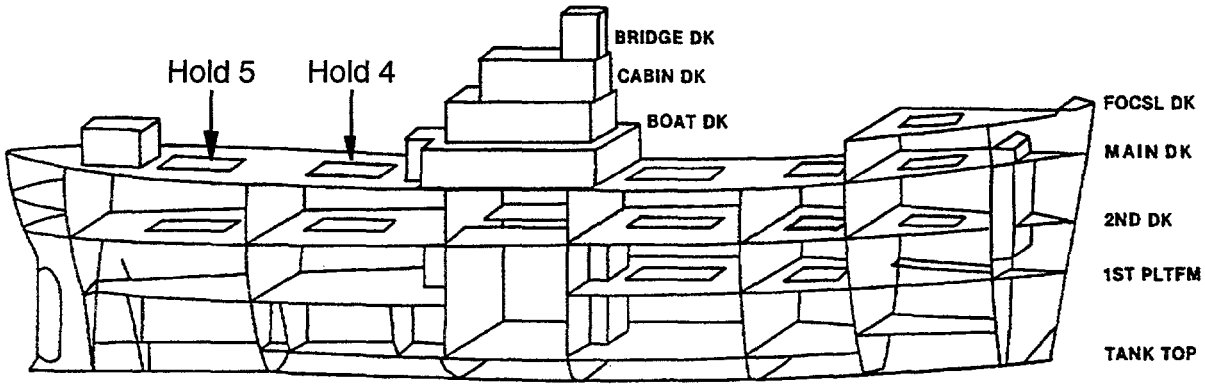

Figure 2. Perspective of *Mayo Lykes*. Tests were conducted in Holds 4 and 5 on first level below the weather deck.

small amounts of diesel fuel in small cavities were sometimes separately burned in conjunction with the heptane. Pool fires were conducted with diesel fuel because this is a commonly used fuel on ships, and because unused stores could be put to good use after the testing. Detailed descriptions of individual tests are presented later in the report.

Eight separate tests were conducted in two series of four tests each, the first series occurring September 11-15, 1995 and the second occurring November 13-17, 1995. A detailed table of the tests is presented later. Thermocouples and other instrumentation permitted measurement of thermal data for pipe calorimeters representing the radioactive material package, and the surrounding ship hold. Pipe calorimeters were chosen to represent the radioactive material package

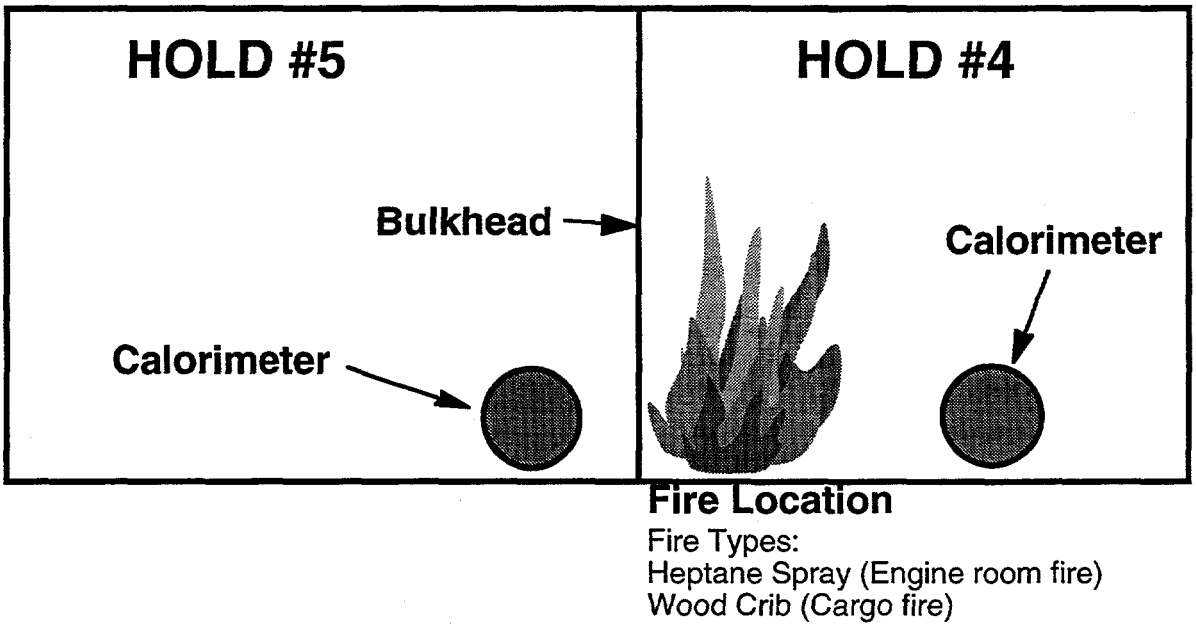

Figure 3. Schematic of tests conducted aboard the *Mayo Lykes*.

for the following reasons:

- Radioactive material packages cover a wide range of weights, sizes and shapes, making the choice of one or two typical packages difficult.
- The pipe calorimeters have a controlled simple geometry and ease of instrumentation that permit a more accurate assessment of heat transfer than would be possible with an actual package.
- The calorimeters are relatively inexpensive, do not risk an actual package, and do not raise possible concerns about radioactivity that could occur, for example, if a previously used package were found and instrumented.
- The pipe calorimeter for this series was chosen to be within the local lifting capacities of the Coast Guard Test Detachment. Larger packages would have required services of a floating crane at the ship.

Tests were terminated if thermocouples indicated that bulkhead or overhead temperatures reached the 540°C (1000°F) temperature that could weaken the carbon steel structure of a ship.

1.2 Test Objectives

The shipboard fire test series was completed with three major objectives in mind. First, general data on heat transfer in the shipboard environment from fires of known size to objects similar to radioactive material casks was to be gathered. These data give an idea of the range of heat fluxes expected from fires on break-bulk type ships. Second, the data should allow direct comparison to computer analyses performed to predict the heat transfer for shipboard fires. Together with the analyses, the major modes of heat transfer can be identified for possible simplification of analysis. For example, if radiation heat transfer is found to dominate in certain arrangements, then simpler analyses can be performed with only radiation considered with confidence that correct results can be obtained. Further, once the analysis methods are confirmed, then larger fires than the experimental series can be analyzed with increased confidence in the results. Finally, the data should provide one of the bases for establishing a simplified model of hold-to-hold fire spread on ships. With such a simplified model of fire spread on ships, improved risk assessments for sea transport of radioactive materials can be conducted.

2.0 EXPERIMENT DESIGN

2.1 Ship Hold Layout

After surveying the ship, Level 1, the highest level in Holds 4 and 5, was selected for the tests. Although Hold 4 contained a large sheet metal engine room mockup previously used for fire suppression testing, and a 1.02 m diameter circular King Post supporting a cargo crane centered in the bulkhead between Holds 4 and 5, these holds were large and allowed easy access to instrumentation in a data acquisition system located on the weather deck. The general arrangements in the holds are shown in Figures 4 and 5. Hold 5 contained a large furnace at the location shown in Figure 5 and other smaller pieces of material, but was generally open. The center of the pipe

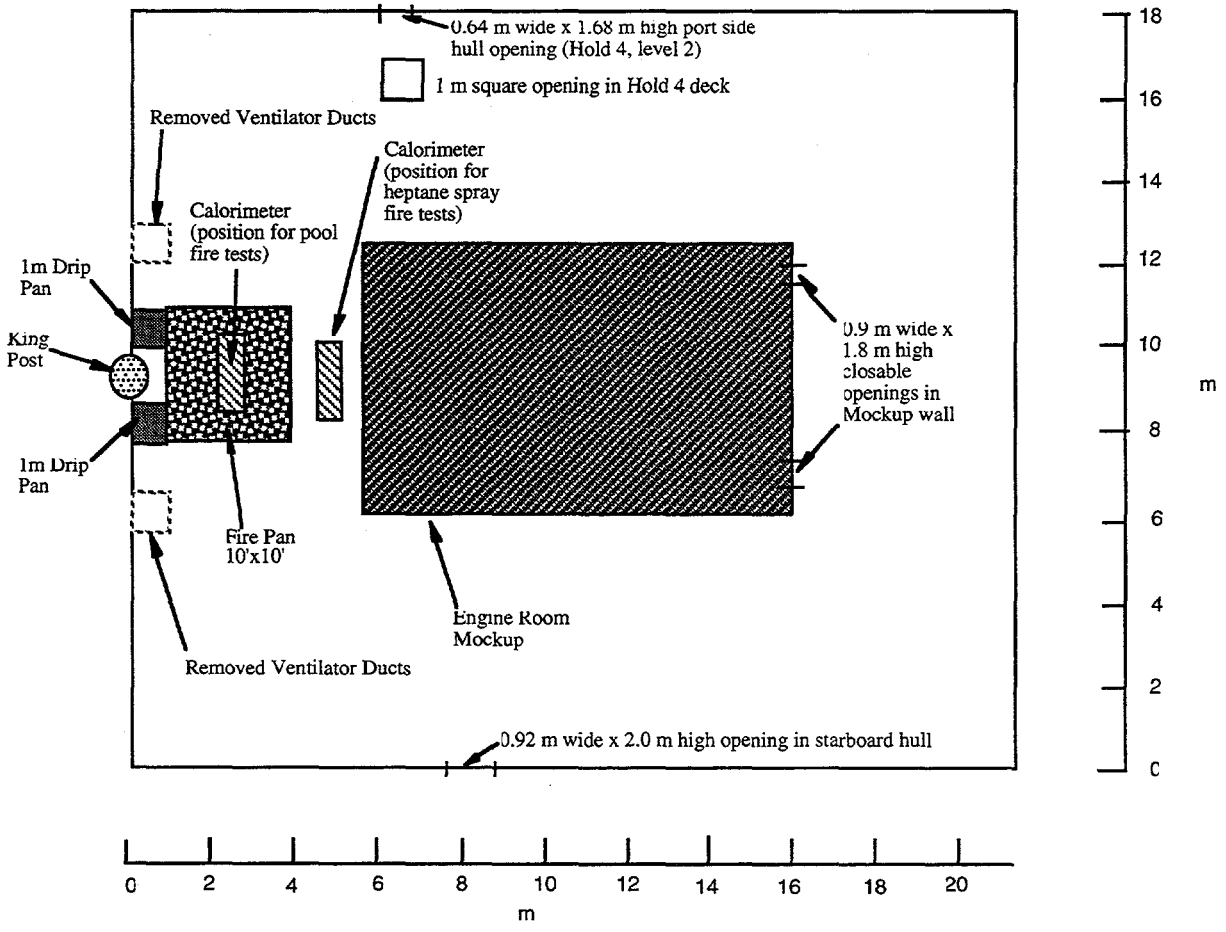

Figure 4. Arrangement in Hold 4. Hold height in test area is 3.66 m.

calorimeter in Hold 5 that simulated radioactive cargo was placed 2 m from the bulkhead between Holds 4 and 5 on the ship centerline as shown in Figure 5. During early surveys of the ship, 0.91 m square ventilation ducts with hold access ladders were found to be located on both sides of the Hold 4 and 5 bulkhead. Since these ducts and ladders could interfere with heat transfer between the holds, they were removed prior to testing. The holes left in the overhead and deck were covered with carbon steel plate of the same nominal thickness as the deck and overhead. The locations of the removed ducts is shown in Figures 4 and 5. The ship was constructed from welded carbon steel

Table 1. Ship Hull, Bulkhead and other Thicknesses

Location	Thickness, mm
Starboard Hull	18.1
Port Hull	19.4
Bulkhead between Holds 4 and 5	8.2
Overhead (Weather Deck)	10.7
Hold 4 and 5 Deck in Test Area	10.7
King Post	34.9

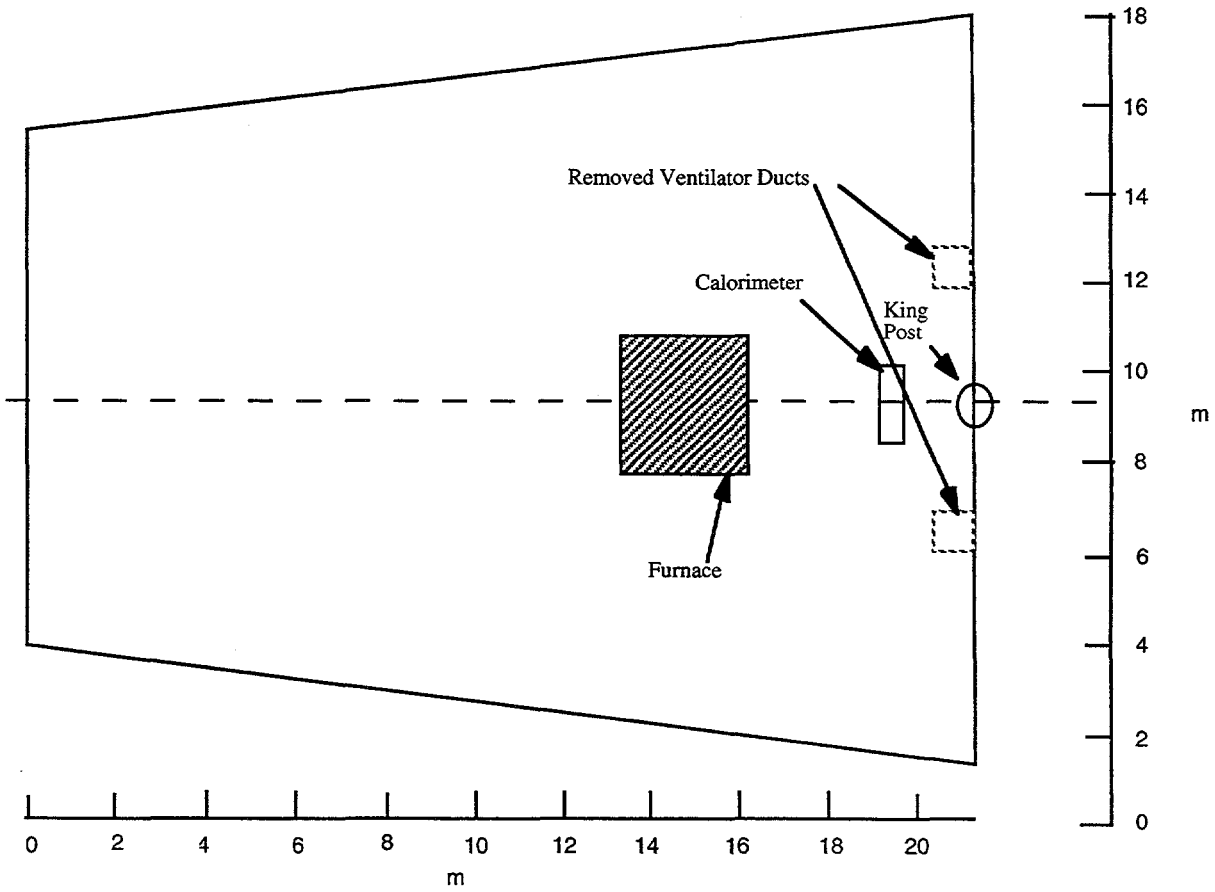

Figure 5. Arrangement of Hold 5. Hold Height in test area is 3.66 m.

plate. Table 1 shows the measured thicknesses of the various ship components used to construct Holds 4 and 5. Differences from standard steel plate thickness are due to corrosion and variations the thicknesses of the plates as originally supplied.

Ventilation to all fires in Hold 4 was provided by openings in the starboard and port hulls as shown in Figure 4. The opening on the port side was a deck level below the hold level where the tests were conducted, but a 1 m square opening in the deck allowed a near symmetry with starboard side and port side ventilation. Closable openings at the end of the engine room mockup shown in Figure 4 were left open for the heptane spray and pool fire tests, but were closed for the wood crib tests. When the openings in the engine room mockups were removed, two 2 m x 3 m panels in the overhead of the engine room mockup were also removed to provide vertical ventilation for the smoke. Other than these openings, all ports and openings were secured during testing.

Measurements of paint flakes obtained various locations in Hold 5 of the Lykes were used to gain information on the thermal emittance of the surfaces. This information can be used in modeling the

Table 2. Calculated Total Normal Emittance Values of Paint Flakes from Hold 5

Sample ID Visual Hue	Temperature (°C)	$\varepsilon_N(T)$
#1	100	0.444
Silver (cracks)	250	0.427
	500	0.411
	750	0.411
	1000	0.413
	1250	0.408
	1500	0.402
#2	100	0.778
Silver - Green	250	0.743
	500	0.695
	750	0.655
	1000	0.619
	1250	0.596
	1500	0.585
#3	100	0.797
Silver - Green	250	0.774
	500	0.735
	750	0.688
	1000	0.638
	1250	0.606
	1500	0.590
#4	100	0.792
Gray - Green	250	0.775
	500	0.753
	750	0.741
	1000	0.736
	1250	0.737
	1500	0.742

radiation heat transfer within the holds. The estimated emittance values [6] for four different paint flakes are shown in Table 2.

2.2 Calorimeter Design

The pipe calorimeters were constructed from two 1.52 m lengths of nominal 2 foot diameter Schedule 60 carbon steel pipe with an outside diameter of 0.61 m and a wall thickness of 0.0244 m. Nominal 1 inch (0.0254 m) thick circular carbon steel plates were bolted to form the ends of the calorimeters. Thermocouples were fastened to the pipe interior and exterior surfaces with thin capacitance-welded Nichrome metal strips at the locations shown in Figures 6 and 7. Calorimeters located in Holds 4 and 5 were identical in construction, with the side containing the larger number of thermocouples facing the bulkhead between Holds 4 and 5. Type K thermocouples, discussed further in Section 2.3, were attached in pairs with one interior and one exterior thermocouple at each location. This permitted measurement of the time history of the pipe wall temperature difference at 12 locations as shown in Figures 6 and 7. Further information on calorimeter thermocouples including data channel identification and cable identification are included in Tables 2 and 3.

After attachment of the thermocouples, the calorimeter interiors were packed with commercial Kaowool insulation material with a nominal density of 8 pounds per cubic foot to provide an insulated boundary condition for data analysis. The insulation also blocked thermal radiation heat transfer inside the calorimeter that would require a complicated interior cavity geometry to be analyzed.

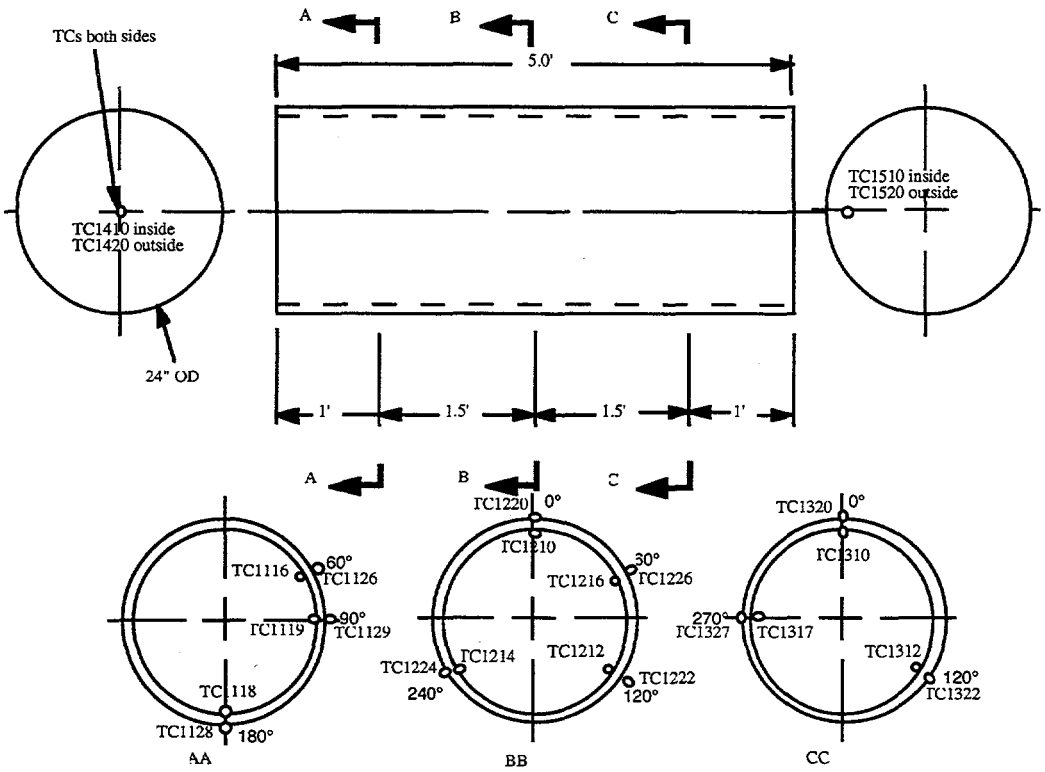

Figure 6. Calorimeter 1 thermocouple locations.

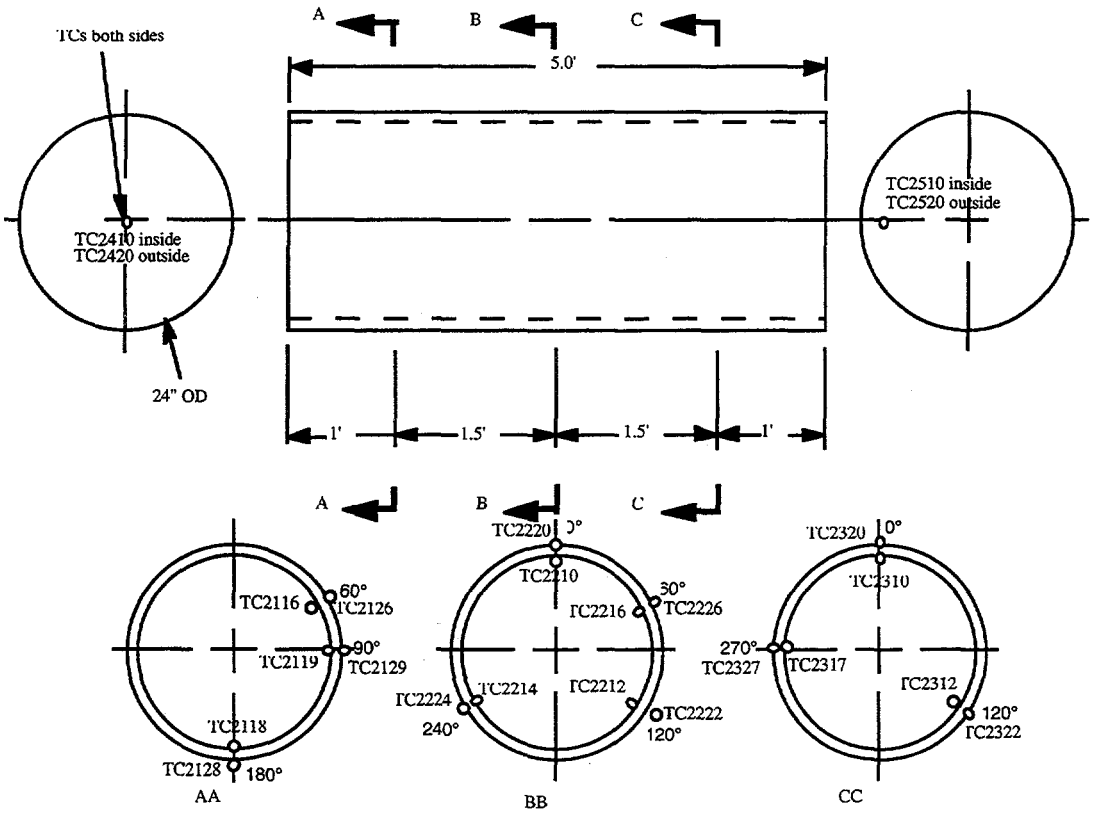

Figure 7. Calorimeter 2 thermocouple locations.

Absorbed heat fluxes to the calorimeter were determined with the use of the Sandia One-Dimensional Direct and Inverse Thermal (SODDIT) computer code [7]. This code can be used to solve inverse heat conduction problems, i.e., rather than solving for the temperatures of an object given the boundary conditions, this code estimates the heat flux boundary conditions given object temperatures. As the name implies, the code assumes a one-dimensional geometry for cylinders, spheres or plates. This approach provides good estimates of the surface heat transfer as long as local peaking of the flux profiles does not produce significant two- or three-dimensional heat transfer near the peak. For example, a test case was run with synthetic thermal data produced from a Topaz [8] two-dimensional finite element computer model. With a uniform circumferential heat flux of 7.5 kW/m^2 applied to the entire circumference combined with an additional cosine peak distribution of 7.5 kW/m^2 applied to one half of the calorimeter surface, the SODDIT code successfully predicted the peak surface heat flux at the beginning of the 60 minute time period, underpredicted the peak by 8 per cent at 30 minutes, and under predicted the peak by 8.6 per cent at the end of the 60 minute simulation. In general, the one-dimensional analysis of two-dimensional effects tends to broaden the peaks of the input distribution with the total heat transfer close to the correct value. The data presented should be viewed with these effects in mind.

With the SODDIT code, absorbed surface heat fluxes could be estimated either from both interior and exterior thermocouples at a location together or from either the interior or exterior thermocouple alone. Tests with the code indicated that any of the approaches could be used successfully for the calorimeters with little change in the estimated heat flux values.

Carbon steel properties assumed for all calorimeter analyses were taken from the Topaz [8] computer code data base, and are shown in Table 3. Density of carbon steel was assumed constant at 7750 kg/m^3. Measured values of surface emittance for the calorimeter [9] are shown in Table 4.

Table 3. Calorimeter 1 Thermocouple Locations

		Calorimeter 1 - Hold 4			
ID Number	Device type	Location	Angle	Cable/Channel	
TC1116	t/c - type k	Section AA - Inside - 60°	60	21/50	
TC1126	t/c - type k	Section AA - Outside - 60°	60	22/51	
TC1119	t/c - type k	Section AA - Inside - 90°	90	23/52	
TC1129	t/c - type k	Section AA - Outside - 90°	90	24/53	
TC1118	t/c - type k	Section AA - Inside - 180°	180	25/54	
TC1128	t/c - type k	Section AA - Outside - 180°	180	26/55	
TC1210	t/c - type k	Section BB - Inside - top	0	27/56	
TC1220	t/c - type k	Section BB - Outside - top	0	28/57	
TC1216	t/c - type k	Section BB - Inside - 60°	60	29/58	
TC1226	t/c - type k	Section BB - Outside - 60°	60	30/59	
TC1212	t/c - type k	Section BB - Inside - 120°	120	31/60	
TC1222	t/c - type k	Section BB - Outside - 120°	120	32/61	
TC1214	t/c - type k	Section BB - Inside - 240°	240	33/62	
TC1224	t/c - type k	Section BB - Outside - 240°	240	34/63	
TC1310	t/c - type k	Section CC - Inside - top	0	35/64	
TC1320	t/c - type k	Section CC - Outside - top	0	36/65	
TC1312	t/c - type k	Section CC - Inside - 120°	120	37/66	
TC1322	t/c - type k	Section CC - Outside - 120°	120	38/67	
TC1317	t/c - type k	Section CC - Inside - 270°	270	39/68	
TC1327	t/c - type k	Section CC - Outside - 270°	270	40/69	
TC1410	t/c - type k	End AA centered inside	n/a	41/70	
TC1420	t/c - type k	End AA centered outside	n/a	42/71	
TC1510	t/c - type k	End CC 90° -inside - 6" in	90	43/72	
TC1520	t/c - type k	End CC 90° -Outside - 6" in	90	44/73	
ID key:					
TC = thermocouple					
First digit = 1 for calorimeter 1					
Second digit = 1 for AA, 2 for BB, 3 for CC, 4 for AA end 5 for CC end					
Third digit = 1 for inside surface, 2 for outside					
Fourth digit = 0 for top, 6 for 60°, 9 for 90°, 2 for 120°, 4 for 240°, 8 for 180°, 7 for 270°					

Table 4. Calorimeter 2 Thermocouple Locations

		Calorimeter 2 - Hold 5			
ID Number	Device type	Location	Angle	Cable/Channel	
TC2116	t/c - type k	Section AA - Inside - 60°	60	A-1/1	
TC2126	t/c - type k	Section AA - Outside - 60°	60	A-2/2	
TC2119	t/c - type k	Section AA - Inside - 90°	90	A-3/3	
TC2129	t/c - type k	Section AA - Outside - 90°	90	A-4/4	
TC2118	t/c - type k	Section AA - Inside - 180°	180	A-5/5	
TC2128	t/c - type k	Section AA - Outside - 180°	180	A-6/6	
TC2210	t/c - type k	Section BB - Inside - top	0	A-7/7	
TC2220	t/c - type k	Section BB - Outside - top	0	A-8/8	
TC2216	t/c - type k	Section BB - Inside - 60°	60	A-9/9	
TC2226	t/c - type k	Section BB - Outside - 60°	60	A-10/10	
TC2212	t/c - type k	Section BB - Inside - 120°	120	A-11/11	
TC2222	t/c - type k	Section BB - Outside - 120°	120	A-12/12	
TC2214	t/c - type k	Section BB - Inside - 240°	240	A-13/13	
TC2224	t/c - type k	Section BB - Outside - 240°	240	A-14/14	
TC2310	t/c - type k	Section CC - Inside - top	0	A-15/15	
TC2320	t/c - type k	Section CC - Outside - top	0	A-16/16	
TC2312	t/c - type k	Section CC - Inside - 120°	120	A-17/17	
TC2322	t/c - type k	Section CC - Outside - 120°	120	A-18/18	
TC2317	t/c - type k	Section CC - Inside - 270°	270	A-19/19	
TC2327	t/c - type k	Section CC - Outside - 270°	270	A-20/20	
TC2410	t/c - type k	End AA centered inside	n/a	61/21	
TC2420	t/c - type k	End AA centered outside	n/a	62/22	
TC2510	t/c - type k	End CC 90° -inside - 6" in	90	63/23	
TC2520	t/c - type k	End CC 90° -Outside - 6" in	90	64/24	
ID key:					
TC = thermocouple					
First digit = 2 for calorimeter 2					
Second digit = 1 for AA, 2 for BB, 3 for CC, 4 for AA end 5 for CC end					
Third digit = 1 for inside surface, 2 for outside					
Fourth digit = 0 for top, 6 for 60°, 9 for 90°, 2 for 120°, 4 for 240°, 8 for 180°, 7 for 270°					

Table 5. Thermal Properties of Carbon Steel from Reference [8].

Temperature, °C	Specific Heat, J/kg	Thermal Conductivity, W/m-°C
-18.05	502.1	43.1
203.95	518.8	42.26
647.95	753.1	32.22
762.85	800.0	27.06
772.85	627.6	26.61
787.85	621.2	25.94
870.85	585.8	26.99
1093.85	606.7	30.86

Table 6. Calculated Total Normal Emittance Values for Oxidized Iron Calorimeters before September 1995 Fire Test

Temperature (°C)	$\varepsilon_N(T)$
100	0.741
250	0.731
500	0.713
750	0.709
1000	0.724
1250	0.766
1500	0.813
5525*	0.870*

*Used averaged measured solar averaged absorptance value; exoatmospheric solar distribution approximates blackbody temperature ≈5800K (5525°C)

2.3 Instrumentation

Besides the thermocouples attached to the pipe calorimeters, instrumentation included thermocouples attached to bulkheads, deck and overhead, flow probes in Holds 4 and 5, radiometers, video cameras, a 35 mm still camera, an infrared camera and an oxygen sensor in the vicinity of the fire. Data recorded by the data acquisition system during the eight tests are included in this report as Appendices A through H.

For temperature measurement, Type K thermocouples were attached at locations shown in Figures 8 and 9. These figures show the interior locations in a manner analogous to the unfolding of a cardboard box with the bulkhead between Holds 4 and 5 as the center of the Figures. Actual physical locations and other information for the thermocouples and other instruments are shown in Tables 7 through 10. The thermocouples were attached to the bulkheads with thin Nichrome strips capacitance tack welded to the steel surfaces. Small areas of steel were ground to base metal to permit attachment of the Nichrome strips. For consistency of temperature measurements, the thermocouples were initially specified to come from the same batch of thermocouple wires, but the thermocouple manufacturer did not have sufficient stock to complete the order, and two different batches of thermocouple wire were supplied. Care was taken with the calorimeters to assure that the two batches of thermocouple were not mixed on the same calorimeter.

For comparison to computational fluid dynamics analyses, flow probes were located at locations shown in Figures 8 and 9 and Tables 9 and 10. These bi-directional probes and transducers were supplied by the Coast Guard, and are described in the Society of Fire Protection Engineers Handbook [9]. The probes were attached to stands or rakes at locations 0.61 and 1.83 m above the deck and oriented to measure flows parallel to the fore-to-aft centerline of the ship. Flows from aft to forward were defined as positive. The formula for velocity determination, taken from [10], is

$$v = 0.0813\sqrt{T\Delta p} \tag{1}$$

where v is the velocity in m/s, T is the absolute temperature of the air in Kelvins, and p is the pressure difference across the probe in Pascals. This equation assumes that air is a perfect gas. Two video cameras were used for most tests, one each in Holds 4 and 5 at locations shown in Figures 8 and 9. These cameras were placed in water cooled jackets. The camera in Hold 4 was aimed at the fire source, and a monitor was located at the data acquisition system to permit remote viewing of the fire. The camera in Hold 5 was aimed at the bulkhead between Holds 4 and 5. The 35 mm still camera was mounted inside a water cooled case in Hold 4. The field of view of the camera was adjusted to be similar to view from the video camera in Hold 4, and a remote control switch for the camera was mounted at the data acquisition unit. An infrared camera with limited temperature range was also located in Hold 5, but the signal quickly saturated in the vicinity of the fire, and was useful only in determining the areas where the heptane spray nozzles impinged on the bulkhead.

To gain a different perspective on the radiant energy from the fires, two Schmidt-Boelter type radiometers were included in the instrumentation. The radiometer in Hold 4 was located in the vicinity of the video camera and pointed at the fire source. This radiometer with a peak response at 200 kW/m^2 had an 11° field of view. The radiometer in Hold 5 had a peak response of 20 kW/m^2 and a 15° field of view, was located near Hold 5 video camera was aimed at the bulkhead between Holds 4 and 5.

A single oxygen sensor was installed in the vicinity of the King Post near the fire location. This permitted a continuous measurement of oxygen levels in the vicinity of the fire.

Data was collected with "Rack 11," a portion of the MIDAS [11] data acquisition system, which is based on an HP 3852A data logger and an HP 380 series UNIX workstation. A total of 102 thermocouple channels and 16 voltage channels representing flow signals, radiometers, etc. were recorded. The data acquisition system was located on the weather deck of the *Lykes* in a small air conditioned shipping container. Sampling interval for all data was 30 seconds.

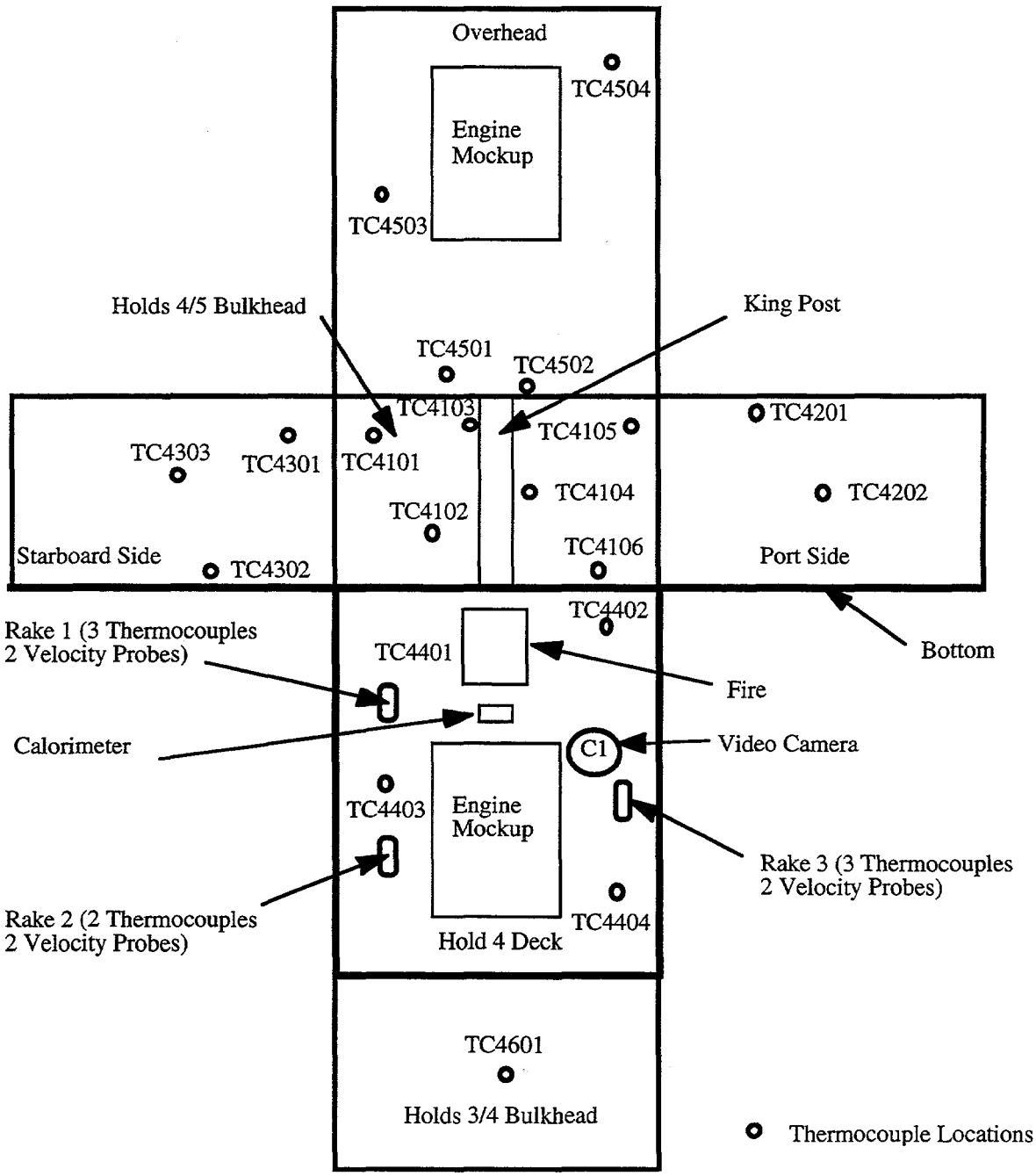

Figure 8. Thermocouples and other instrumentation in Hold 4.

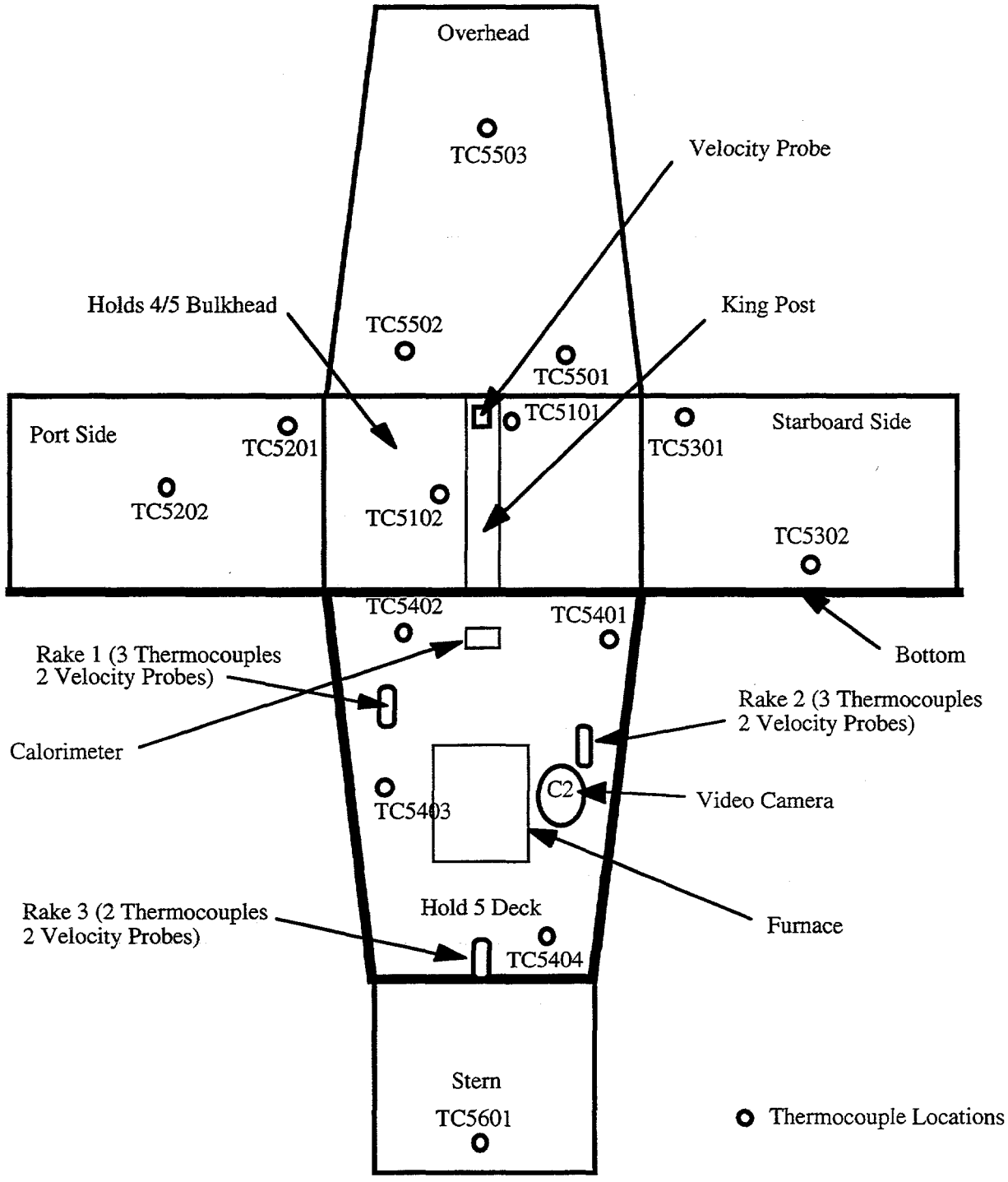

Figure 9. Thermocouples and other instrumentation in Hold 5.

Table 7. Thermocouple Locations in Hold 4

Hold 4 Thermocouple Locations						
		Distance from	Distance from	Distance above		
		Centerline	Forward Bulkhead	Deck		
ID Number	Device type	x, m	y, m	z, m	Comments	Cable/Channel
TC4101	t/c - type k	8.41	0	2.74	Aft bullkhead	59/74
TC4102	t/c - type k	9.27	0	1.83	"	58/75
TC4103	t/c - type k	1.42	0	3.1	"	48/26
TC4104	t/c - type k	-1.32	0	1.42	"	108/28
TC4105	t/c - type k	-8.41	0	2.74	"	114/94
TC4106	t/c - type k	-12.67	0	0.61	"	121/101
TC4201	t/c - type k	-8.8	3.18	2.9	Port bulkhead	113/93
TC4202	t/c - type k	-8.8	9.6	1.52	"	111/91
TC4301	t/c - type k	8.8	1.35	2.82	Starboard bulkhead	60/76
TC4302	t/c - type k	8.8	9.6	1.22	"	49/77
TC4303	t/c - type k	8.8	15.2	2.69	"	55/78
TC4401	t/c - type k	3.51	3.2	0	Deck	51/79
TC4402	t/c - type k	-4.75	3.05	0	"	118/98
TC4403	t/c - type k	7.21	12.09	0	"	54/80
TC4404	t/c - type k	-7.42	15.65	0	"	109/89
TC4501	t/c - type k	0.508	0	3.68	Overhead	57/81
TC4502	t/c - type k	-0.508	0	3.07	"	110/90
TC4503	t/c - type k	5.7	11.1	3.3	"	52/82
TC4504	t/c - type k	5.71	15.65	3.07	"	115/95
TC4601	t/c - type k	0	21.05	2.54	Forward bulkhead	120/100
TC4801	t/c - type k	0.61	5.33	1.52	Eng. Rm. Mockup	56/88
TC4802	t/c - type k	-1.29	5.33	1.22	" " "	119/99
ID key:						
TC = thermocouple, x-Dimensions: Port side negative, Starboard positive						
First Digit = 4 for hold 4						
Second Digit = Bulkhead number, 1 = Aft bulkhead, 2 = Port bulkhead, 3 = Starboard bulkhead,						
4 = deck, 5 = overhead, 6 = forward bulkhead						
Third and fourth digits = sequence number						

Table 8. Instrument Rake Locations in Hold 4

		Instrumentation Rakes & Misc. - Hold 4				
		Distance from	Distance from	Distance above		
		Centerline	Aft Bulkhead	Deck		
ID Number	Device type	x, m	y, m	z, m	Comments	Cable/Circuit
TC4711	t/c - type k	6.6	4.42	0.91	Rake 1	50/83
TC4712	t/c - type k	6.6	4.42	1.52	"	47/84
TC4713	t/c - type k	6.6	4.42	2.13	"	46/85
TC4721	t/c - type k	6.88	13.31	0.91	Rake 2	53/86
TC4722	t/c - type k	6.88	13.31	2.13	"	45/87
TC4731	t/c - type k	-6.48	11.73	0.91	"	117/97
TC4732	t/c - type k	-6.48	11.73	1.52	Rake 3	116/96
TC4733	t/c - type k	-6.48	11.73	2.13	"	119/99
FP4711	Flow, 19 m/s	6.6	4.42	0.91	Rake 1	Aux. 5
FP4713	Flow, 19 m/s	6.6	4.42	2.13	"	Aux. 6
FP4721	Flow, 19 m/s	6.88	13.31	0.91	Rake 2	Aux. 3
FP4722	Flow, 19 m/s	6.88	13.31	2.13	"	Aux. 4
FP4731	Flow, 19 m/s	-6.48	11.73	0.91	Rake 3	Aux. 1
FP4733	Flow, 19 m/s	-6.48	11.73	2.13		Aux. 2
RA4001	Radiometer	-1.3	5.33	1.3	11° Radiometer	Aux. 16
O2	Oxygen Sensor	0	0.5	1	Approx. location from photos	Aux. 13
ID key:						
TC = thermocouple, FP = flow probe, RA = radiometer						
First digit = 4 for hold 4						
Second digit = 7 for rake						
Third digit = number of rake						
Fourth digit = sequence number						

Table 9. Thermocouple Locations in Hold 5

Hold 5 Thermocouple Locations						
		Distance from Centerline	Distance from Forward Bulkhead	Distance above Deck		
ID Number	Device type	x, m	y, m	z, m	Comments	Cable/Channel
TC5101	t/c - type k	1.42	0	3.1	Forward bullkhead	65/25
TC5102	t/c - type k	-1.32	0	1.42	"	66/27
TC5201	t/c - type k	-8.8	-1.52	2.74	Port bulkhead	101/43
TC5202	t/c - type k	-8.8	-9.75	1.47	"	102/44
TC5301	t/c - type k	8.8	-1.27	1.6	Starboard bulkhead	67/29
TC5302	t/c - type k	8.8	-6.88	0.61	"	68/30
TC5401	t/c - type k	5.08	-0.99	0	Deck	69/31
TC5402	t/c - type k	-3.35	-1.83	0	"	70/32
TC5403	t/c - type k	-3.35	-7.92	0	"	71/33
TC5404	t/c - type k	4.72	-10.97	0	"	72/34
TC5501	t/c - type k	2.74	-0.29	3.81	Overhead (Approx.)	73/35
TC5502	t/c - type k	-2.74	-0.3	3.81	" "	74/36
TC5503	t/c - type k	0	-15.94	3.48	"	75/37
TC5601	t/c - type k	1.41	-22.9	2.92	Aft bulkhead	106/48
TC5801	t/c - type k				Intrinsic t/c-furnace	107/49
ID key:						
TC = thermocouple, x-Dimensions: Port side negative, Starboard positive						
First Digit = 5 for hold 5						
Second Digit = Bulkhead number, 1 = Forward bulkhead, 2 = Port bulkhead, 3 = Starboard bulkhead,						
4 = deck, 5 = overhead, 6 = Aft bulkhead						
Third and fourth digits = sequence number						

Table 10. Instrument Rake Locations in Hold 5

		Instrumentation Rakes & Misc. - Hold 5				
		Distance from	Distance from	Distance above		
		Starboard side	Aft Bulkhead	Deck		
ID Number	Device type	x, m	y, m	z, m	Comments	Cable/Circuit
TC5711	t/c - type k	-3.12	-3.99	0.91	Rake 1	76/38
TC5712	t/c - type k	-3.12	-3.99	1.52	"	77/39
TC5713	t/c - type k	-3.12	-3.99	2.13	"	78/40
TC5721	t/c - type k	4.75	-6.15	0.91	Rake 2	79/41
TC5722	t/c - type k	4.75	-6.15	1.52	"	80/42
TC5723	t/c - type k	4.75	-6.15	2.13	"	103/45
TC5731	t/c - type k	-4.75	-19.13	0.91	Rake 3	104/46
TC5732	t/c - type k	-4.75	-19.13	2.13	"	105/47
FP5711	Flow, 19 m/s	-3.12	-3.99	0.91	Rake 1	Aux. 9
FP5713	Flow, 19 m/s	-3.12	-3.99	2.13	"	Aux. 10
FP5721	Flow, 19 m/s	4.75	-6.15	0.91	Rake 2	Aux. 11
FP5723	Flow, 19 m/s	4.75	-6.15	2.13	"	Aux. 12
FP5731	Flow, 19 m/s	-4.75	-19.13	0.91	Rake 3	Aux. 7
FP5732	Flow, 19 m/s	-4.75	-19.13	2.13	"	Aux. 8
RA5001	Radiometer	-1.12	-4.37	1.07	15° Radiometer	Aux. 15
FP5101	Flow, 19 m/s	0	-1.19	2.51	Mounted above calorimeter	Aux. 13
ID key:						
TC = thermocouple, FP = flow probe, RA = radiometer						
First digit = 4 for hold 4						
Second digit = 7 for rake						
Third digit = number of rake						
Fourth digit = sequence number						

3.0 TEST SEQUENCE

The total of 8 tests consisted of three basic types: heptane spray tests simulating an engine room or galley fire, wood crib fires simulating a cargo fire, and open pool fires intended to permit comparison with regulatory pool fires typical of land transport situations. The test sequence is shown in Table 11. A detailed description of each experimental fire configuration follows. Test numbers are not sequential because pretest instrumentation check runs with the data logger are also assigned a permanent sequence number.

Table 11. Test Sequence

Test Number	Date, Time and Duration	Type of Test	Peak Thermal Power, MW
5037	9/12/95 2:09 PM CDT 60 Minutes	2 burner heptane spray test	2.2
5040	9/14/95 9:13 AM CDT 20 Minutes	Wood crib fire test with 17 L heptane accelerant	4.1
5041	9/14/95 12:21 PM CDT 60 Minutes	2 burner heptane spray test with diesel fuel in drip pans for smoke	2.2
5043	9/15/95 8:26 AM CDT 20 Minutes	Wood crib fire test with 17 L heptane accelerant	4.1
5045	11/13/95 12:02 PM CDT 60 Minutes	4 burner heptane spray test	5.6
5046	11/13/95 2:46 PM CDT 60 Minutes	4 burner heptane spray test with diesel fuel in drip pans for smoke	5.6
5048	11/14/95 3:09 PM CDT 27 Minutes	Diesel pool fire in Hold 4	15.7
5049	11/15/95 2:20 PM CDT 32 Minutes	Diesel pool fire on weather deck	18.8

3.1 Two Burner Heptane Spray Test (5037)

For these tests simulating a fire in an engine room or galley, heptane in a pressurized reservoir was fed through nominal 3/8 inch, 0.035 inch wall thickness stainless steel tubing to two nozzles located in Hold 4. The general arrangement for theses tests is shown in Figures 10 and 11. Stainless steel BETE model P54 fine atomization spray nozzles were used to create a 90° cone

shaped fog spray that was manually ignited with a propane torch. The nozzles were located 0.91 m to either side of the hold centerline. The nozzles were located 1 m above the deck, 1 m from the bulkhead between Holds 4 and 5, and were aimed at the bulkhead at an angle of 45° above horizontal.

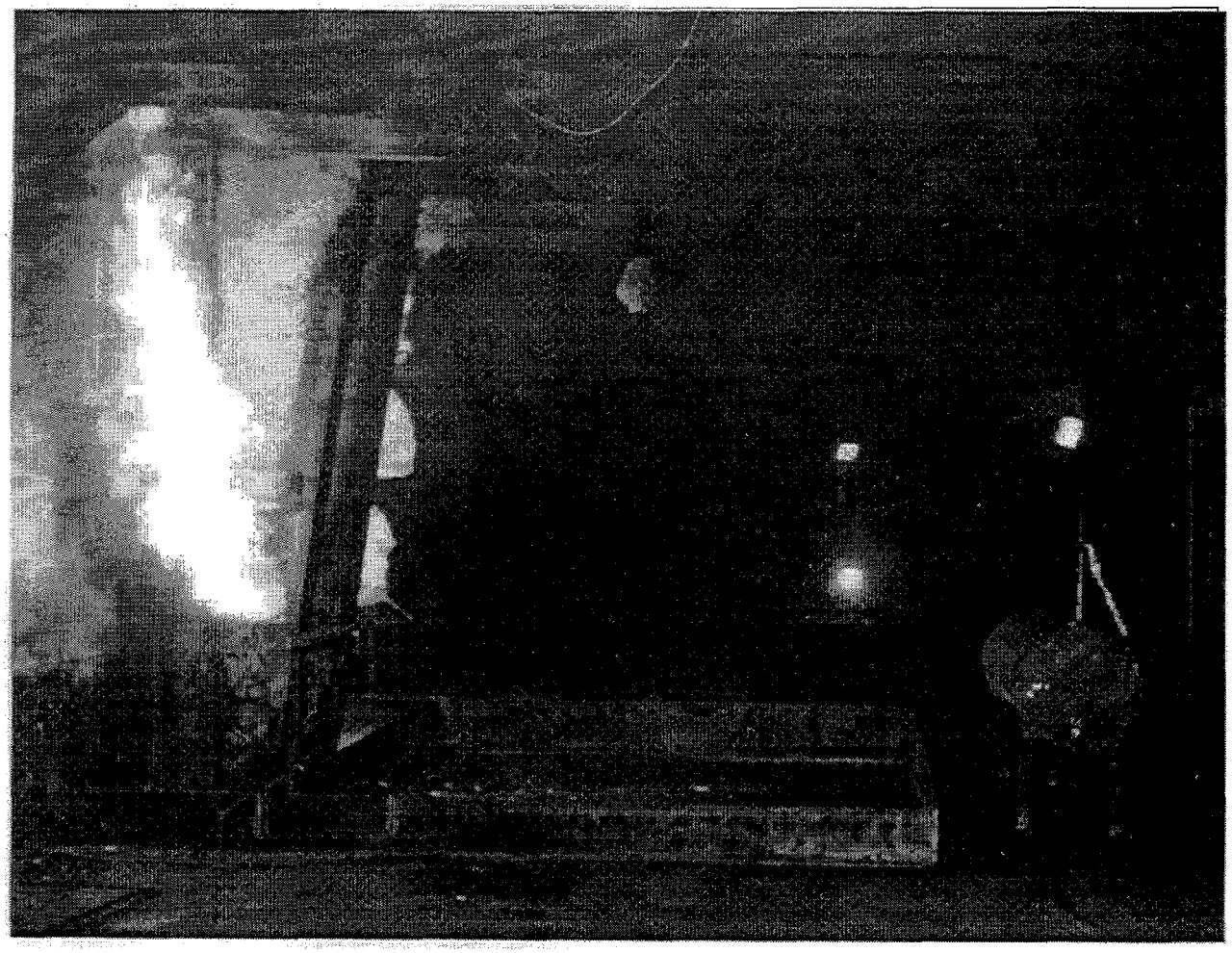

Figure 10. Two burner test arrangement in Hold 4. Note calorimeter location at right.

The heat release of a spray nozzle was estimated by correcting the spray nozzle factor, k, in the equation

$$q = k\sqrt{\Delta p} \tag{2}$$

where q is the flow in m^3/s, k is the nozzle flow constant, and p is the pressure drop in MPa, for heptane density rather than the water density data listed in the BETE catalog as follows

$$k_{heptane} = k_{water}\sqrt{\rho_{water}/\rho_{heptane}} \tag{3}$$

where ρ is the density of the fluid. Since heptane is less dense than water, the nozzle flows increases by a factor of about 20 per cent above water flow for the fluid temperatures considered. Pressure drop from the reservoir to the nozzles was estimated with standard fluid pressure drop formulas for flows in piping. For the estimated 0.21 MPa pressure difference across the nozzle, a

0.0.024 kg/s mass flow rate results through each nozzle. For heptane with a heat of combustion of 44.6 MJ/kg, this gives a thermal output of each nozzle for full combustion of 1.1 MW. The two nozzle configuration shown in Figure 10 doubles this to a total thermal output of the fire to 2.2 MW.

During this test, a rain shower passed over the ship. Thermocouple data of overhead and hull temperatures show significant dips caused by cooling from the rain water.

3.2 Wood Crib Fire Test (5040)

Wood cribs built from clear Douglas fir were used to simulate a cargo fire adjacent to the radioactive cargo. The general arrangement for the crib fires is shown in Figures 11 and 12, and a photograph of a completed crib during combustion is shown in Figure 13. The general wood crib design is based on UL Standard 711 [4], and is consistent with the size designated as 20-A in that standard. To estimate the heat release from the crib, equations were taken from Walton [5]. First the cross sectional area of the exposed surface, A_E, is calculated from the equation

$$A_E = 2nb^2[(2(l/b)+1)N - n(N-1)] \tag{4}$$

where b is the stick thickness in m, n is the number of sticks per layer, N is the number of layers and l is the length of the wood sticks. Since the wood used was rectangular in cross section, the stick thickness b was taken to be one-fourth of the perimeter dimension. The heat release rate is then obtained from the equation

$$\dot{q} = A_E E C b^{-0.5} \tag{5}$$

where $\dot{q}$ is the heat release rate in MW, A_E is the cross-sectional area from Equation (4) in m^2, E is the heat released from the combustion of pyrolysis products in kJ/kg, and C is an empirical constant for the mass of pyrolysis product produced per unit surface area and unit time in $kg/(m^{1.5}s)$. Walton suggests a value of 0.65×10^{-3} $kg/(m^{1.5}s)$ for single cribs of Douglas fir. Application of these equations to the UL 711 size 20-A crib give a heat release of 2.4 MW. The UL standard also specifies that to initiate the fire, 17 L of heptane accelerant are to be ignited in a 1 m square pan under the crib. Observation of the experimental data indicated that this accelerant burned for about five minutes giving an experimental recession rate of 0.038 $kg/(m^2s)$, and a corresponding output of 1.7 MW. Combining the heat release of the wood crib and the heptane accelerant gives an initial thermal output of 4.1 MW for the first 5 minutes of the fire, then a steady heat release of 2.4 MW as the crib alone burns. Inspection of the data for the calorimeter in Hold 4 indicates that the wood crib heat release decreased rapidly 15 minutes after ignition indicating that most wood had burned.

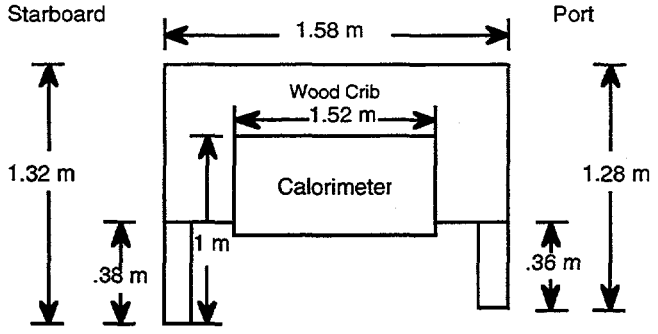

Figure 11. Wood crib arrangement looking aft. Wood crib is centered on ship forward to aft centerline.

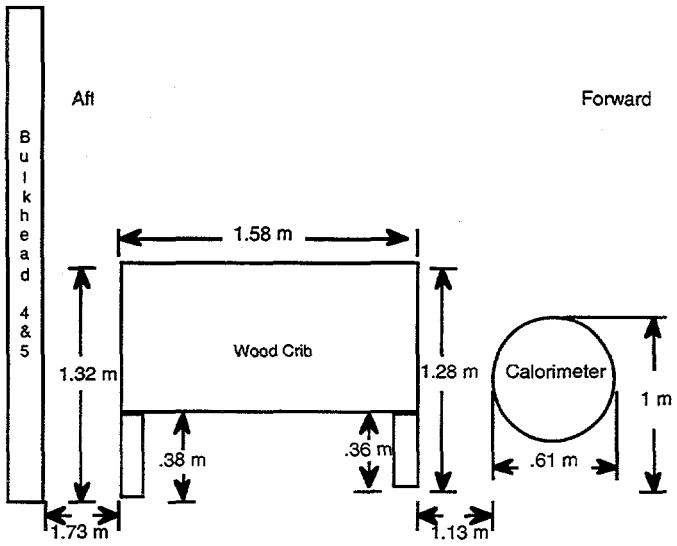

Figure 12. Wood crib arrangement as viewed from starboard side of ship.

Figure 13. Wood crib fire viewed from near video camera on port side of the *Mayo Lykes*.

3.3 Two Burner Heptane Spray Test with Diesel Fuel (5041)

This test was essentially a repeat of Test 5037, the two-burner heptane spray test, with the exception that 4 L quantities of diesel fuel were ignited in the 1 m drip pans located just outside the fire pan in Hold 4 (See Figure 4). Since heptane is an extremely clean burning fuel, the purpose of the diesel fuel fires was to create smoke in the hold to simulate a smoky fire. As the test proceeded, a smoke layer formed at the overhead, and proceeded to lower and visibly cover the upper half of the hold. Inspection of the calorimeter data indicates that the diesel burned out at about 5 minutes into the test, and visible smoke remained in the hold for about the next 10 minutes.

3.4 Wood Crib Fire Test (5043)

The major purpose of this test was to check the reproducibility of wood crib fires. The configuration was an intentional repeat of Test 5040, and the calculations for heat release reported for that test should apply equally to this test.

3.5 Four Burner Heptane Spray Test (5045)

After inspecting the calorimeter results from the first series of two-burner heptane spray tests, a second series with larger nozzles in a four-burner arrangement were conducted with as shown in Figure 14 for test 5046. For this test, in addition the nozzle locations 0.91 m to each side of the ship centerline, additional nozzles were located 3.05 m to each side of the centerline. As with the two burner tests, nozzles were 1 m above the deck, 1 m from the Hold 4 and 5 bulkhead, and aimed at the bulkhead at an angle of 45° above horizontal. For the test the larger BETE P66 nozzles were used with a 0.55 MPa pressure maintained at the fuel reservoir. This gives an estimated nozzle pressure difference of 0.17 MPa and a flow from each nozzle of 0.031 kg/s. This yields an estimated power release of 1.4 MW for each burner, and a total release of 5.6 MW total for all burners.

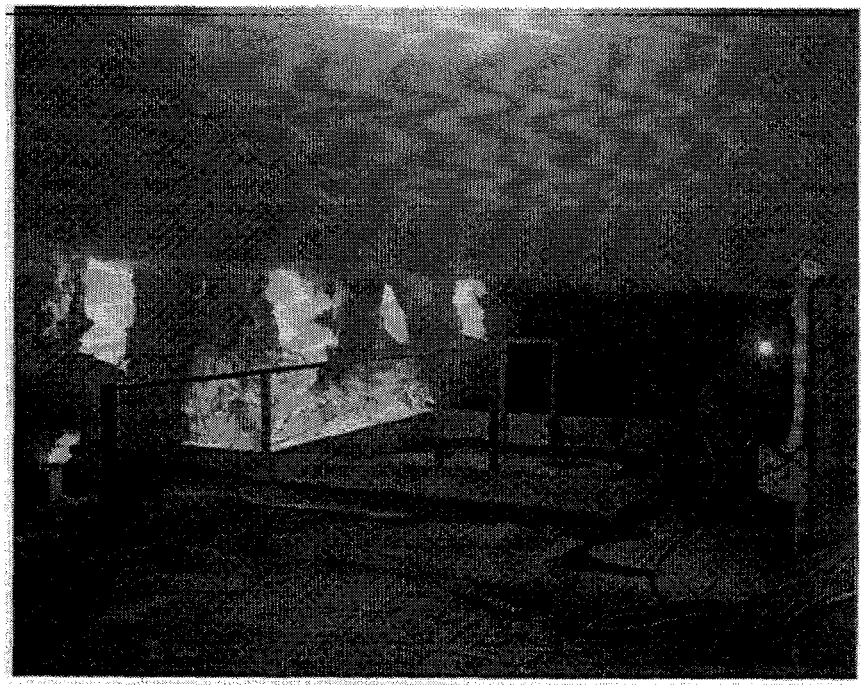

Figure 14. Four burner test with diesel fuel added for smoke. Note smoke obscuration at time near burnout of diesel fuel.

3.6 Four Burner Heptane Spray Test with Diesel Fuel (5046)

As with the two burner tests, a second four burner test was conducted with 4 L of diesel fuel in the drip pans as shown in Figure 14. Smoke built from the overhead in a pattern similar to encountered in the two burner tests. Except for the first five minutes while the diesel burned, the energy output for this test was the same as for Test 5045.

3.7 In-Hold Pool Fire (5048)

Although pool fires in ship holds, especially those holds selected for shipment of radioactive cargoes, are highly unlikely, a comparison of conditions encountered in such a fire to pool fire conditions commonly conducted for land-based regulatory testing was considered to be useful. One argument held that a pool fire in a ship hold may actually be more severe because the energy produced by the fire would be reflected by the ship bulkheads, increasing the heat transfer to the cargo. On the other hand, arguments that reduced oxygen availability in the hold would limit the fire thermal output were also proposed. In order to provide a basis for comparison, and in-hold pool fire was conducted with the test configuration shown in Figure 4. The fire pan used is shown in Figure 10. At the start of the burn, the bottom of the calorimeter was 1 m above the fuel surface. This is consistent with the height above the pool used for regulatory tests on land. Because of its ready availability and usefulness for other purposes if not all the fuel was consumed, diesel fuel was selected for this test. The fuel was floated on a pool of water in the specially built containment area adjacent to the bulkhead between Holds 4 and 5. To avoid a possible explosion, openings in the hull provided adequate oxygen to the fire. In an actual shipboard fire, this free availability of oxygen is unlikely.

For this test the calorimeter in Hold 4 was moved to be centered above the pool, 1 m above the fuel surface at the start of the test. This arrangement is the same as used for land-based pool fire tests and permits direct comparison of ship fire results to typical land based pool fire tests. During the test 7.6 cm depth out of a total depth of 13 cm of diesel fuel were burned before overhead temperatures exceeded 540°C at 24 minutes into the test, and the fire was extinguished with foam at 27 minutes. At this point the fire was extinguished with foam to prevent further damaging the ship structure. From this information a fuel recession rate of 0.0443 kg/m^2-s was calculated. With a typical diesel heat of combustion of 42.75 MJ/kg this leads to an average heat release of 15.7 MW during the test.

For the pool fires a Directional Flame Thermometer (DFT) based on a basic design from Burgess and Fry [12] were used to estimate the temperatures of the engulfing flames. These devices, resembling a vegetable can, have thin metal ends that rapidly approach flame temperatures. Thermocouples attached on the inside of the thin metal ends provide an estimate of flame temperatures in the direction that the end faces in the fire. The cans are filled with insulation to prevent internal heat transfer within the DFT.

3.8 Outdoor Diesel Pool Fire (5049)

For comparison to the in-hold fire test, a 3 m x 3 m pool was built on the weather deck of the *Mayo Lykes* on the port side amidships. The pool was constructed to closely follow the dimensions of the pool built in Hold 4. The calorimeter from Hold 5 was centered above the pool, 1 m above the fuel surface at the start of the test. A depth of 13 cm of diesel fuel gave a 32 minute burn, typical of a regulatory pool fire. Calculation of the recession rate for this fire led to an estimated average thermal output of 18.8 MW. A strong off-shore wind tended to lay the fire plume over, often uncovering the flames from the calorimeter as shown in Figure 15. This effect, visible in the data as highly variable heat fluxes to the calorimeter, is not typical of land based tests that are conducted when the wind is relatively calm.

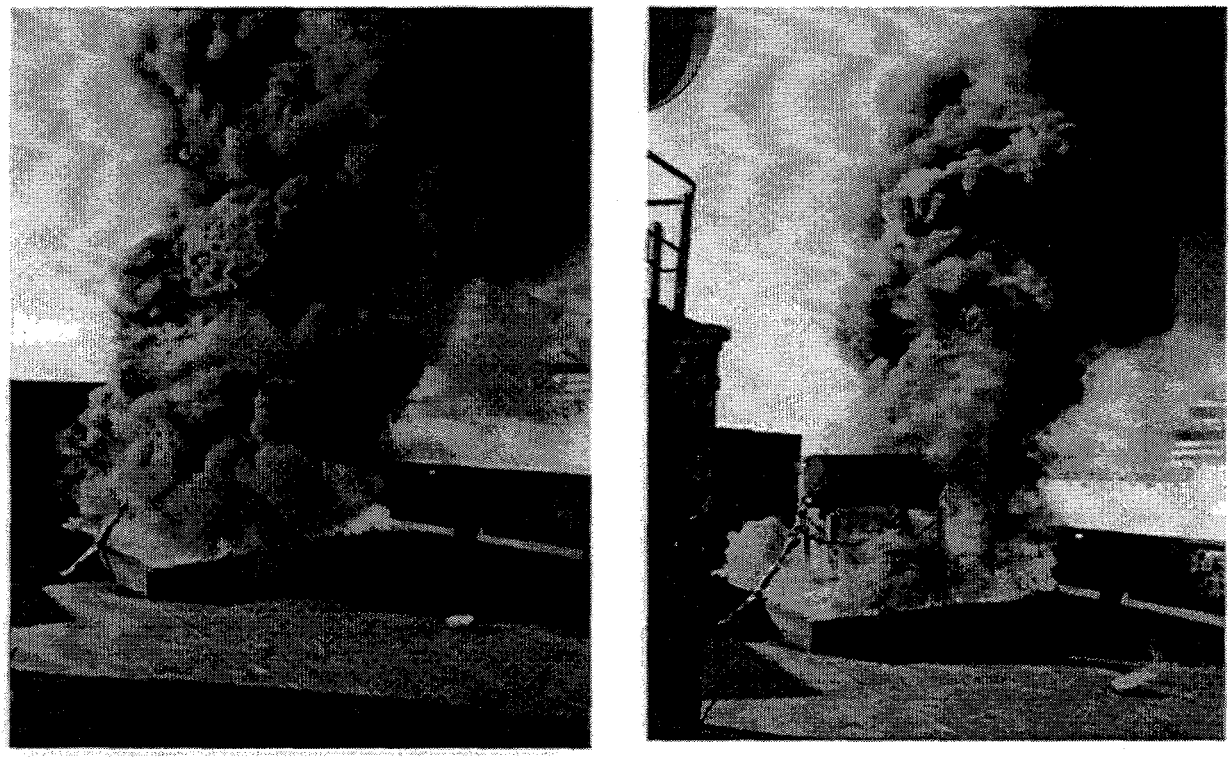

Figure 15. Diesel pool fire on deck of *Mayo Lykes*. In view at right, high wind has blown flames away from calorimeter.

4.0 RESULTS AND CONCLUSIONS

Data from the eight tests for bulkhead, calorimeters and flow probes are presented in Appendices A through H. The fires ranged in size from 2.2 MW for the two burner heptane tests, to 18.8 MW for the outdoor pool fire test, leading to a wide variation in temperatures, heat fluxes and flows. Inspection of the results leads to several conclusions regarding the fires. More will be learned after simulations based on computational fluid dynamics techniques are completed and described in a second report on these tests. After the simulation methods are verified, then the successful approaches can be used to extend the results to other shipboard fire situations.

Calorimeter results for both Hold 4 and Hold 5 tests indicate that for fires in adjacent holds, and adjacent to the burning object in the same hold, heat fluxes are well below current regulatory limits. Even in the case of the fully engulfing pool fire in Hold 4, heat fluxes are in the typical range reported for outdoor pool fires on land [13]. This indicates that the heat fluxes encountered are not higher than previously anticipated, and the duration of the fire must also be considered. For Hold 5, the heat fluxes to the calorimeter never exceeded 1 kW/m^2, even with the large pool fire in Hold 4.

For the heptane spray fires in Hold 4 representing an adjacent engine room fire or galley fire, Tests 5037, 5041,5045, and 5046, heat fluxes to the Hold 5 calorimeter never exceeded 0.8 kW/m^2. This is significantly below the typical 65 kW/m^2 maximum heat fluxes implied by Safety Series 6 or 10CFR71. Even with the large pool fire of Test 5048, heat fluxes in Hold 5 do not exceed 1.8 kW/m^2 indicating that even large fires in adjacent holds would not usually create concerns for radioactive materials packages.

For both the heptane spray and wood crib fires, analysis of the calorimeter heat flux plots in the Appendices shows that the absorbed heat fluxes are much higher on the side facing the fire. This indicates that thermal radiation is the dominant heat transfer mechanism, since convection would lead to a more uniform heating with hot gases flowing around the entire circumference of the calorimeter. Accurate fire simulations will aid in determining the partitioning of the heat transfer mechanisms involved.

Steel cargo holds typically do not contain the combustible carpets, wall coverings and other easily combustible materials such as furniture and paper that lead to the flashover conditions typical of building fires on land. At the flashover point, room temperatures and thermal radiation combine to ignite simultaneously most combustible materials in the room. This condition was not observed for any of the tests conducted. The calorimeter measurements of heat fluxes, coupled with ignition models, could be used to estimate the time required for spread of a ship hold fire from one combustible cargo to another.

To avoid potentially explosive conditions with the heptane spray and in-hold pool fires, adequate oxygen was supplied to Hold 4 via openings in the hull. Measurements indicate that oxygen levels in the vicinity of the fire were usually near normal atmospheric content. In sealed shiphold fires at sea, oxygen would be more limited, leading to smoldering fires with even lower heat flux levels

than experimentally measured. The experimental fires reported here represent conditions more typical of a fire that could occur during ship loading or unloading in port.

Inspection of the estimated heat transfer plots for Holds 4 and 5 shows some rapid fluctuations in the estimated heat flux values, especially for Hold 5. Since the heat fluxes to the calorimeter in Hold 5 are generally much lower than the values for the calorimeter in Hold 4, any noise in the Hold 5 data are displayed as proportionately larger variations on the heat flux signal than occur for Hold 4 data. Although the SODDIT code permits multiple time point analyses that smooth the results, the decision was made to display the single time point analysis results to enable a better understanding of the signal-to-noise ratios involved in the data analysis.

Wood crib fires in Tests 5040 and 5043 led to estimated peak heat fluxes on the calorimeters of near 30 kW/m^2 during the burning of the heptane accelerant, and heat fluxes of near 10 kW/m^2 while the wood crib alone burned. Again these heat fluxes are significantly below the regulatory values, and are applied to only one half of the calorimeter surface. The heat flux peaks at the start of the fire are likely not as large as shown on the Figures in Appendices B and D. This is because a surface thermocouple on the calorimeter, when exposed to rapid changes in radiant energy levels, does not respond in the same manner as the steel surface of the calorimeter. Having less mass, the thermocouple bead responds more rapidly than the surface, and, under these rapid heating conditions, does not accurately represent the calorimeter surface temperature. The inverse heat conduction program interprets this as a rapid increase in the bead temperature as the temperature of the steel surface of the calorimeter. The result is an estimated peak in the heat transfer that is significantly higher than when the inside thermocouple alone is used for the data analysis. Since these effects tend to overestimate rather than underestimate the early heat transfer transients, the results are conservative (high) values, and were chosen for display of the wood crib and heptane spray results in the report.

Heat fluxes to the calorimeter for the in-hold pool fire test, 5048, are in the range of 150 to 200 kW/m^2 for the first 3 to 5 minutes of the test. These values are consistent with values measured in outdoor pool fires on land [13], indicating that even in the confines of a ship hold, the heat transfer to a radioactive material package is not increased above values observed for open air accidents on land. This discounts the concept that the hold bulkheads reflect the energy, leading to higher heat transfer. A possible explanation for the lack of the reflected energy is that smoke from the fire blocks thermal radiation, converting the heat transfer to a convection dominated regime. Studies with analysis codes can be used to confirm this effect.

The in-hold pool fire is a highly unlikely event, and was conducted only to provide a basis of comparison for land-based regulatory fires. To accumulate a large pool of flammable liquid in the same hold with a radioactive material package requires multiple failures or breaching of the IMDG code for loading of hazardous materials.

For the pool fires of Test 5048 and 5049, data analyzed with both inside and outside thermocouples proved extremely noisy for reasons related to the method of attachment for outside thermocouples discussed above for wood crib fires. For this reason, and to be consistent with methods previously used for land based experiments, only the thermocouples located inside the calorimeter were used to analyze heat transfer in these tests. Figures in Appendices G and H indicate this fact.

Winds tended to blow the flames from the calorimeter during Test 5049. This leads to a much wider variation in the heat transfer than observed in the in-hold Test 5048. This also demonstrates why regulatory tests are done under conditions with low wind velocities. Despite the wind, peak heat transfer values to the calorimeter are in the same range for both in-hold and outdoor tests, and the peak temperature are reached at similar times.

Inspection of the traces for the flow probes lead to questions regarding the accuracy and reliability of the data. Many traces show little variation during the tests indicating possible problems with the pressure transducers or the amplifiers used during the tests. Caution should be used when comparing these data to other fires or computer simulations. In contrast, the temperature data from the instrument rakes appear consistent and accurate, giving good estimates of the gas temperatures at various levels above the deck during the fires. Oxygen data must also be considered carefully. For example, the drop in the oxygen level observed in Test 5040 (Figure B.28), was attributed to a soot blockage in the tube that routed the air from the fire zone to the oxygen sensor. After the blockage was removed, later tests reveal a significant recovery in oxygen level after termination of the fire. The trace from Test 5048 (Figure G.29) for the in-hold pool fire indicates a total blockage of the oxygen sensor line about 6 minutes after fire ignition.

During Test 5048, several of the thermocouple cables were damaged by the hot deck across which the cables were routed. The erratic bahavior of the data traces after 24 minuteswas caused by this damage, and should be considered when analyzing these data.

Analysis of the data does not indicate that shipboard fires are likely to lead to increased heat transfer when compared to land based regulatory fires. In general, the heat transfer seems to be lower than for the fully engulfing pool fire considered for land based accidents. This leads to the consideration of the duration of shipboard fires, a study that may be better based on historical data rather than experiment.

These experimental results are primarily intended to serve as a means of confirming and refining analytical heat transfer models of shipboard fires. No general conclusions regarding the adequacy or inadequacy of regulatory tests as applied to the shipboard fire environment can be drawn directly from the tests. Any risk assessment model of fires must also include the probabilities of initiating events, as well as details of crew response and allowances for use of fire suppression systems.

The testing here applies primarily to the break-bulk freighters typically used to transport radioactive materials. The work does not apply to container ships, where the IMDG rules differ from those applied to break-bulk ships. Further investigations would be necessary to assess typical fire conditions aboard container cargo ships.

REFERENCES

1. International Maritime Organization, *International Maritime Dangerous Goods Code*, International Maritime Organization, 1992.

2. International Maritime Organization, *Code for the Safe Carriage of Irradiated Nuclear Fuel in Flasks on Board Ships*, International Maritime Organization, 1995.

3. International Atomic Energy Agency, *Regulations for the Safe Transport of Radioactive Material 1985 Edition (As Amended 1990), Safety Series No. 6*, IAEA, Vienna, 1990.

4. Underwriters Laboratories, *Rating and Fire Testing of Fire Extinguishers*, Standard for Safety, UL 711, Underwriters Laboratories, 1990.

5. W. D. Walton, *Suppression of Wood Crib Fires with Sprinkler Sprays: Test Results*, U. S. Dept. of Commerce, NBSIR 88-3696, National Bureau of Standards, National Engineering Laboratory, Gaithersburg, MD, January 1988.

6. A. R. Mahoney, Sandia National Laboratories Memo dated January 14, 1997, *Measured Thermal Emittance of Ship Hold Paint Flakes.*

7. B. F. Blackwell, R. W. Douglas, and H. Wolf, *A User's Manual for the Sandia One-Dimensional Direct and Inverse Thermal (SODDIT) Code*, SAND85-2478, Sandia National Laboratories, Albuquerque, NM, 1987.

8. A. B. Shapiro and A. L. Edwards, *TOPAZ2D Heat Transfer Code Users Manual and Thermal Property Data Base*, UCRL-ID-104558, Lawrence Livermore National Laboratory, Livermore, CA, 1990.

9. A. R. Mahoney, Sandia National Laboratories Memo dated April 22, 1996, *Measured Thermal Emittance of Iron Oxidized Calorimeters.*

10. P. J. DiNemmo, Ed., *Society of Fire Protection Engineers Handbook of Fire Protection Engineering*, National Fire Protection Association, Quincy, MA, 1990.

11. *MIDAS - Mobile Instrumentation Data Acquisition System*, SAND90-2916, Sandia National Laboratories, Albuquerque, NM, 1990.

12. M. H. Burgess and C. J. Fry, "Fire Testing for Package Approval," *Radioactive Material Transportation*, Vol. 1, No. 1, pp. 7-16, 1990.

13. J. J. Gregory, N. R. Keltner and R. Mata, Jr., "Thermal Measurements in Large Pool Fires, *Journal of Heat Transfer*, " No. 111, pp. 446-454, 1989.

Appendix A
Test 5037
Two Burner Heptane Spray Test

conducted 9/12/95
2:09 PM CDT

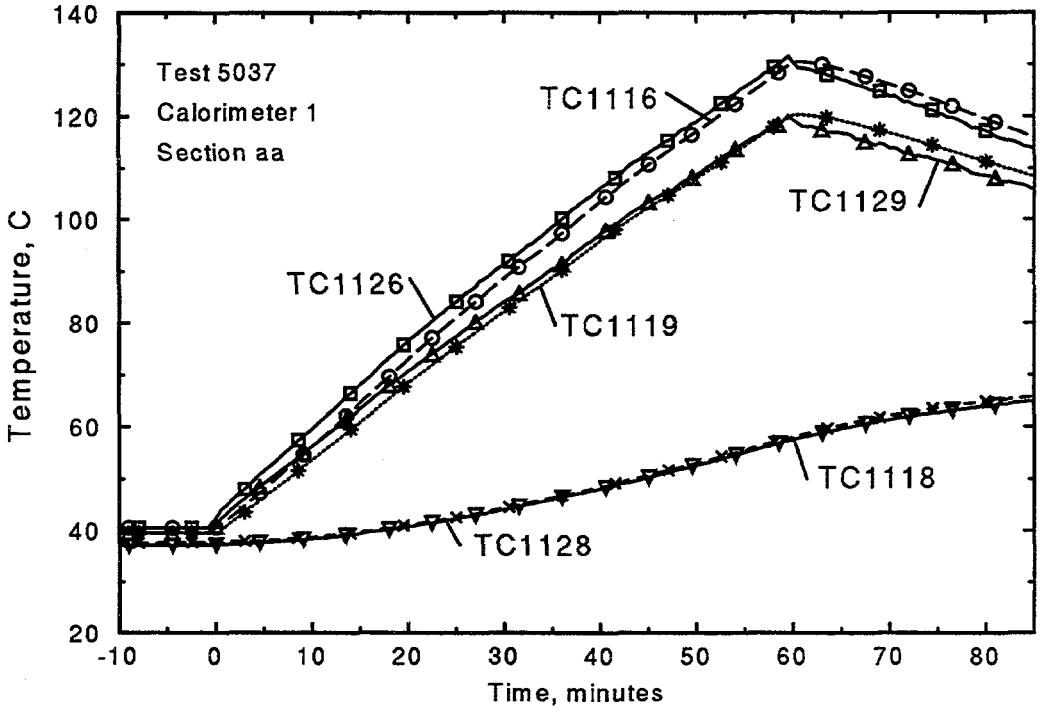

Figure A.1: Thermocouple response of Calorimeter 1, section aa

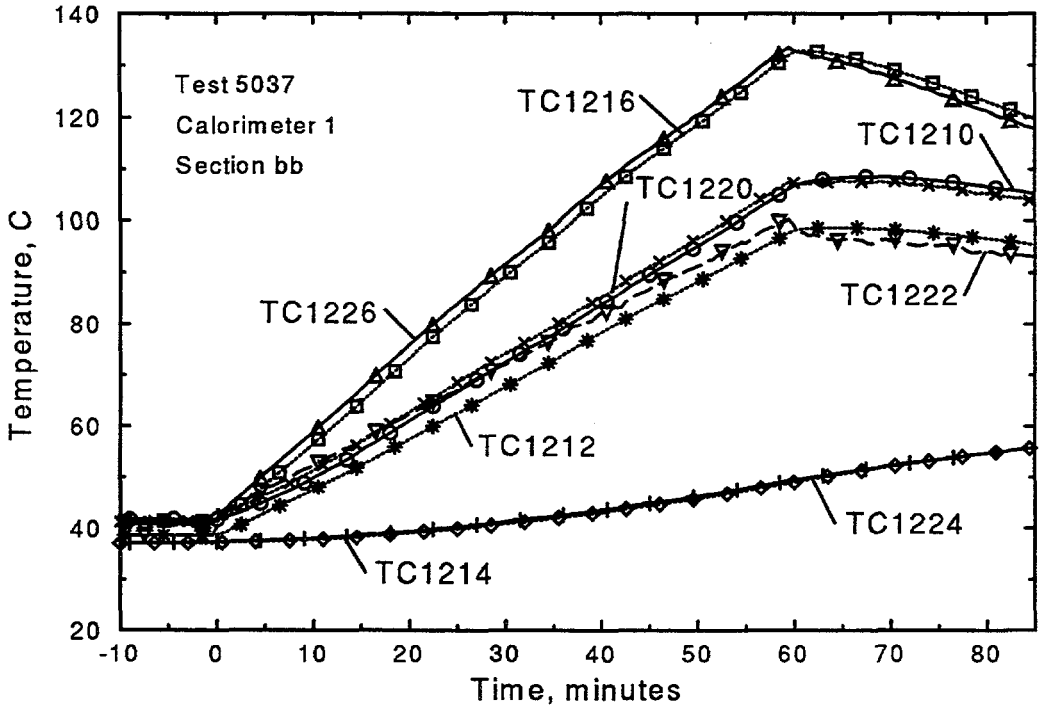

Figure A.2: Thermocouple response of Calorimeter 1, section bb

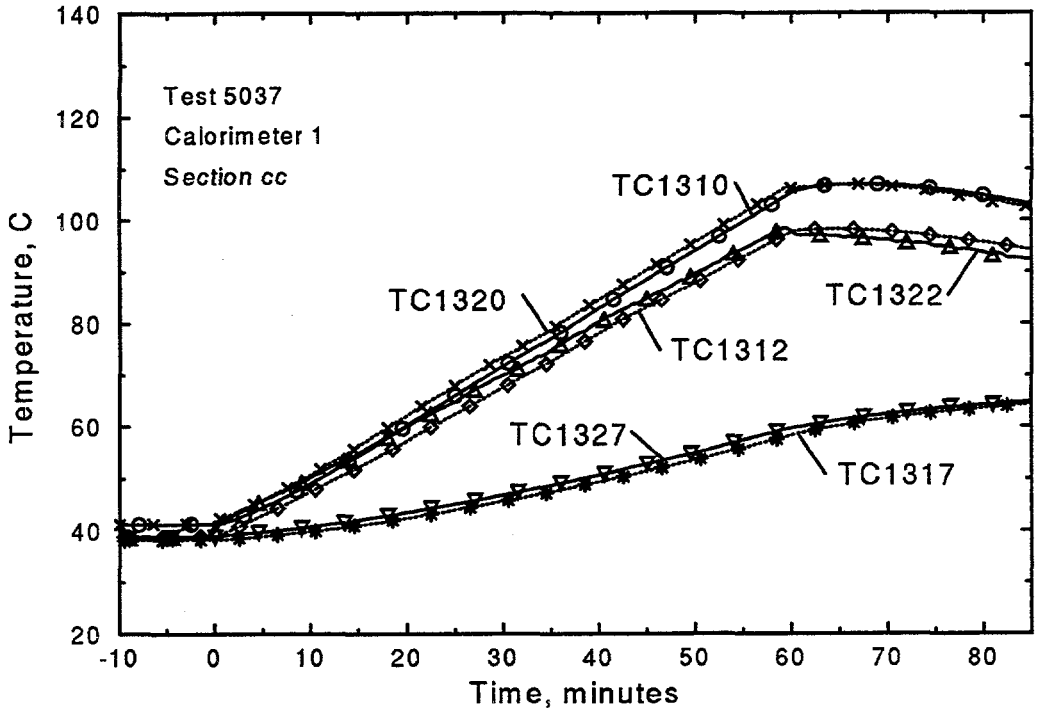

Figure A.3: Thermocouple response of Calorimeter 1, section cc

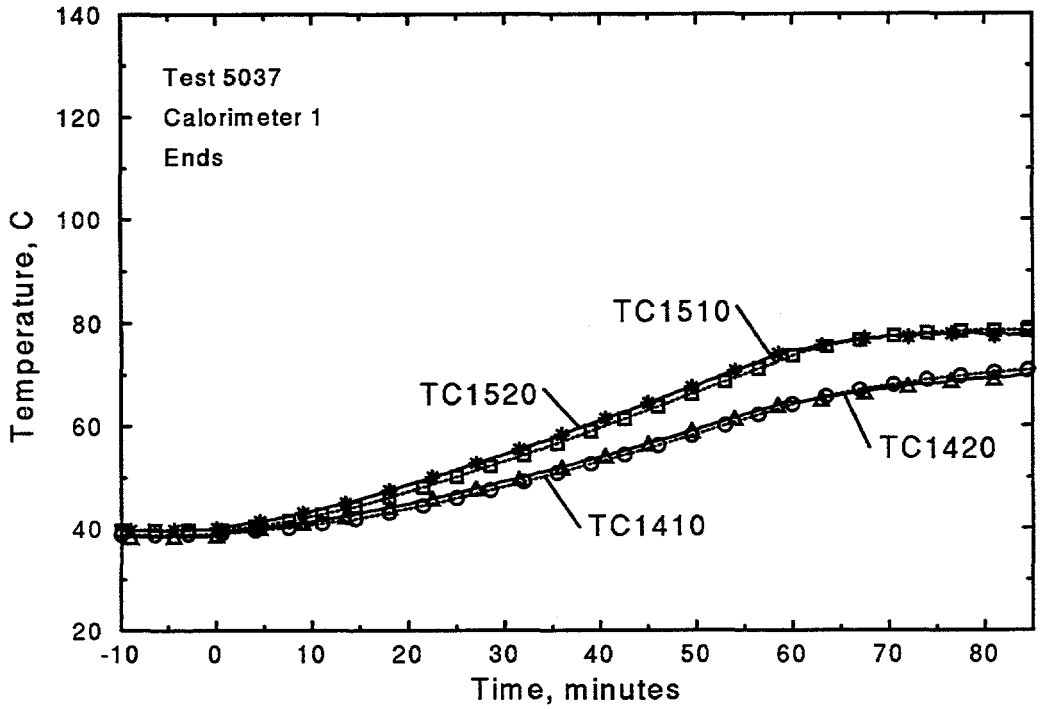

Figure A.4: Thermocouple response of Calorimeter 1, ends

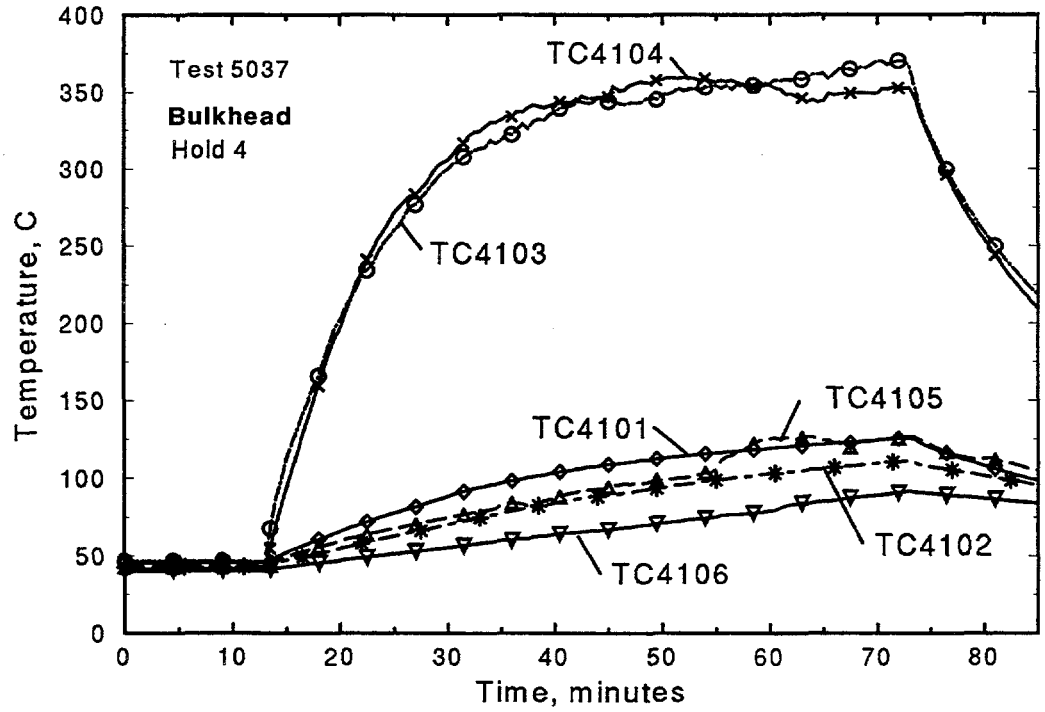

Figure A.5: Thermocouple response of Hold 4 Bulkhead

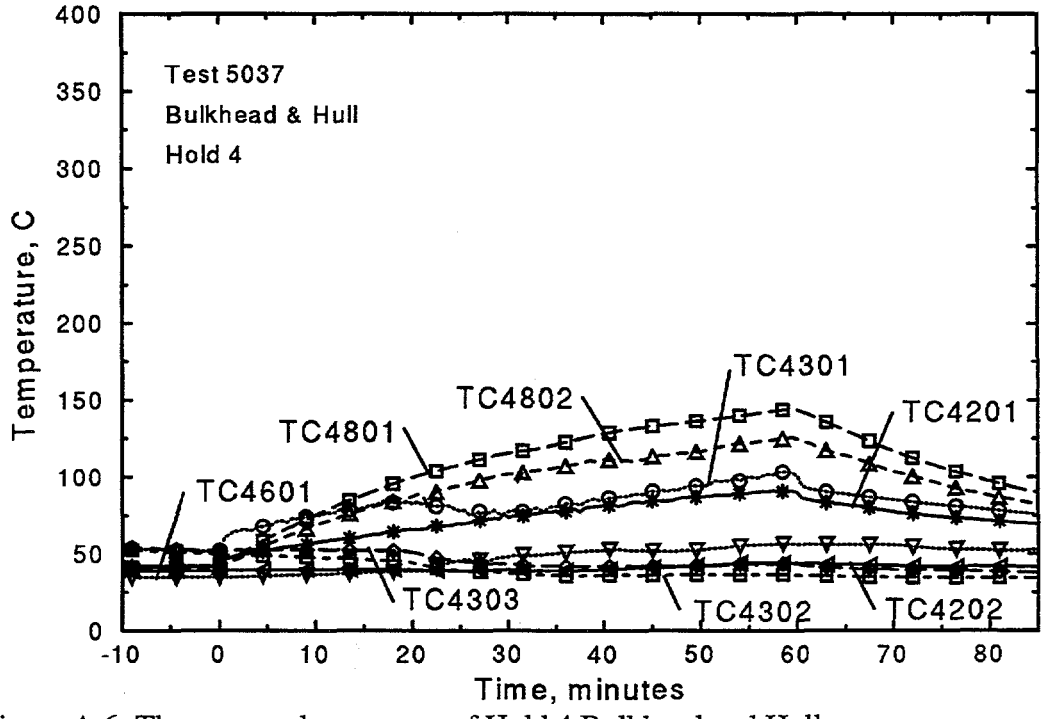

Figure A.6: Thermocouple response of Hold 4 Bulkhead and Hull

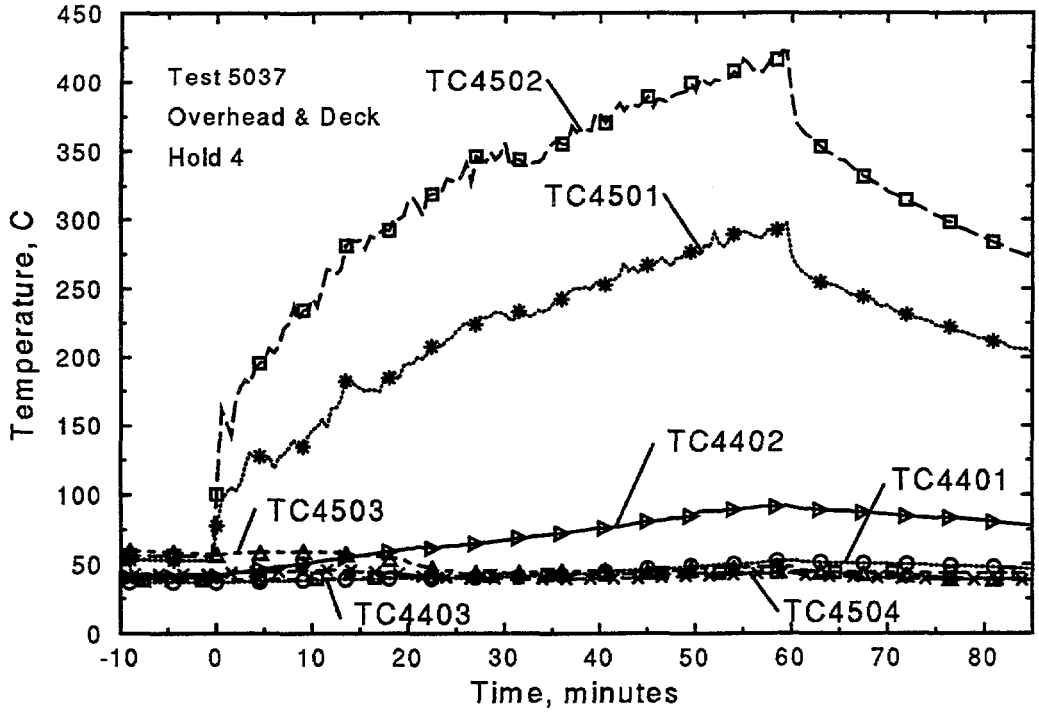

Figure A.7: Thermocouple response of Hold 4 Overhead and Deck

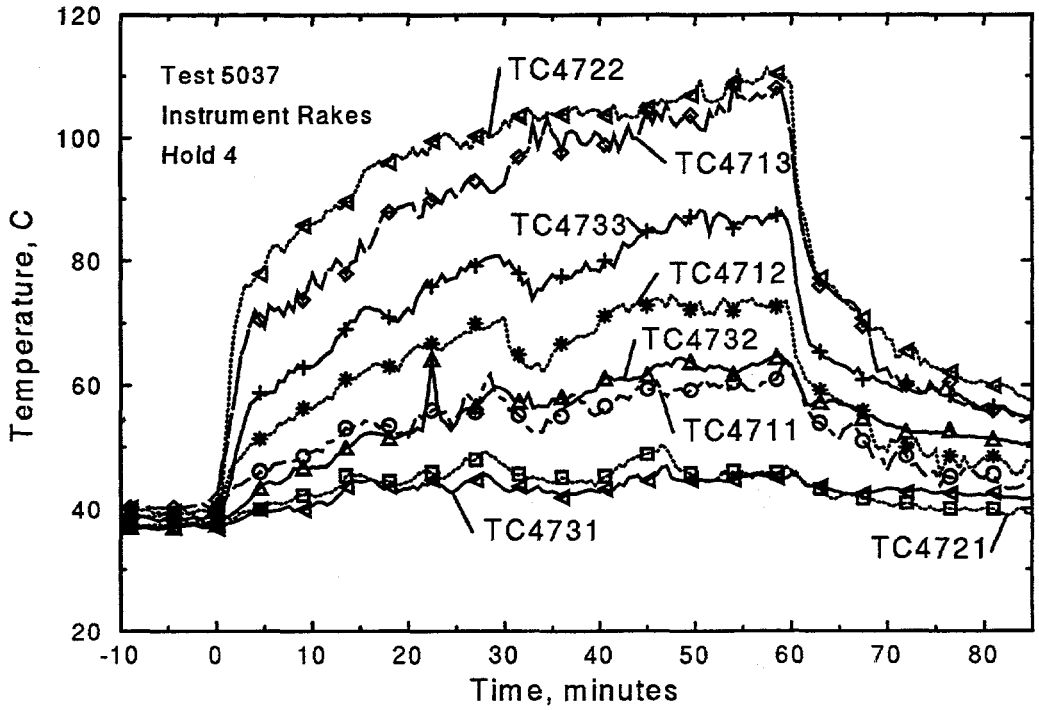

Figure A.8: Thermocouple response of Hold 4 Instrument Rakes

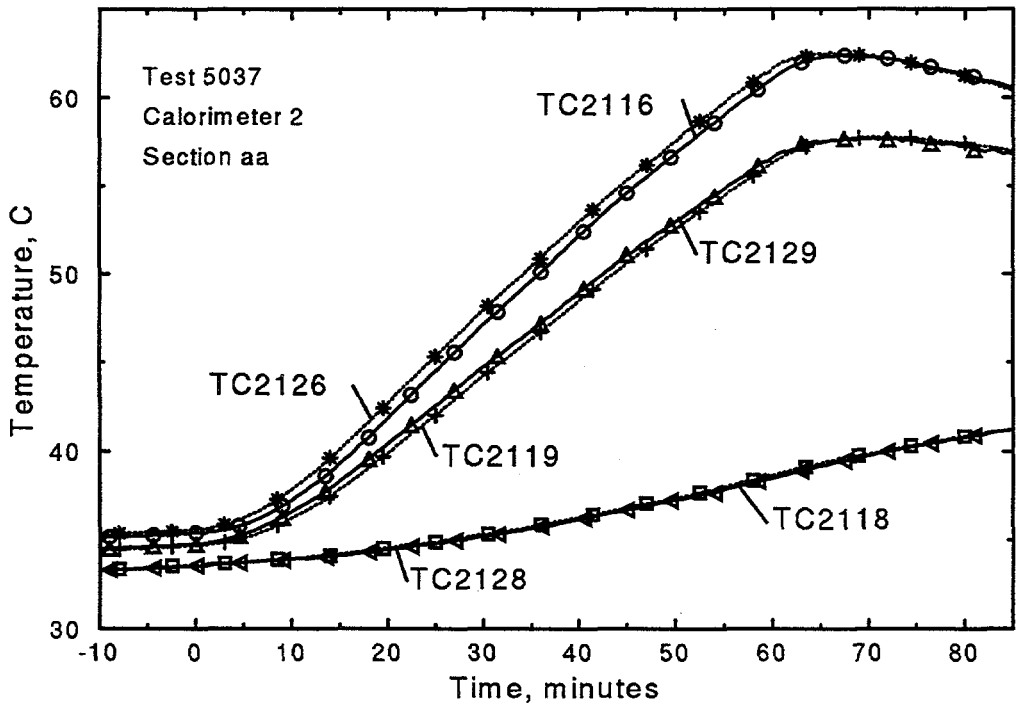

Figure A.9: Thermocouple response of Calorimeter 2, section aa

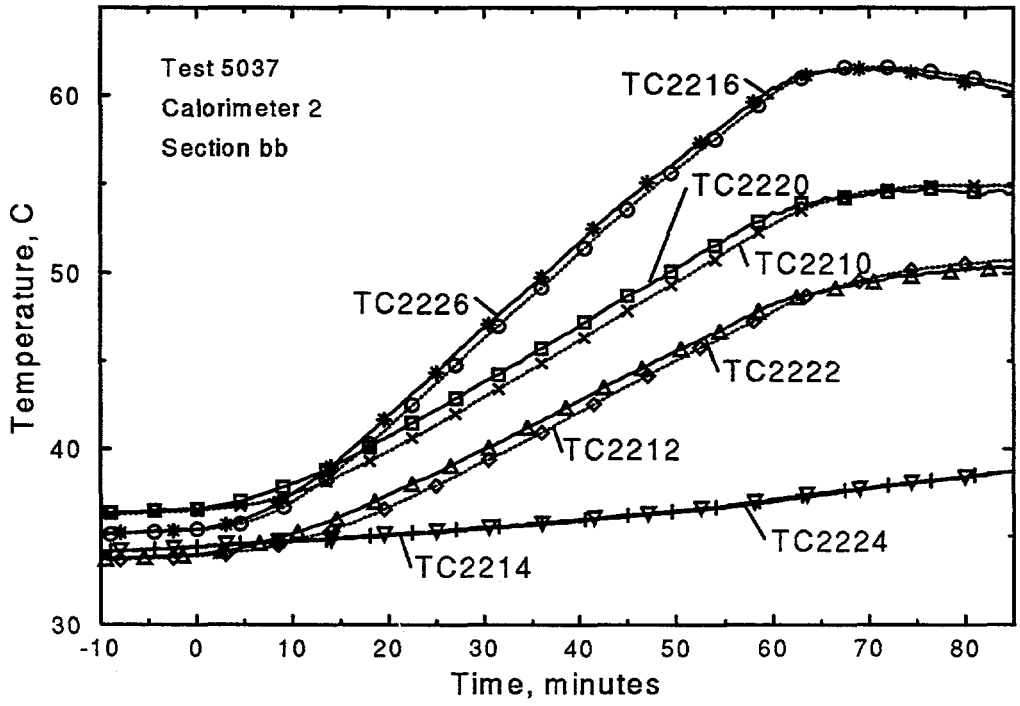

Figure A.10: Thermocouple response of Calorimeter 2, section bb

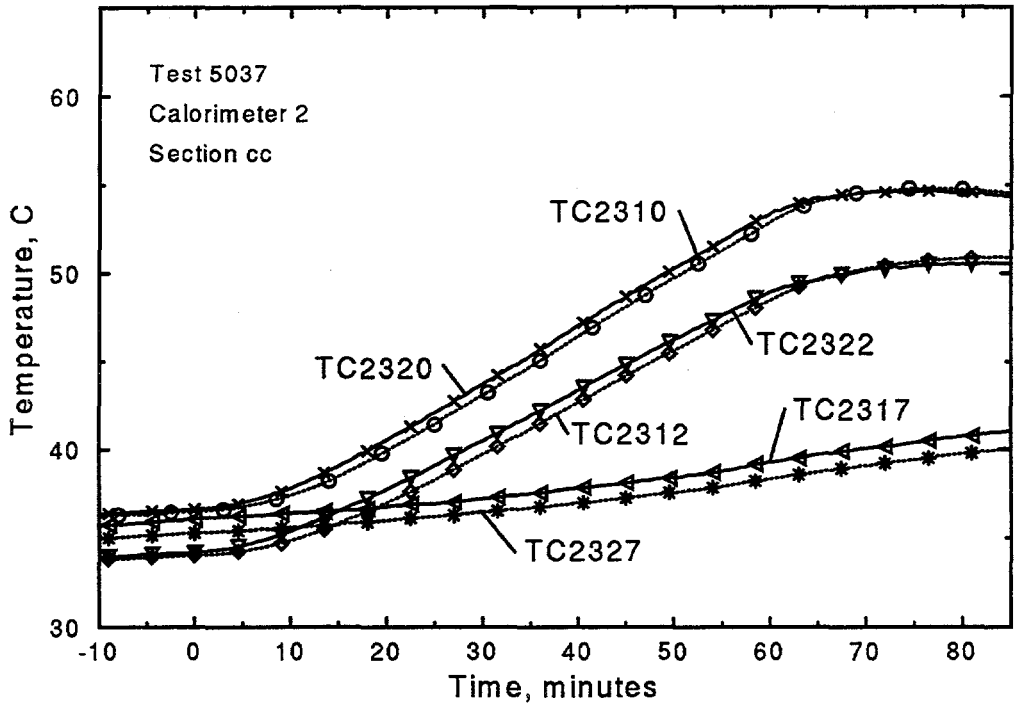

Figure A.11: Thermocouple response of Calorimeter 2, section cc

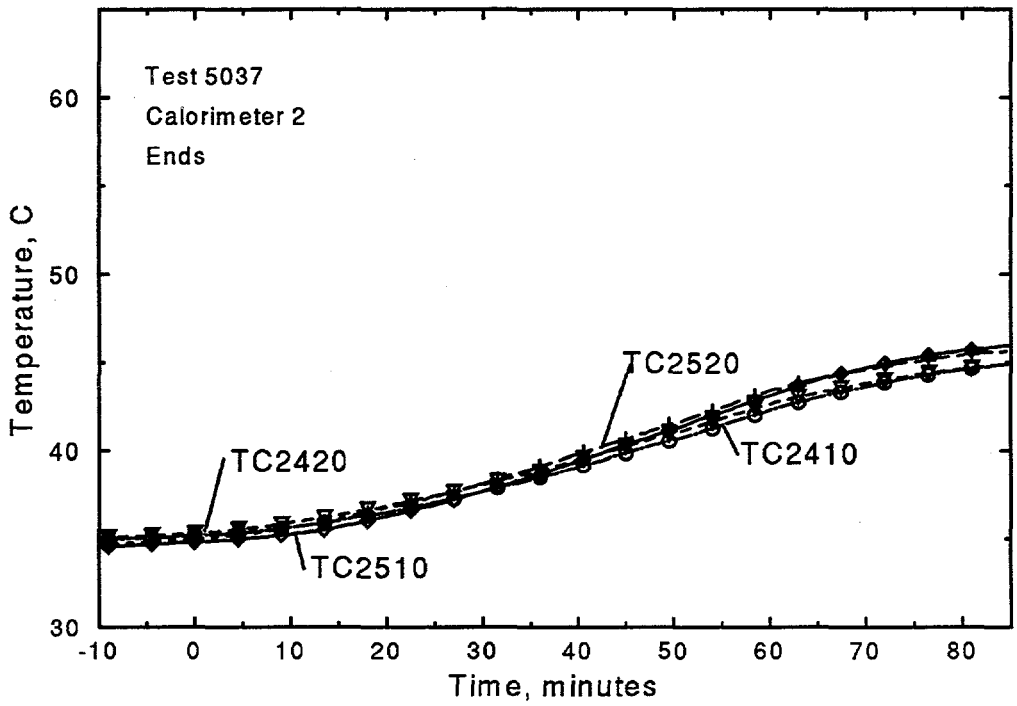

Figure A.12: Thermocouple response of Calorimeter 2, ends

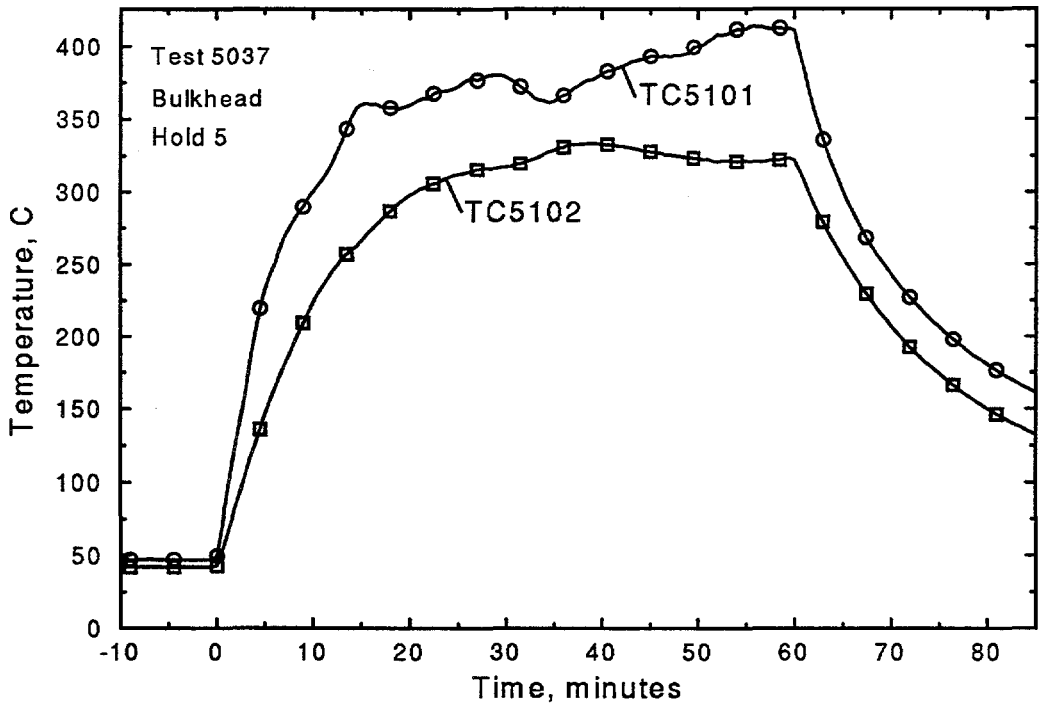

Figure A.13: Thermocouple response of Hold 5 Bulkhead

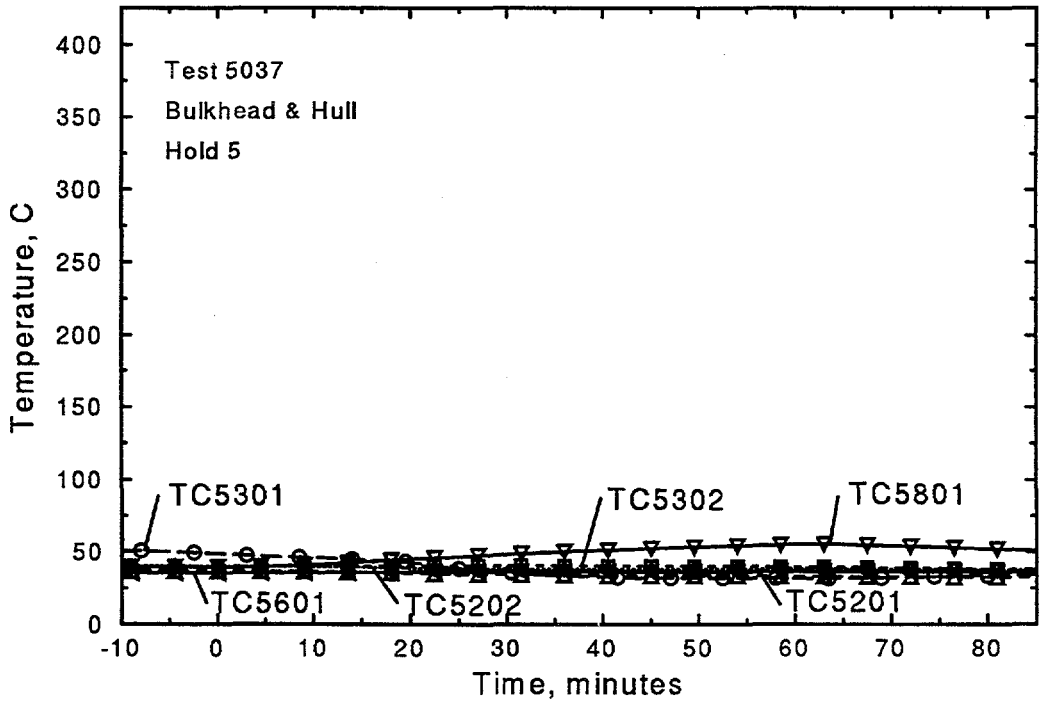

Figure A.14: Thermocouple response of Hold 5 Bulkhead and Hull

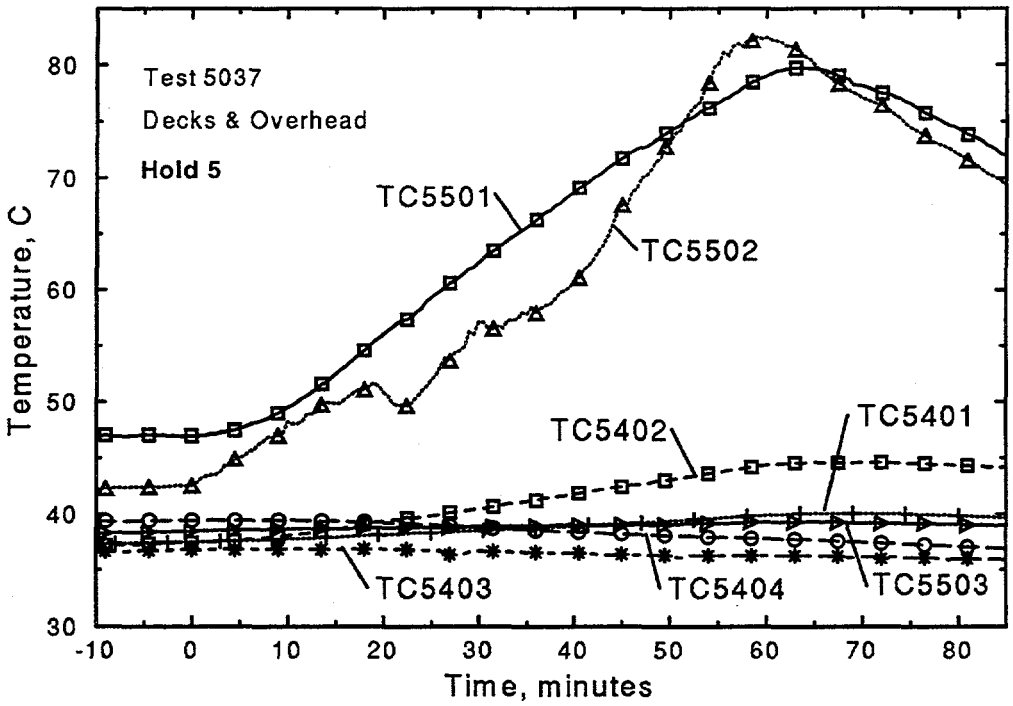

Figure A.15: Thermocouple response of Hold 5 Overhead and Deck

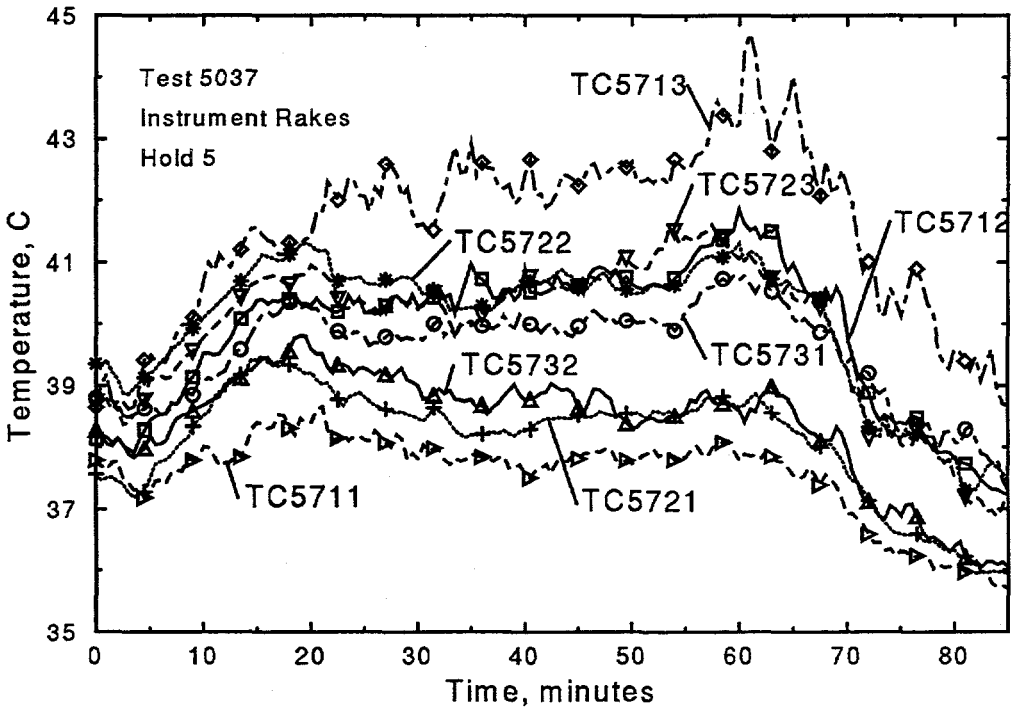

Figure A.16: Thermocouple response of Hold 5 Instrument Rakes

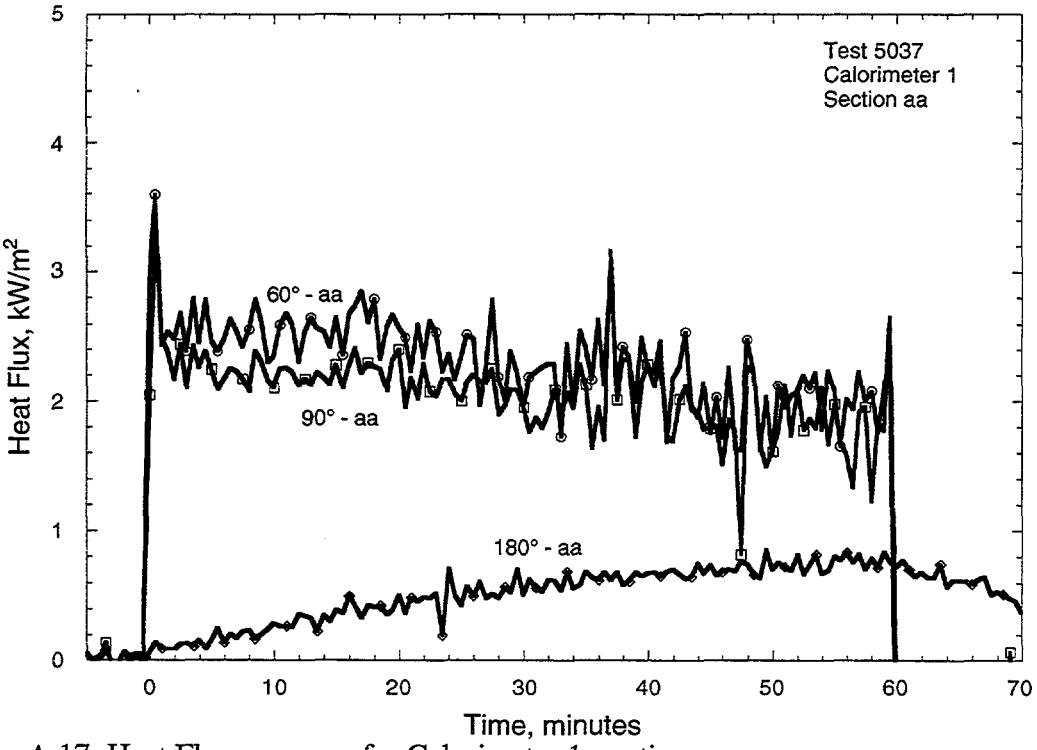

Figure A.17: Heat Flux response for Calorimeter 1, section aa

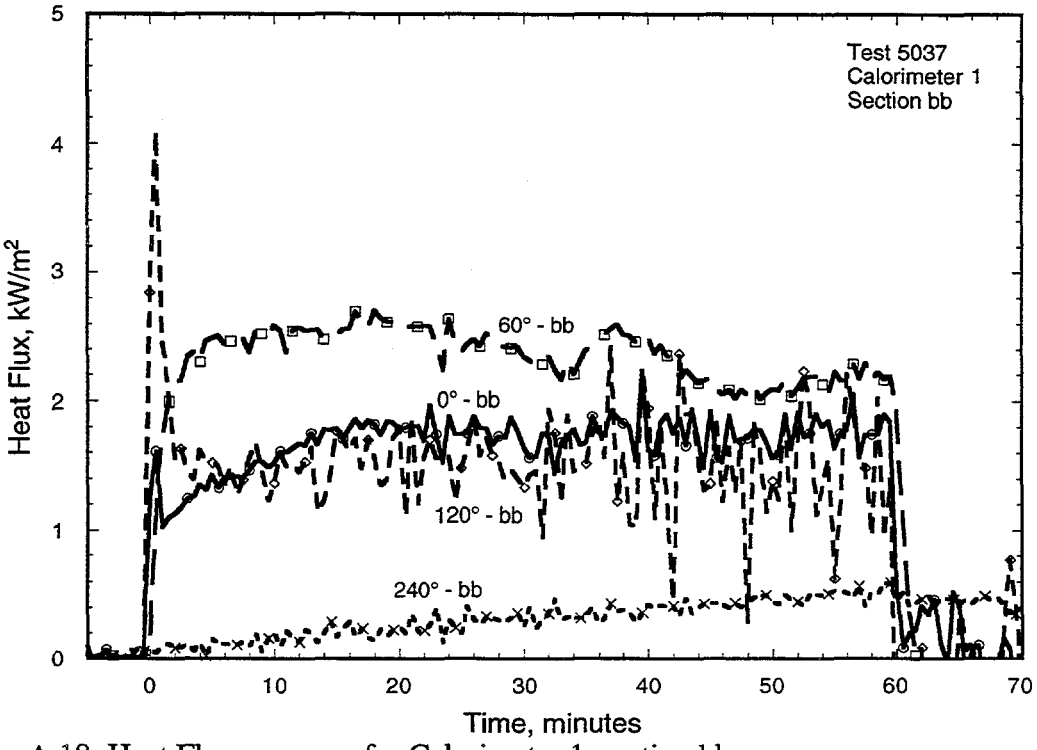

Figure A.18: Heat Flux response for Calorimeter 1, section bb

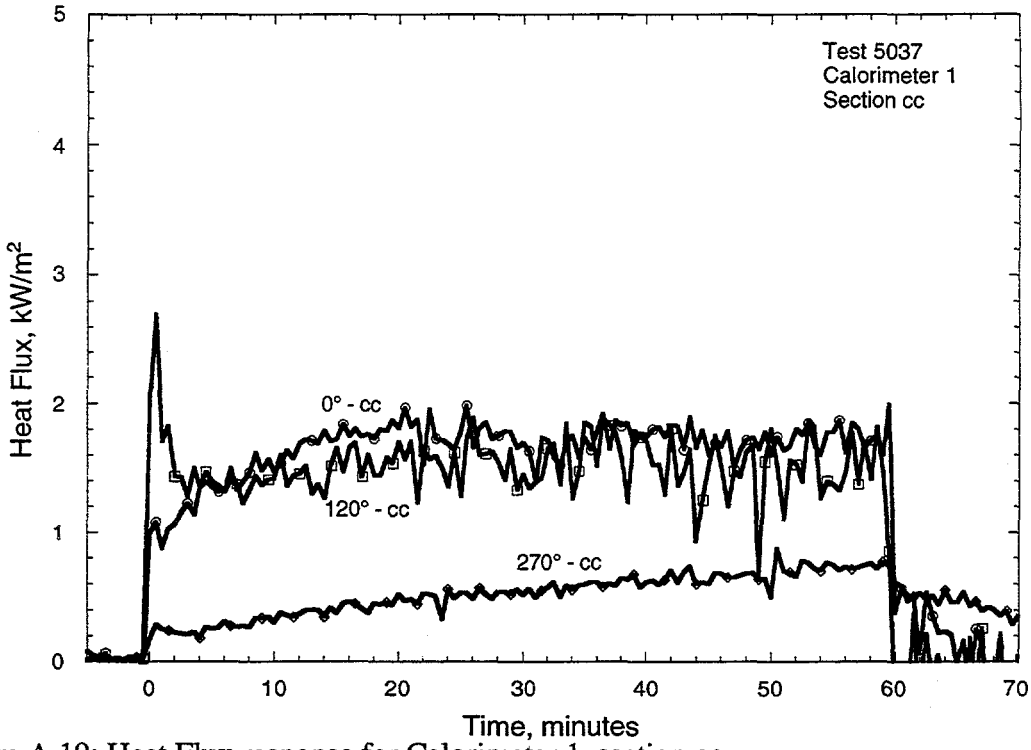

Figure A.19: Heat Flux response for Calorimeter 1, section cc

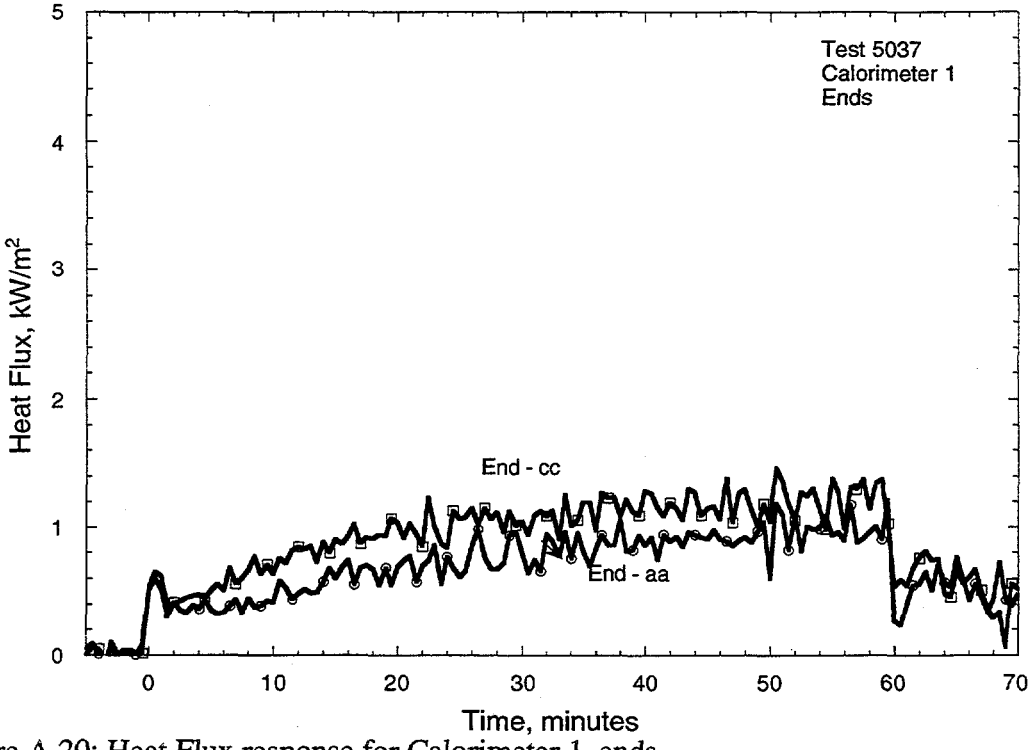

Figure A.20: Heat Flux response for Calorimeter 1, ends

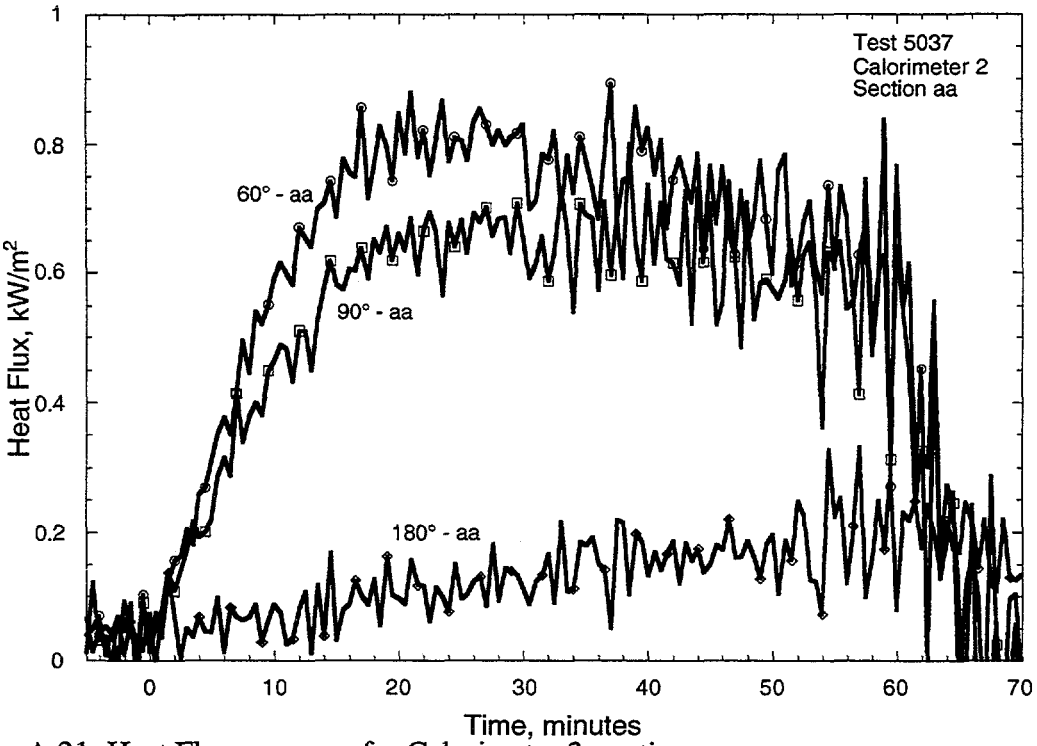

Figure A.21: Heat Flux response for Calorimeter 2, section aa

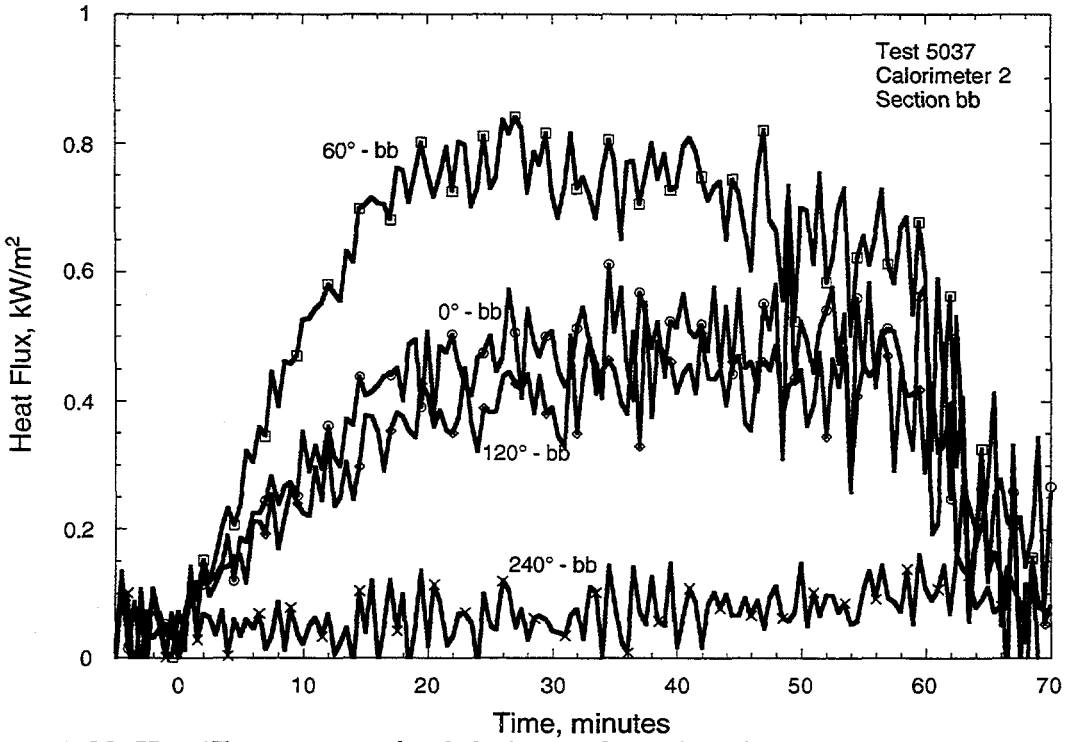

Figure A.22: Heat Flux response for Calorimeter 2, section bb

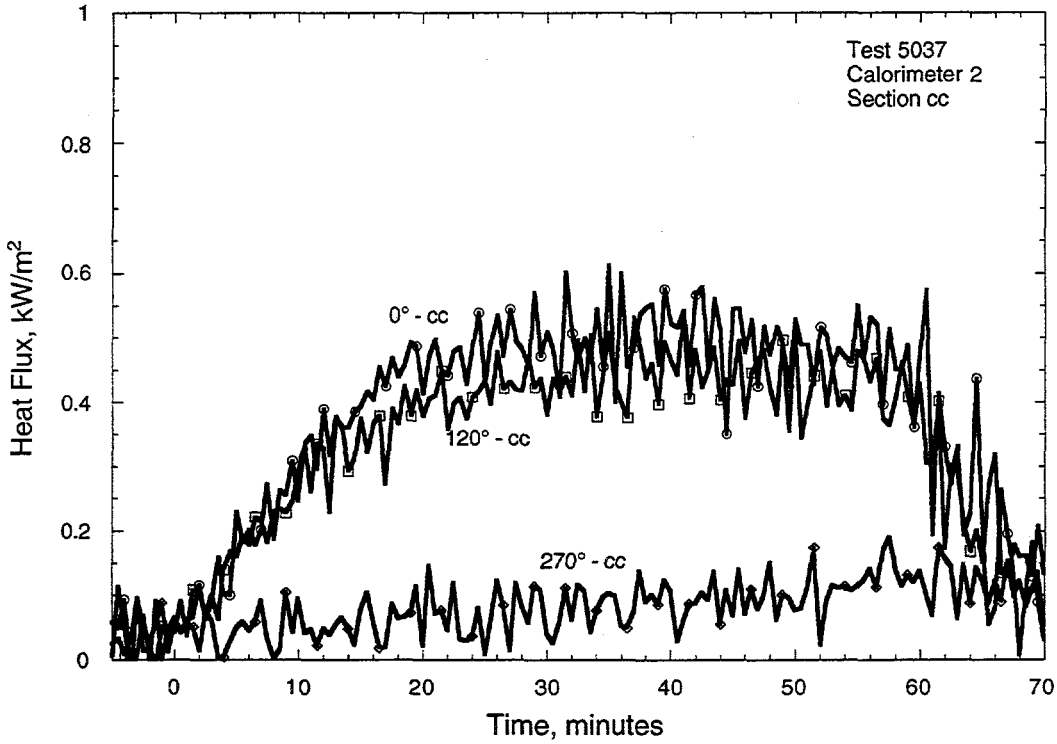

Figure A.23: Heat Flux response for Calorimeter 2, section cc

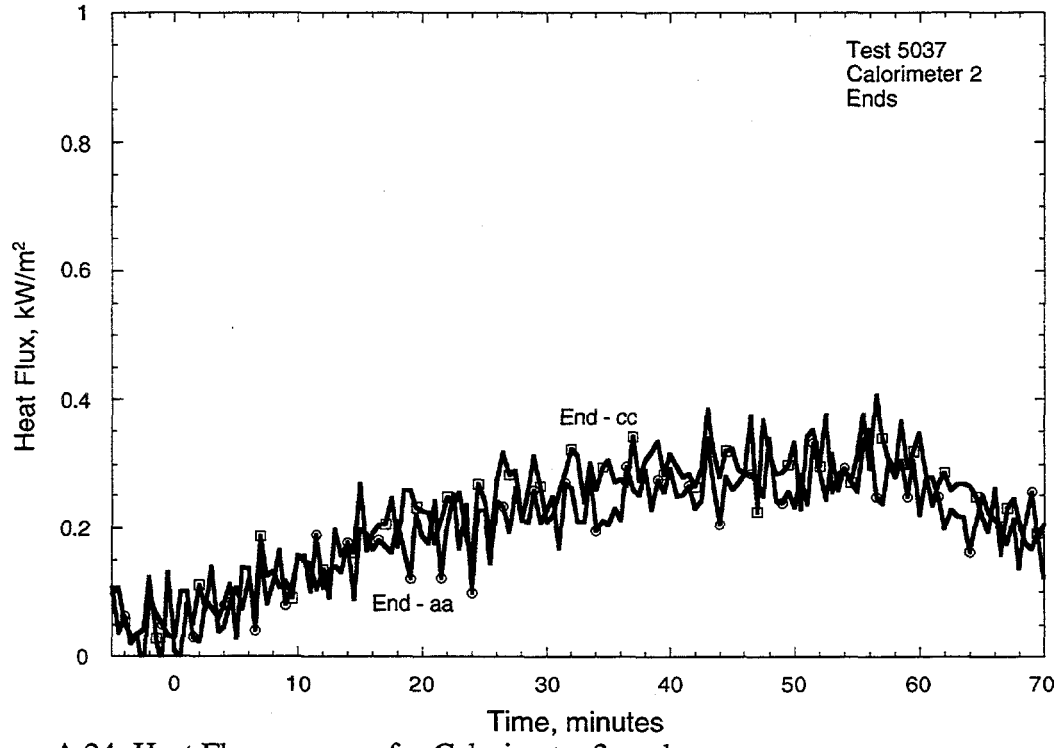

Figure A.24: Heat Flux response for Calorimeter 2, ends

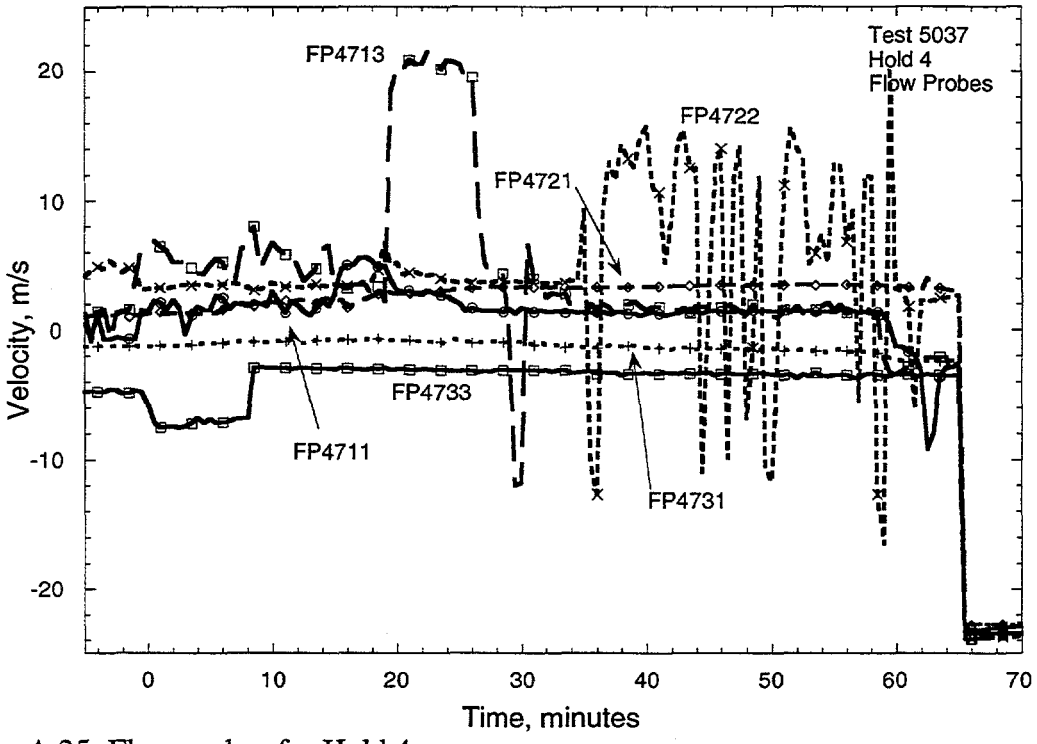

Figure A.25: Flow probes for Hold 4

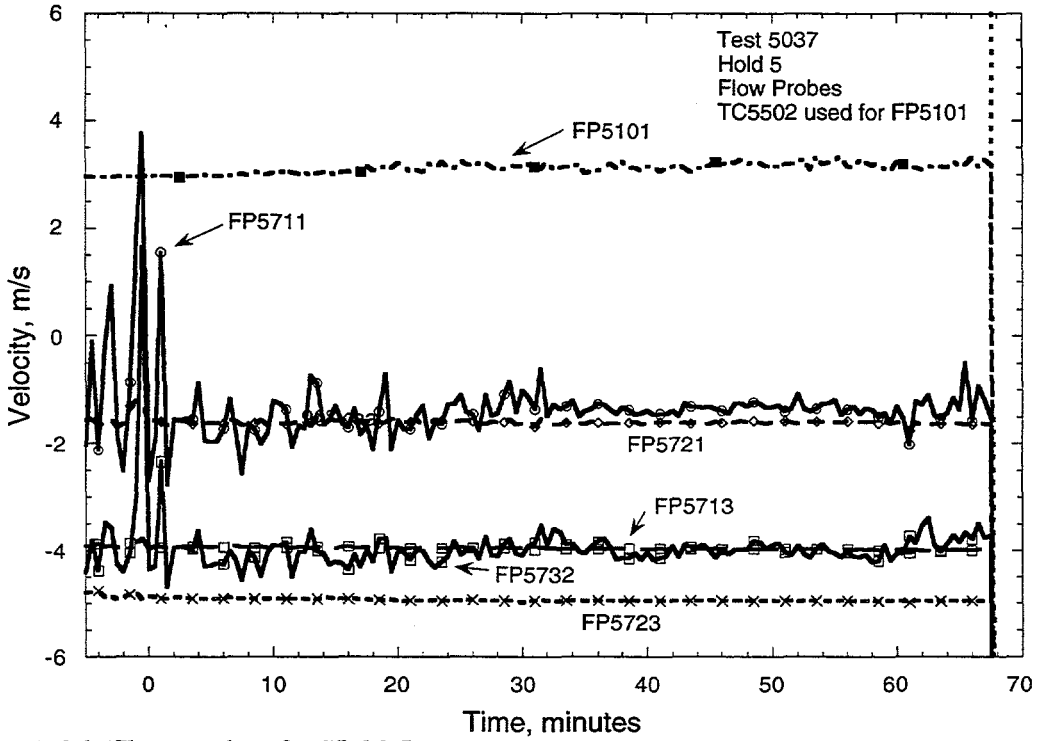

Figure A.26: Flow probes for Hold 5

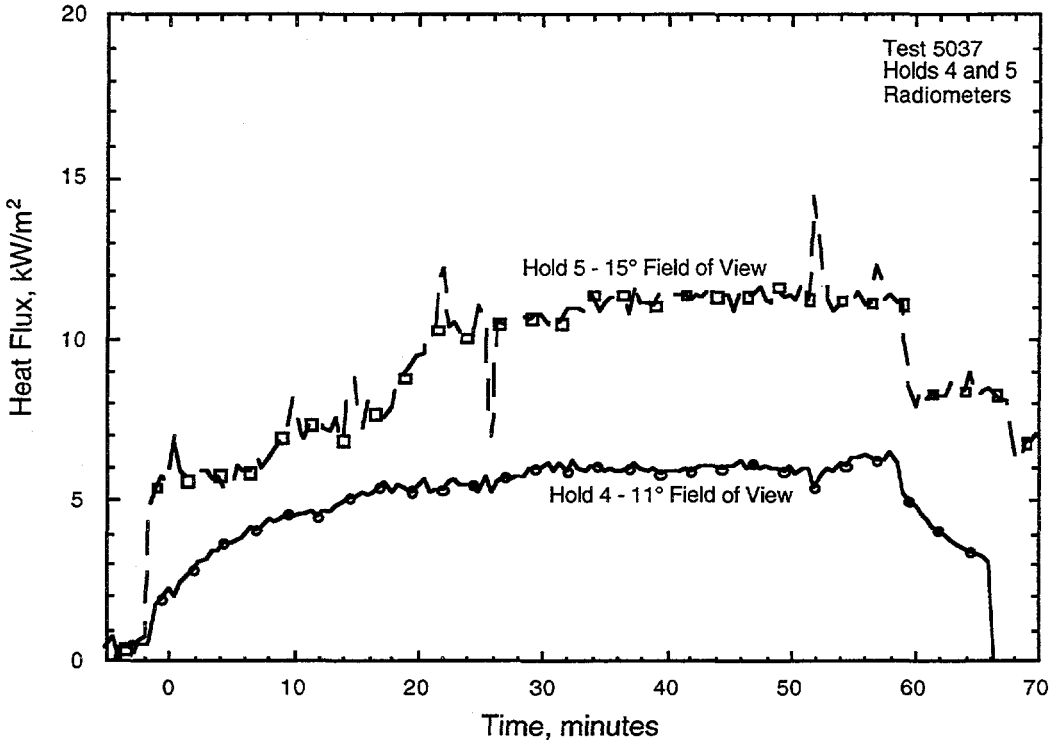

Figure A.27: Holds 4 & 5 Radiation Plot

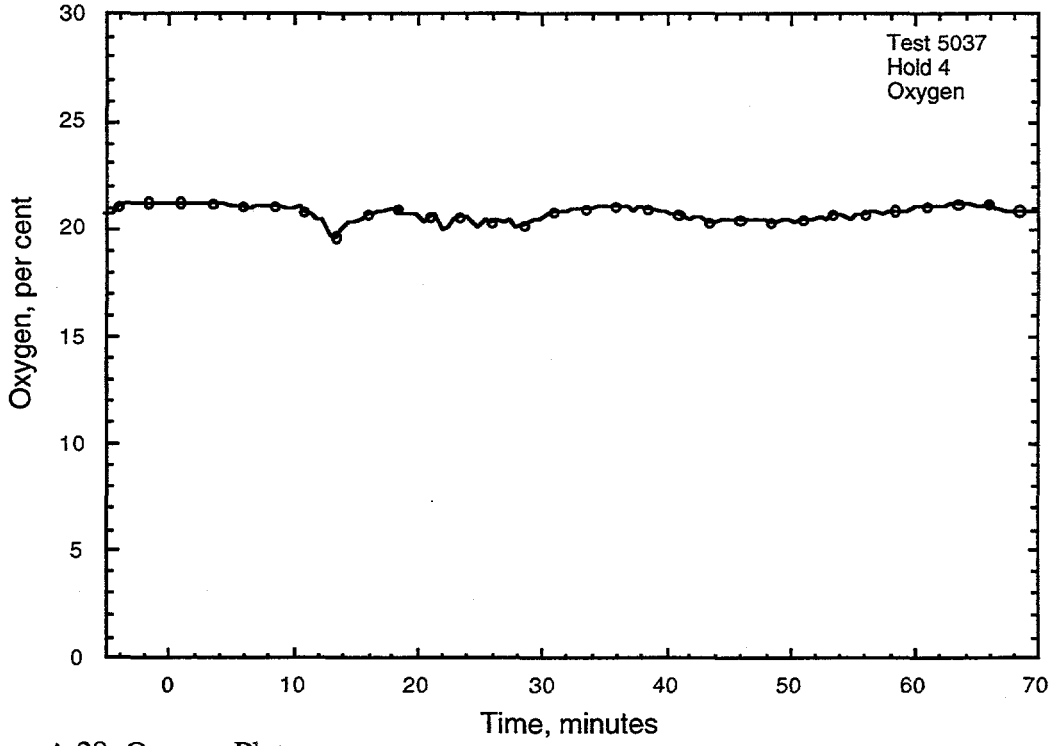

Figure A.28: Oxygen Plot

Appendix B
Test 5040
Wood Crib Fire Test with Heptane Accelerant

conducted 9/14/95
9:13 AM CDT

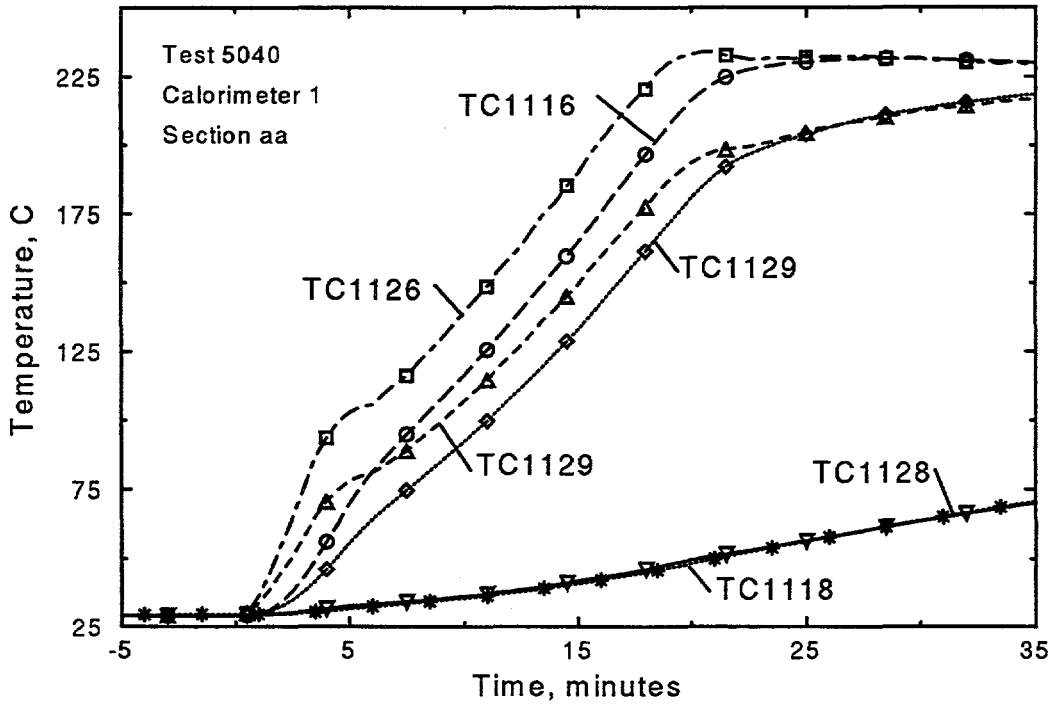

Figure B.1: Thermocouple response of Calorimeter 1, Hold 4, section aa

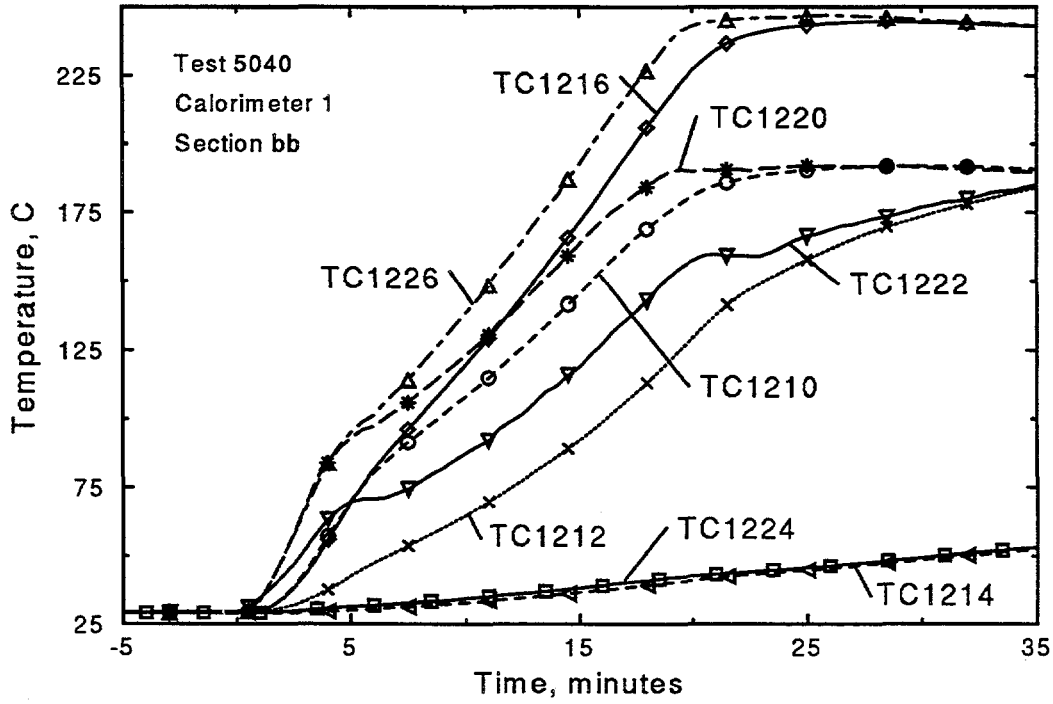

Figure B.2: Thermocouple response of Calorimeter 1, Hold 4, section bb

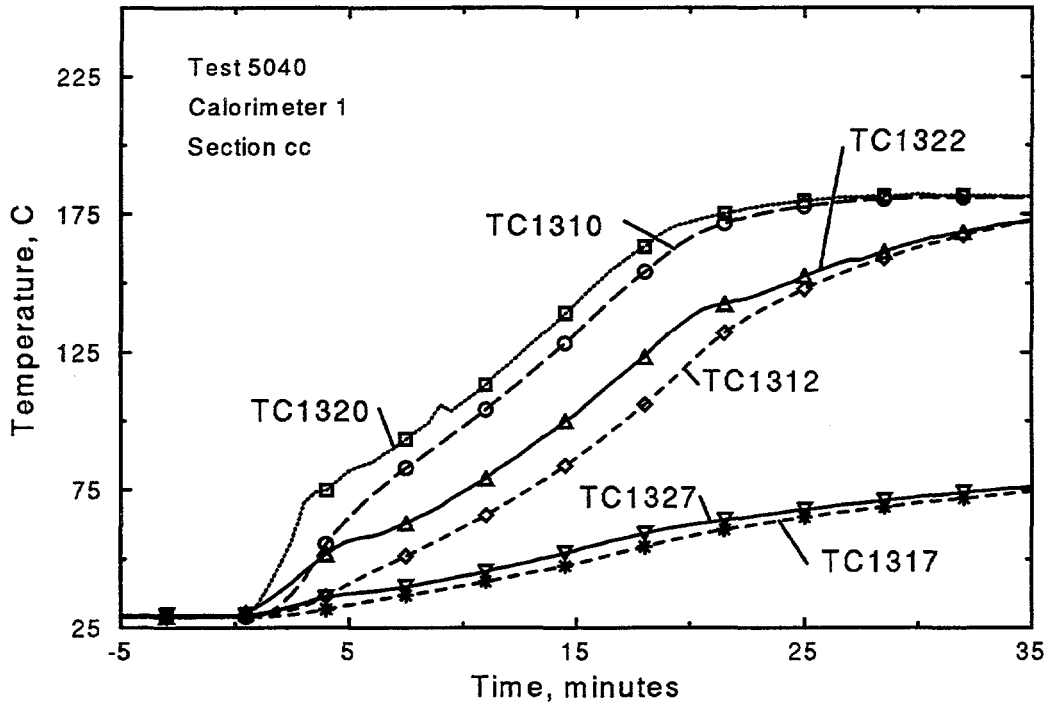

Figure B.3: Thermocouple response of Calorimeter 1, Hold 4, section cc

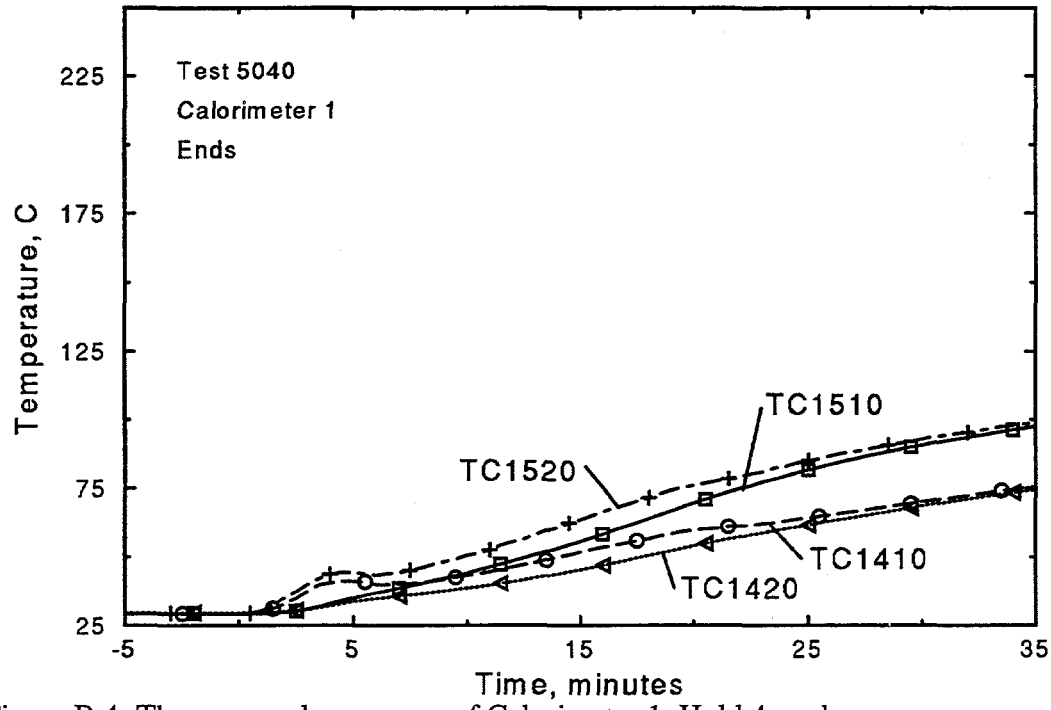

Figure B.4: Thermocouple response of Calorimeter 1, Hold 4, ends

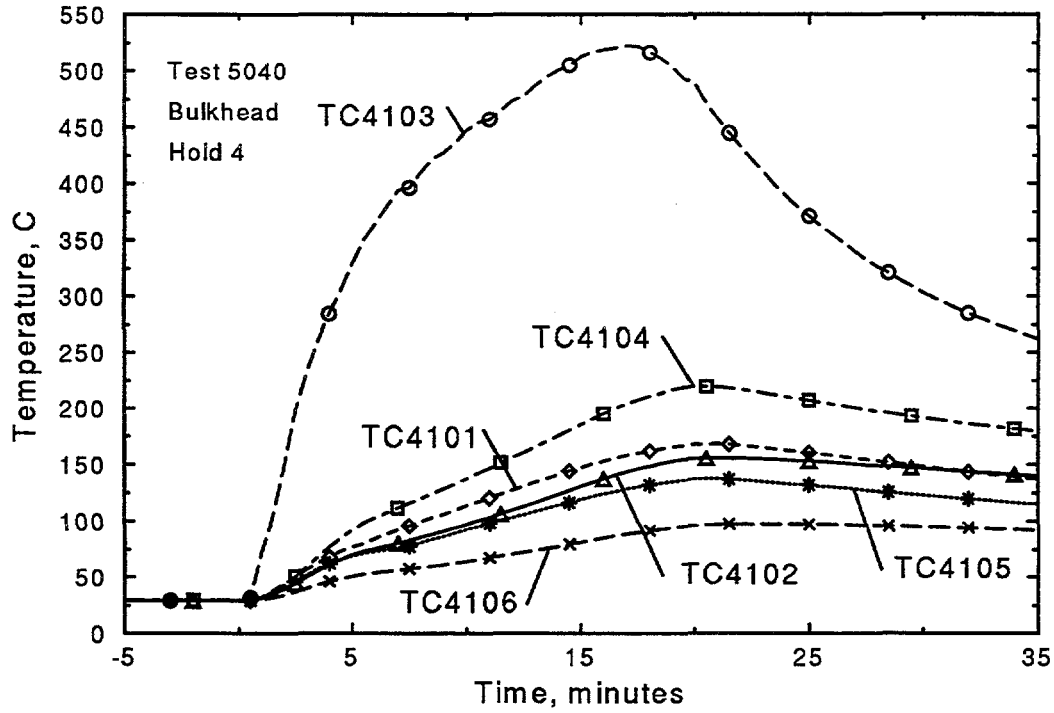

Figure B.5: Thermocouple response of Hold 4 Bulkhead

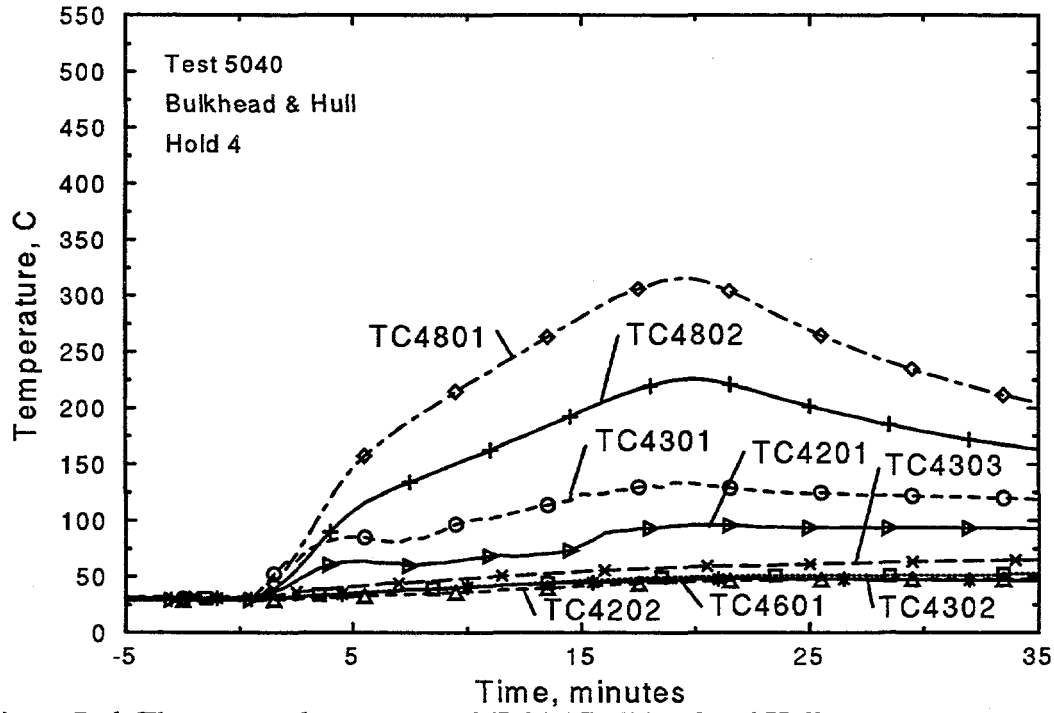

Figure B.6: Thermocouple response of Hold 4 Bulkhead and Hull

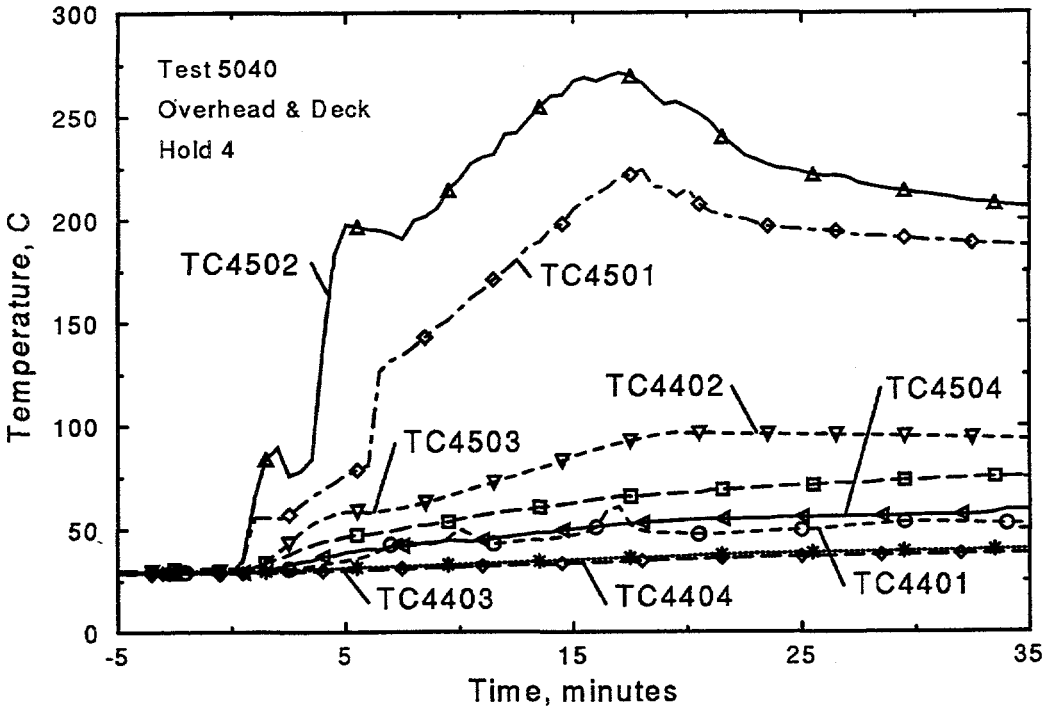

Figure B.7: Thermocouple response of Hold 4 Overhead and Deck

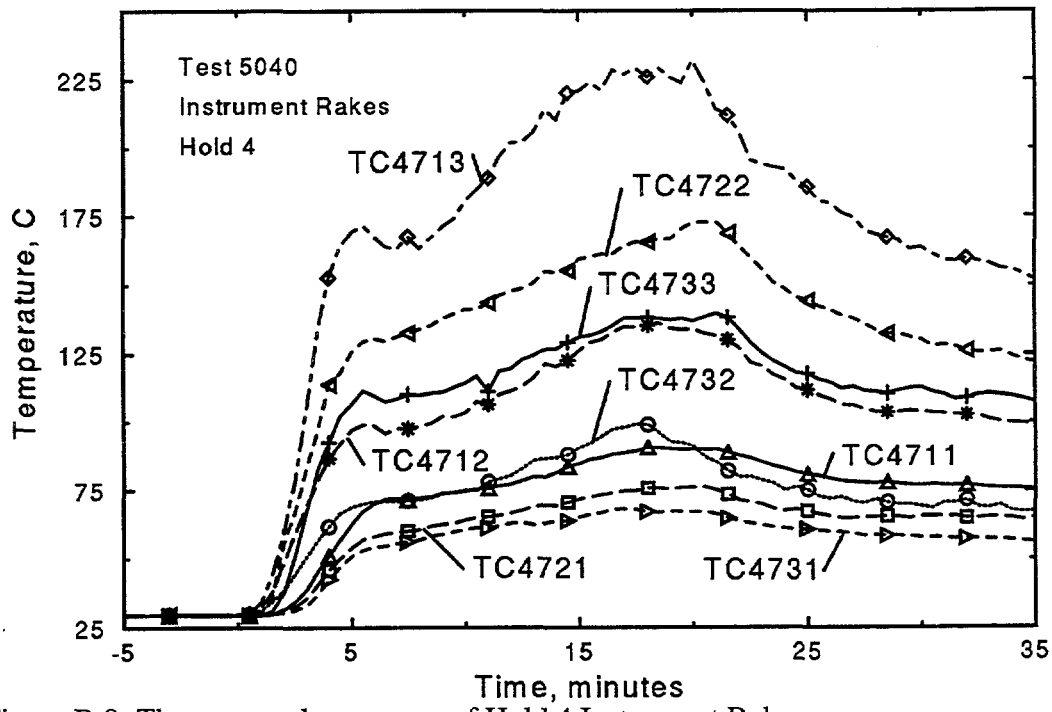

Figure B.8: Thermocouple response of Hold 4 Instrument Rakes

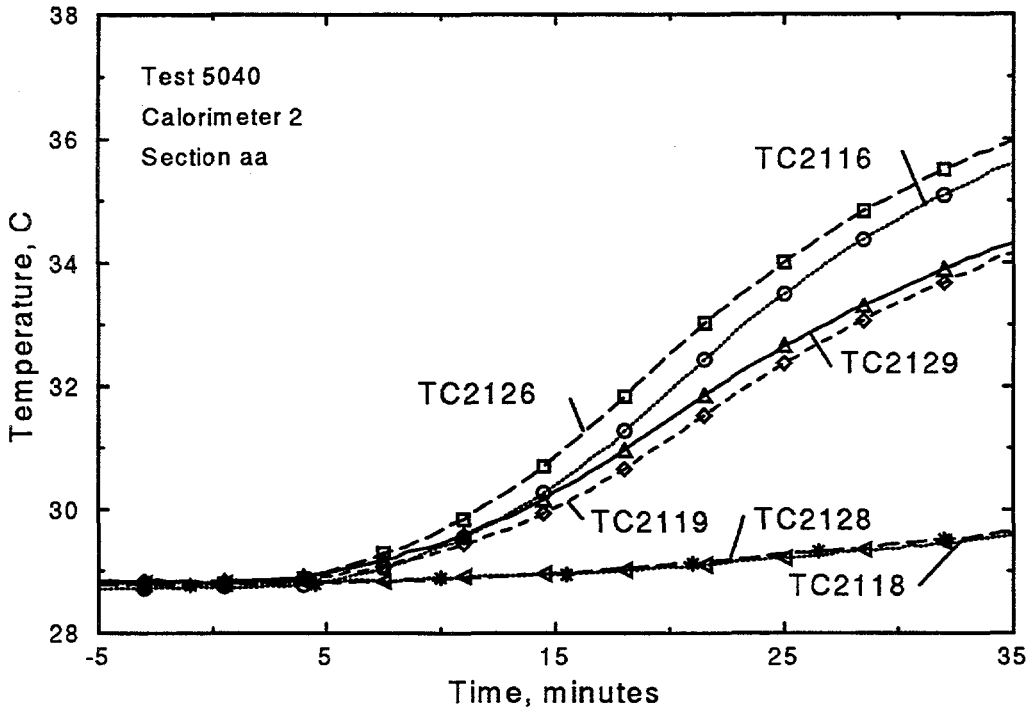

Figure B.9: Thermocouple response of Calorimeter 2, section aa

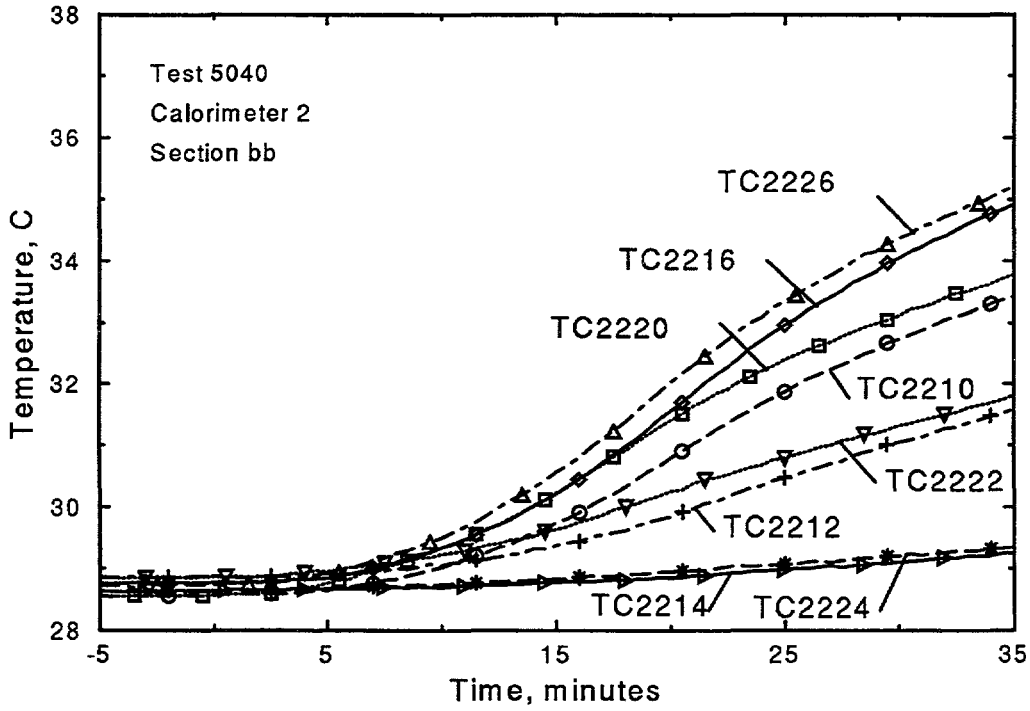

Figure B.10: Thermocouple response of Calorimeter 2, section bb

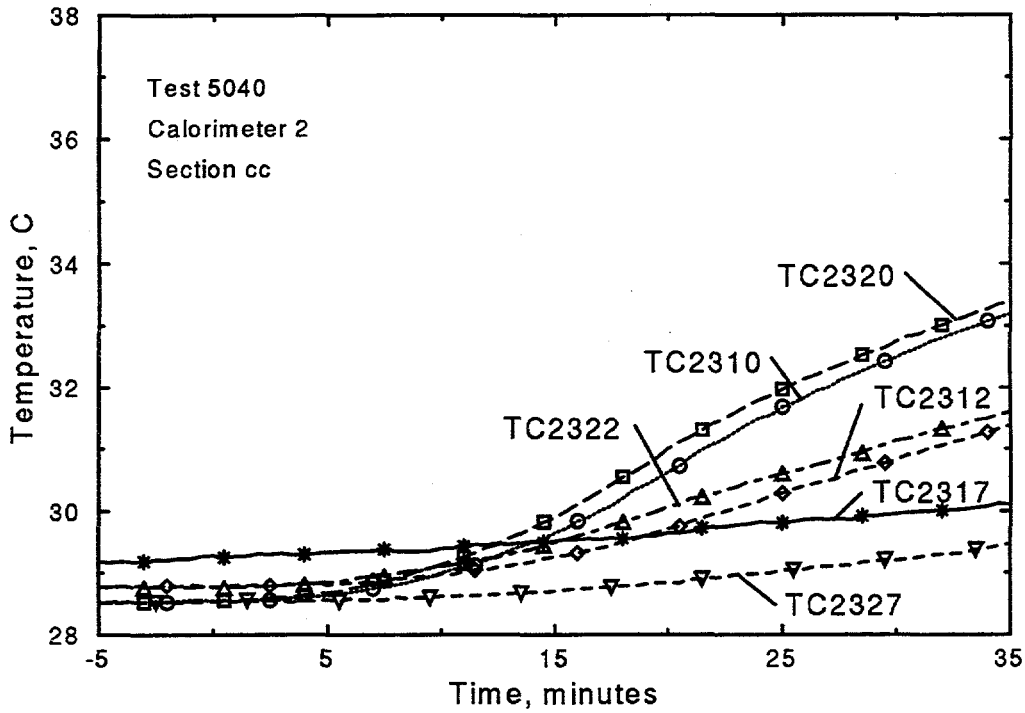

Figure B.11: Thermocouple response of Calorimeter 2, section cc

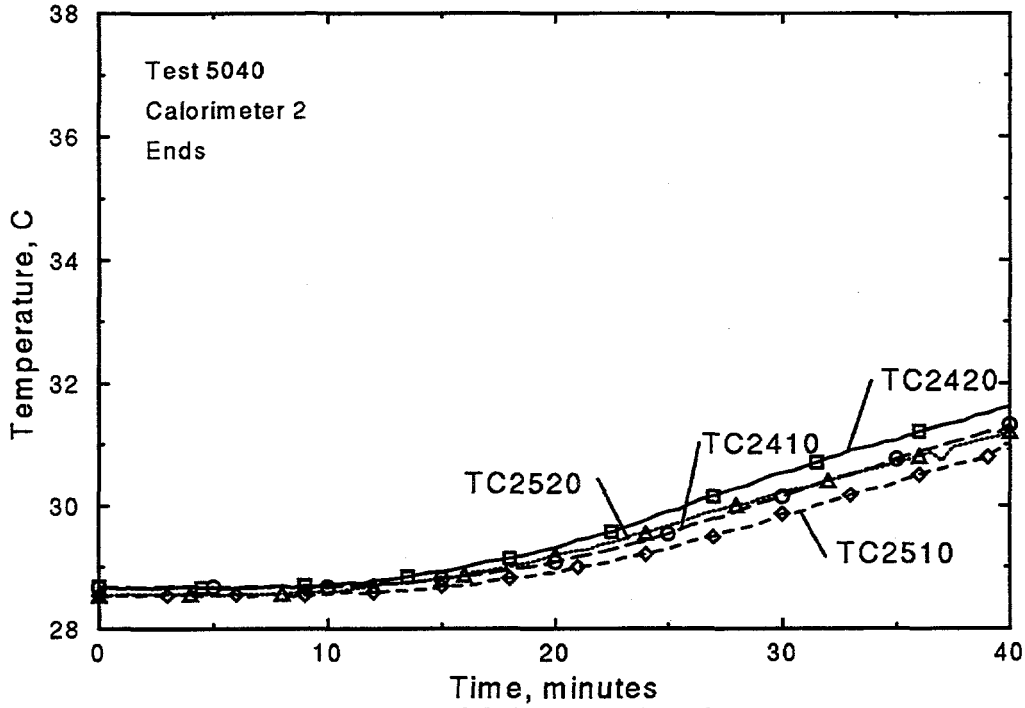

Figure B.12: Thermocouple response of Calorimeter 2, ends

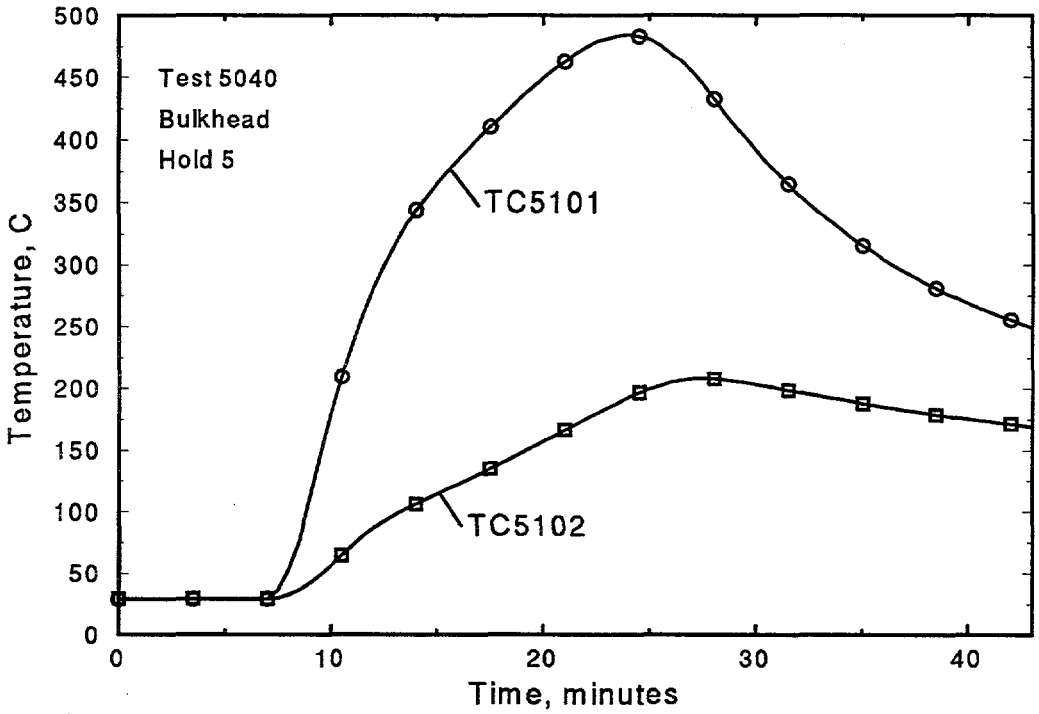

Figure B.13: Thermocouple response of Hold 5 Bulkhead

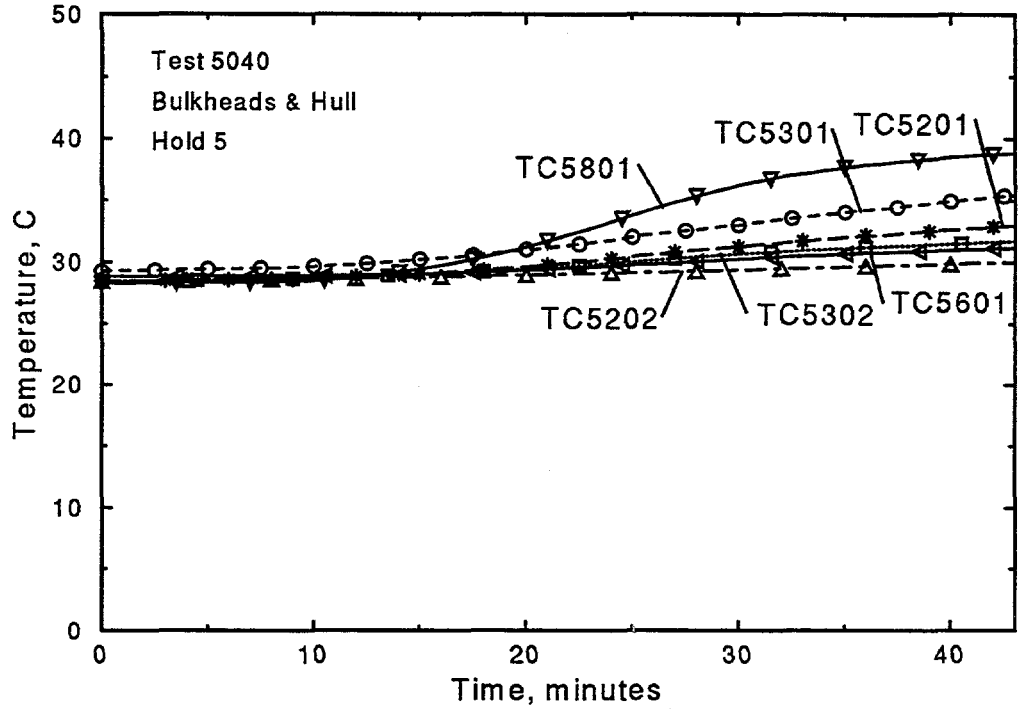

Figure B.14: Thermocouple response of Hold 5 Bulkhead and Hull

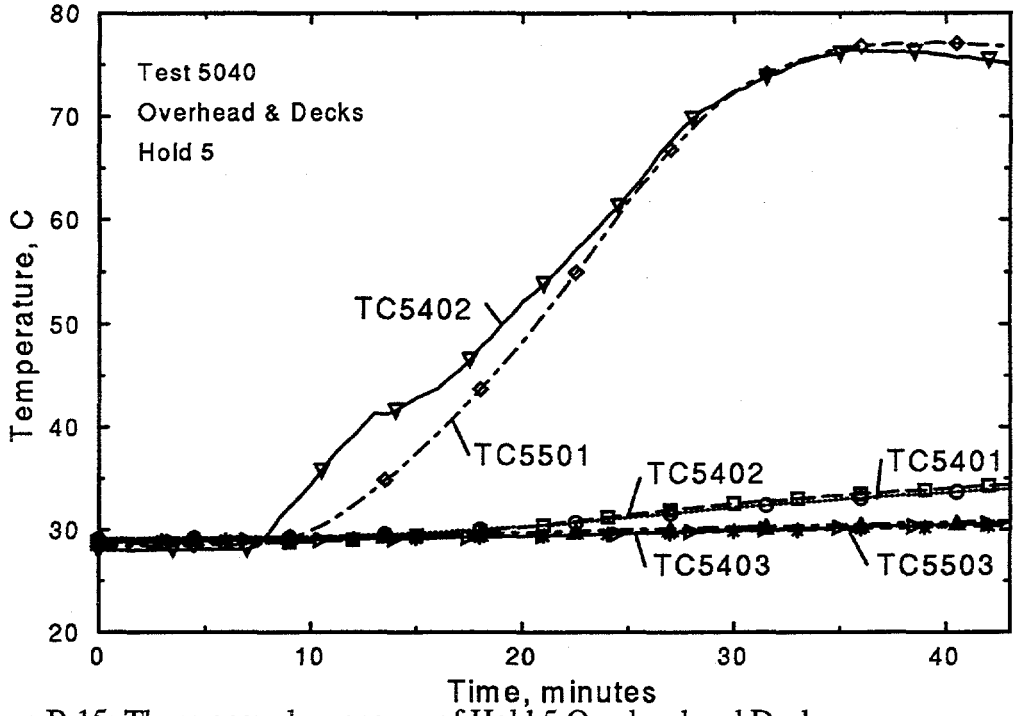

Figure B.15: Thermocouple response of Hold 5 Overhead and Deck

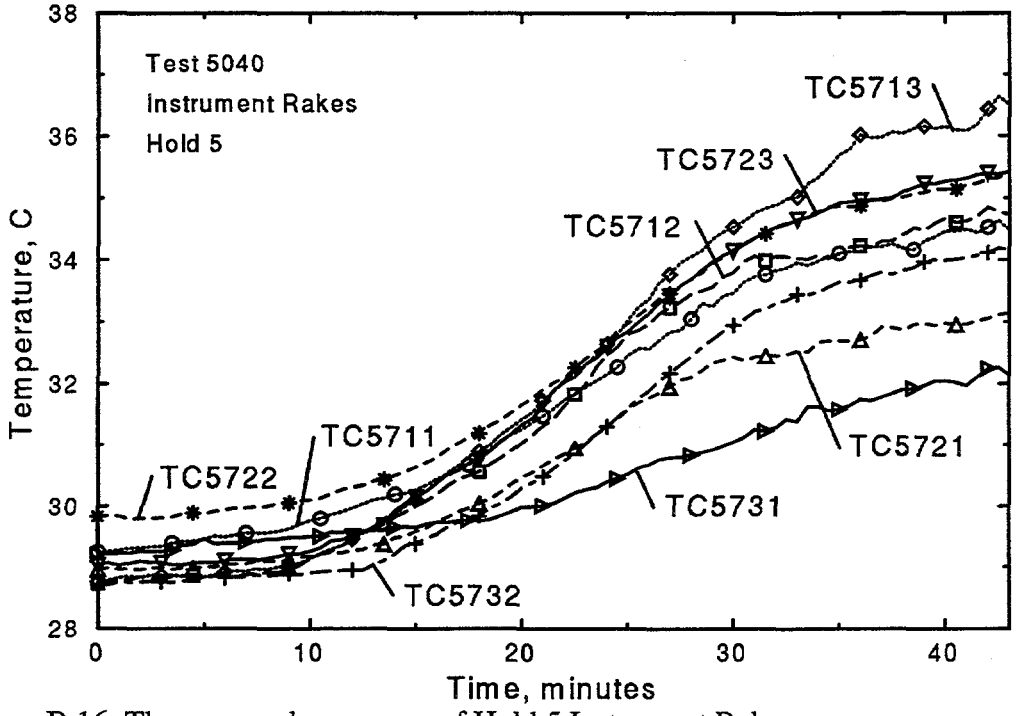

Figure B.16: Thermocouple response of Hold 5 Instrument Rakes

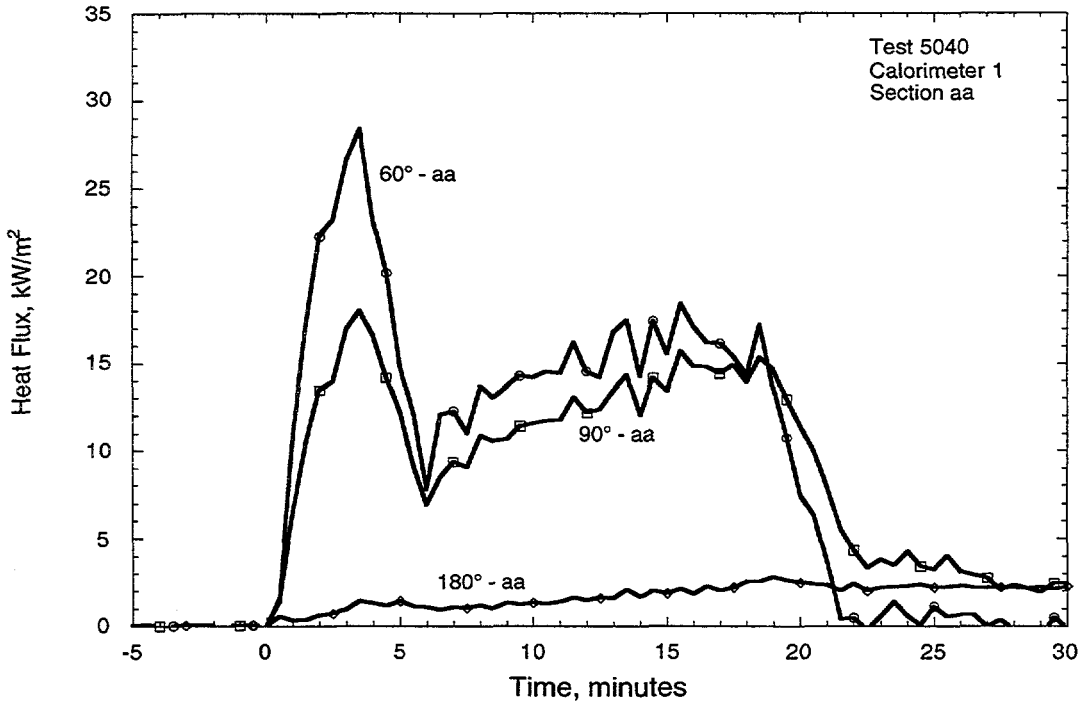

Figure B.17: Heat Flux response for Calorimeter 1, section aa

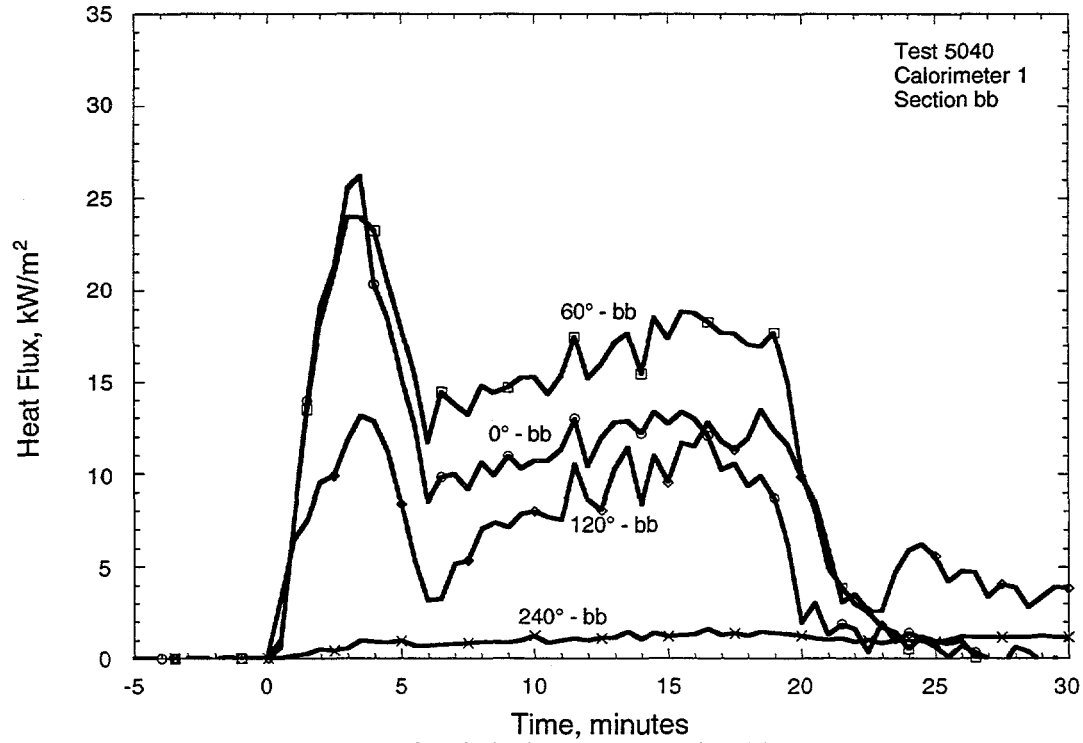

Figure B.18: Heat Flux response for Calorimeter 1, section bb

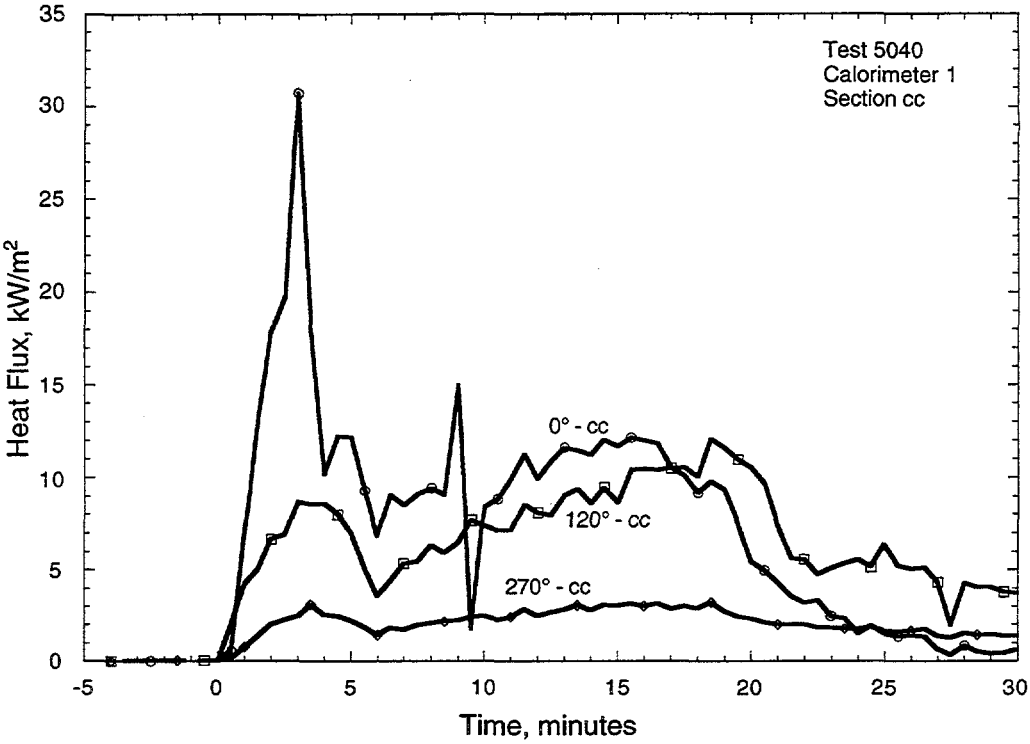

Figure B.19: Heat Flux response for Calorimeter 1, section cc

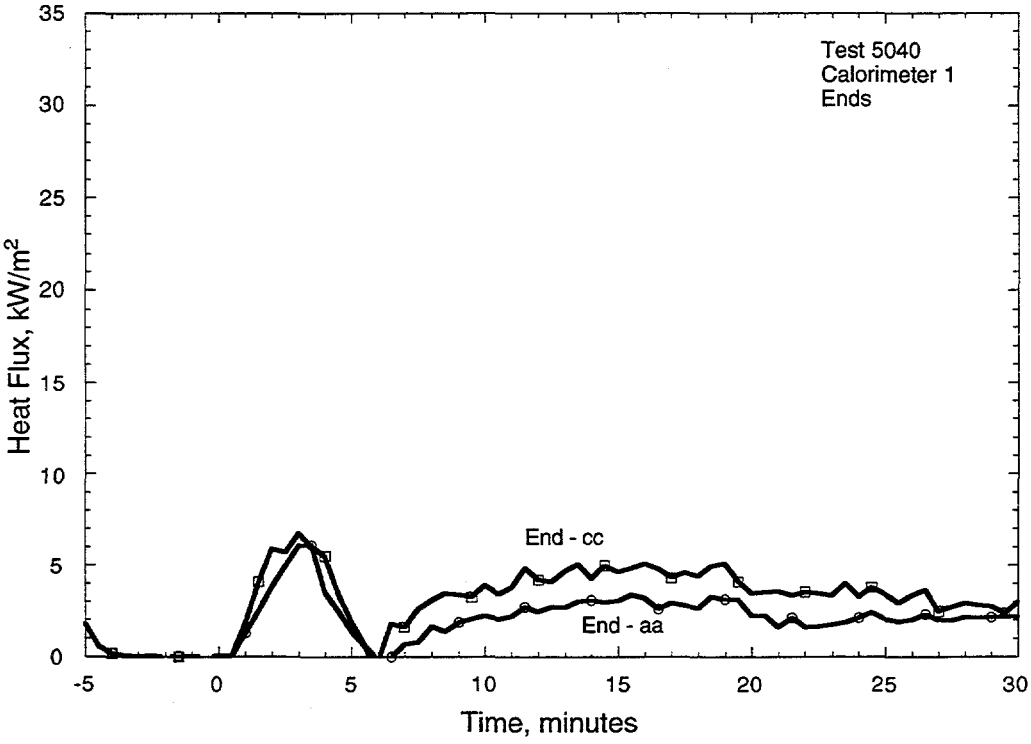

Figure B.20: Heat Flux response for Calorimeter 1, ends

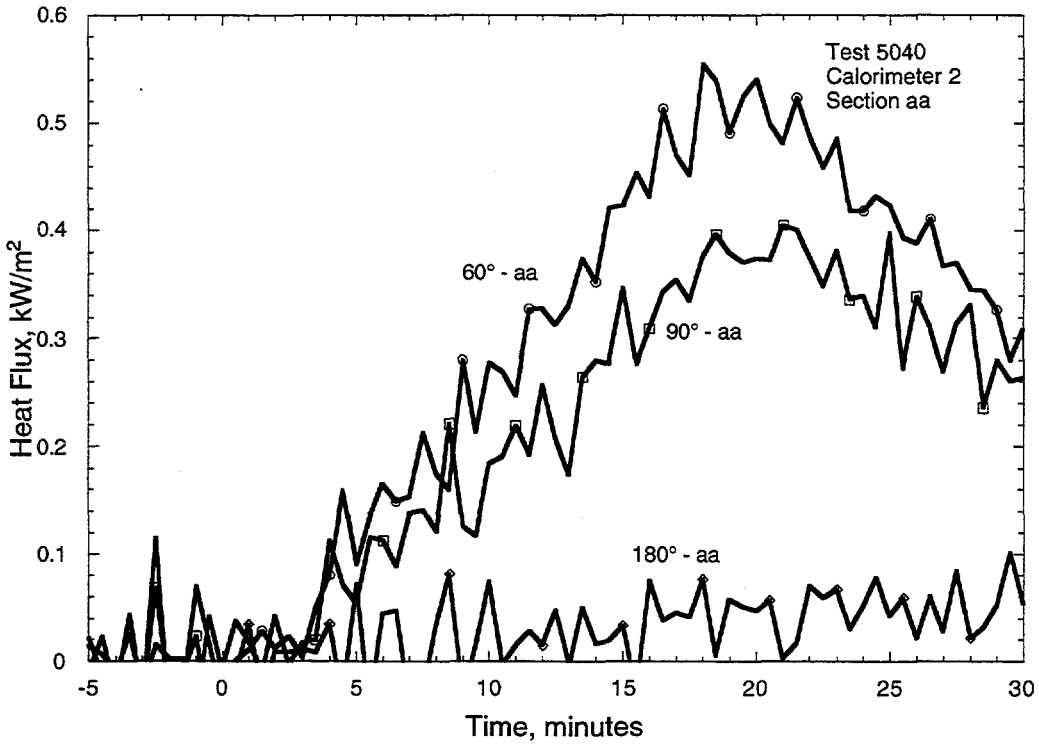

Figure B.21: Heat Flux response for Calorimeter 2, section aa

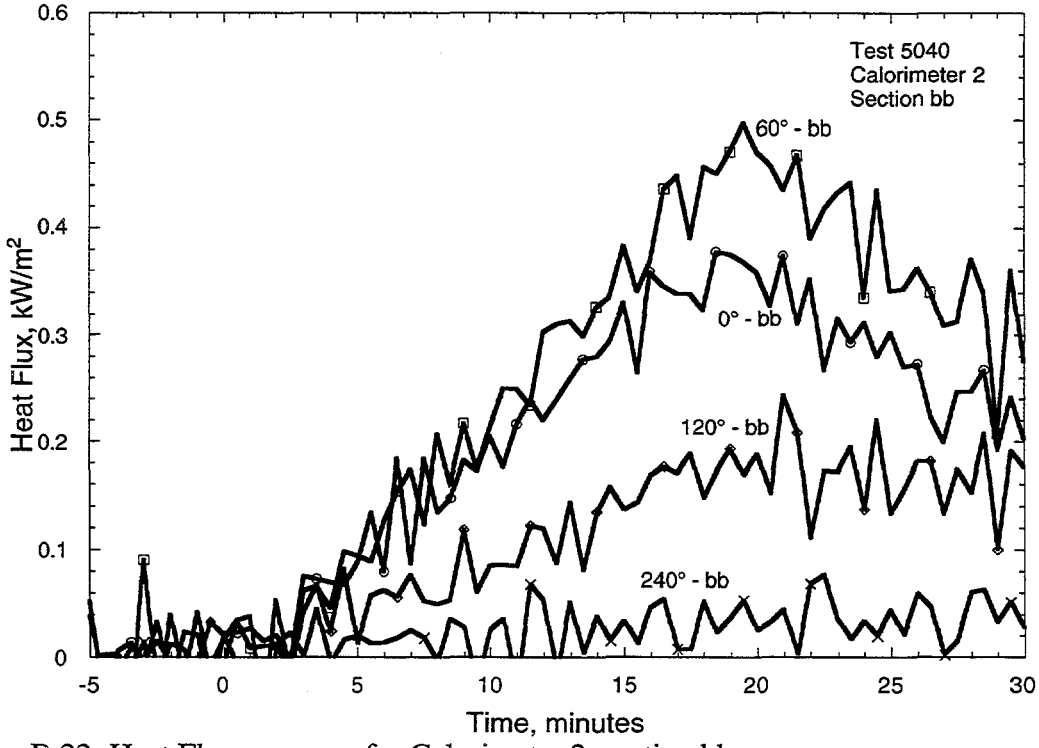

Figure B.22: Heat Flux response for Calorimeter 2, section bb

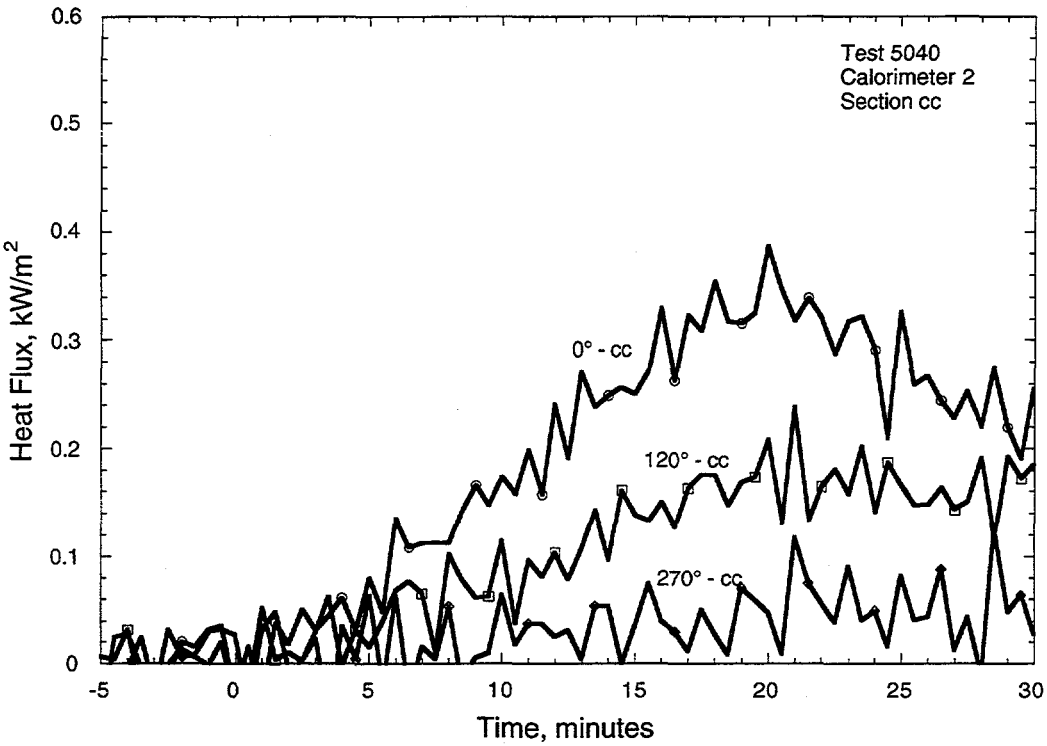

Figure B.23: Heat Flux response for Calorimeter 2, section cc

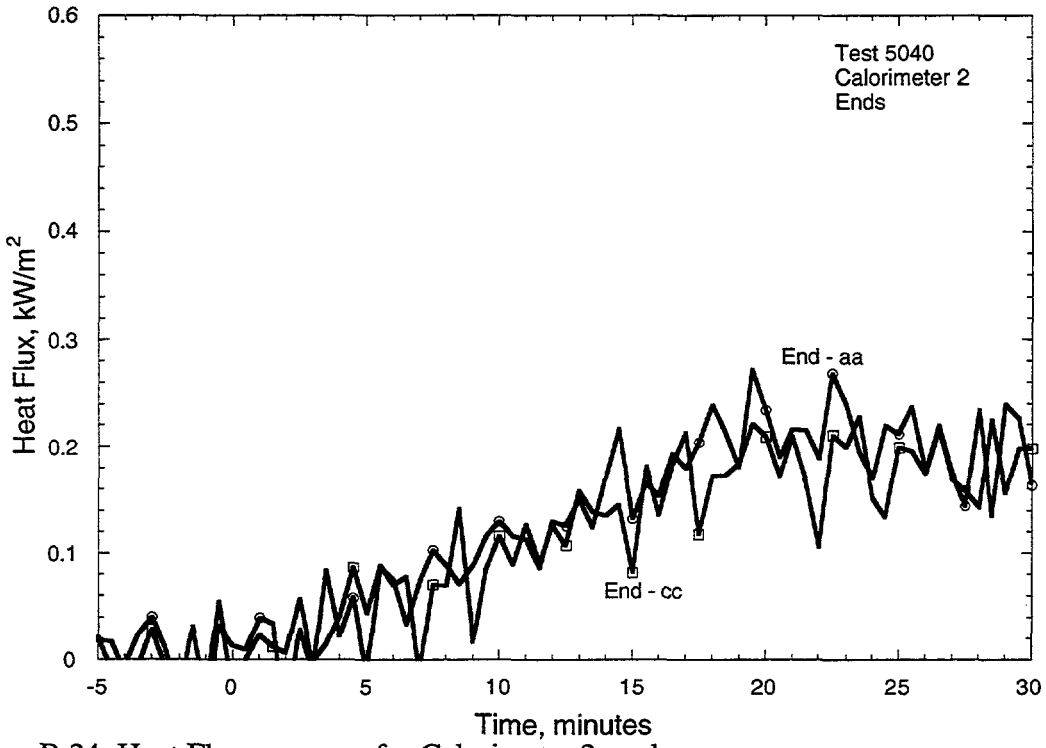

Figure B.24: Heat Flux response for Calorimeter 2, ends

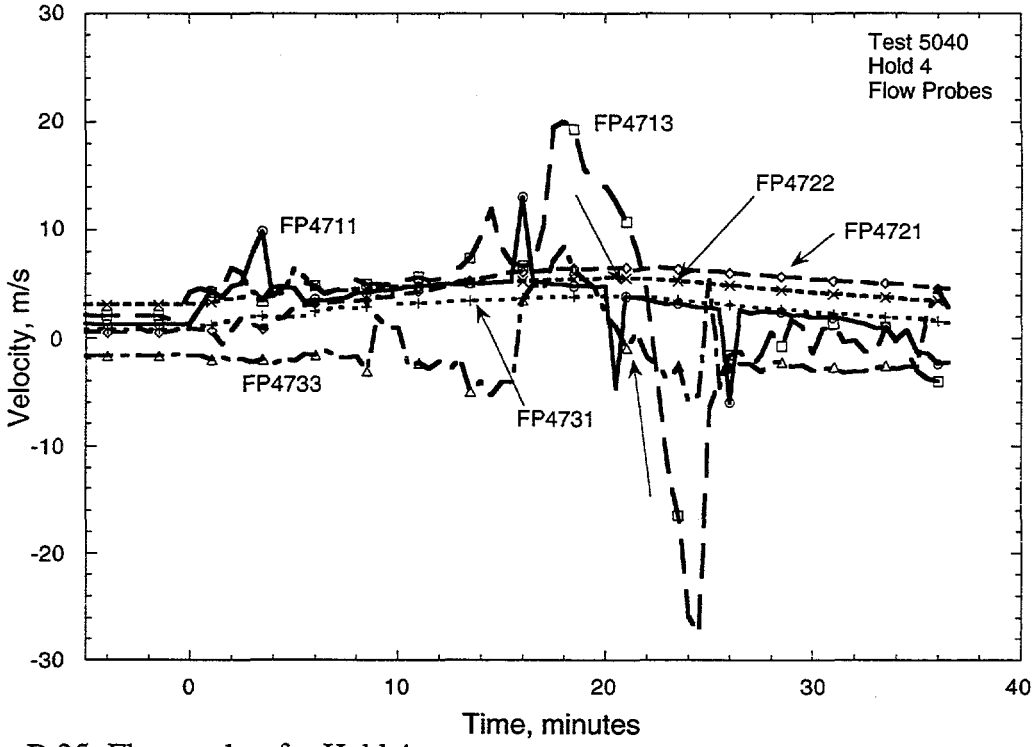

Figure B.25: Flow probes for Hold 4

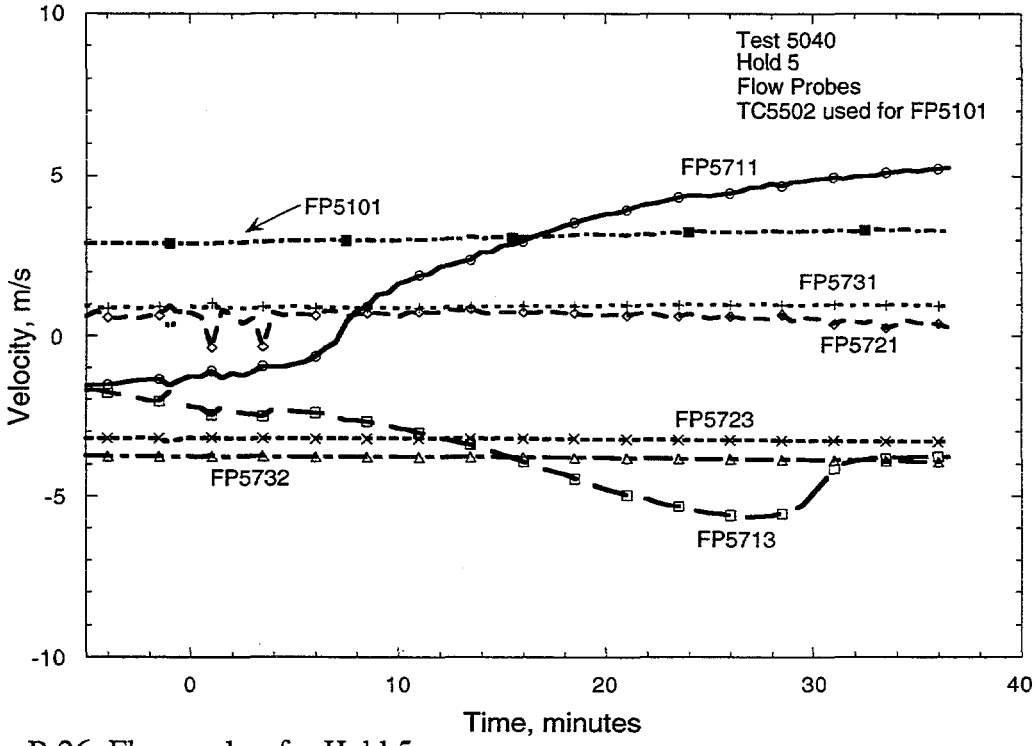

Figure B.26: Flow probes for Hold 5

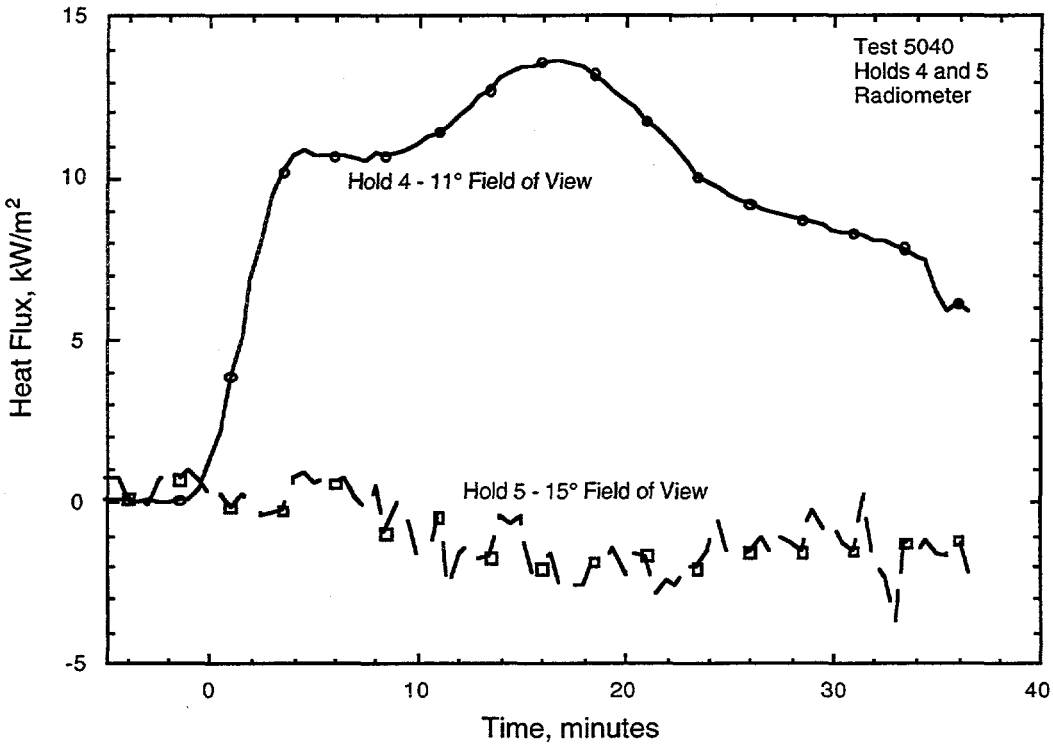

Figure B.27: Holds 4 & 5 Radiation Plot

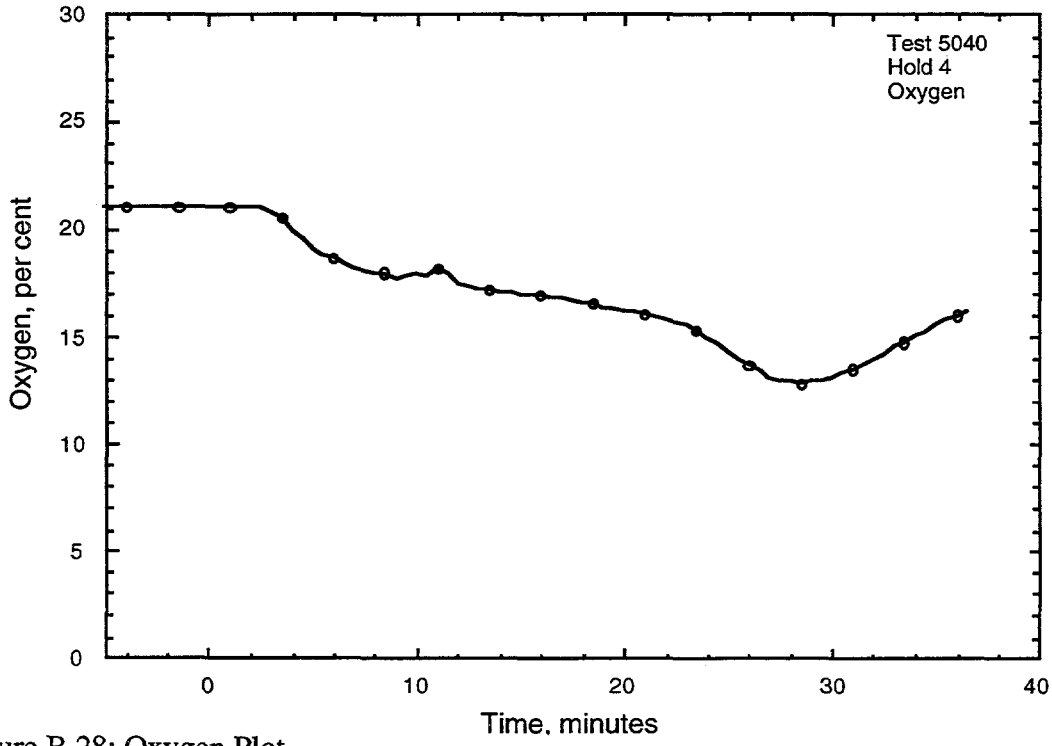

Figure B.28: Oxygen Plot

Appendix C
Test 5041
Two Burner Heptane Spray Test with Smoke

conducted 9/14/95
12:21 PM CDT

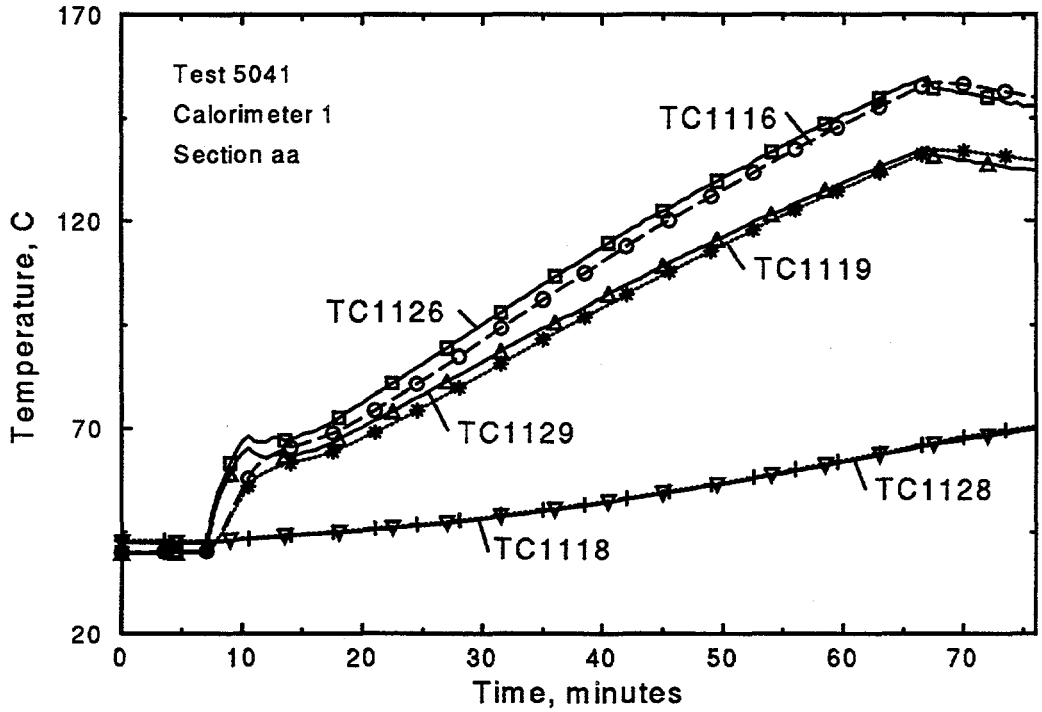

Figure C.1: Thermocouple response for Calorimeter 1, section aa

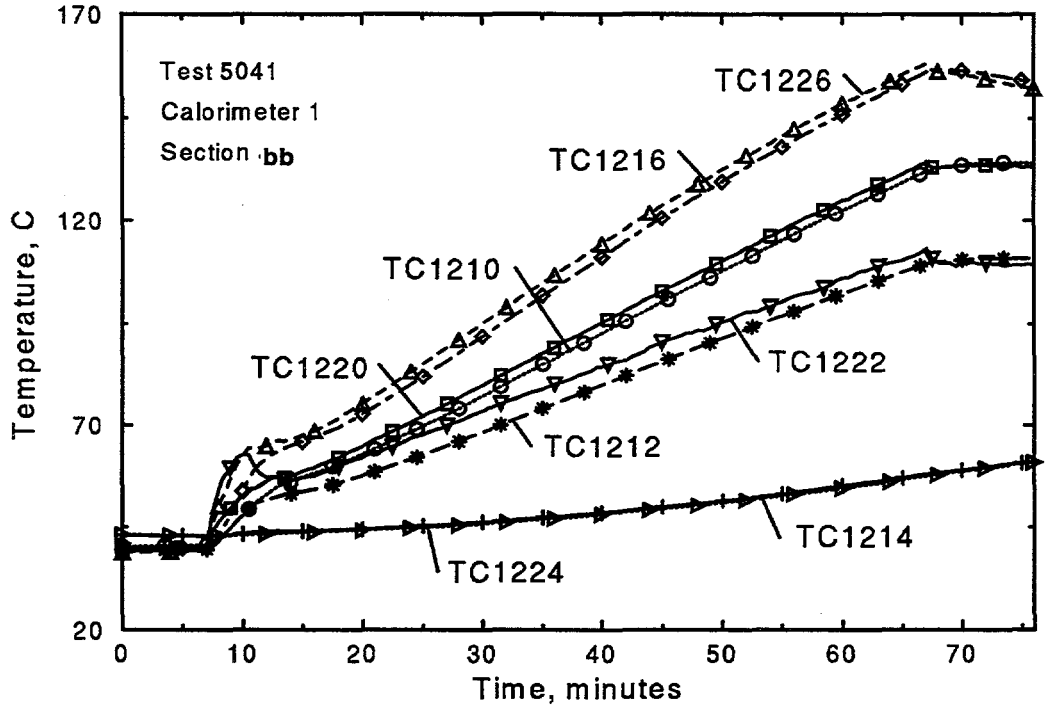

Figure C.2: Thermocouple response for Calorimeter 1, section bb

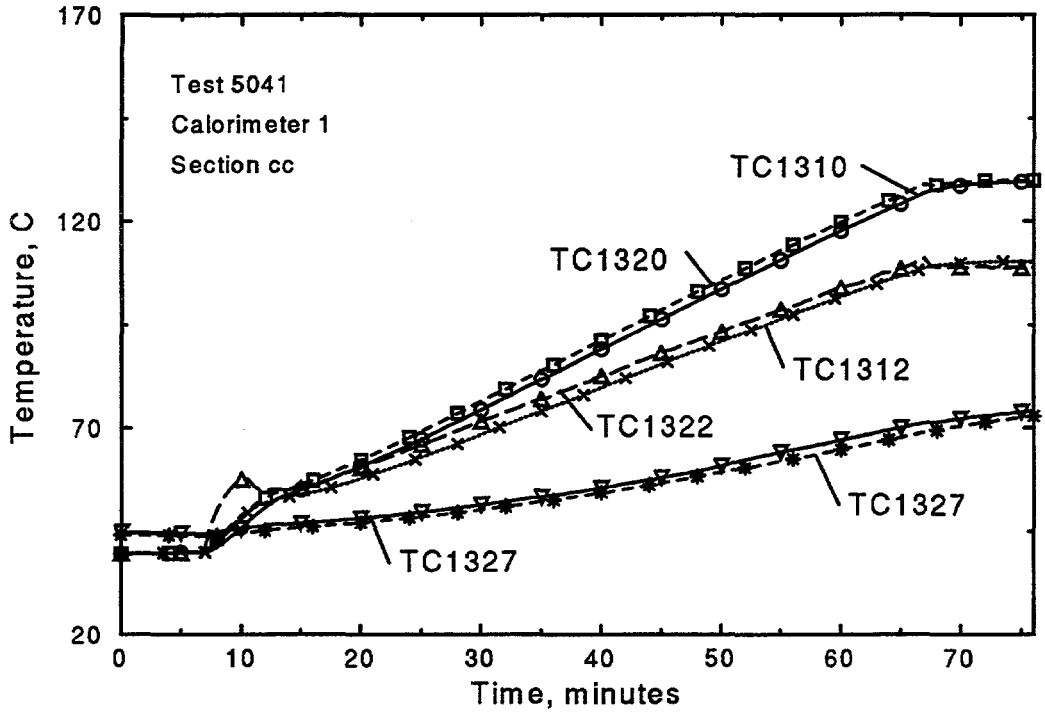

Figure C.3: Thermocouple response for Calorimeter 1, section cc

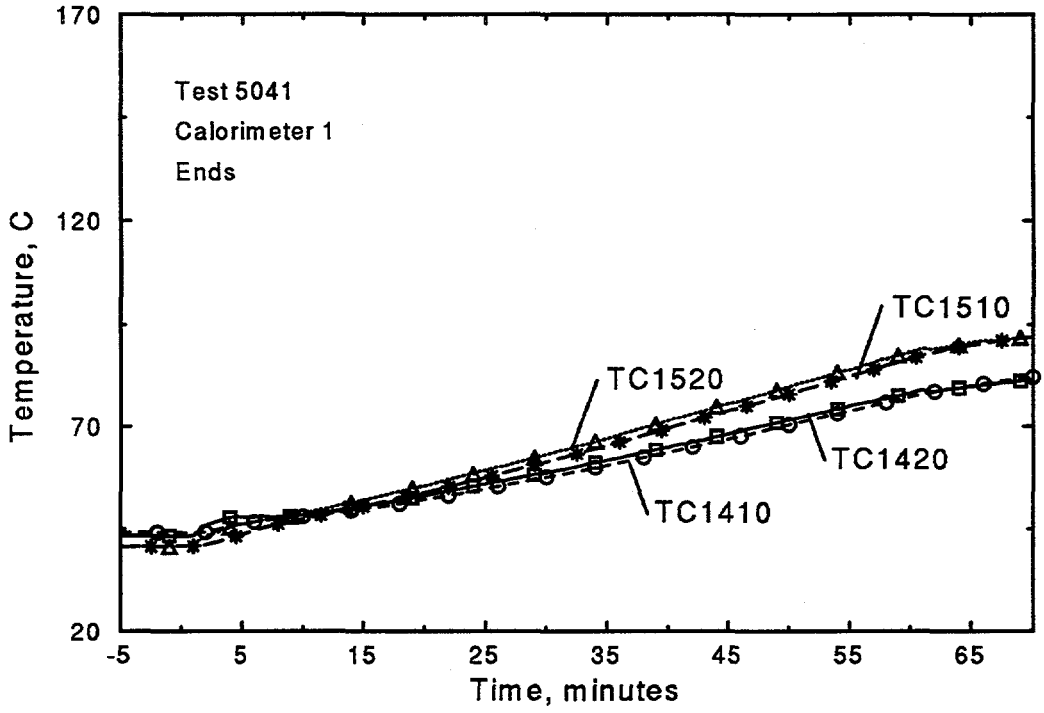

Figure C.4: Thermocouple response for Calorimeter 1, ends

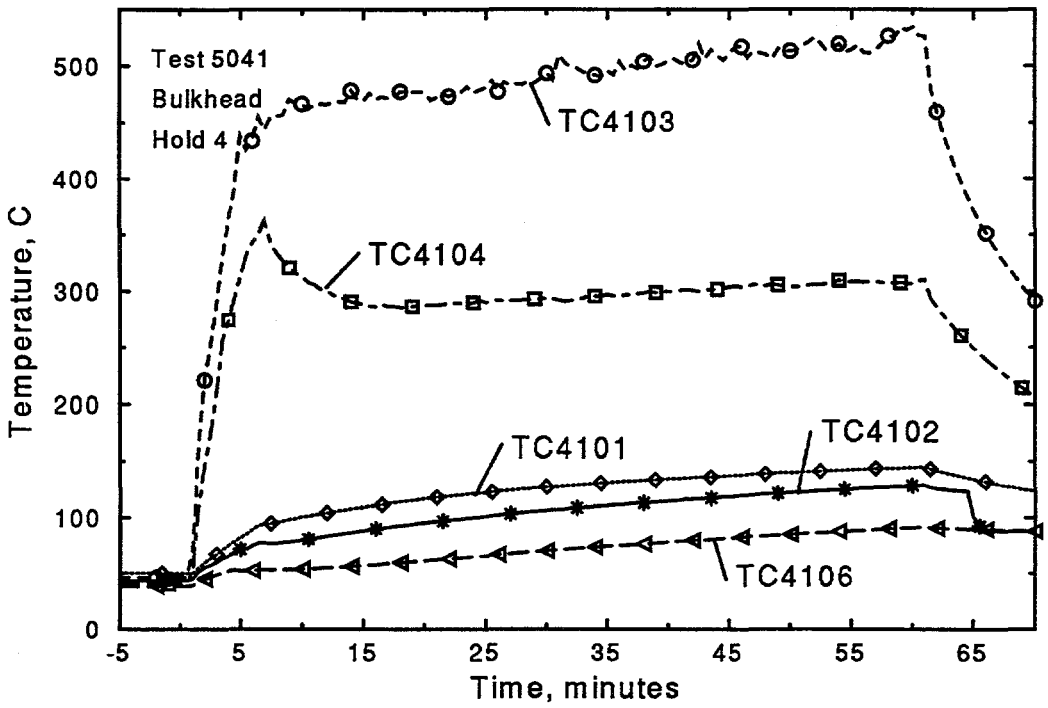

Figure C.5: Thermocouple response of Hold 4 Bulkhead

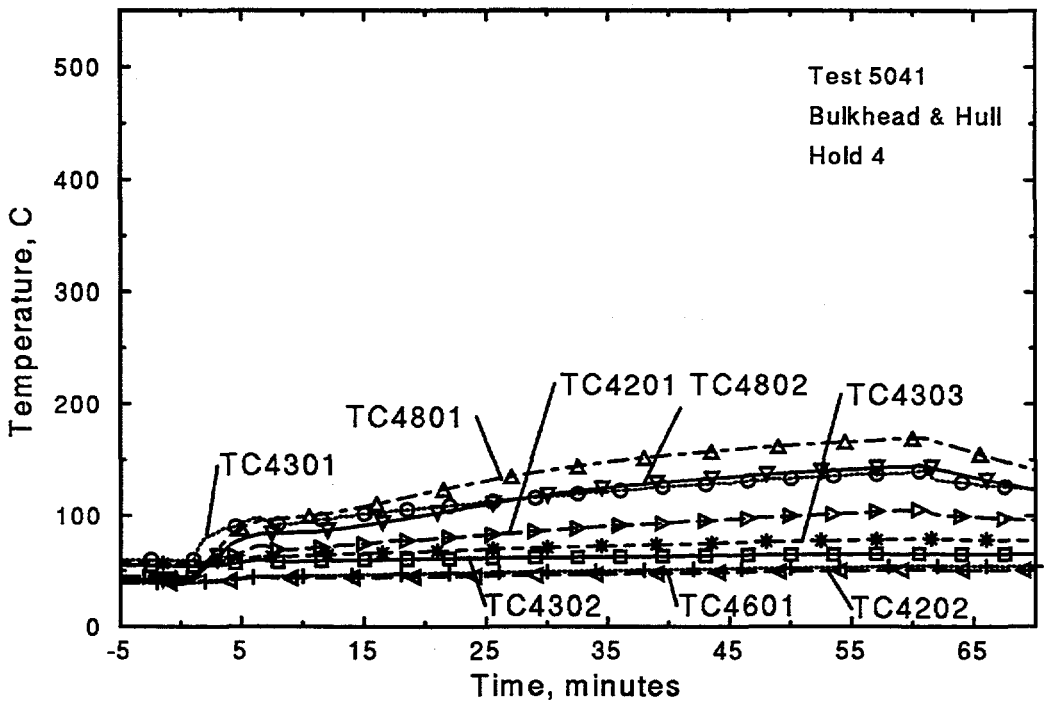

Figure C.6: Thermocouple response of Hold 4 Bulkhead and Hull

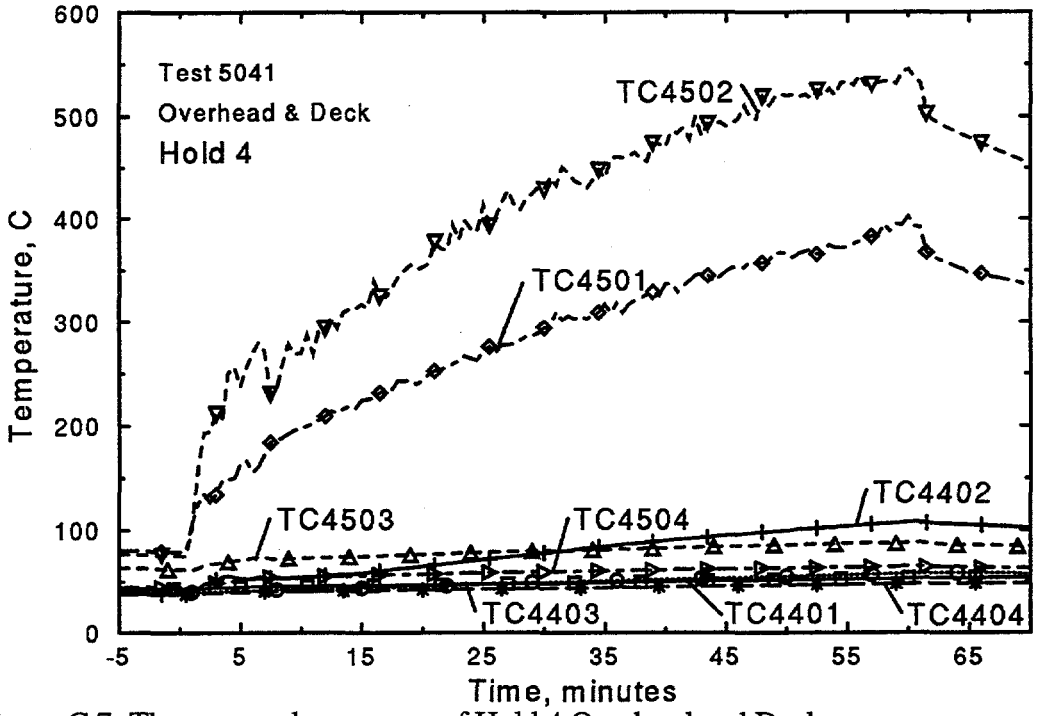

Figure C.7: Thermocouple response of Hold 4 Overhead and Deck

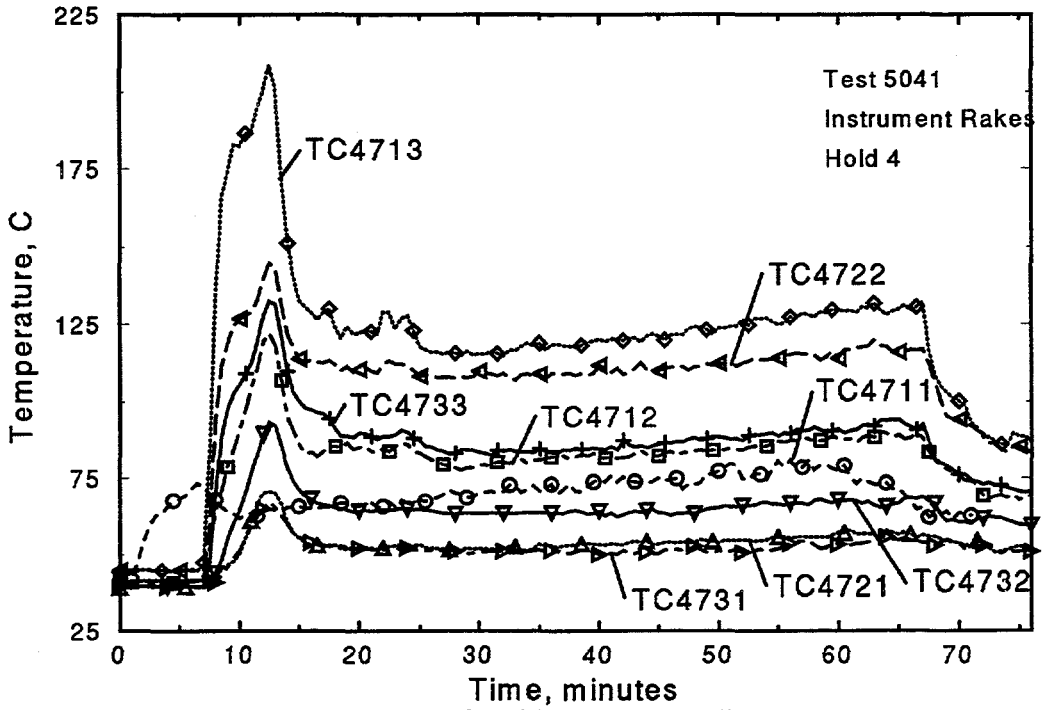

Figure C.8: Thermocouple response of Hold 4 Instrument Rakes

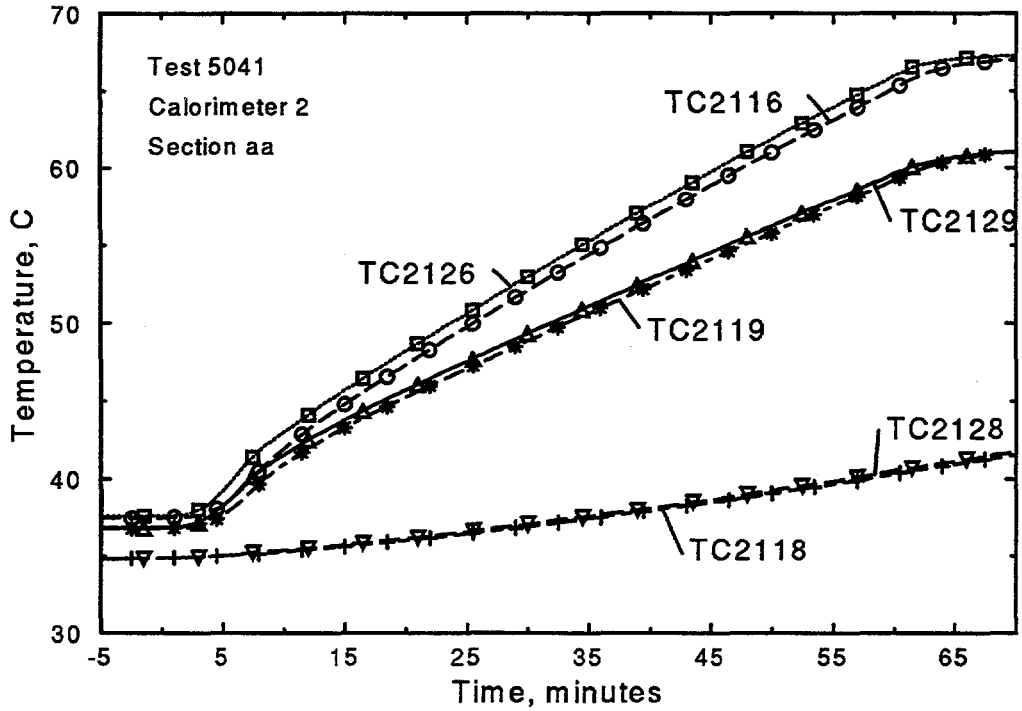

Figure C.9: Thermocouple response of Calorimeter 2, section aa

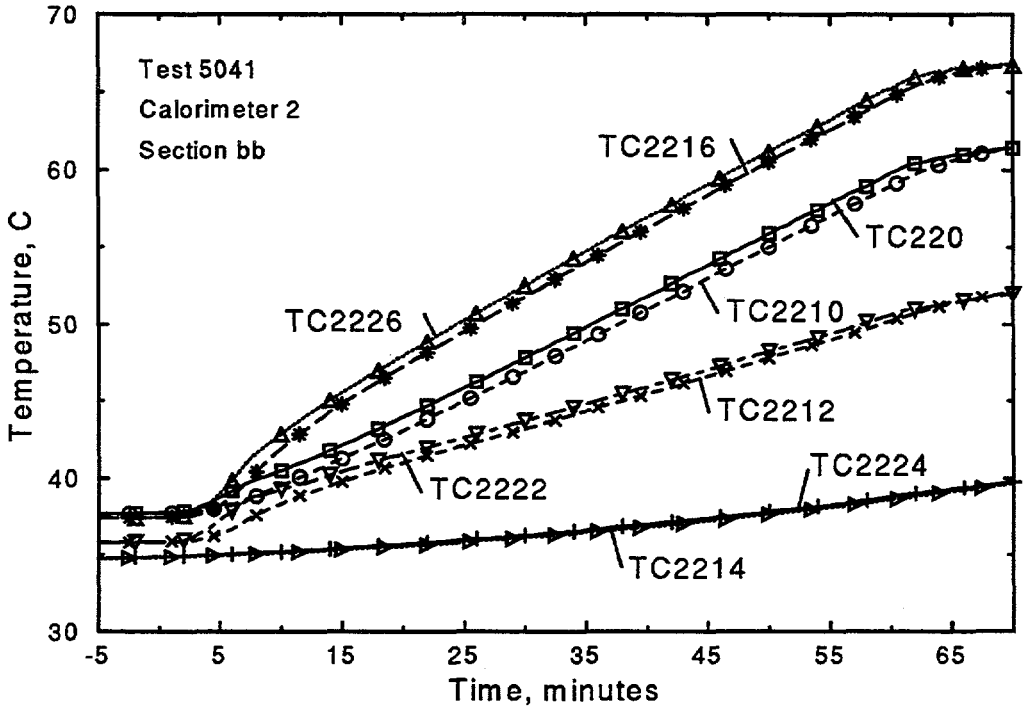

Figure C.10: Thermocouple response of Calorimeter 2, section bb

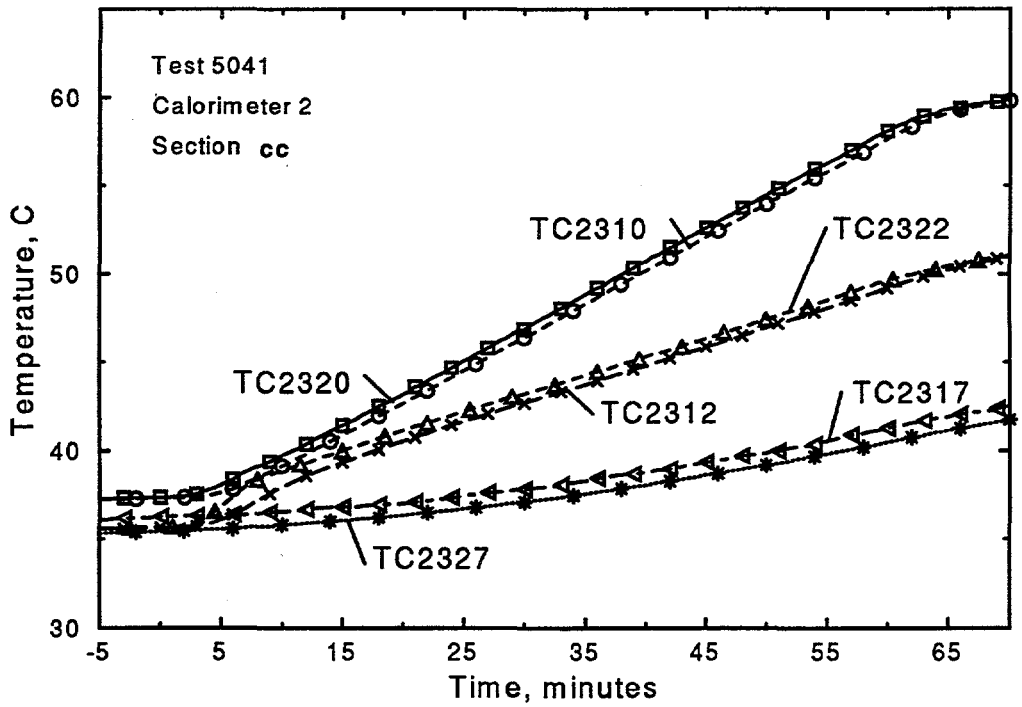

Figure C.11: Thermocouple response of Calorimeter 2, section cc

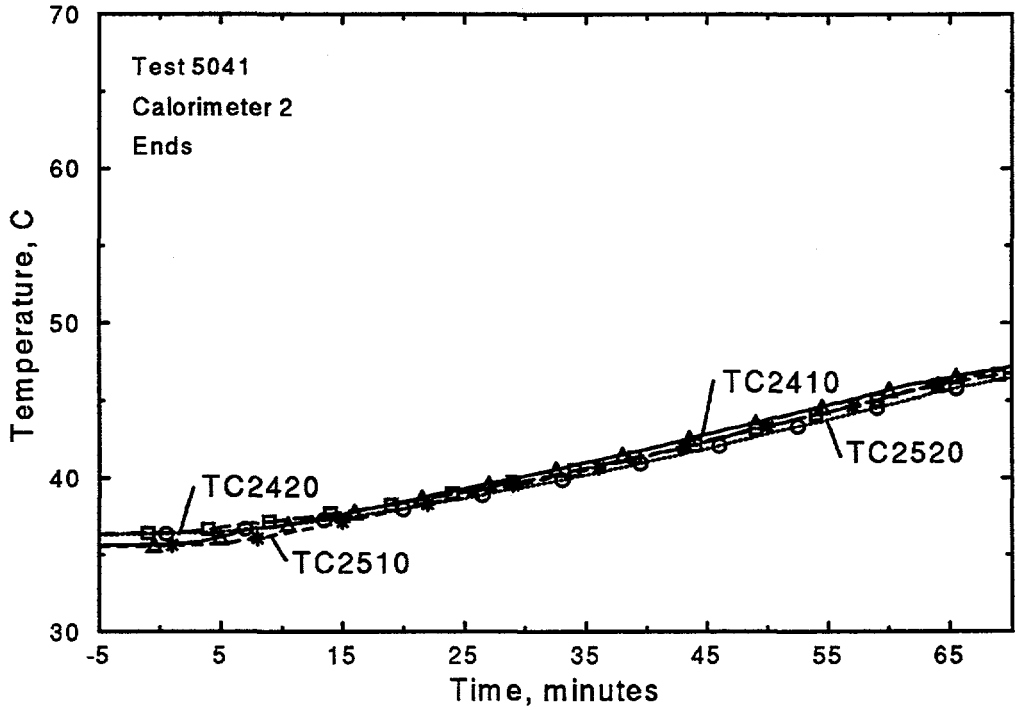

Figure C.12: Thermocouple response of Calorimeter 2, ends

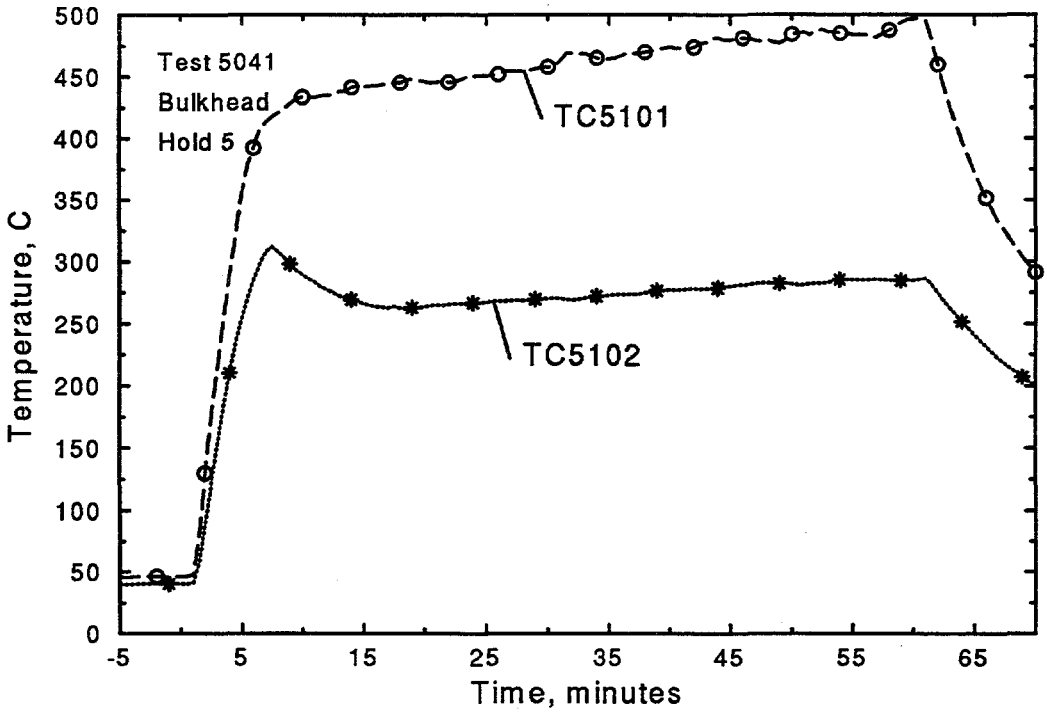

Figure C.13: Thermocouple response of Hold 5 Bulkhead

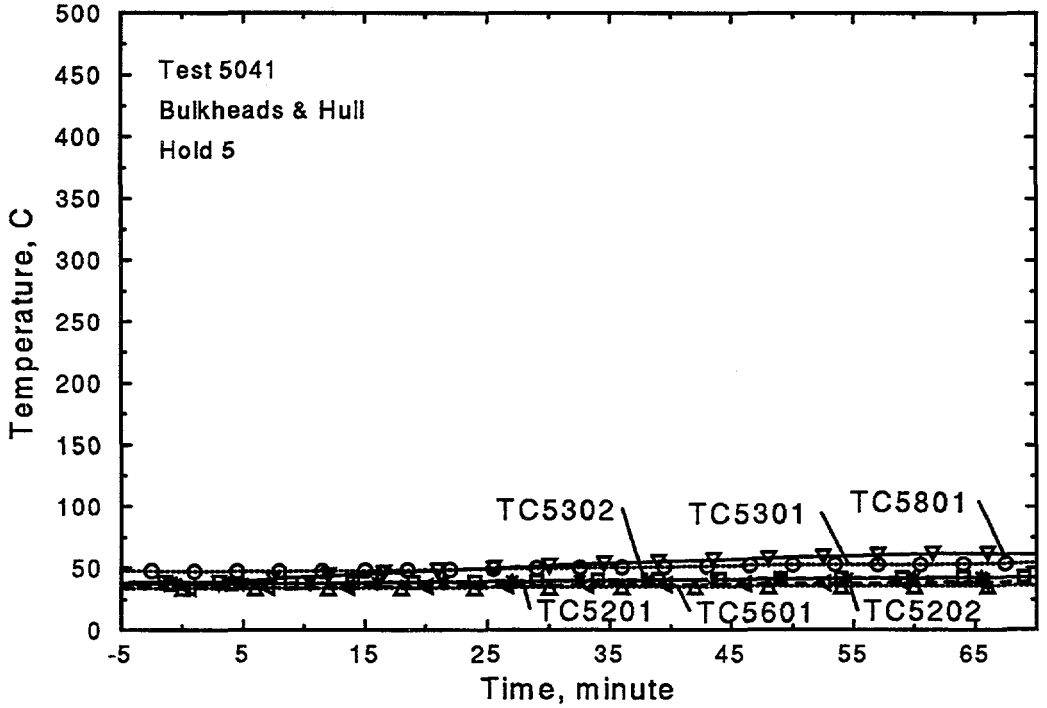

Figure C.14: Thermocouple response of Hold 5 Bulkhead and Hull

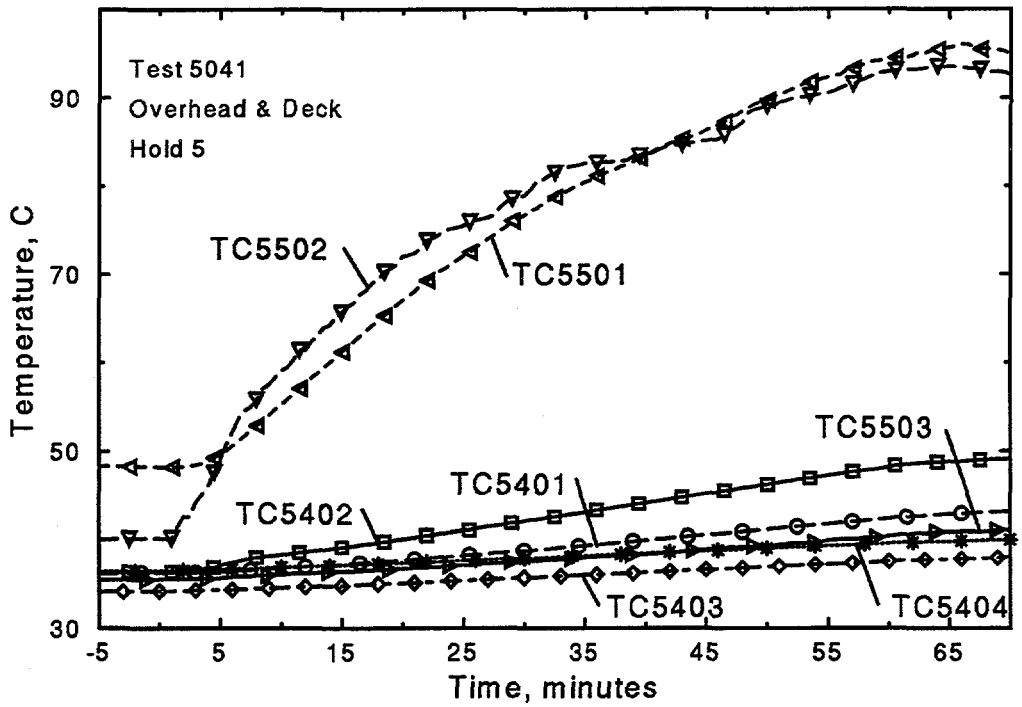

Figure C.15: Thermocouple response of Hold 5 Overhead and Deck

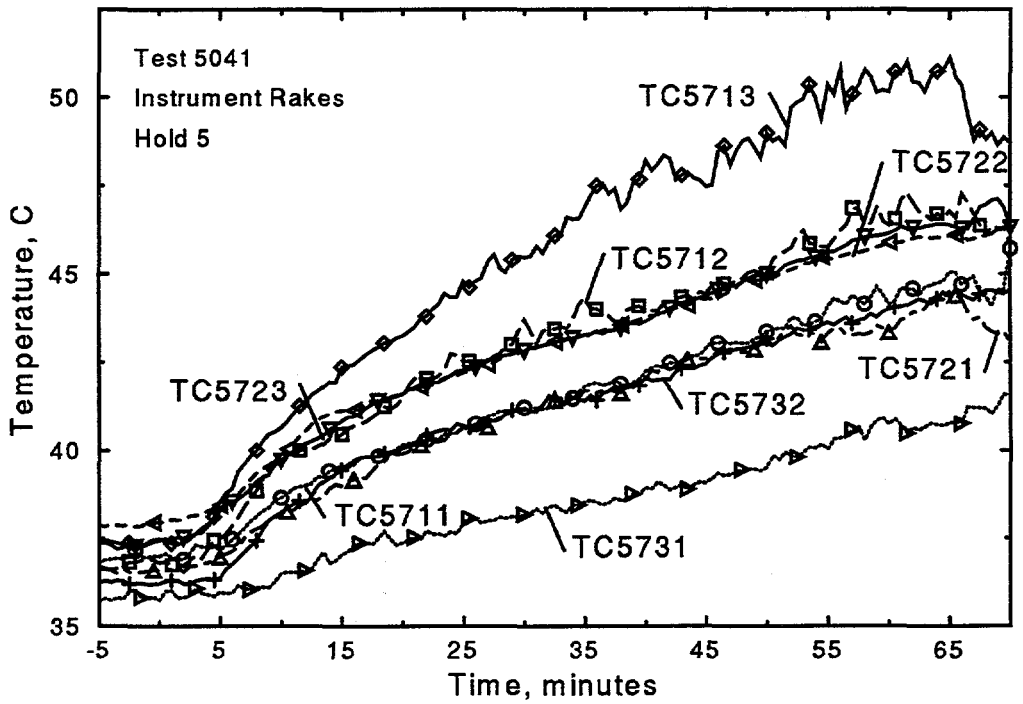

Figure C.16: Thermocouple response of Hold 5 Instrument Rakes

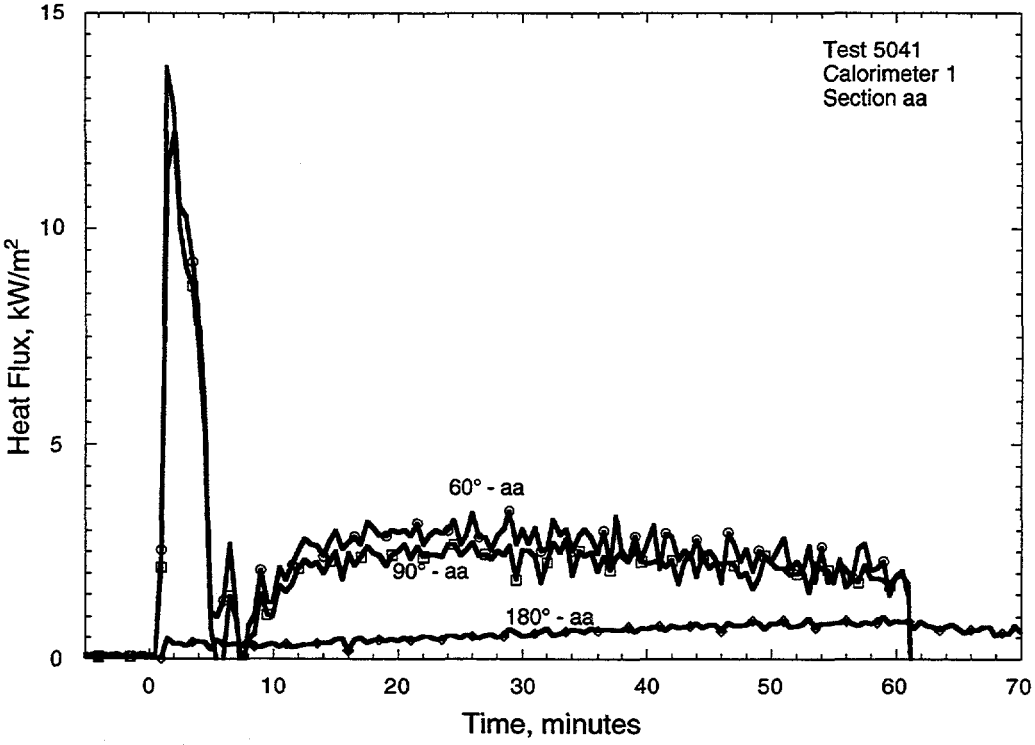

Figure C.17: Heat Flux response for Calorimeter 1, section aa

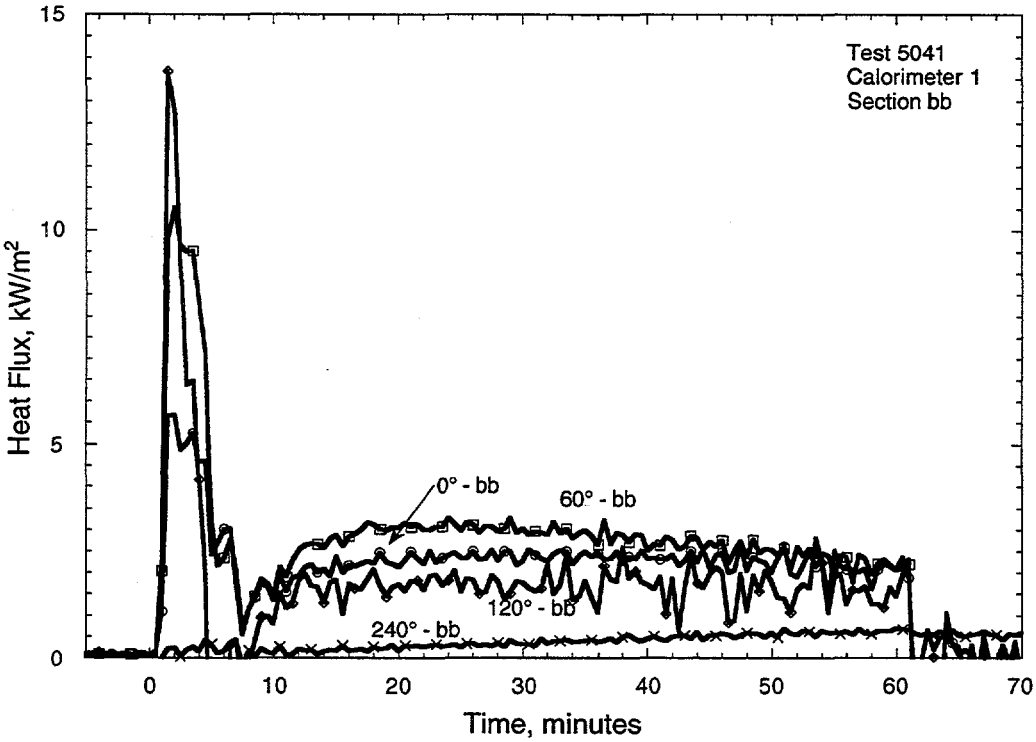

Figure C.18: Heat Flux response for Calorimeter 1, section bb

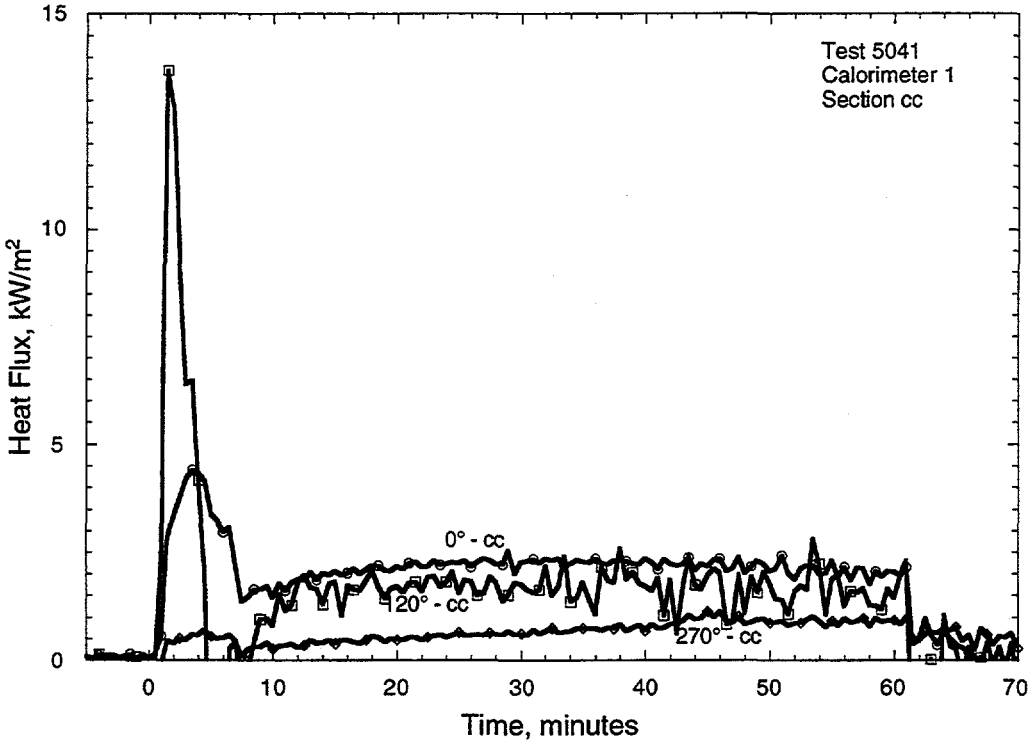

Figure C.19: Heat Flux response for Calorimeter 1, section cc

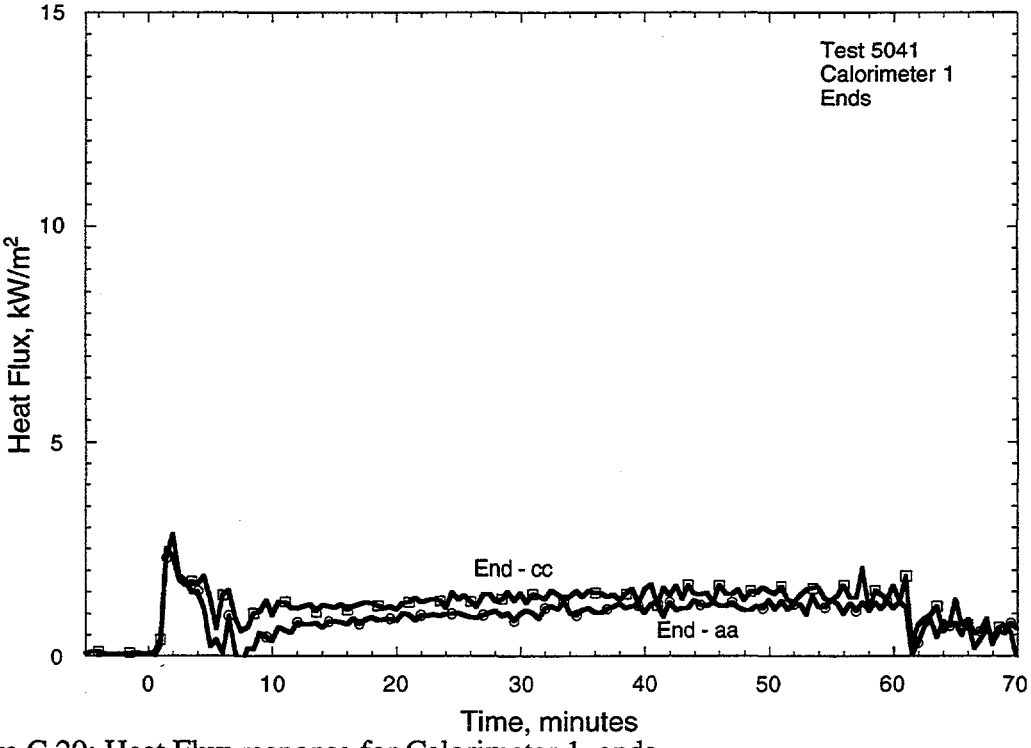

Figure C.20: Heat Flux response for Calorimeter 1, ends

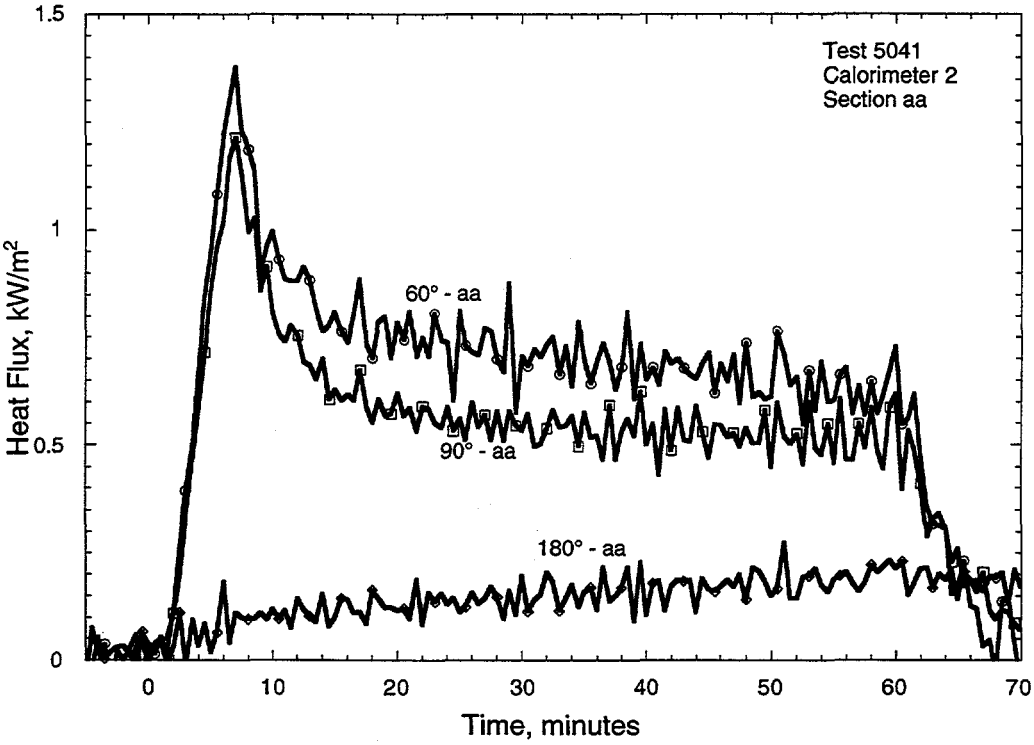

Figure C.21: Heat Flux response for Calorimeter 2, section aa

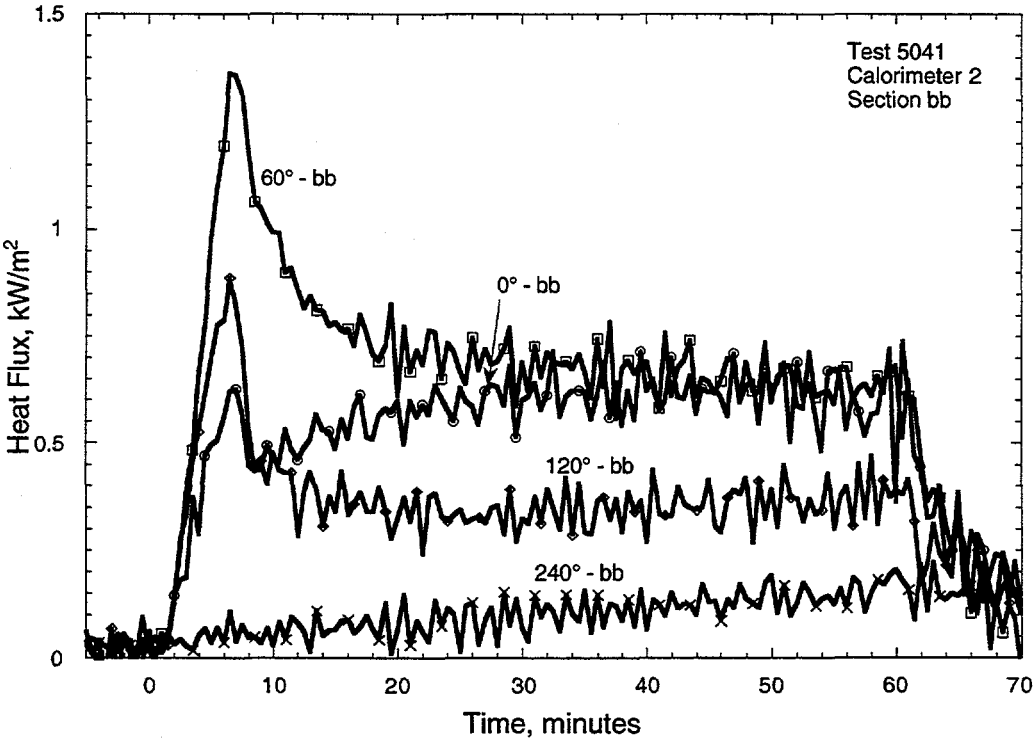

Figure C.22: Heat Flux response for Calorimeter 2, section bb

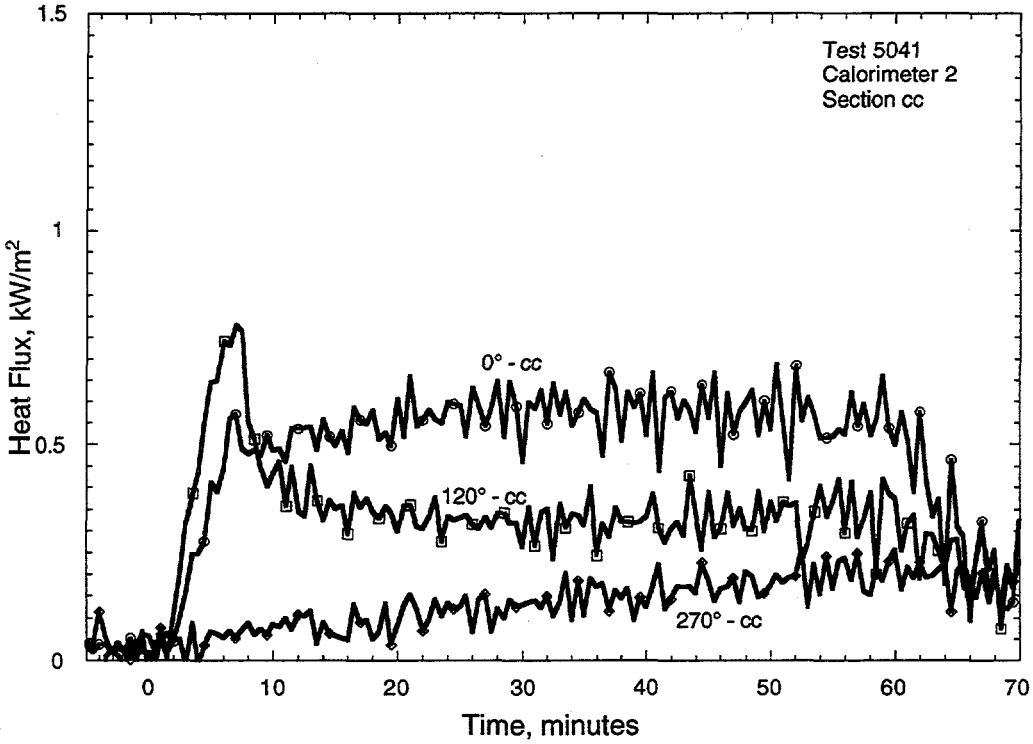

Figure C.23: Heat Flux response for Calorimeter 2, section cc

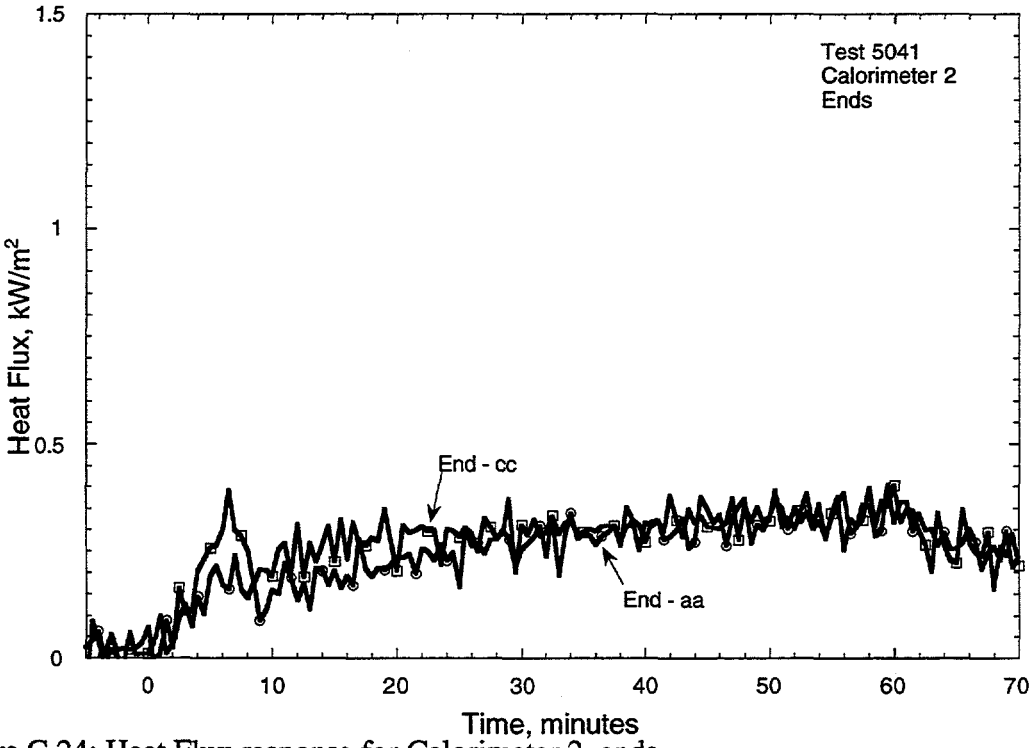

Figure C.24: Heat Flux response for Calorimeter 2, ends

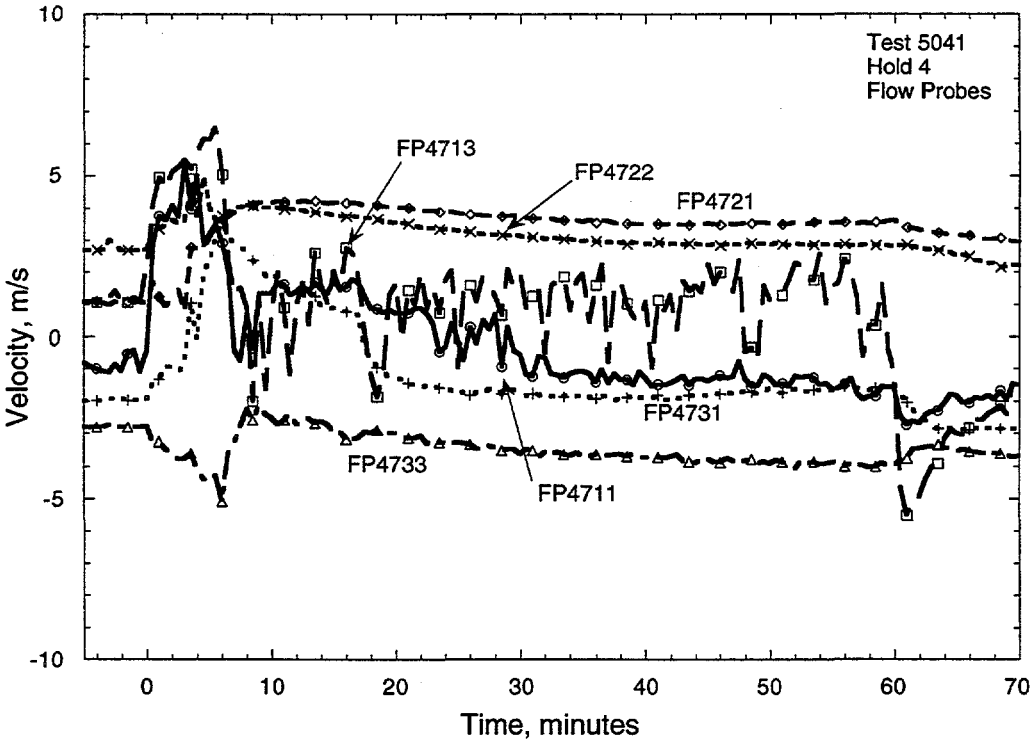

Figure C.25: Flow probes for Hold 4

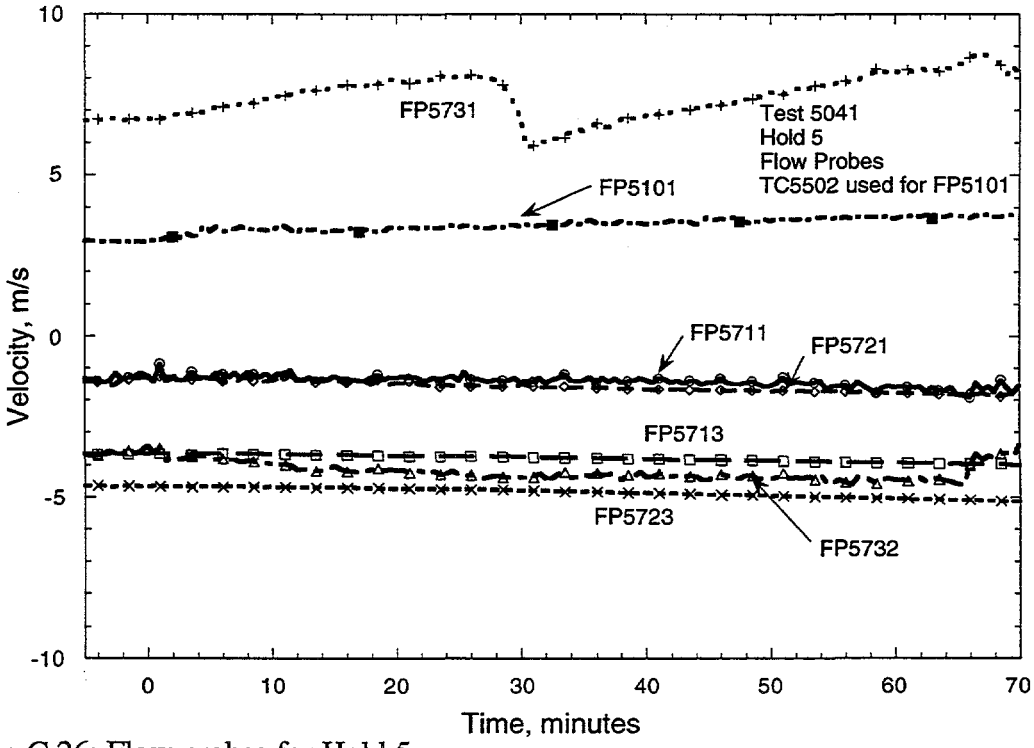

Figure C.26: Flow probes for Hold 5

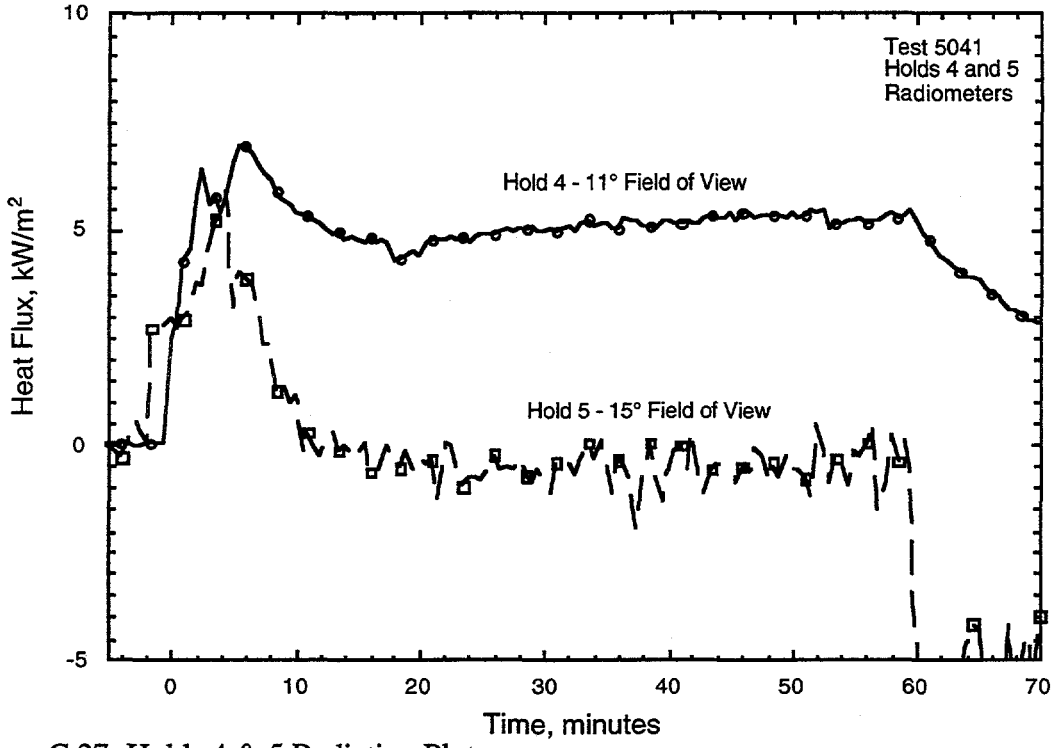

Figure C.27: Holds 4 & 5 Radiation Plot

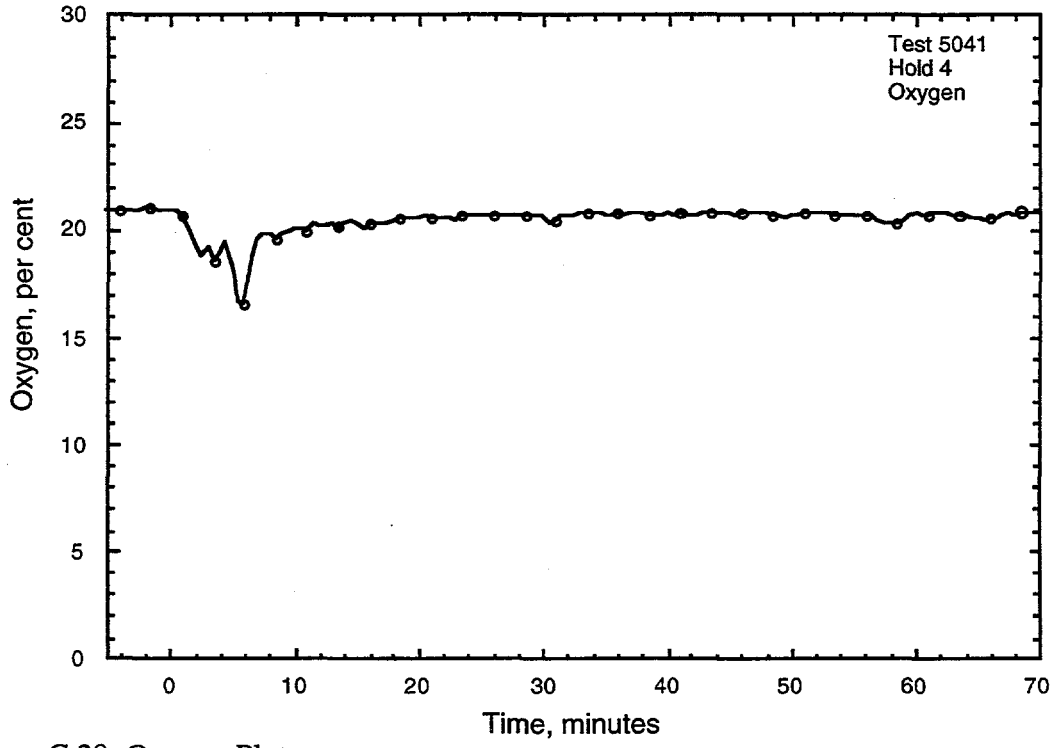

Figure C.28: Oxygen Plot

Appendix D
Test 5043
Wood Crib Fire Test with Heptane Accelerant

conducted 9/15/95
8:26 AM CDT

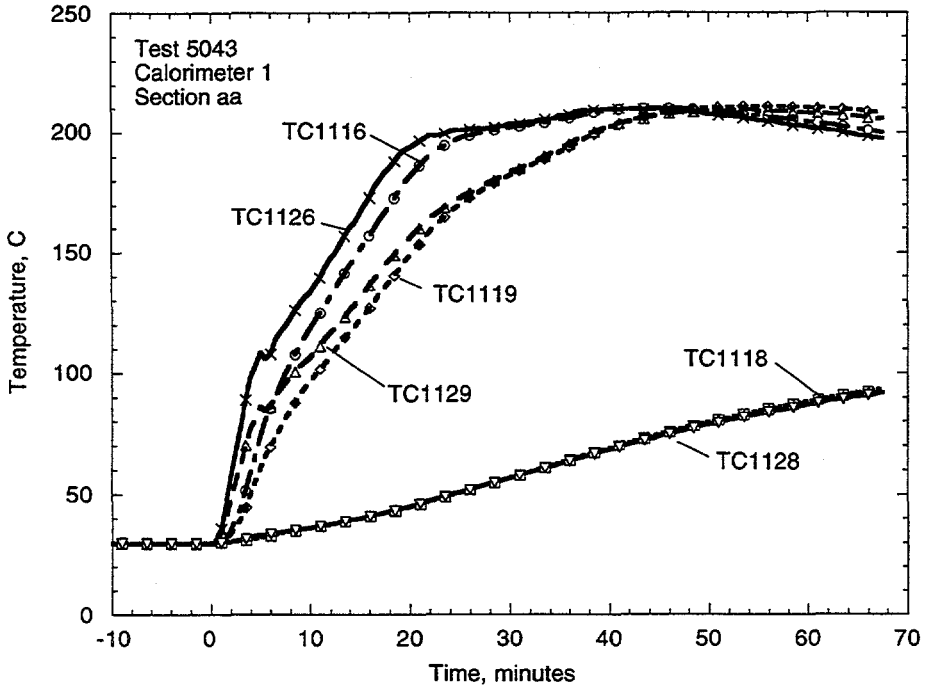

Figure D.1: Thermocouple response of Calorimeter 1, section aa

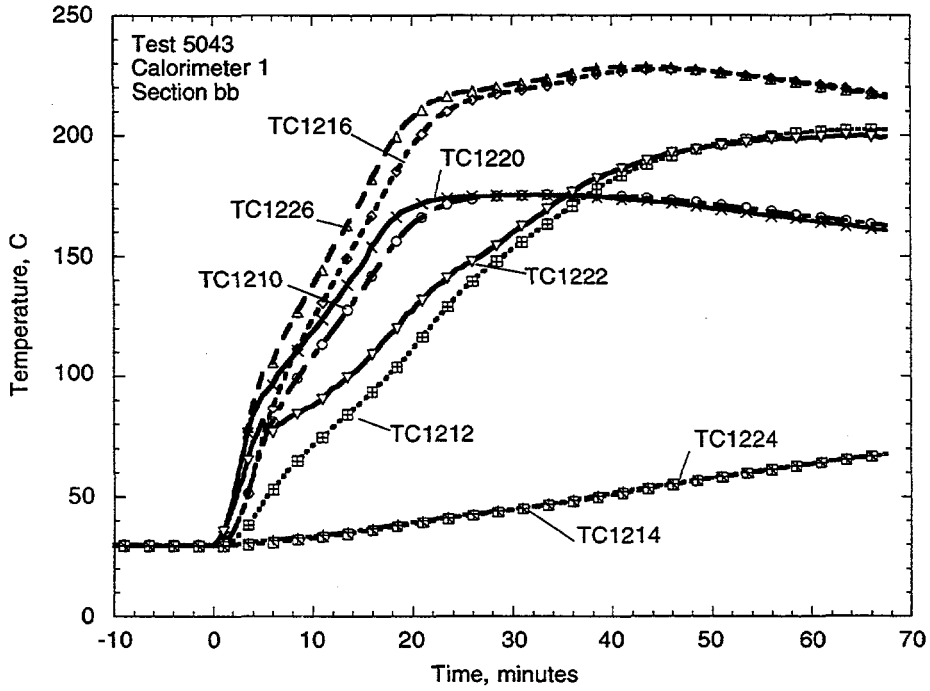

Figure D.2: Thermocouple response of Calorimeter 1, section bb

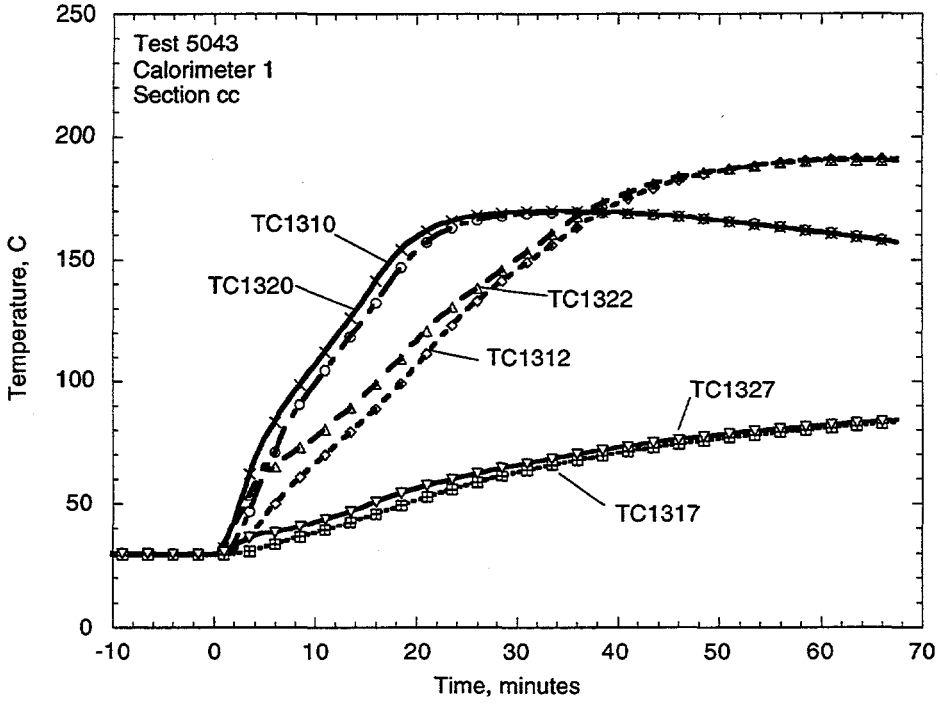

Figure D.3: Thermocouple response of Calorimeter 1, section cc

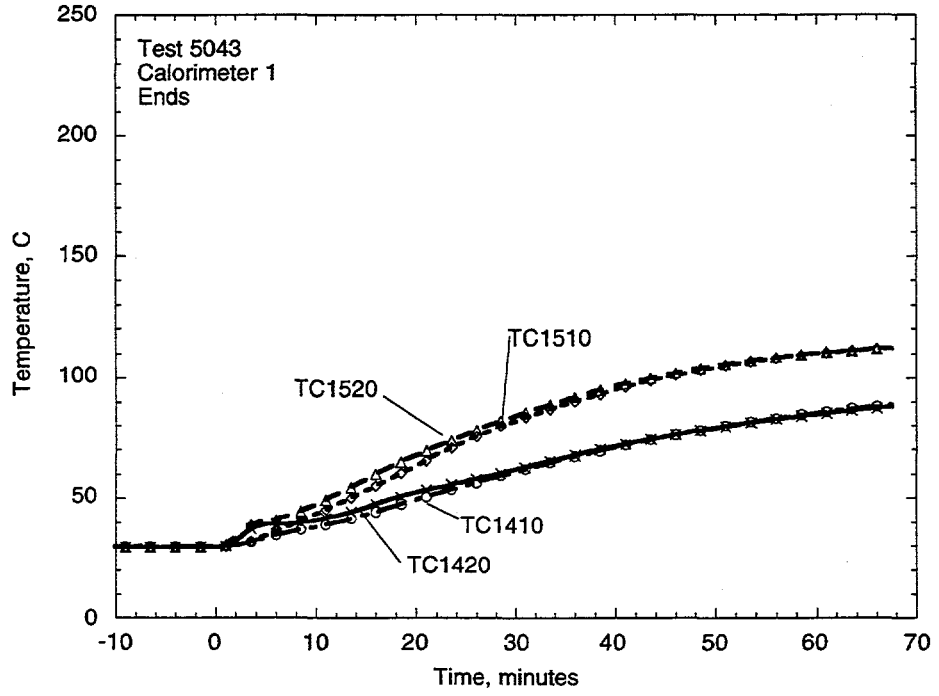

Figure D.4: Thermocouple response of Calorimeter 1, ends

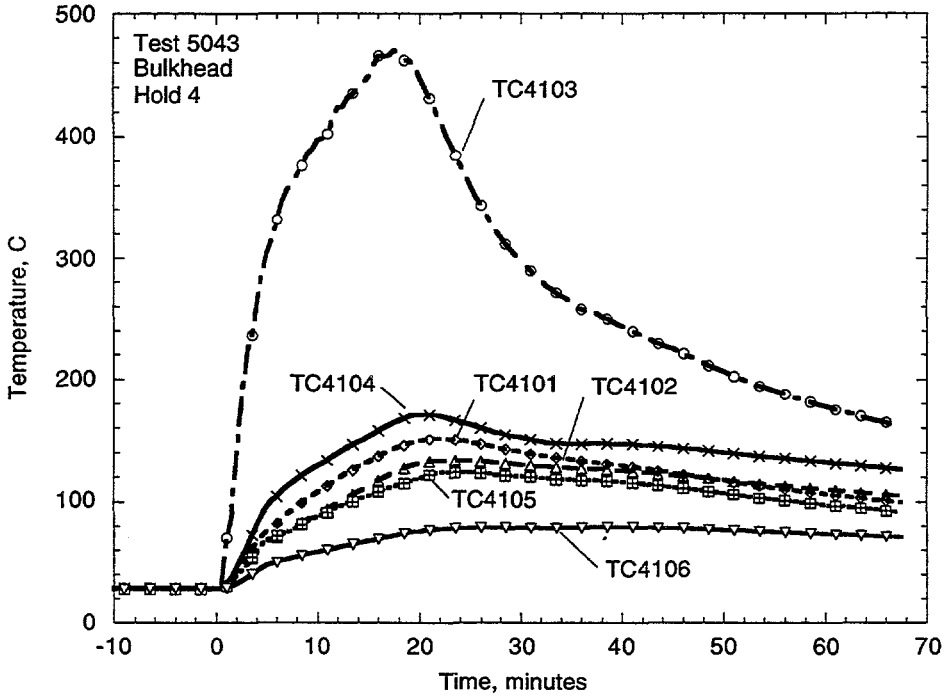

Figure D.5: Thermocouple response of Hold 4 Bulkhead

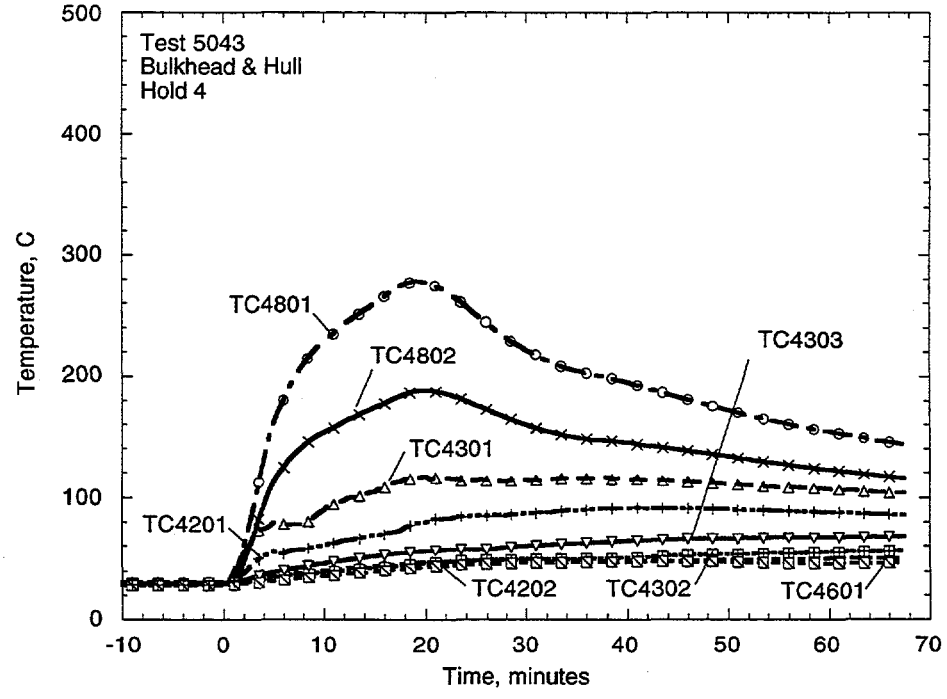

Figure D.6: Thermocouple response of Hold 4 Bulkhead and Hull

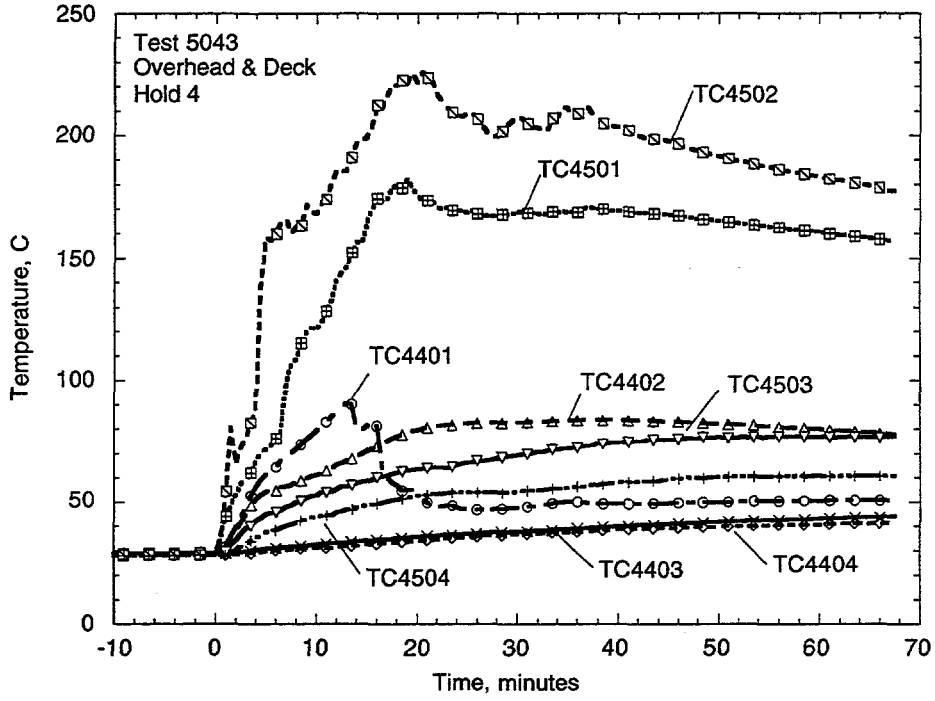

Figure D.7: Thermocouple response of Hold 4 Overhead and Deck

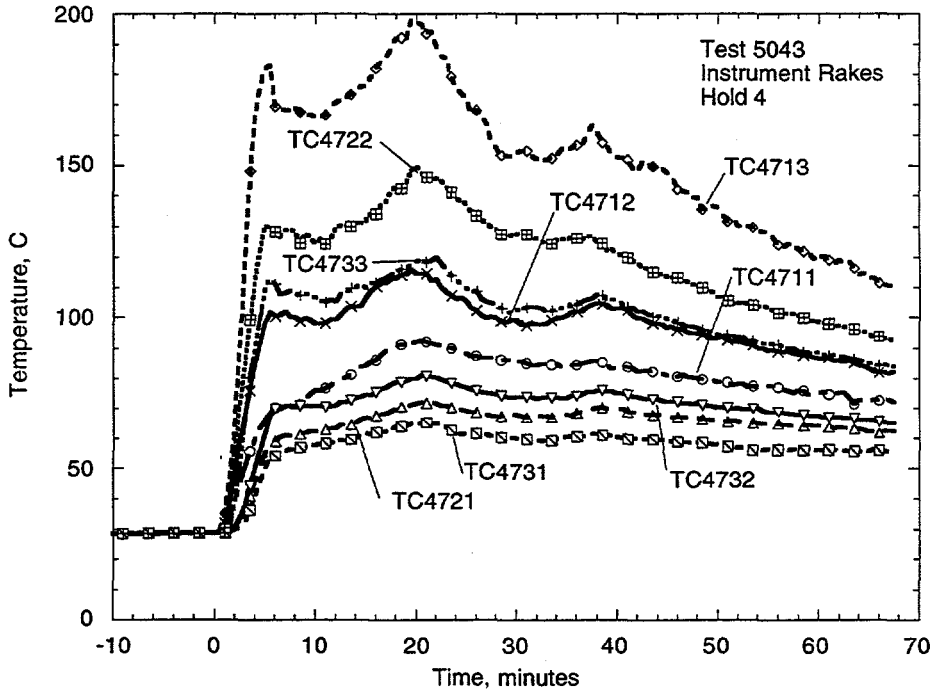

Figure D.8: Thermocouple response of Hold 4 Instrument Rakes

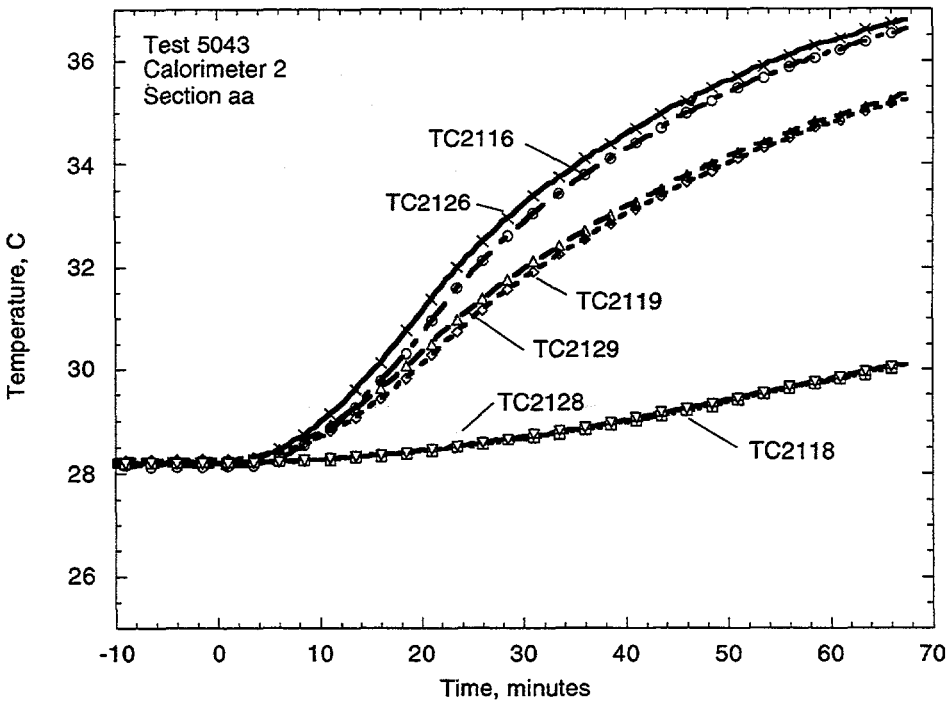

Figure D.9: Thermocouple response of Calorimeter 2, section aa

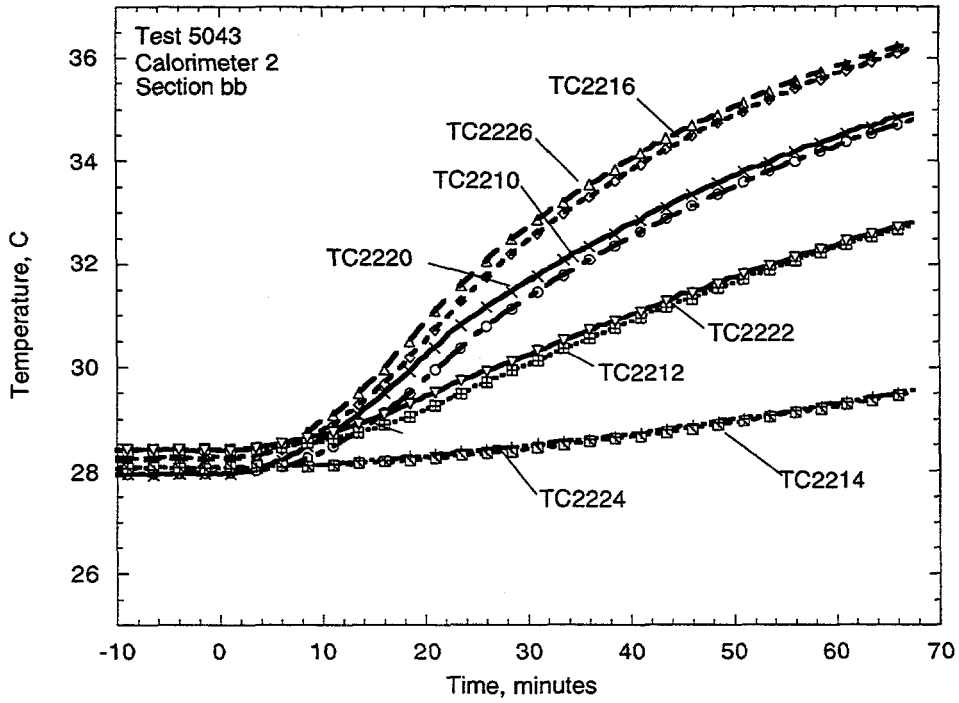

Figure D.10: Thermocouple response of Calorimeter 2, section bb

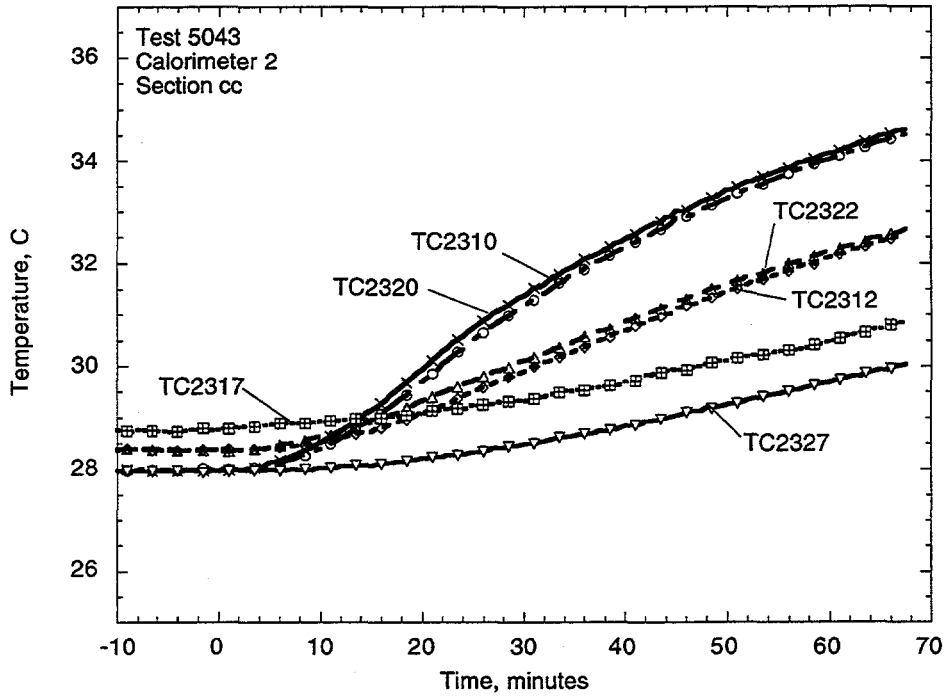

Figure D.11: Thermocouple response of Calorimeter 2, section cc

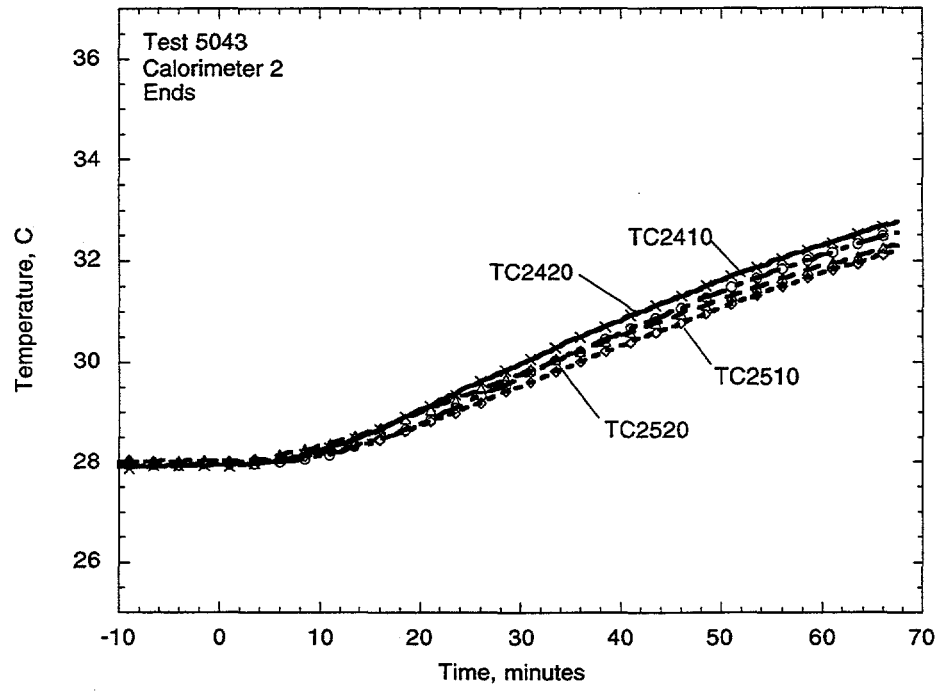

Figure D.12: Thermocouple response of Calorimeter 2, ends

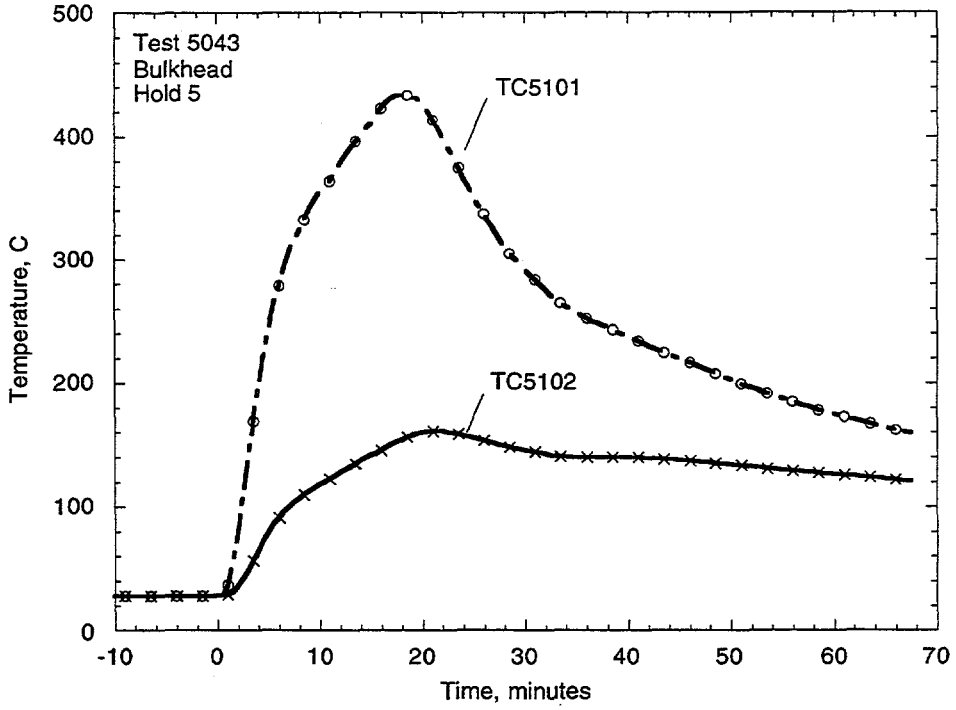

Figure D.13: Thermocouple response of Hold 5 Bulkhead

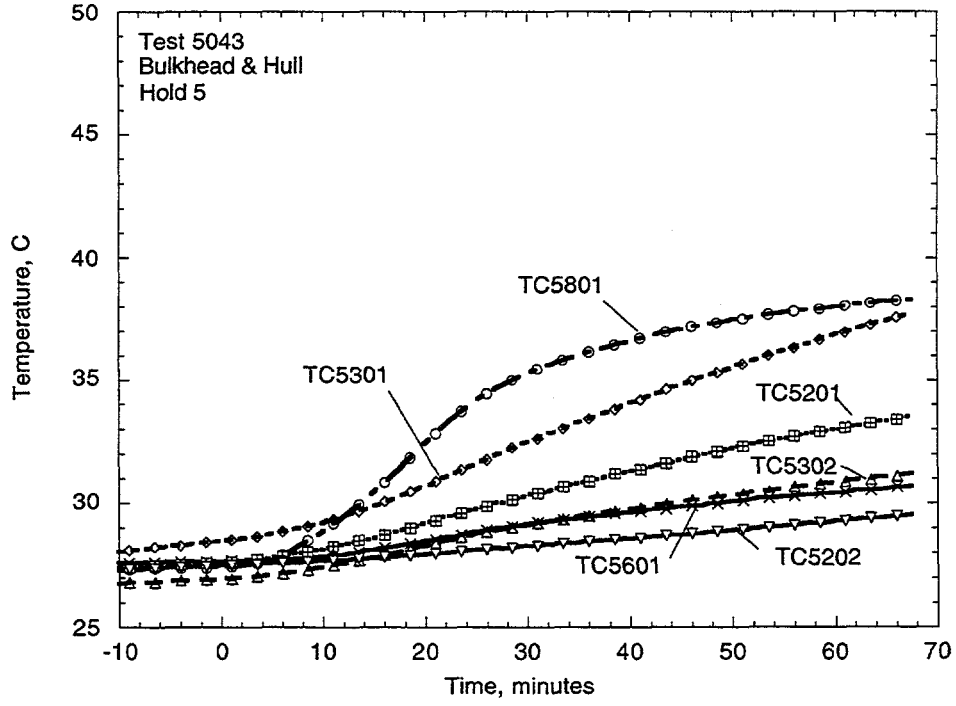

Figure D.14: Thermocouple response of Hold 5 Bulkhead and Hull

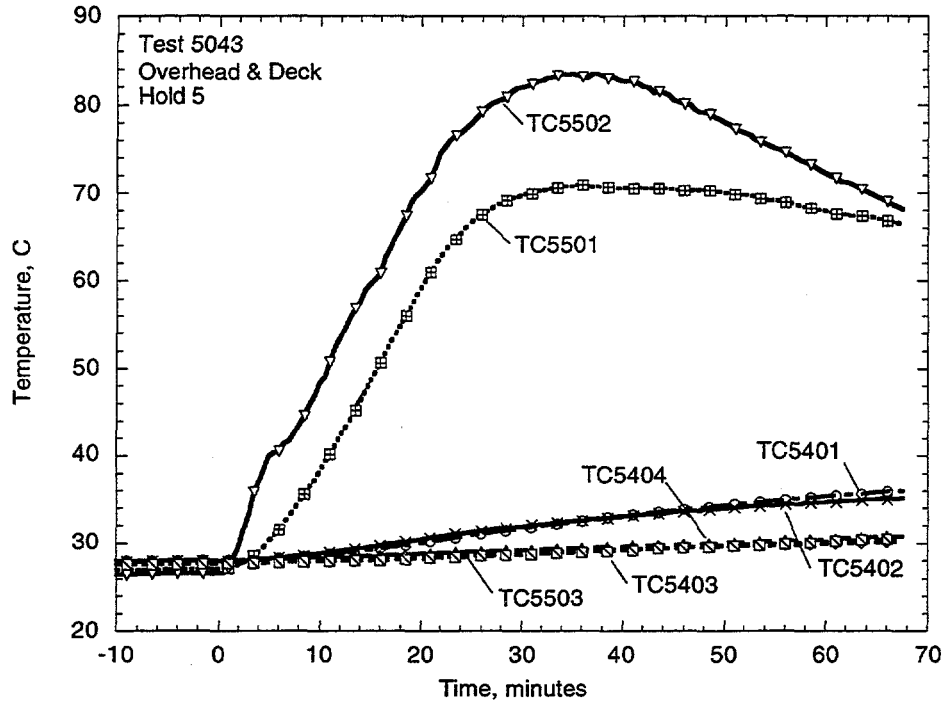

Figure D.15: Thermocouple response of Hold 5 Overhead and Deck

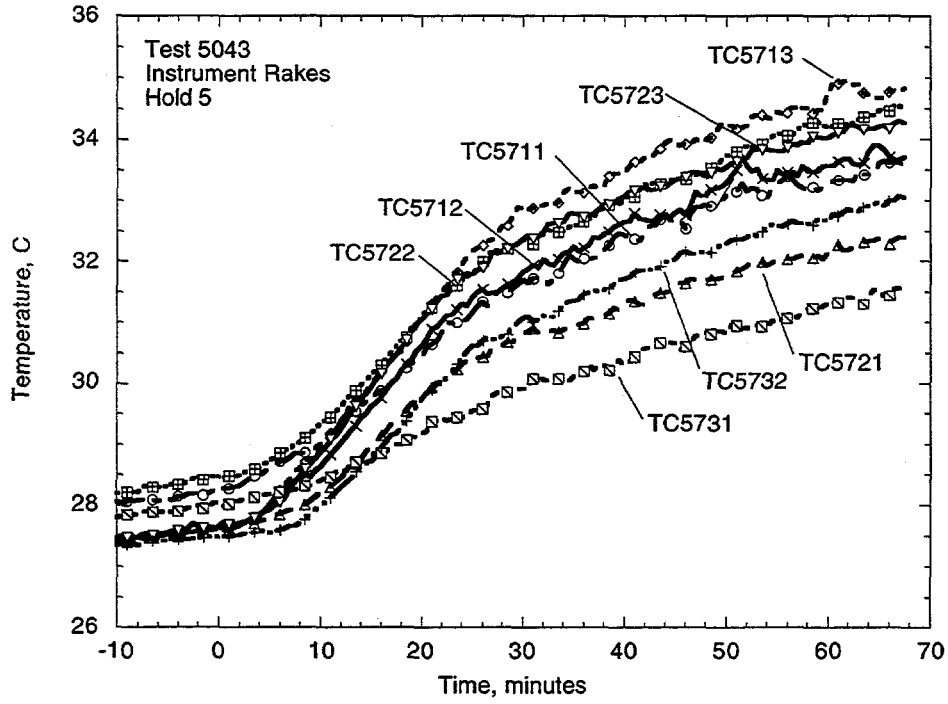

Figure D.16: Thermocouple response of Hold 5 Instrument Rakes

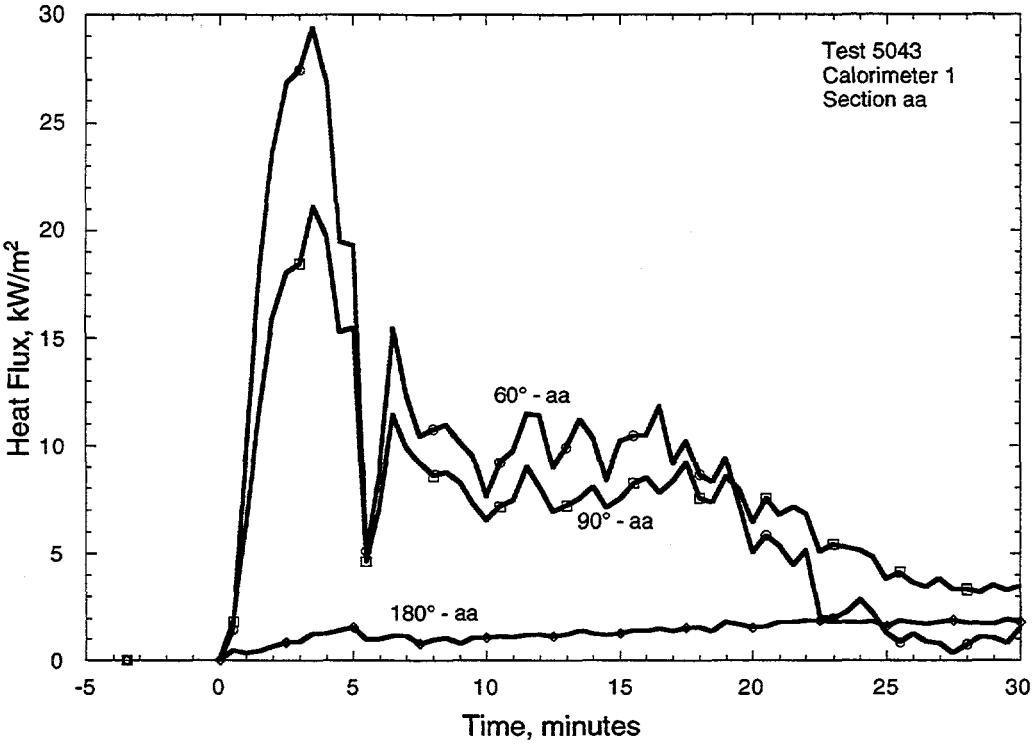

Figure C.17: Heat Flux response for Calorimeter 1, section aa

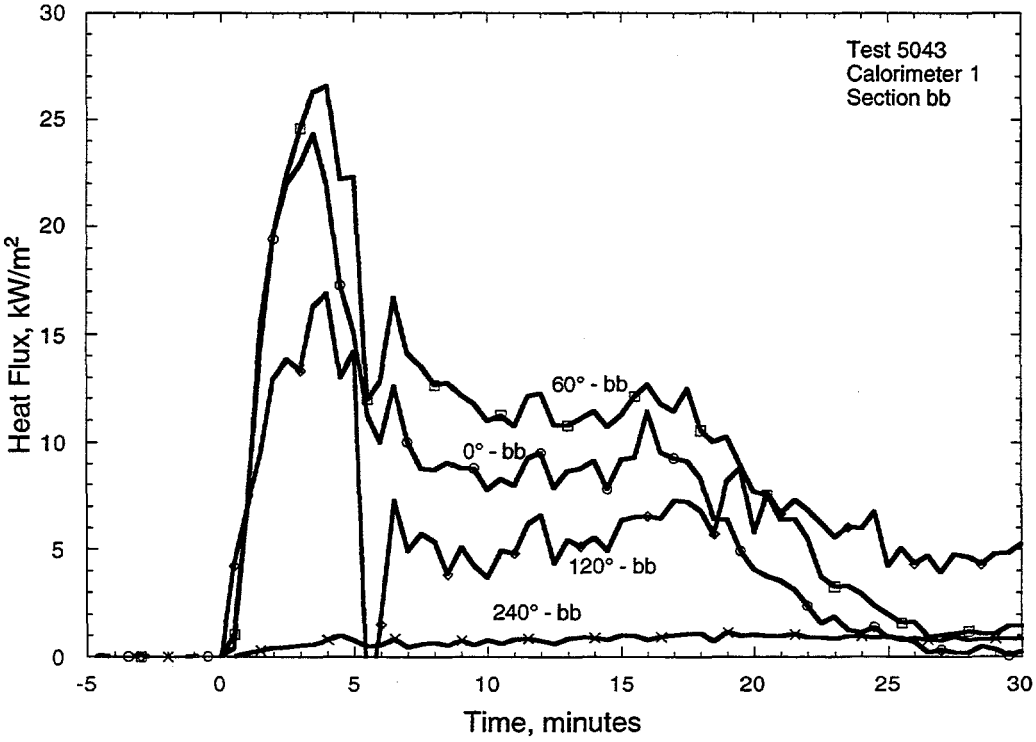

Figure D.18: Heat Flux response for Calorimeter 1, section bb

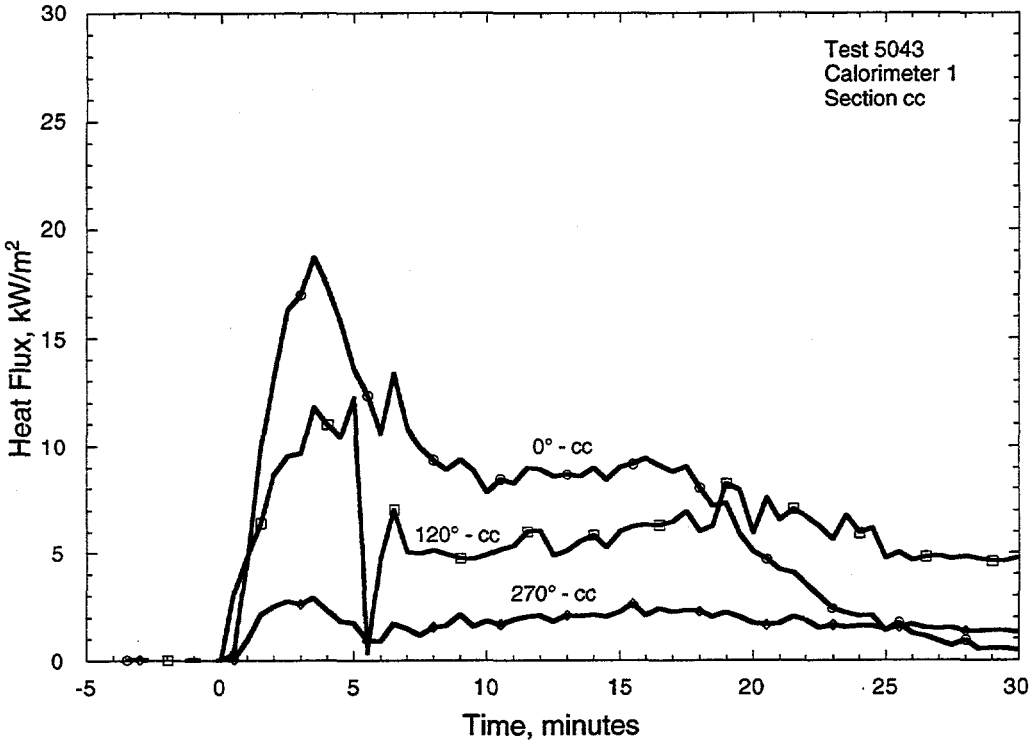

Figure D.19: Heat Flux response for Calorimeter 1, section cc

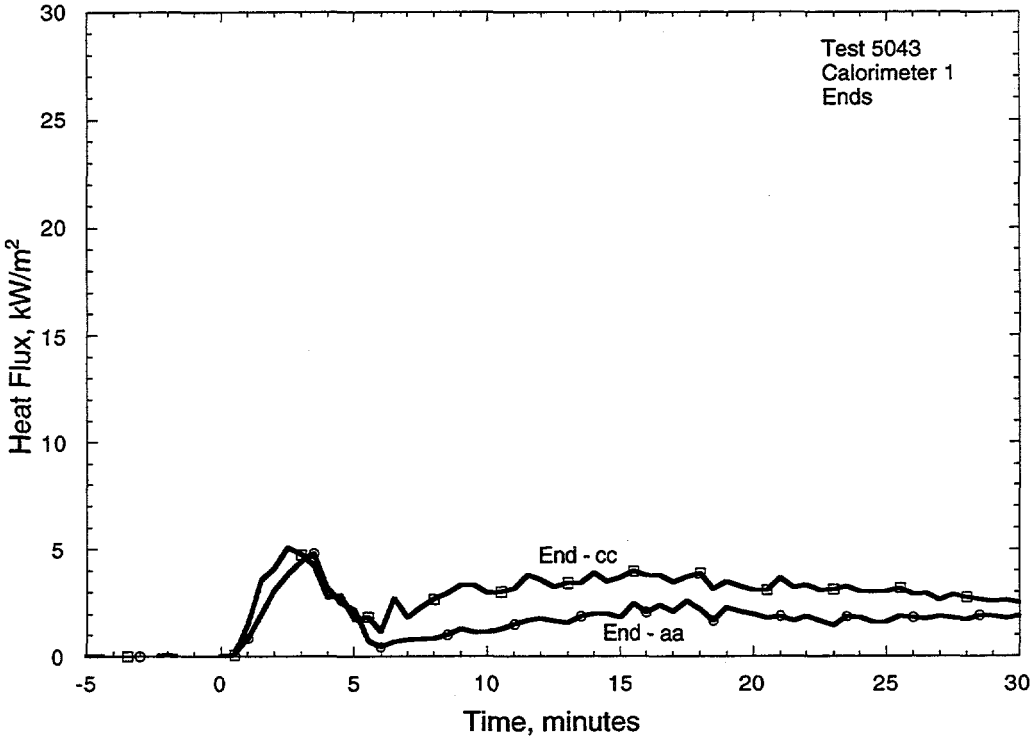

Figure D.20: Heat Flux response for Calorimeter 1, ends

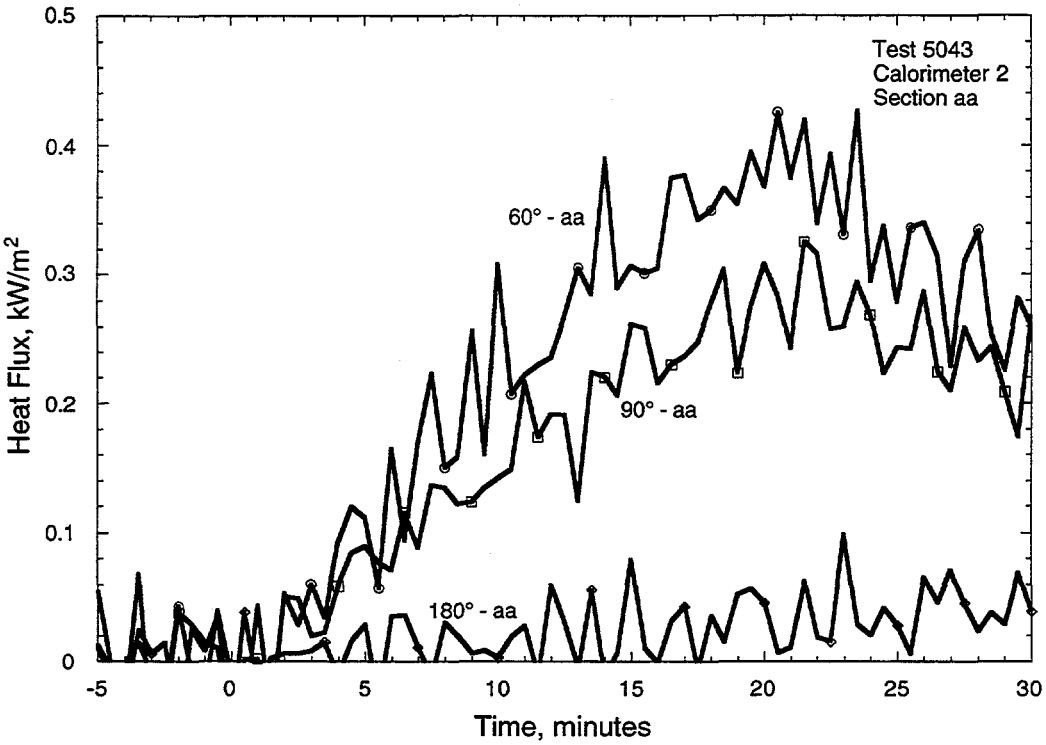

Figure D.21: Heat Flux response for Calorimeter 2, section aa

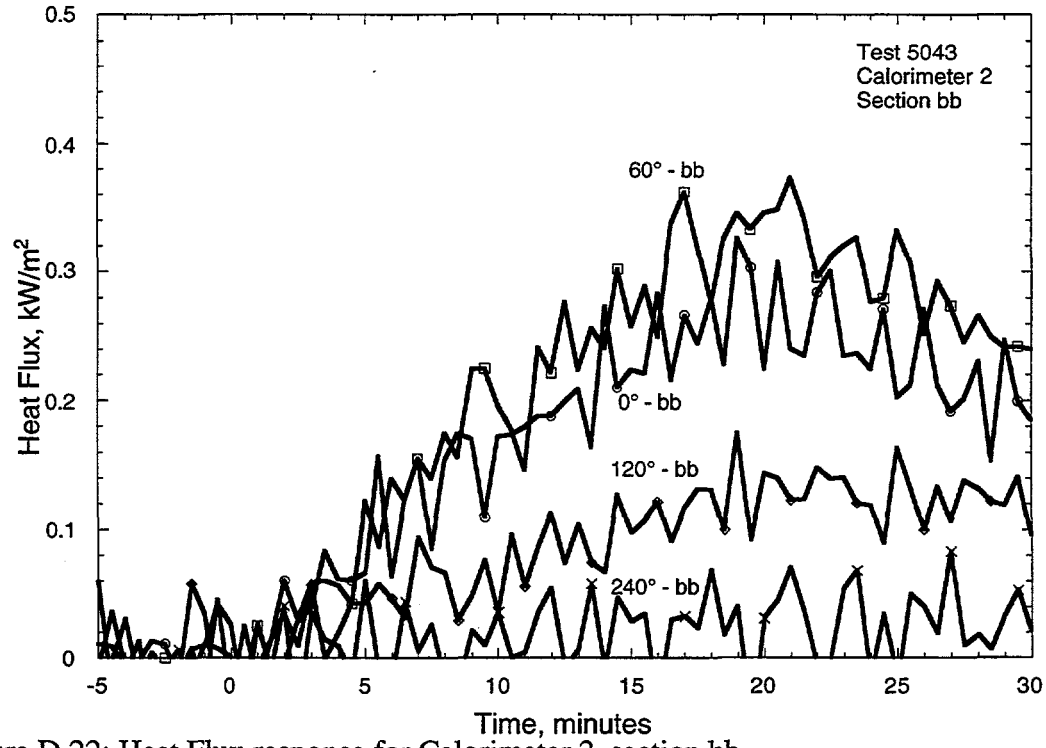

Figure D.22: Heat Flux response for Calorimeter 2, section bb

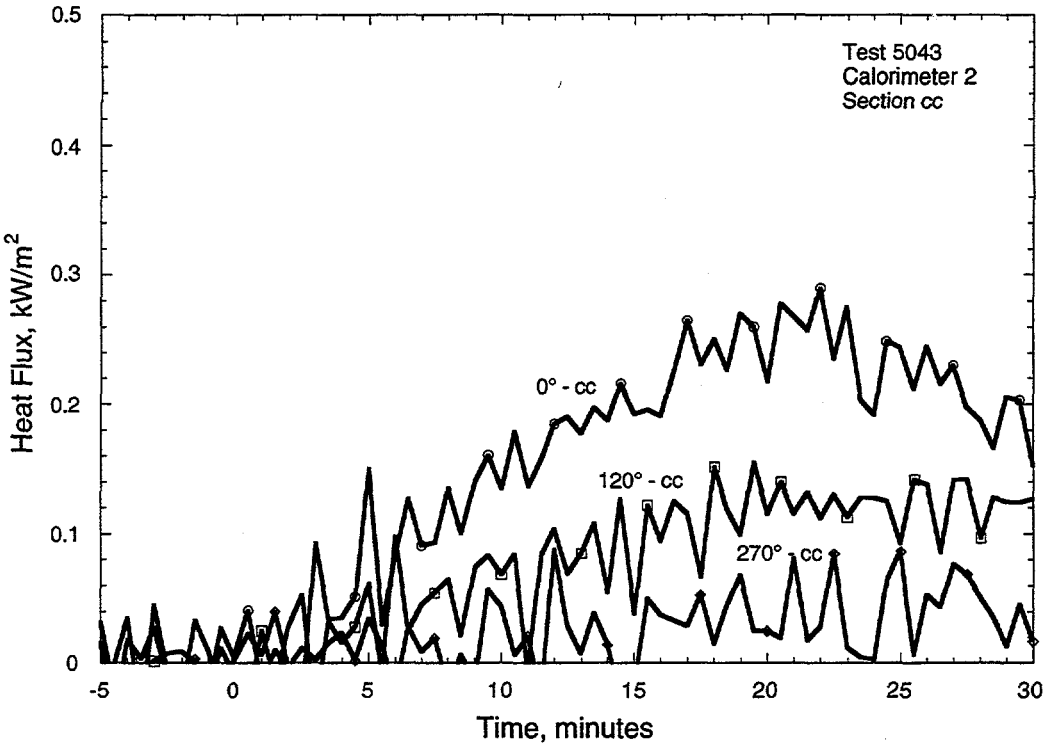

Figure D.23: Heat Flux response for Calorimeter 2, section cc

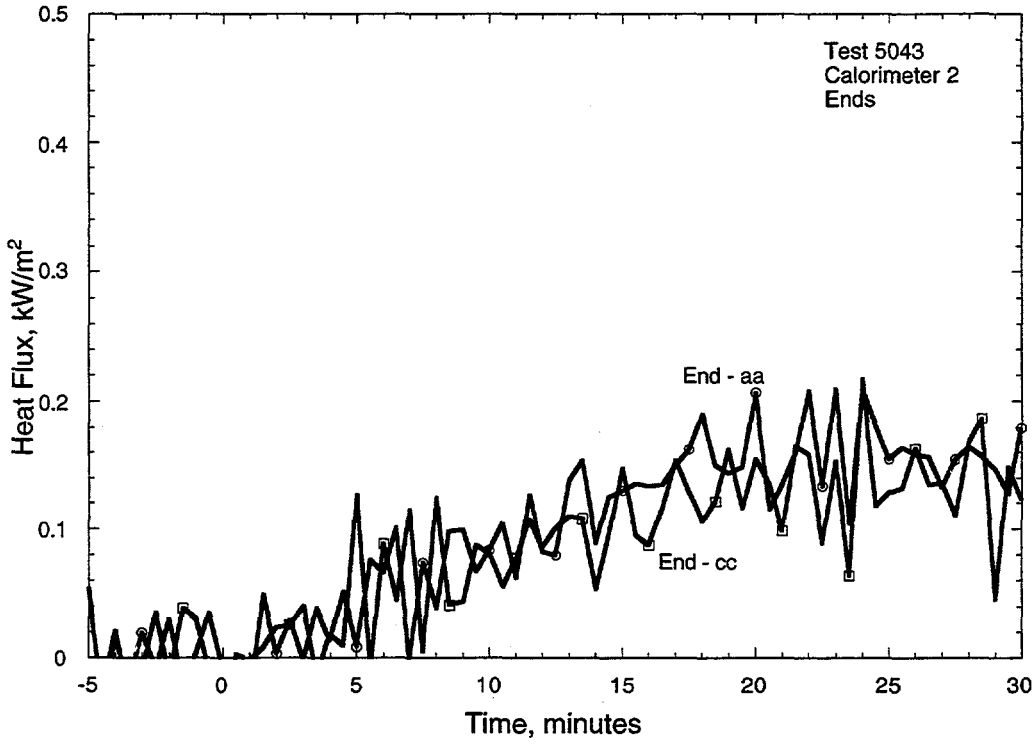

Figure D.24: Heat Flux response for Calorimeter 2, ends

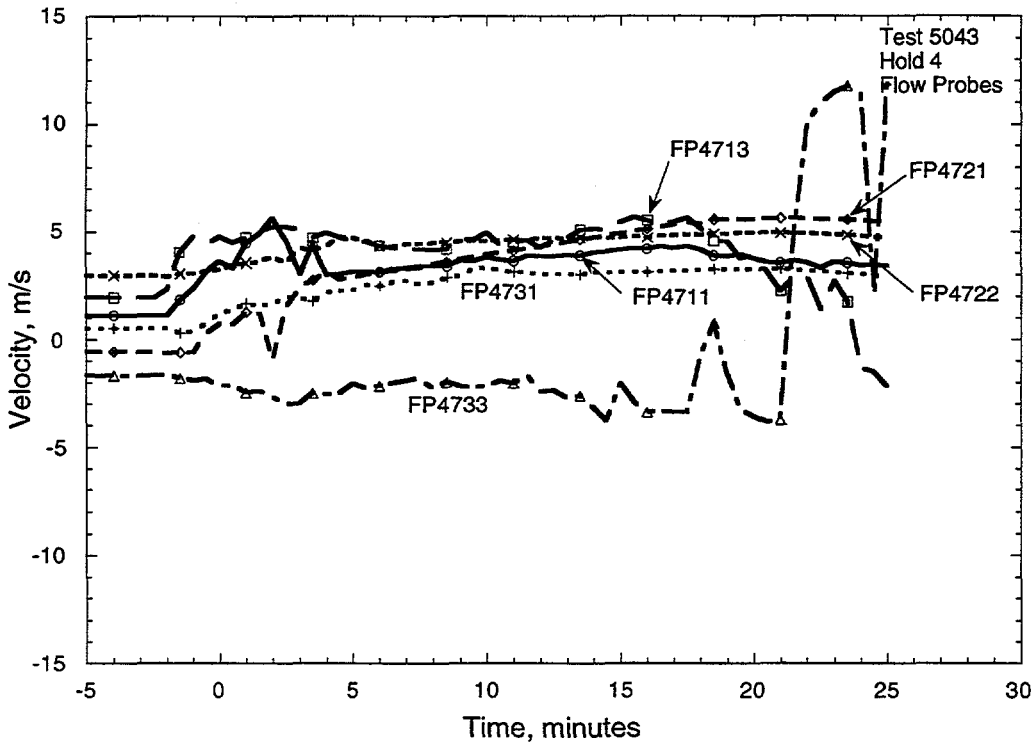

Figure D.25: Flow probes for Hold 4

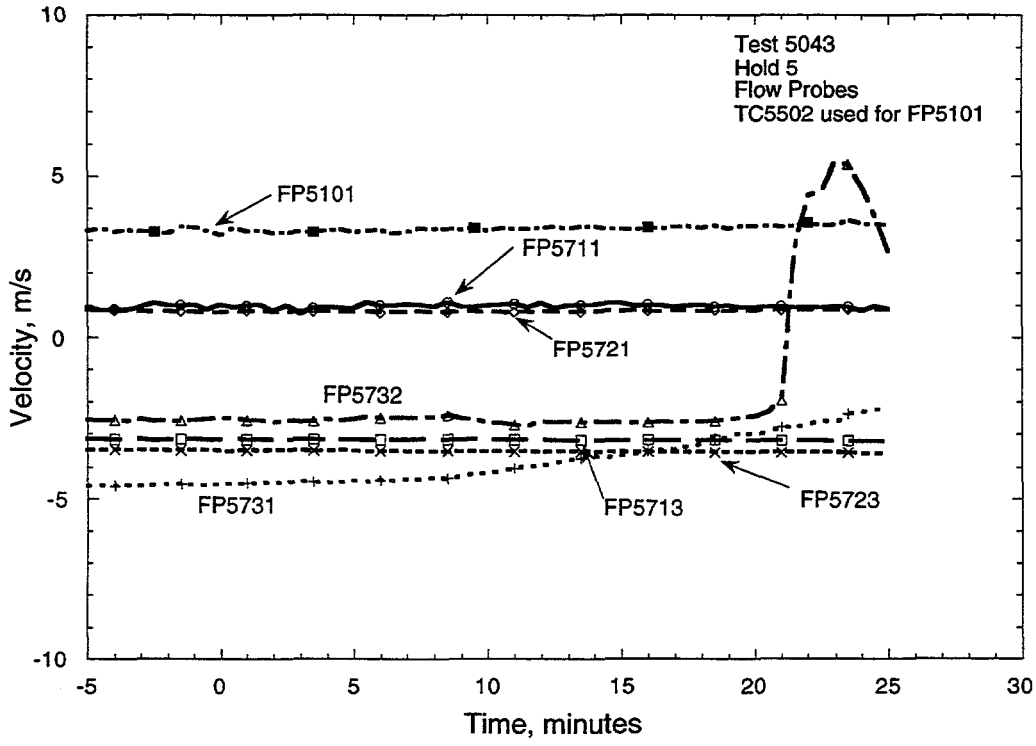

Figure D.26: Flow probes for Hold 5

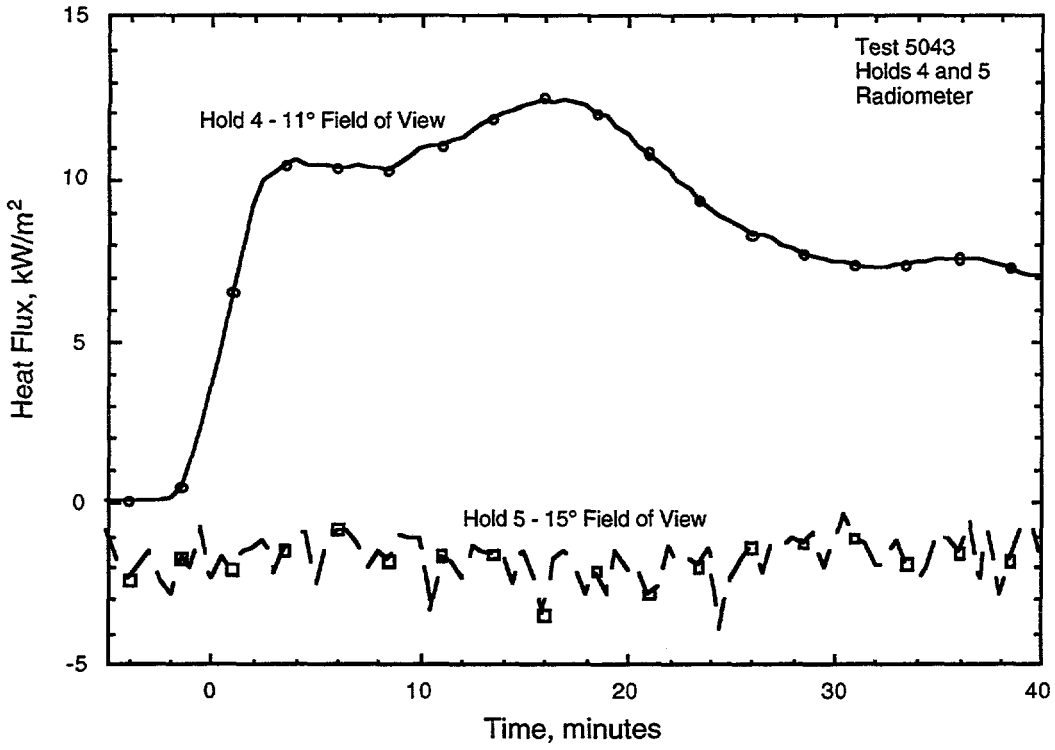

Figure D.27: Holds 4 & 5 Radiation Plot

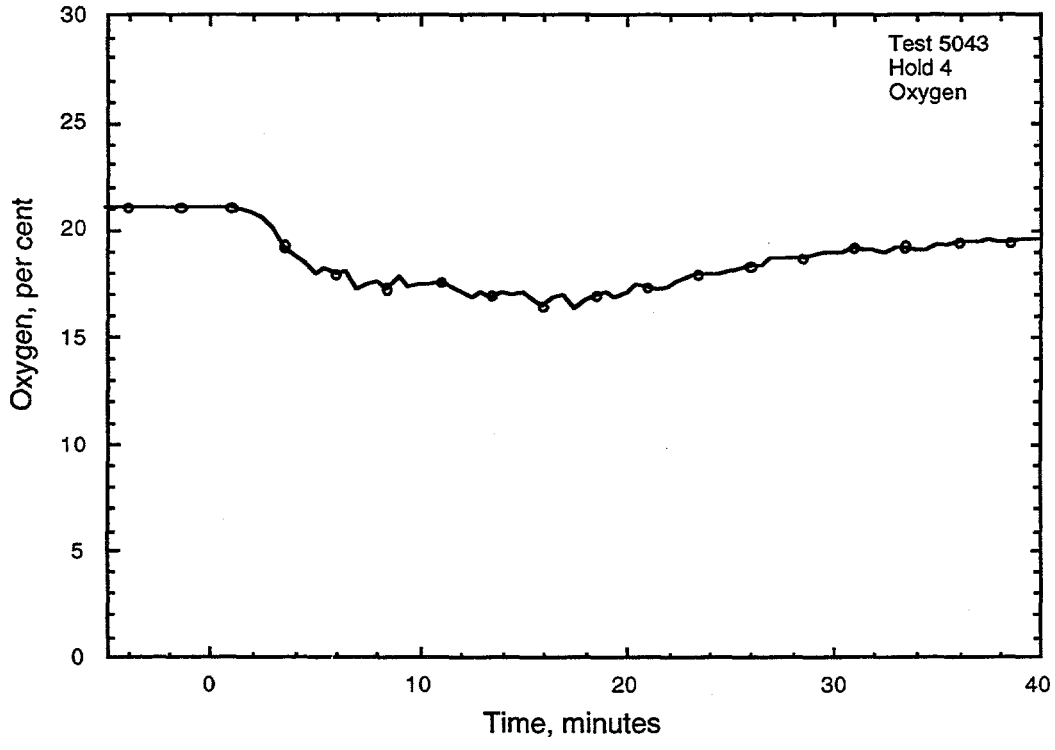

Figure D.28: Oxygen Plot

Appendix E
Test 5045
Four Burner Heptane Spray Test

conducted 11/13/95
12:02 PM CDT

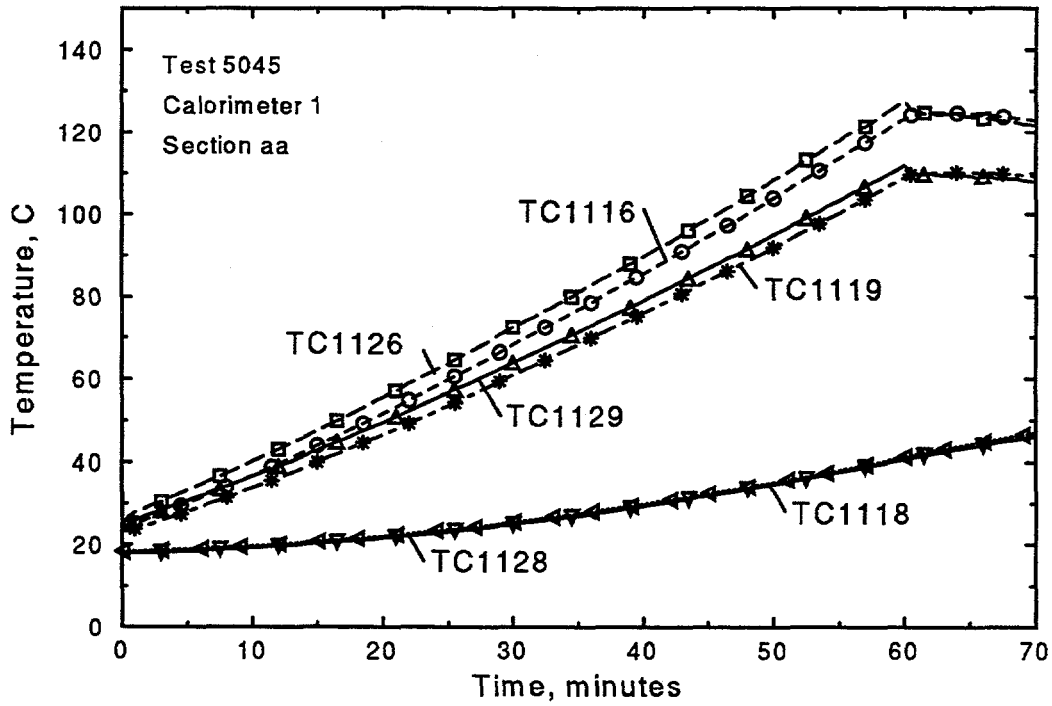

Figure E.1: Thermocouple response of Calorimeter 1, section aa

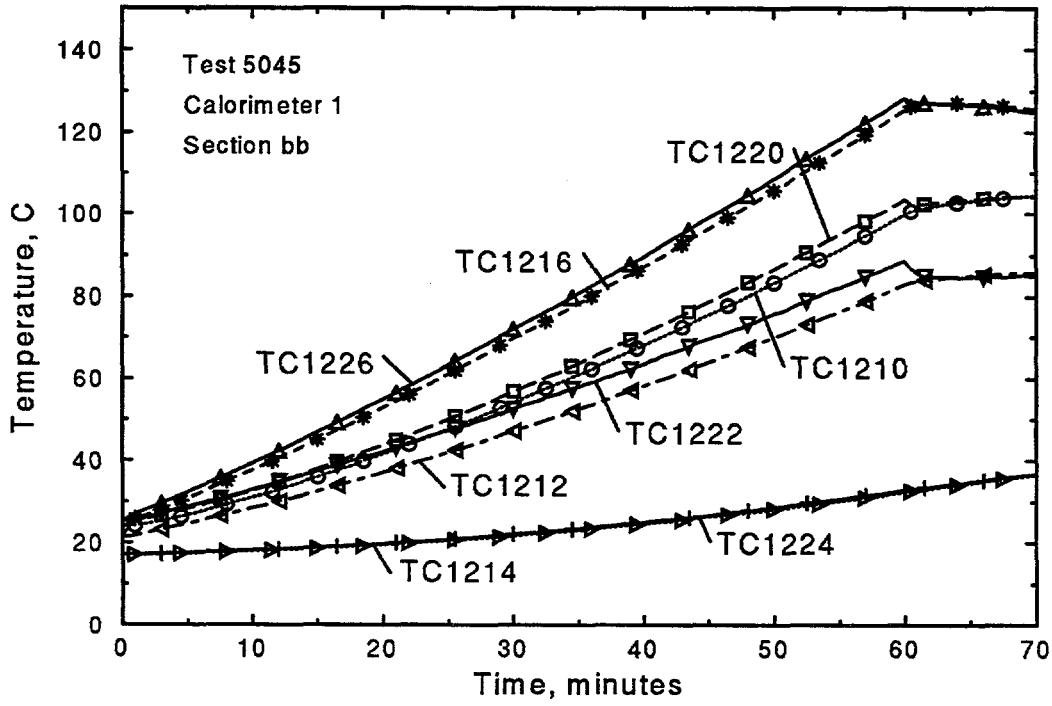

Figure E.2: Thermocouple response of Calorimeter 1, section bb

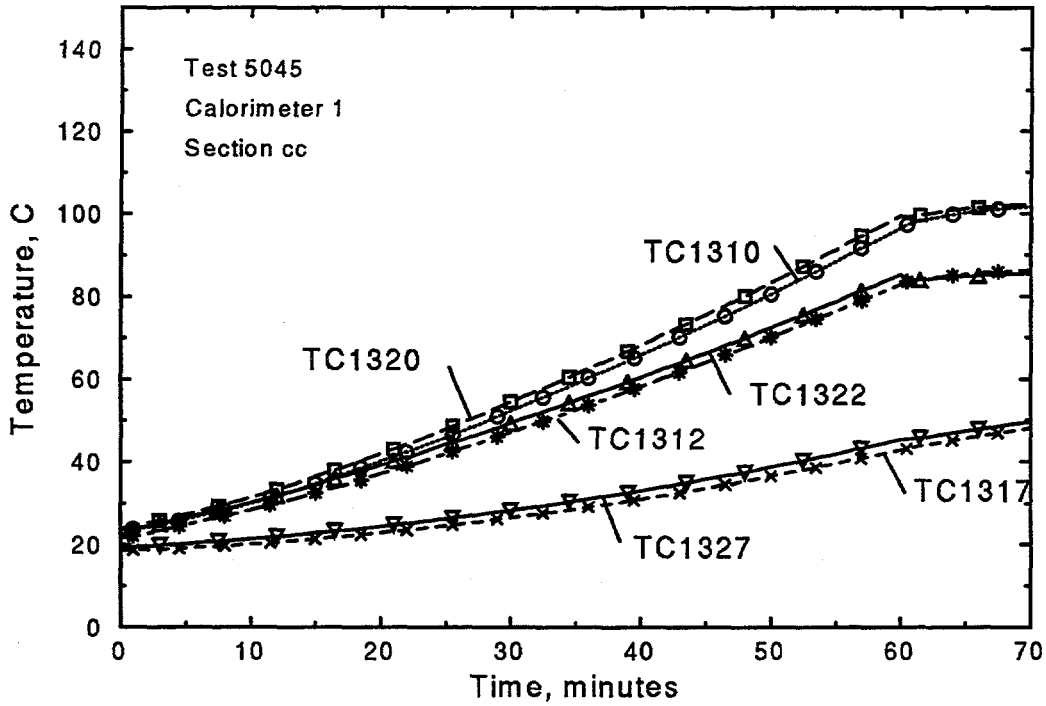

Figure E.3: Thermocouple response of Calorimeter 1, section cc

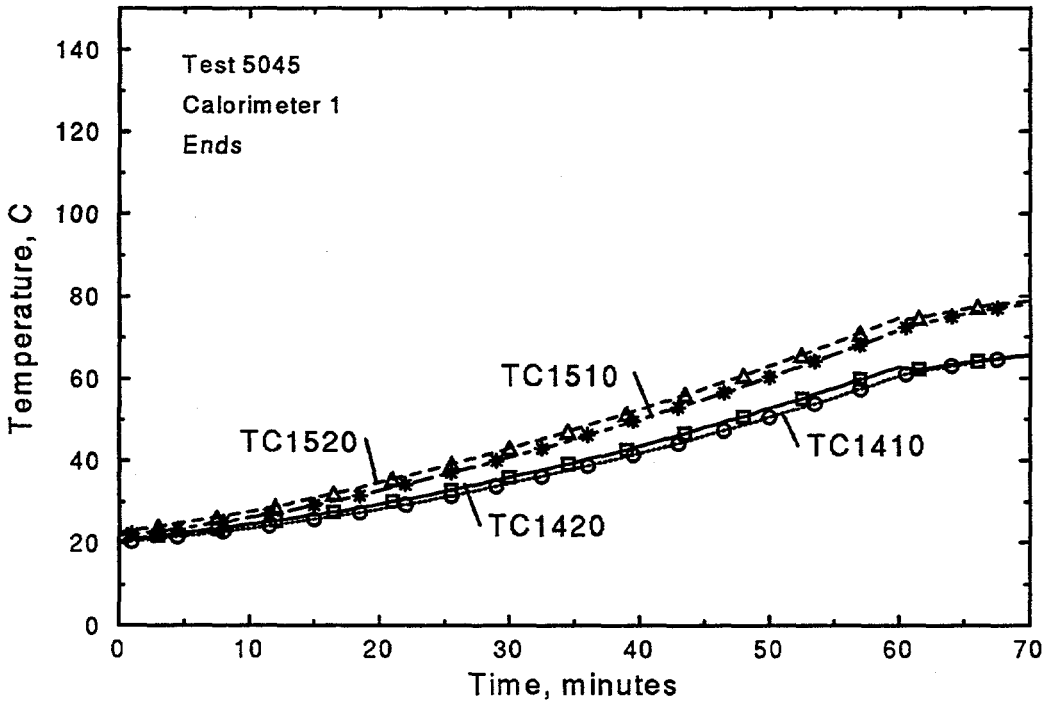

Figure E.4: Thermocouple response of Calorimeter 1, ends

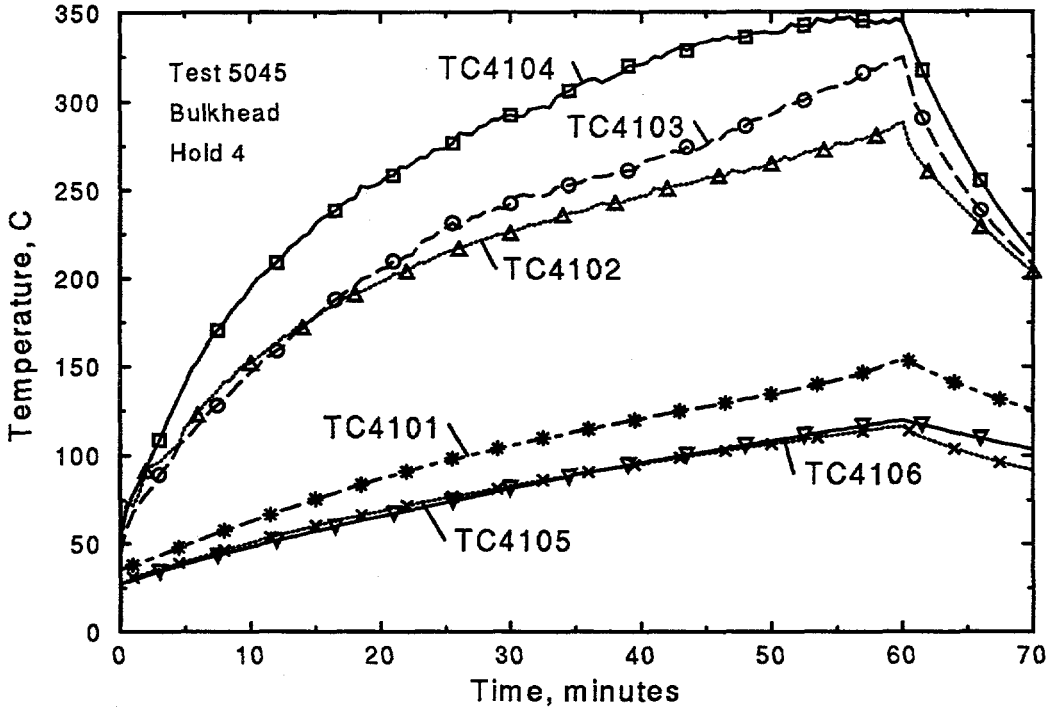

Figure E.5: Thermocouple response of Hold 4 Bulkhead

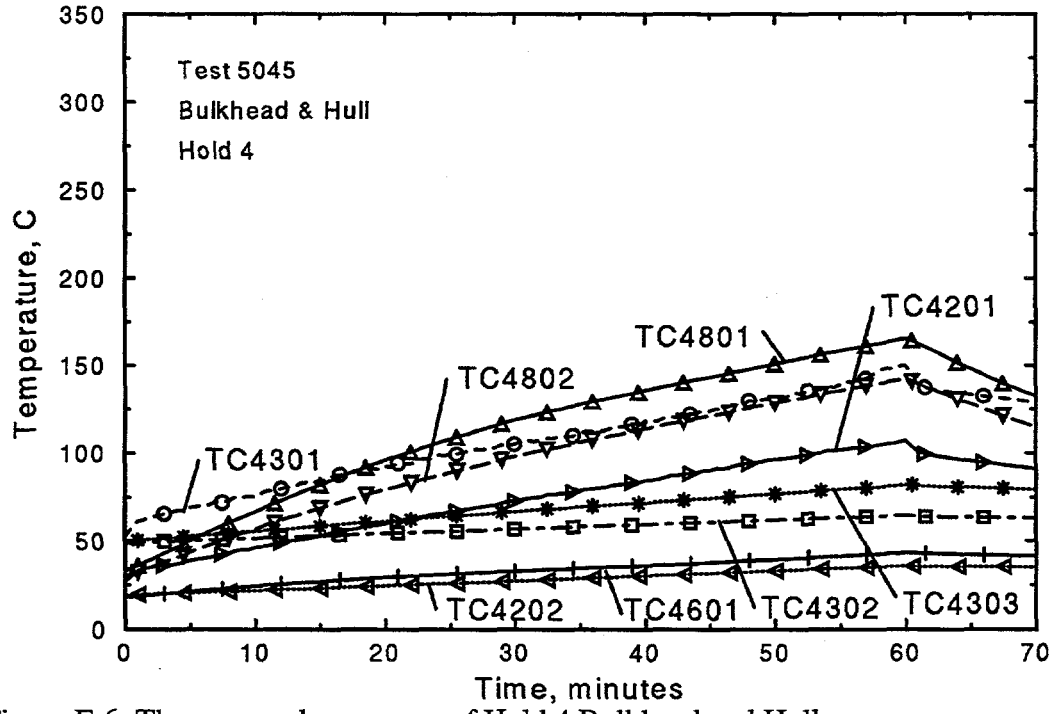

Figure E.6: Thermocouple response of Hold 4 Bulkhead and Hull

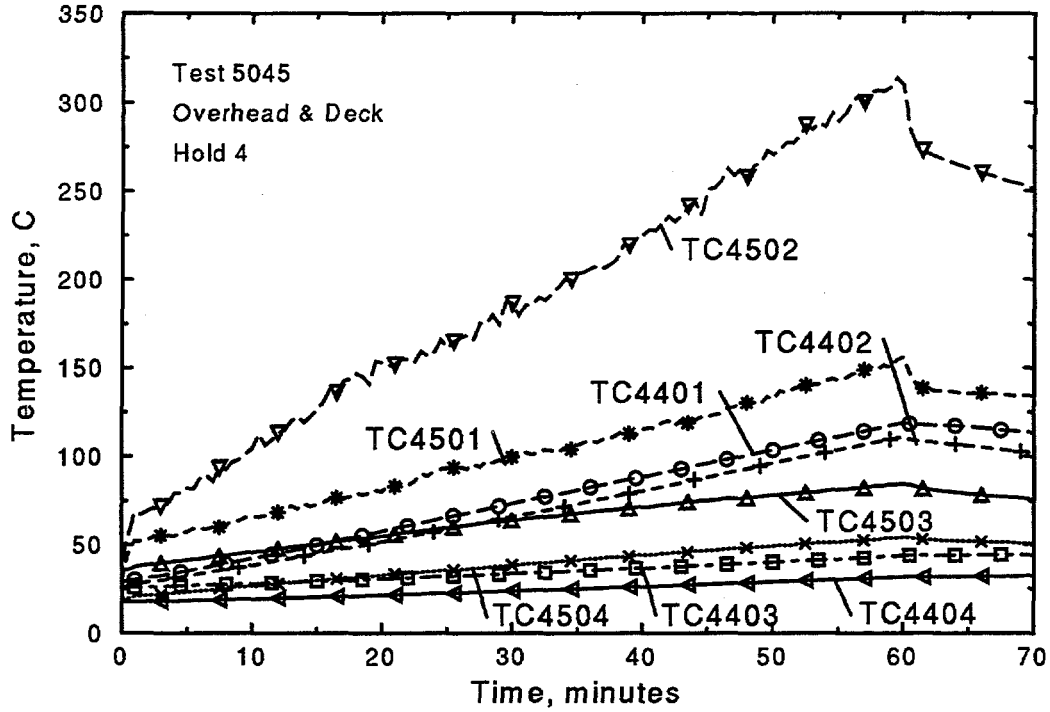

Figure E.7: Thermocouple response of Hold 4 Overhead and Deck

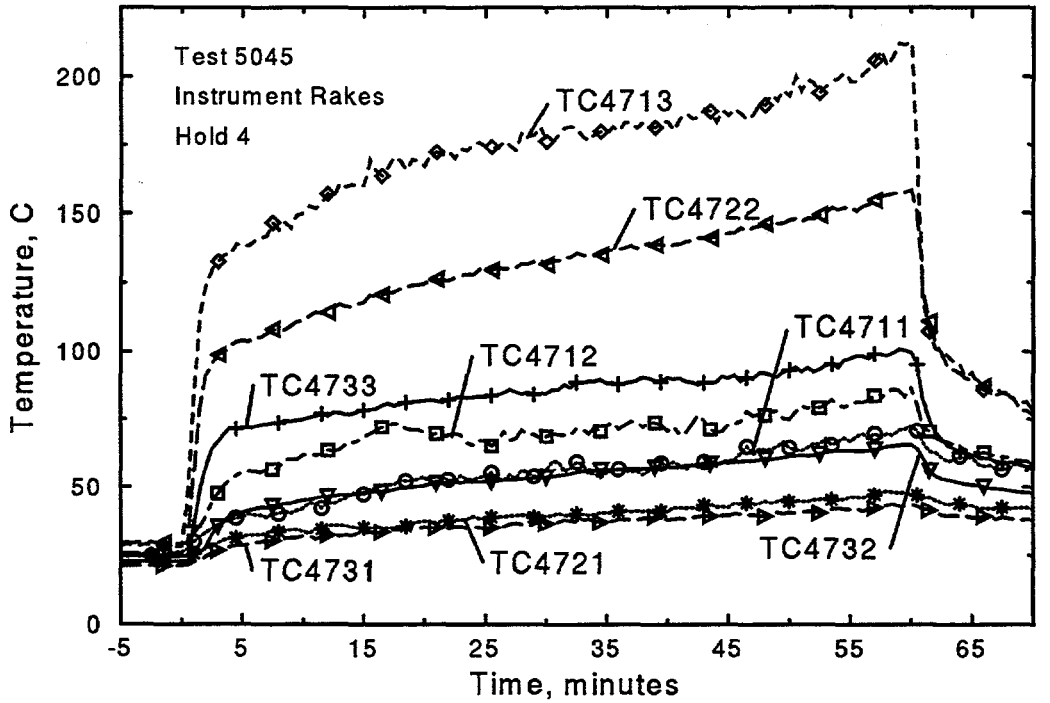

Figure E.8: Thermocouple response of Hold 4 Instrument Rakes

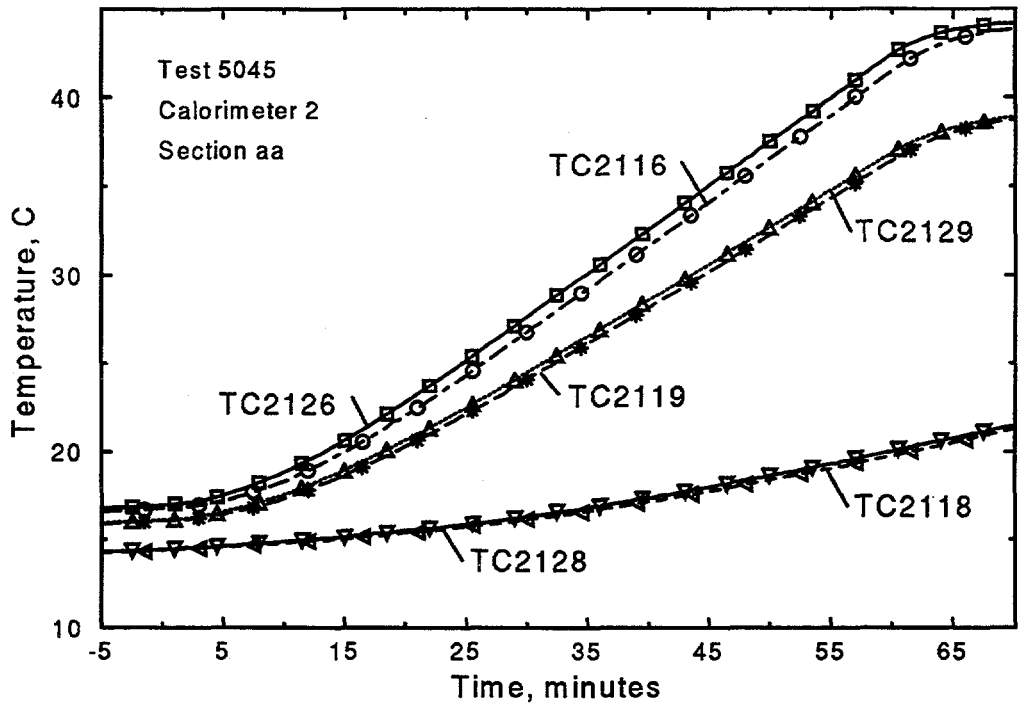

Figure E.9: Thermocouple response of Calorimeter 2, section aa

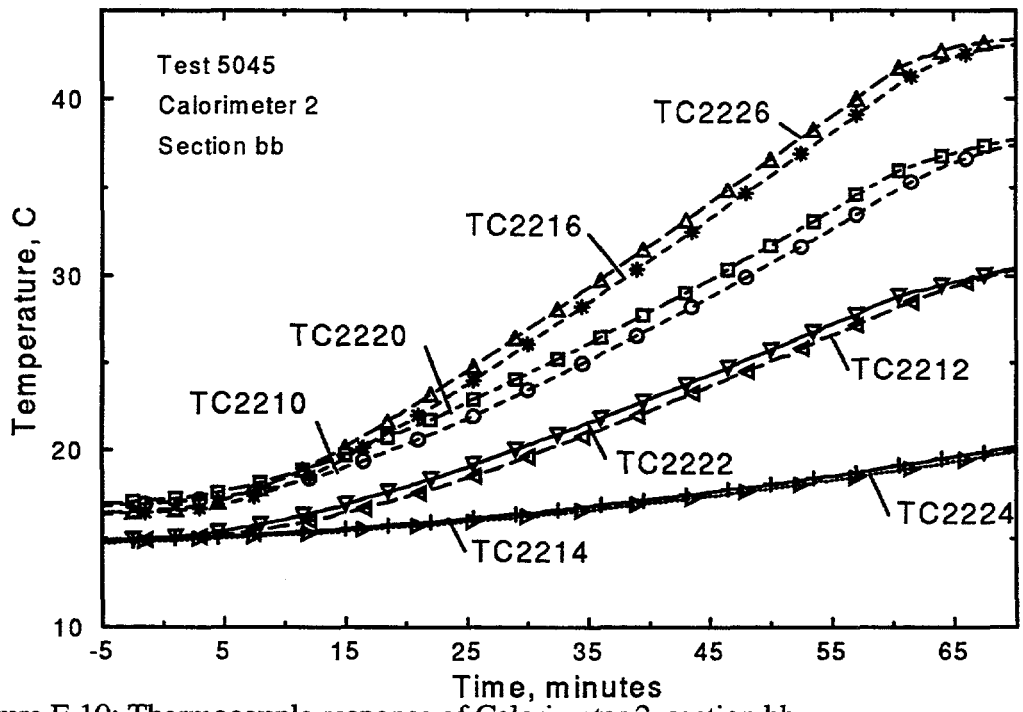

Figure E.10: Thermocouple response of Calorimeter 2, section bb

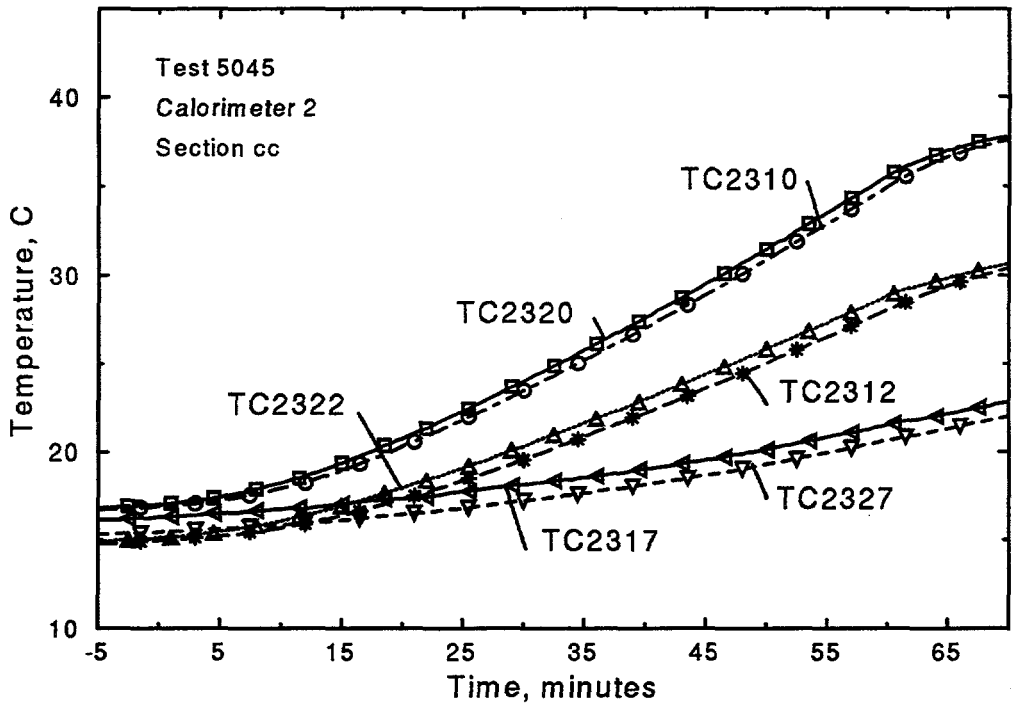

Figure E.11: Thermocouple response of Calorimeter 2, section cc

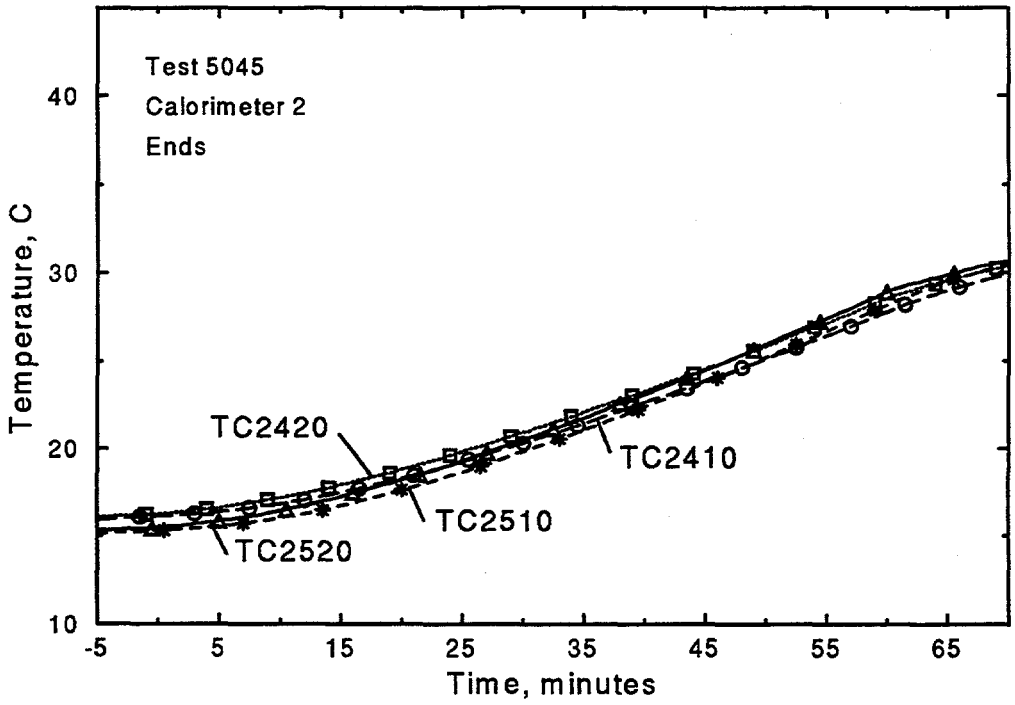

Figure E.12: Thermocouple response of Calorimeter 2, ends

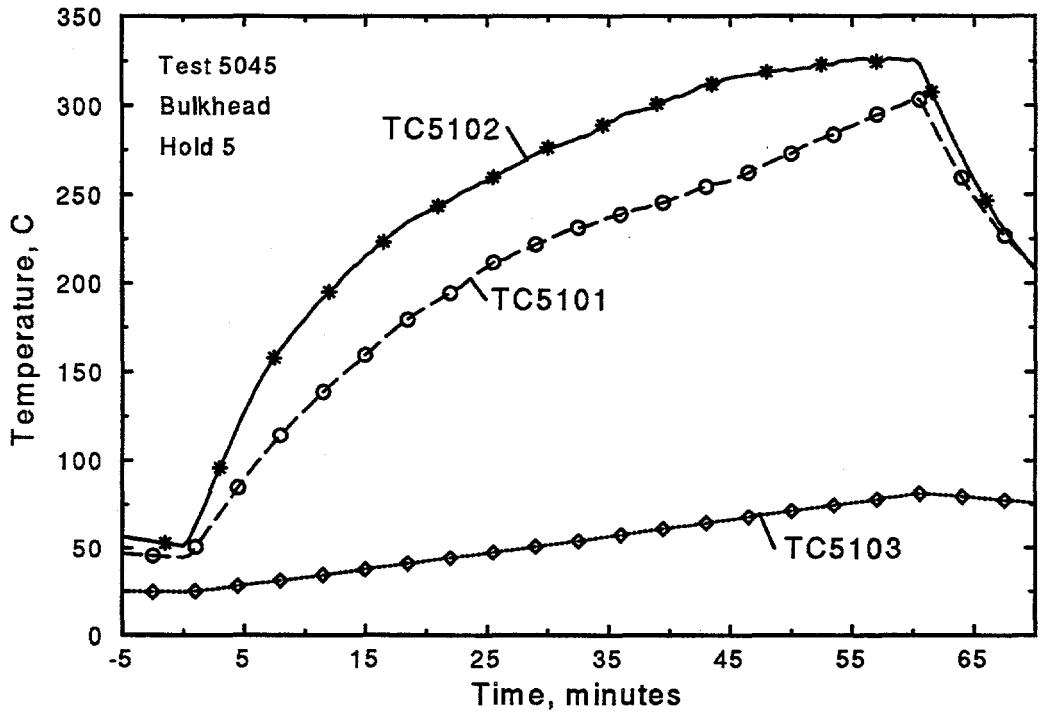

Figure E.13: Thermocouple response of Hold 5 Bulkhead

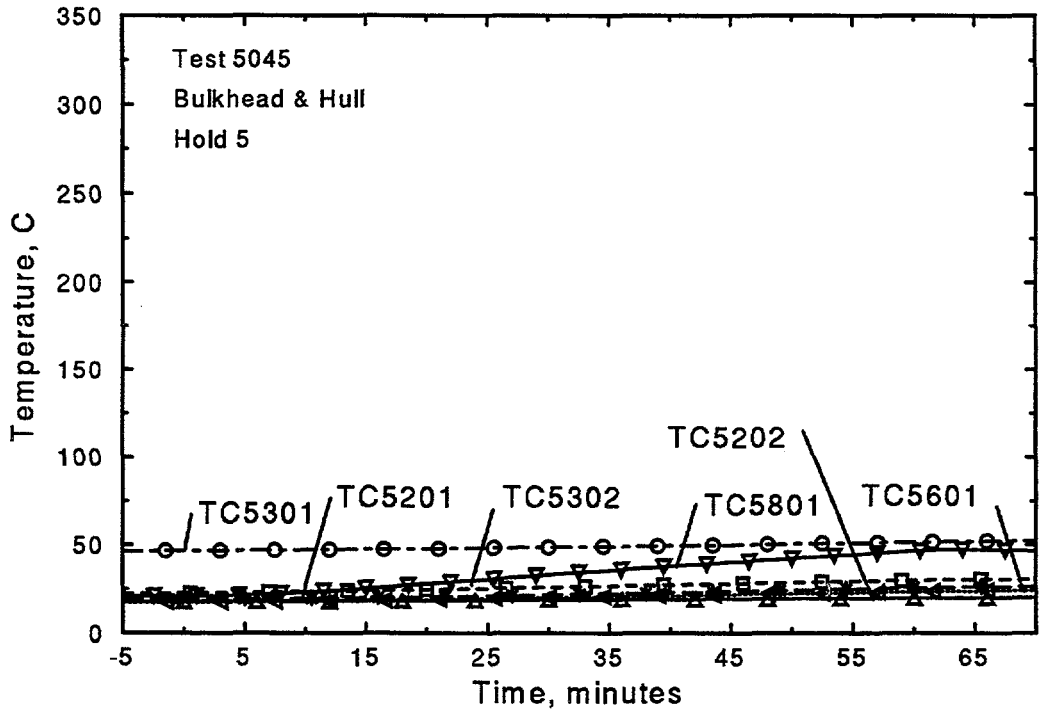

Figure E.14: Thermocouple response of Hold 5 Bulkhead and Hull

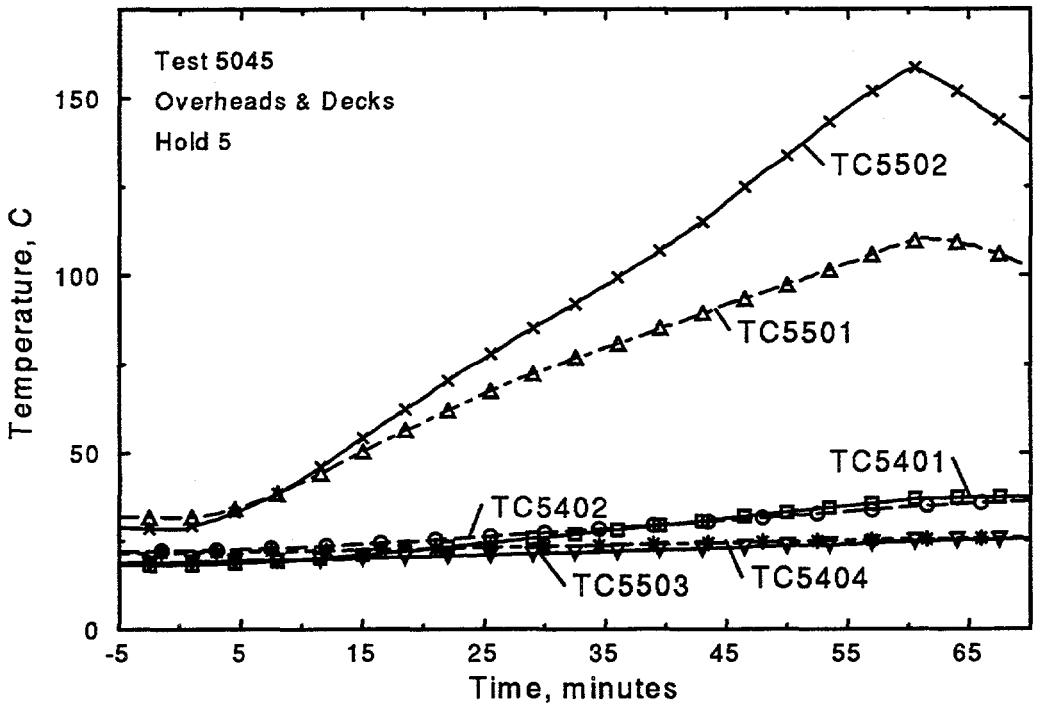

Figure E.15: Thermocouple response of Hold 5 Overhead and Deck

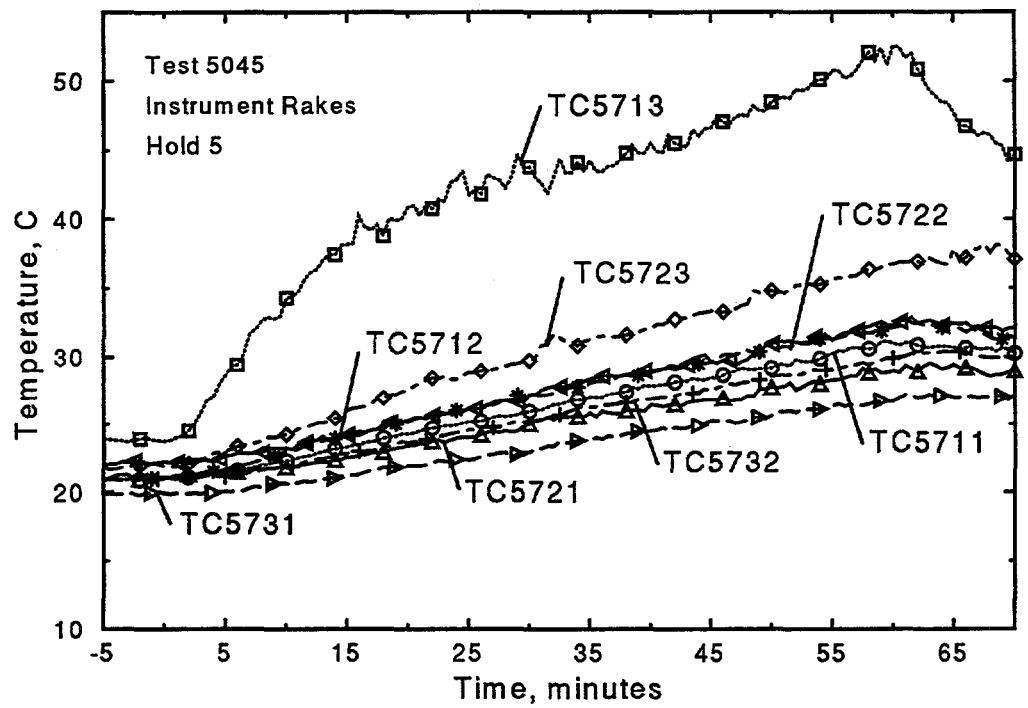

Figure E.16: Thermocouple response of Hold 5 Instrument Rakes

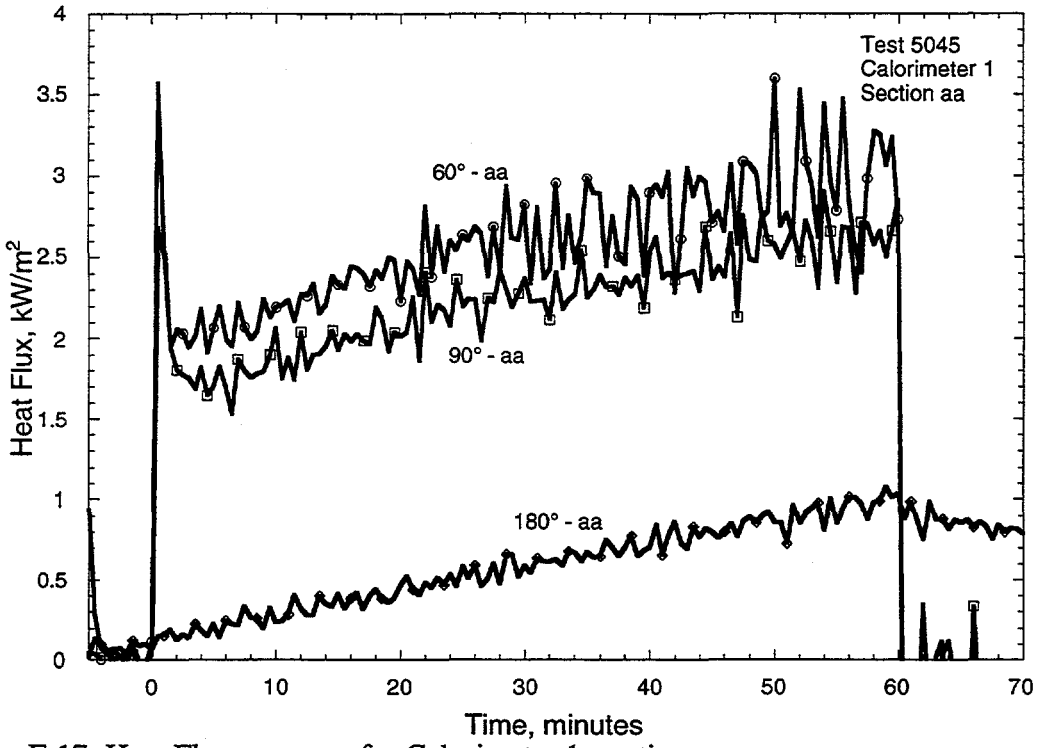

Figure E.17: Heat Flux response for Calorimeter 1, section aa

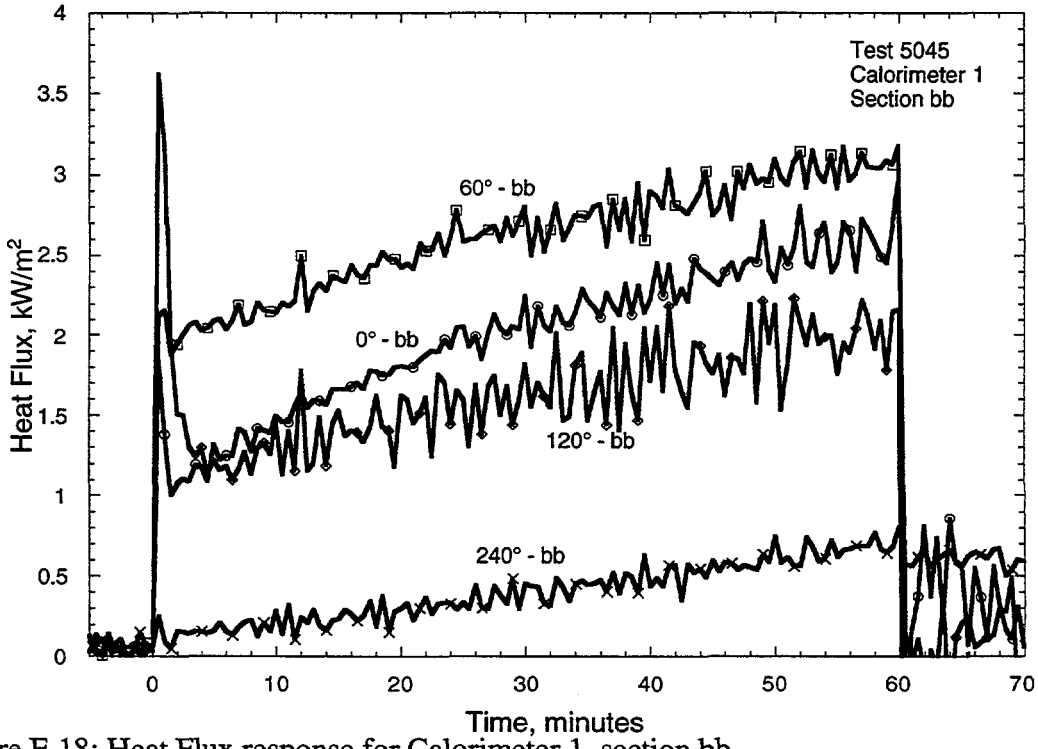

Figure E.18: Heat Flux response for Calorimeter 1, section bb

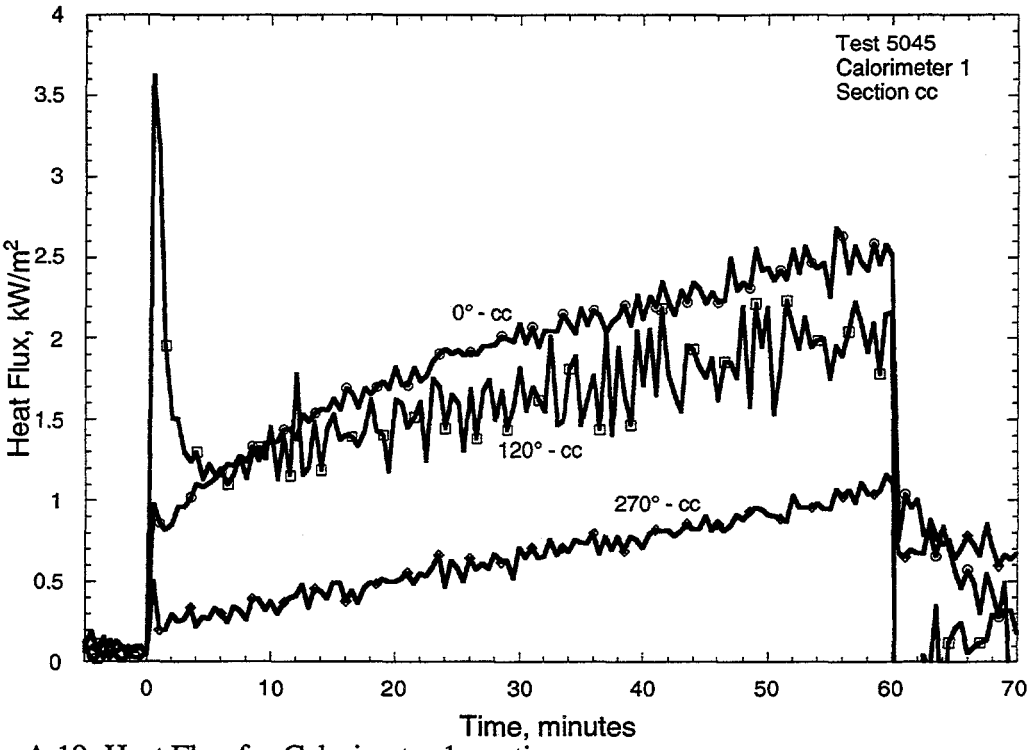

Figure A.19: Heat Flux for Calorimeter 1, section cc

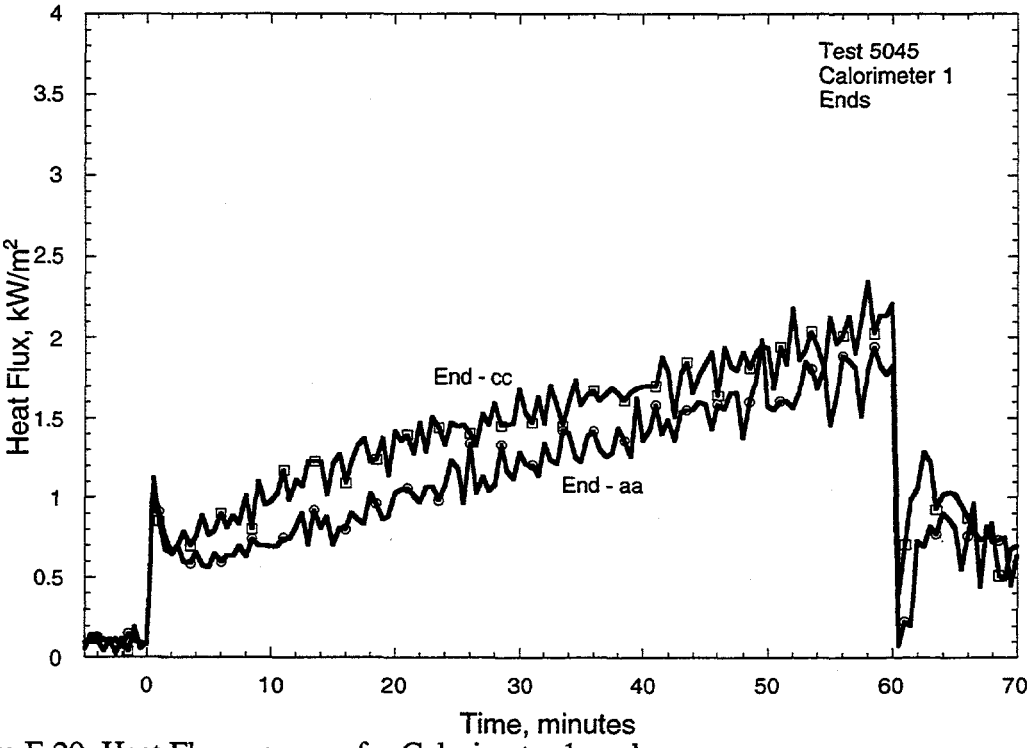

Figure E.20: Heat Flux response for Calorimeter 1, ends

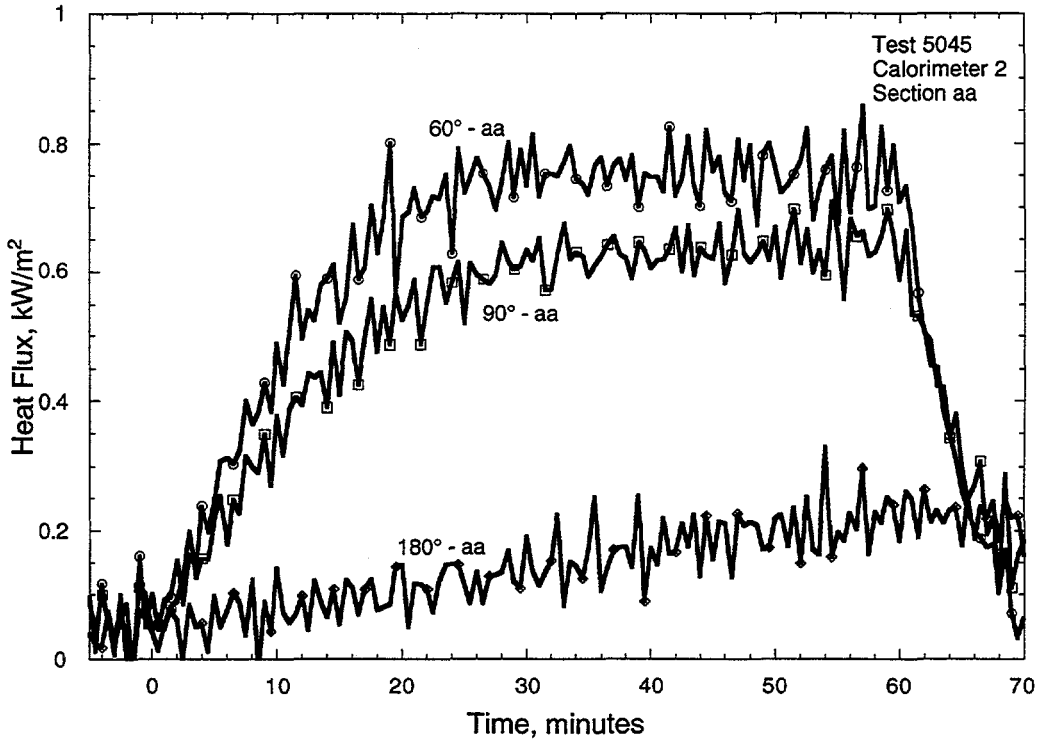

Figure E.21: Heat Flux response for Calorimeter 2, section aa

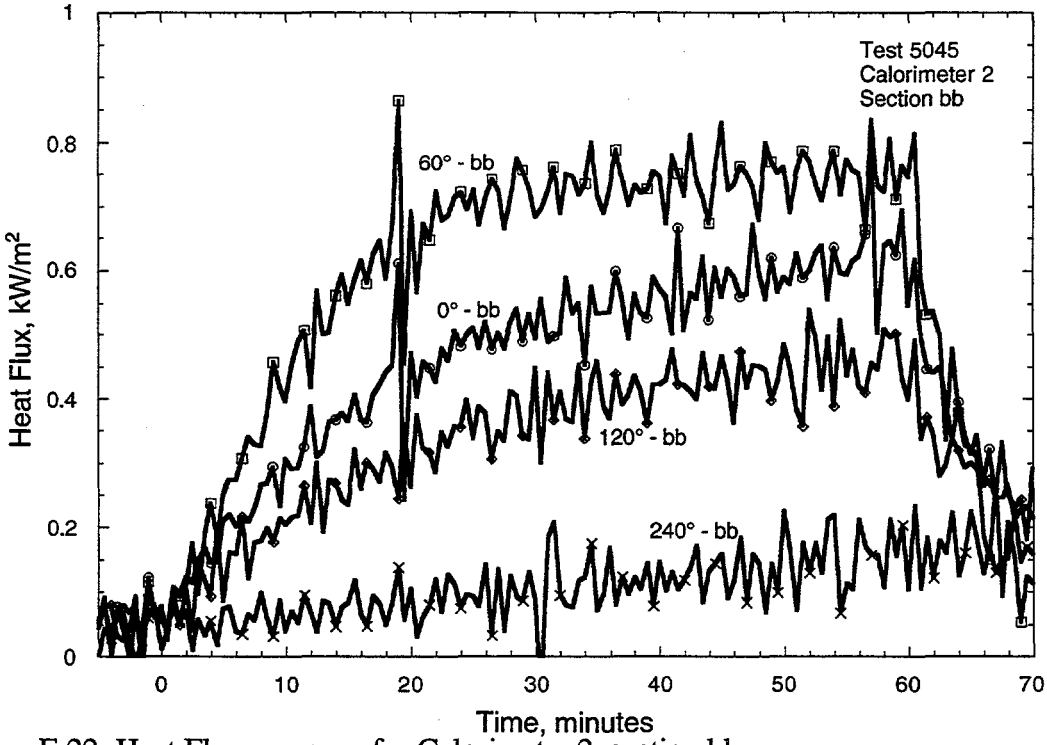

Figure E.22: Heat Flux response for Calorimeter 2, section bb

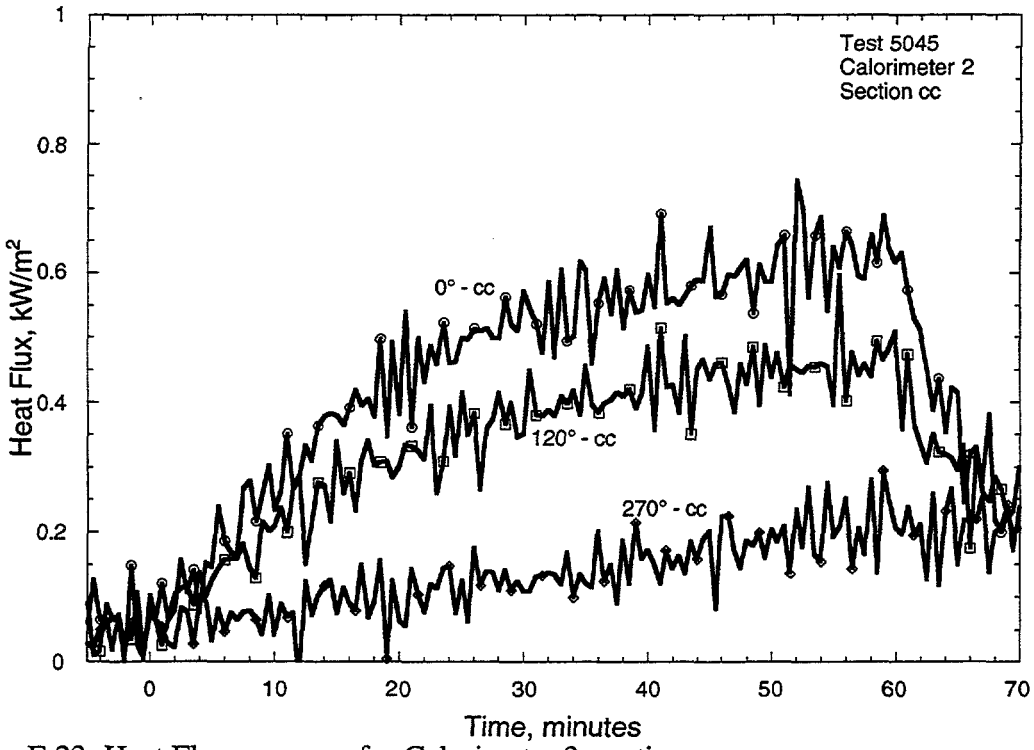

Figure E.23: Heat Flux response for Calorimeter 2, section cc

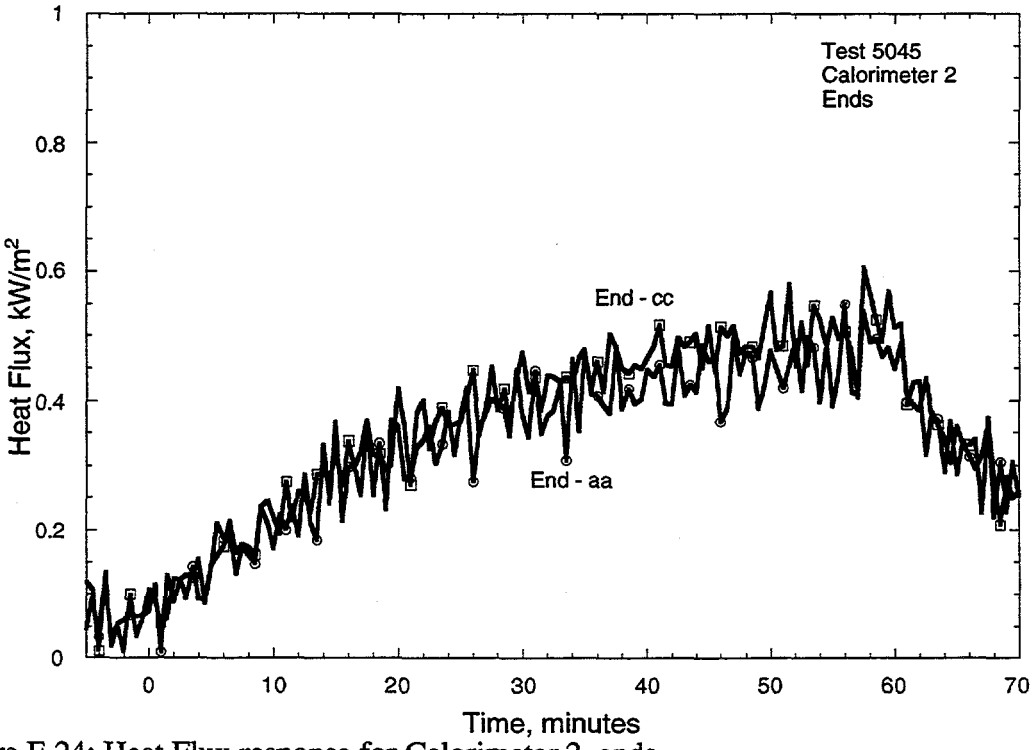

Figure E.24: Heat Flux response for Calorimeter 2, ends

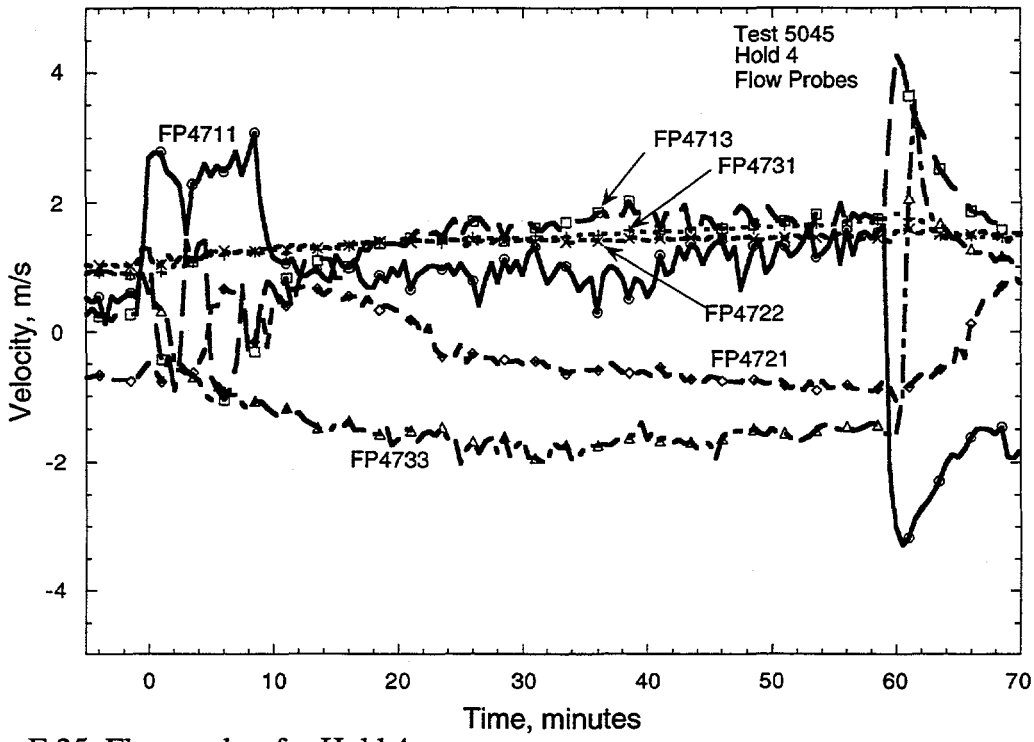

Figure E.25: Flow probes for Hold 4

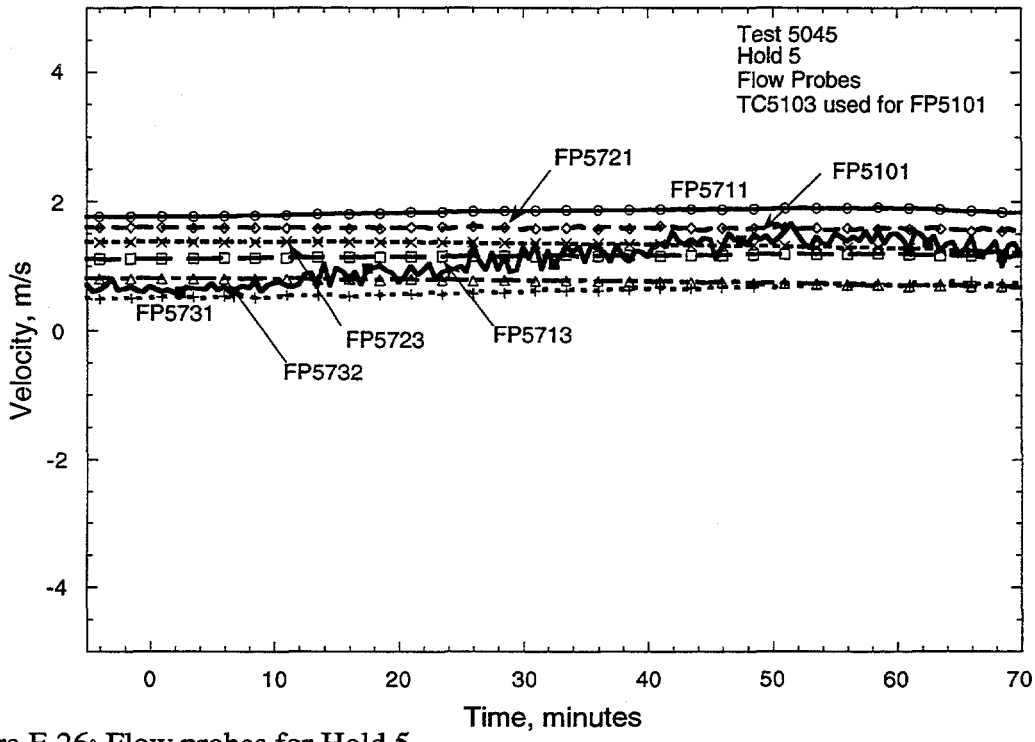

Figure E.26: Flow probes for Hold 5

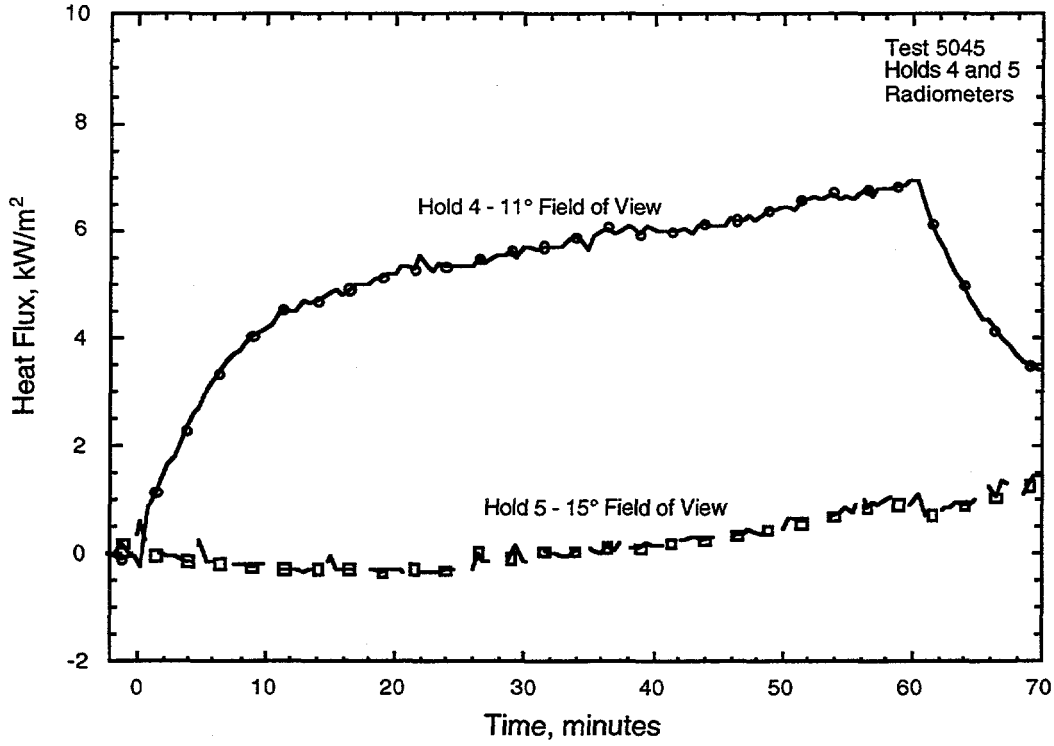

Figure E.27: Holds 4 & 5 Radiation Plot

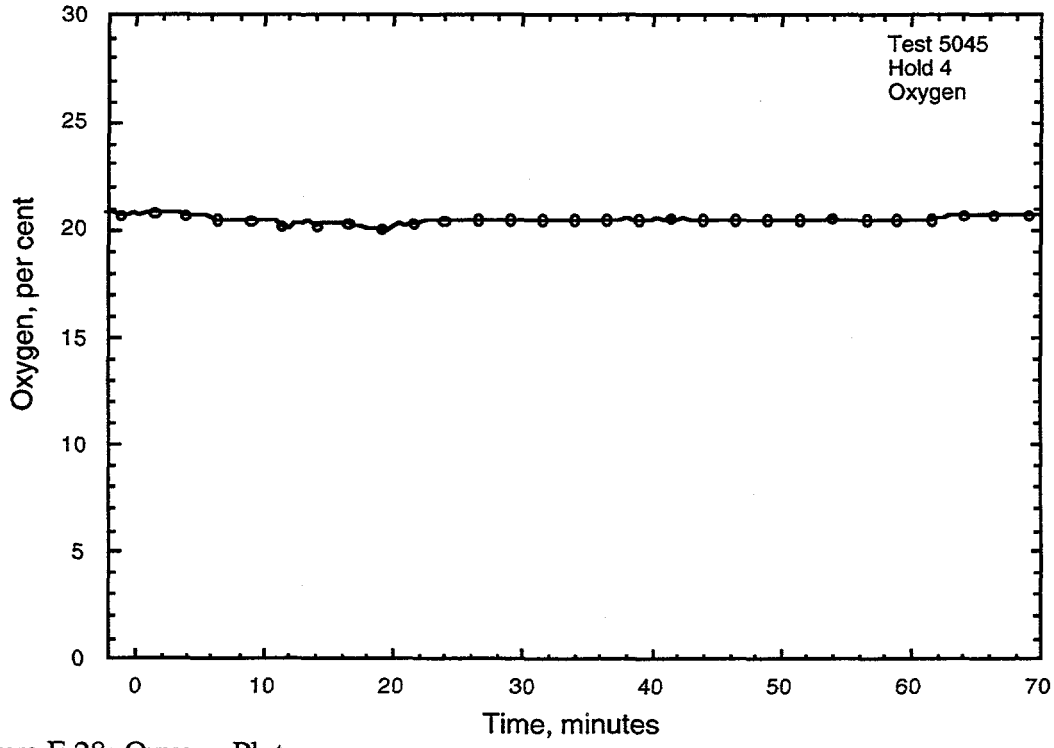

Figure E.28: Oxygen Plot

Appendix F
Test 5046
Four Burner Heptane Spray Test with Smoke

conducted 11/13/95
2:46 PM CDT

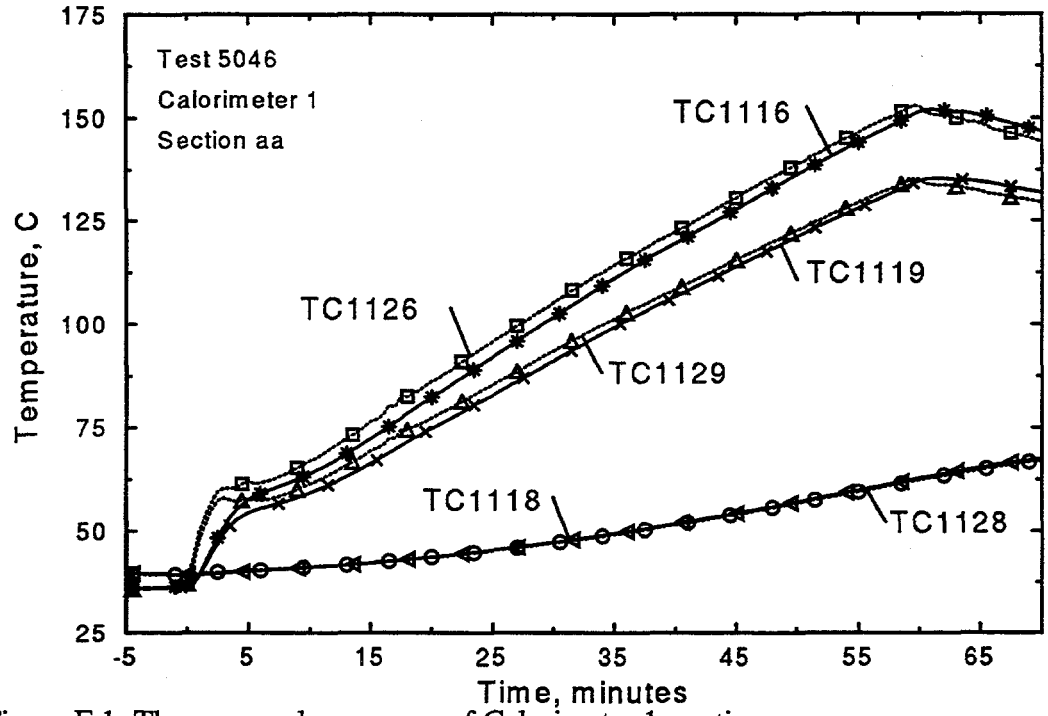

Figure F.1: Thermocouple response of Calorimeter 1, section aa

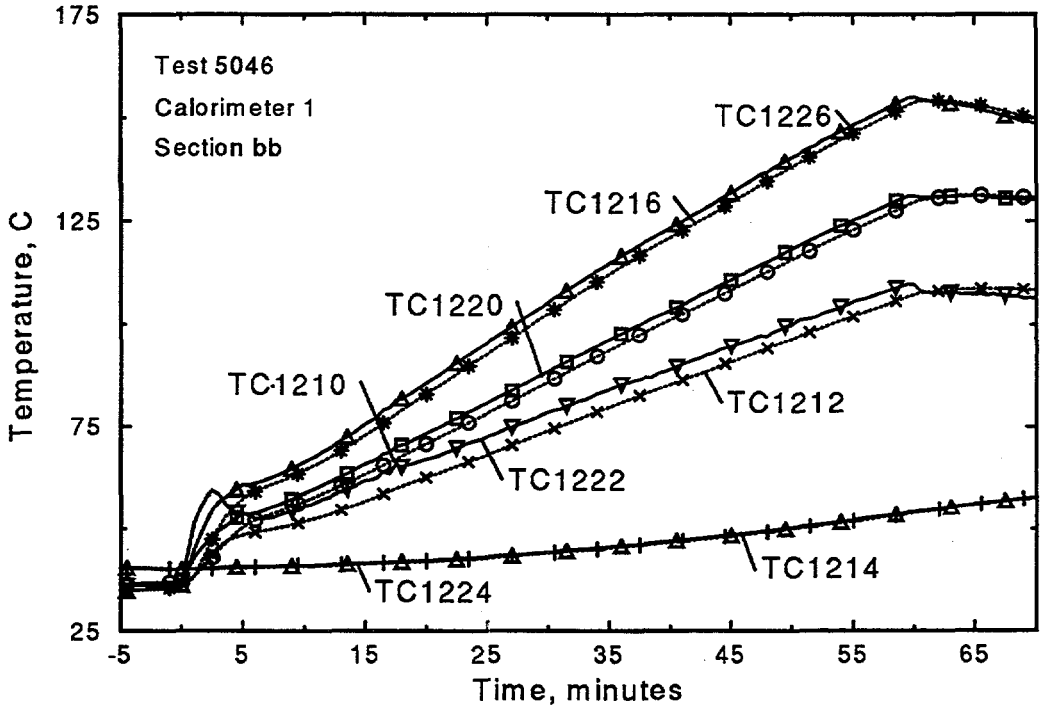

Figure F.2: Thermocouple response of Calorimeter 1, section bb

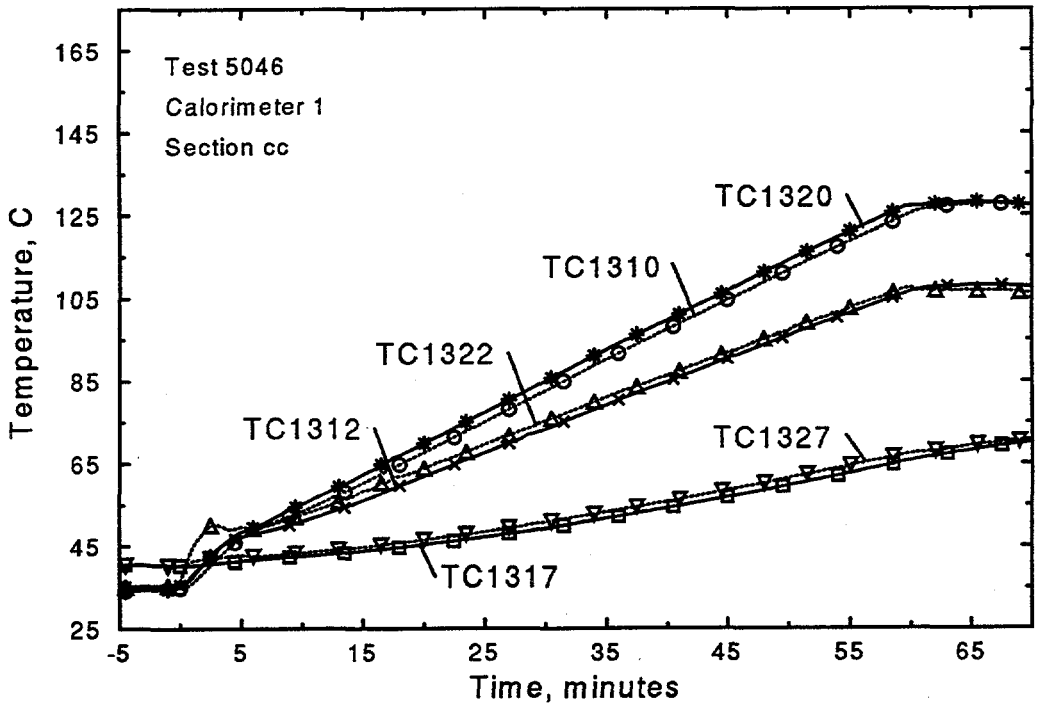

Figure F.3: Thermocouple response of Calorimeter 1, section cc

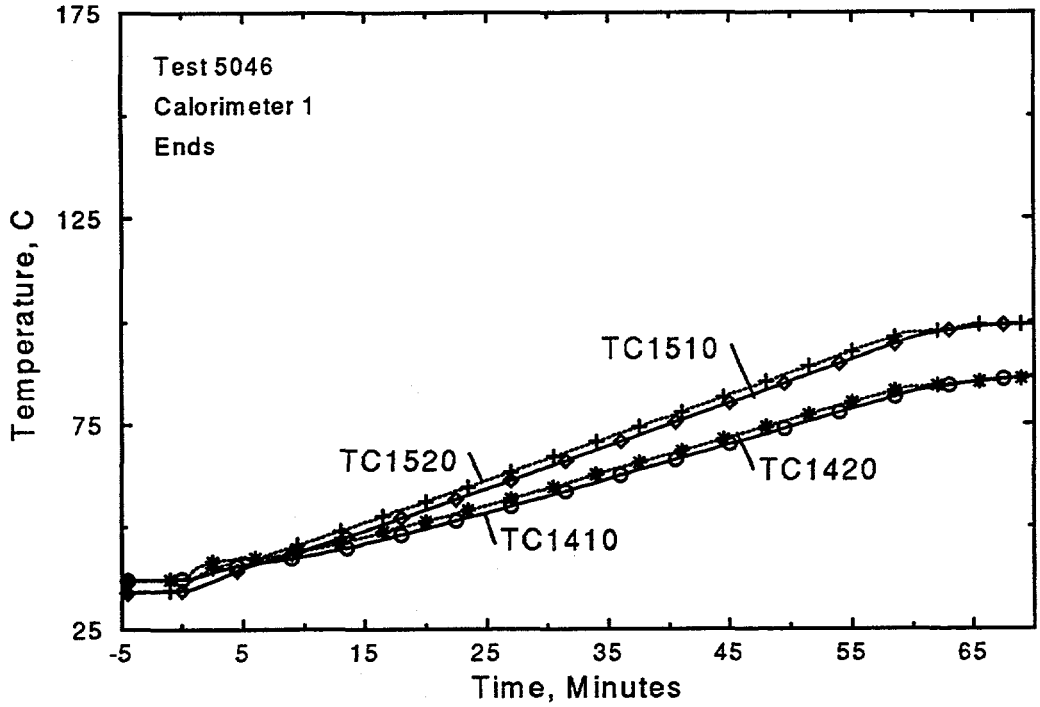

Figure F.4: Thermocouple response of Calorimeter 1, ends

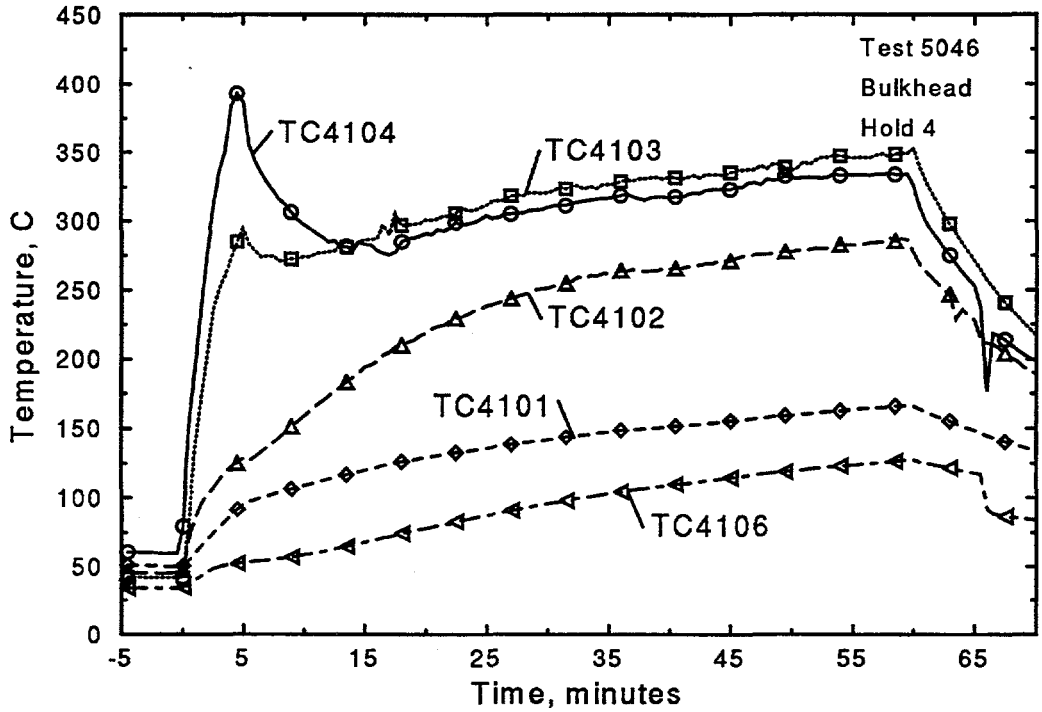

Figure F.5: Thermocouple response of Hold 4 Bulkhead

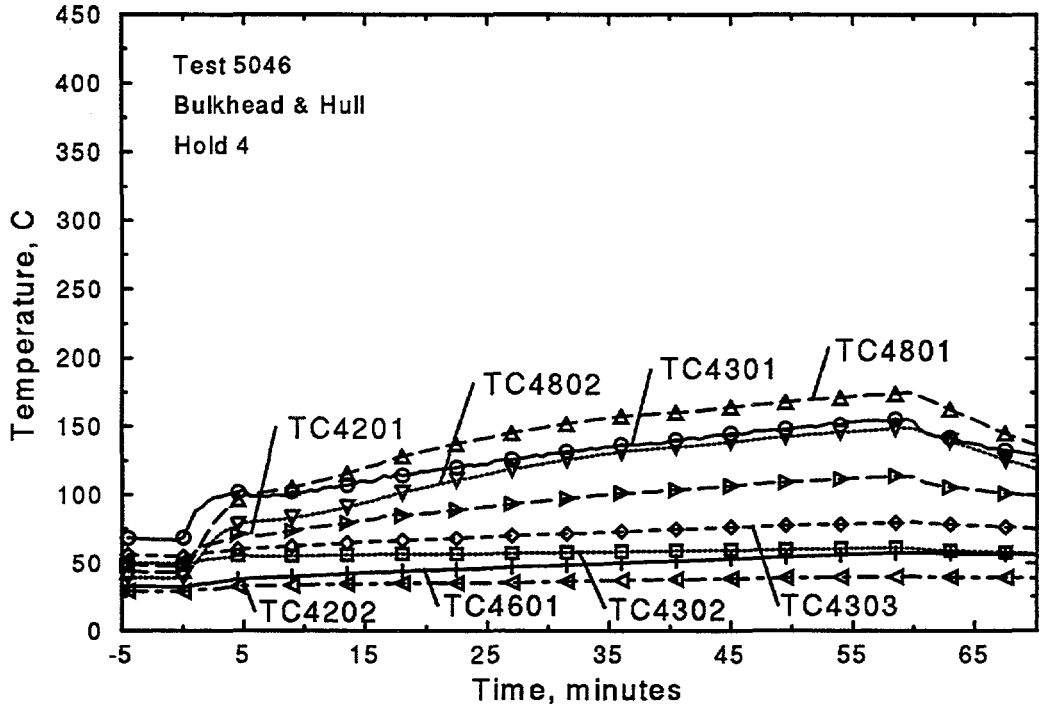

Figure F.6: Thermocouple response of Hold 4 Bulkhead and Hull

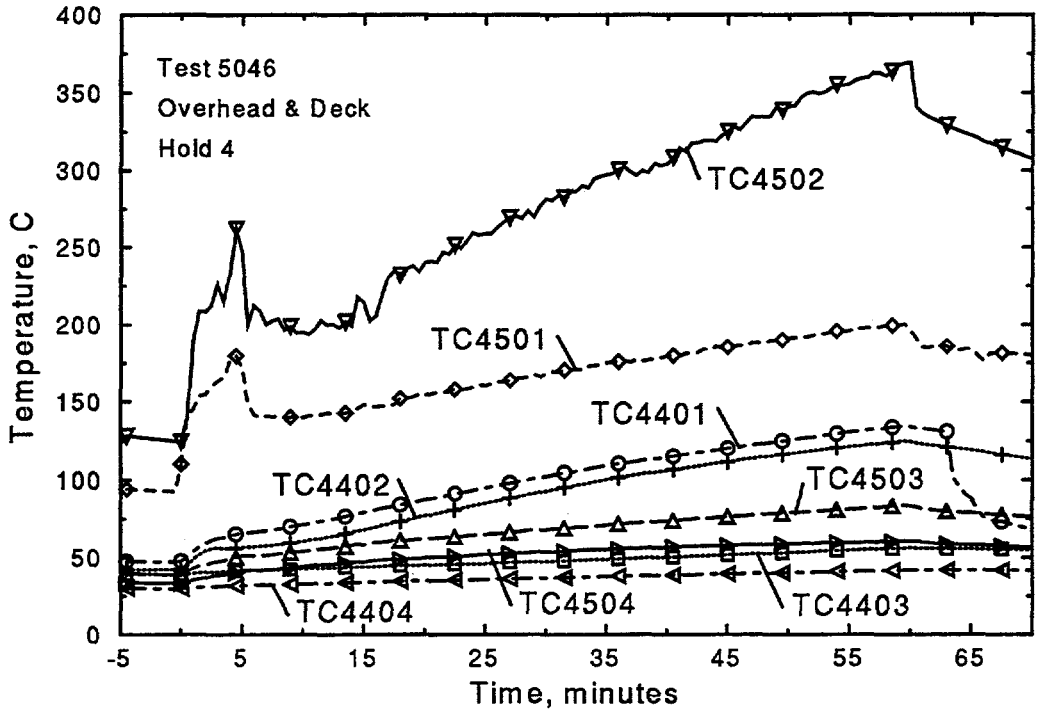

Figure F.7: Thermocouple response of Hold 4 Overhead and Deck

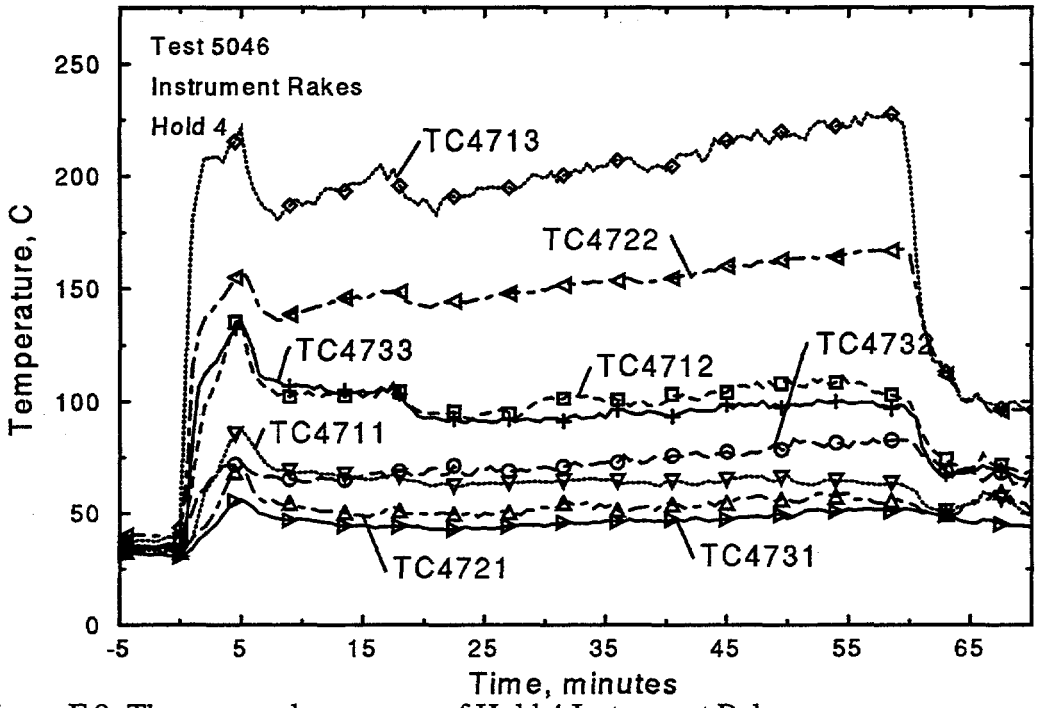

Figure F.8: Thermocouple response of Hold 4 Instrument Rakes

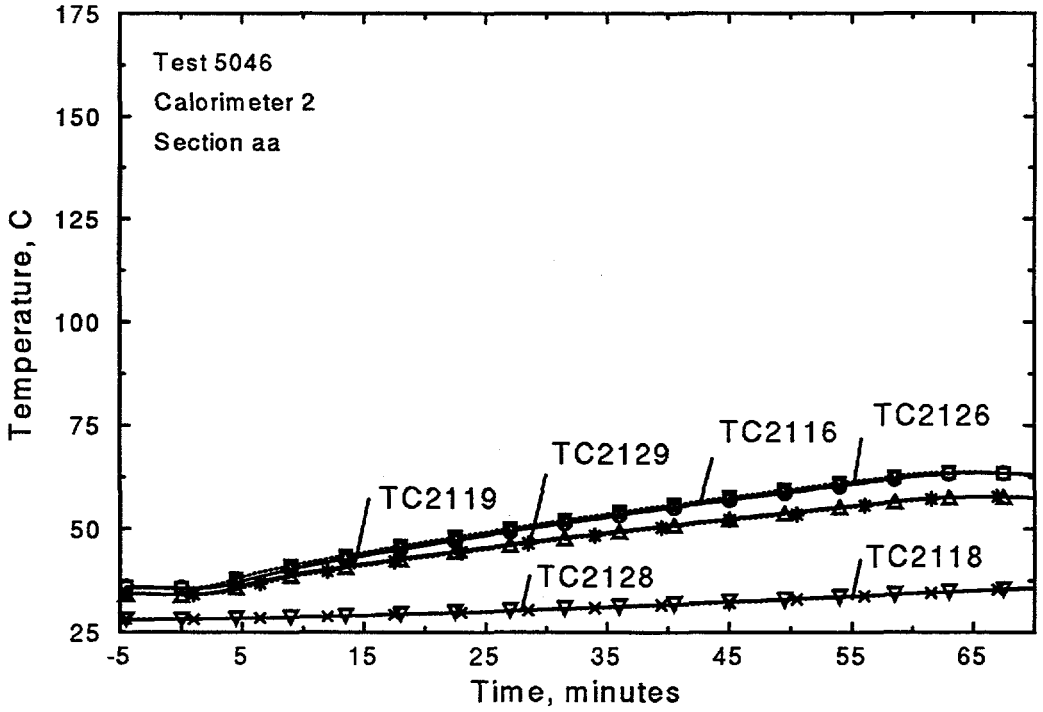

Figure F.9: Thermocouple response of Calorimeter 2, section aa

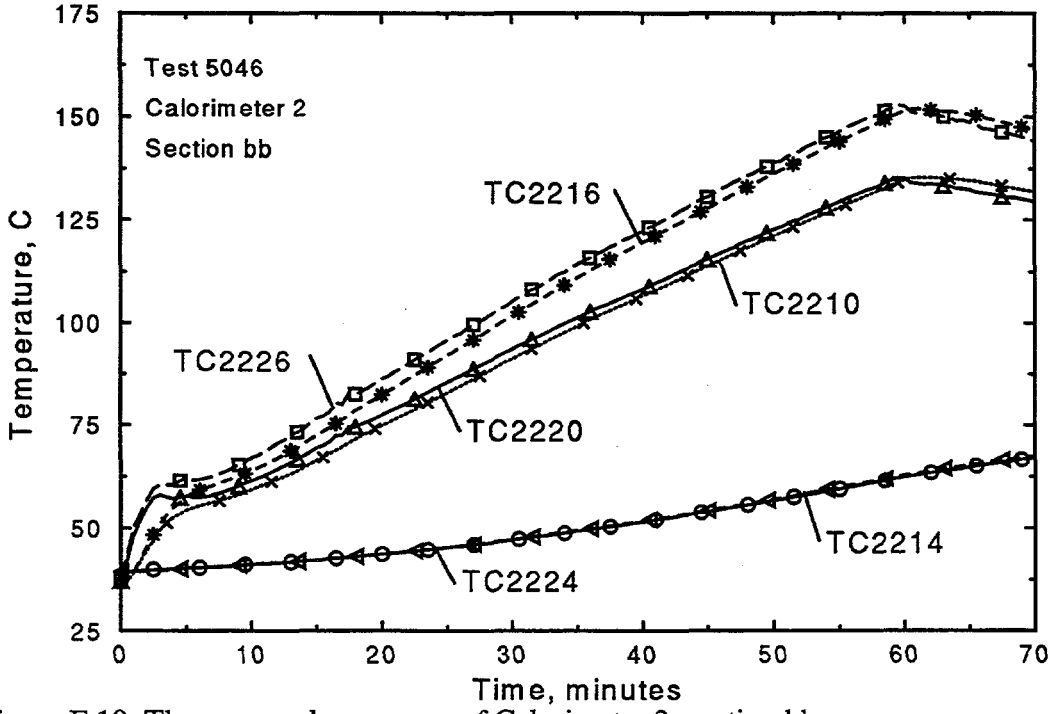

Figure F.10: Thermocouple response of Calorimeter 2, section bb

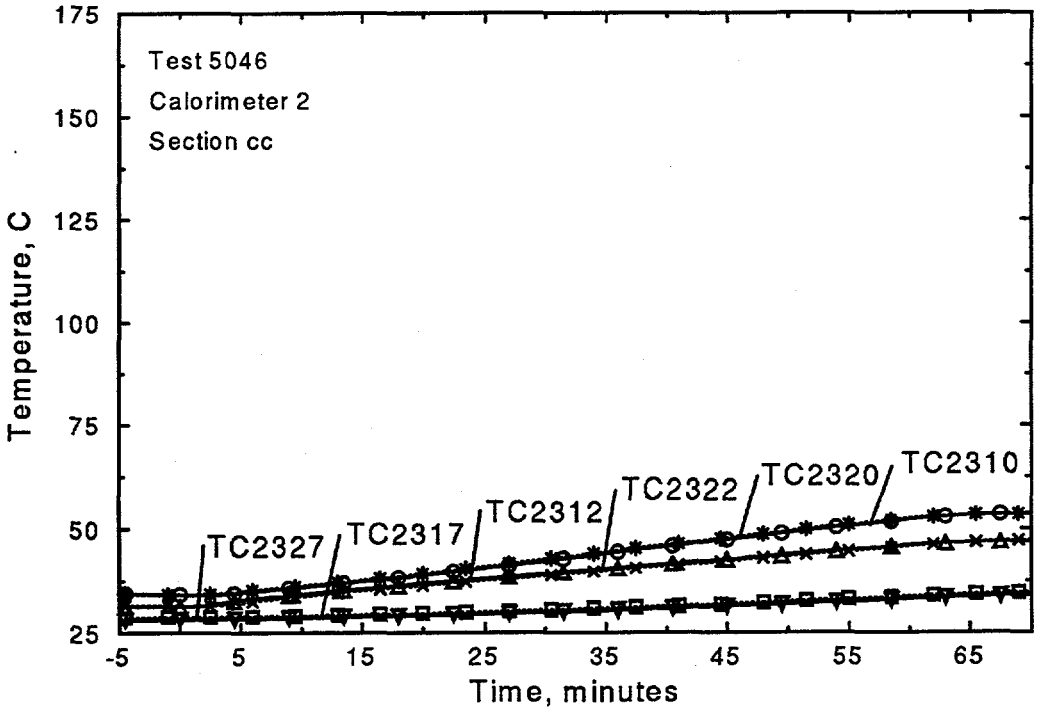

Figure F.11: Thermocouple response of Calorimeter 2, section cc

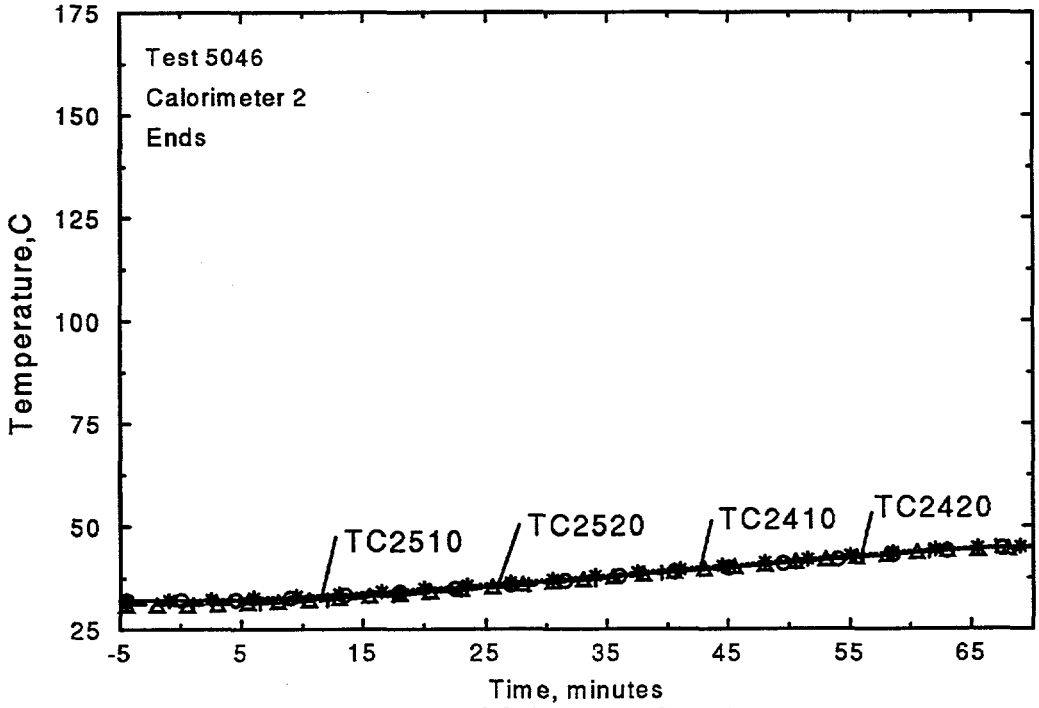

Figure F.12: Thermocouple response of Calorimeter 2, ends

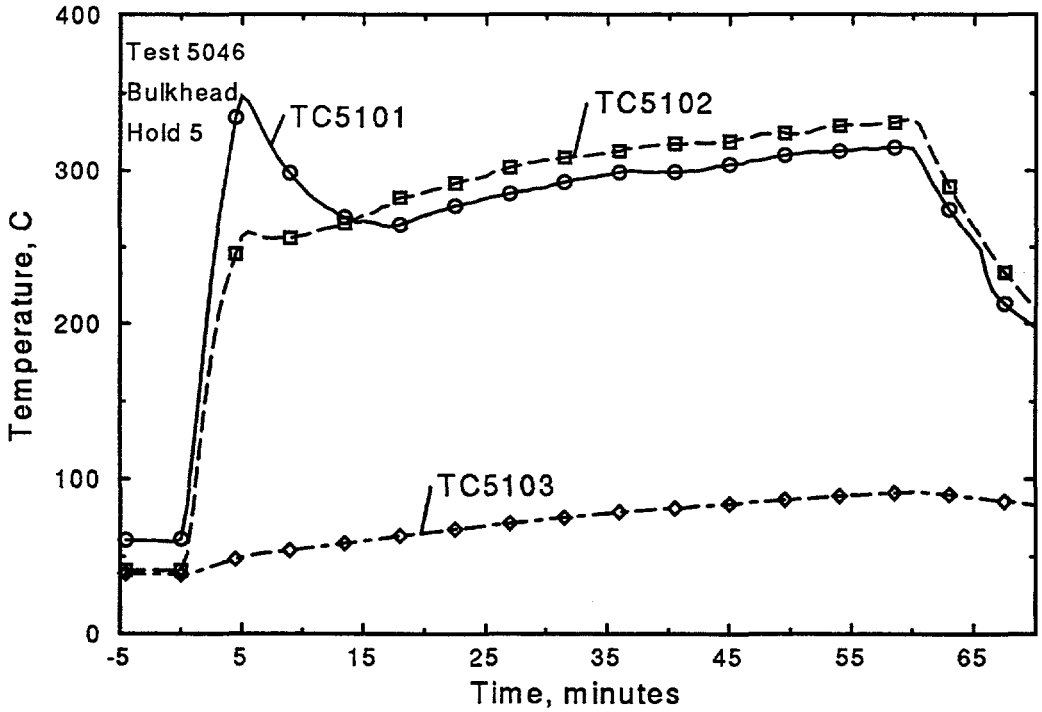

Figure F.13: Thermocouple response of Hold 5 Bulkhead

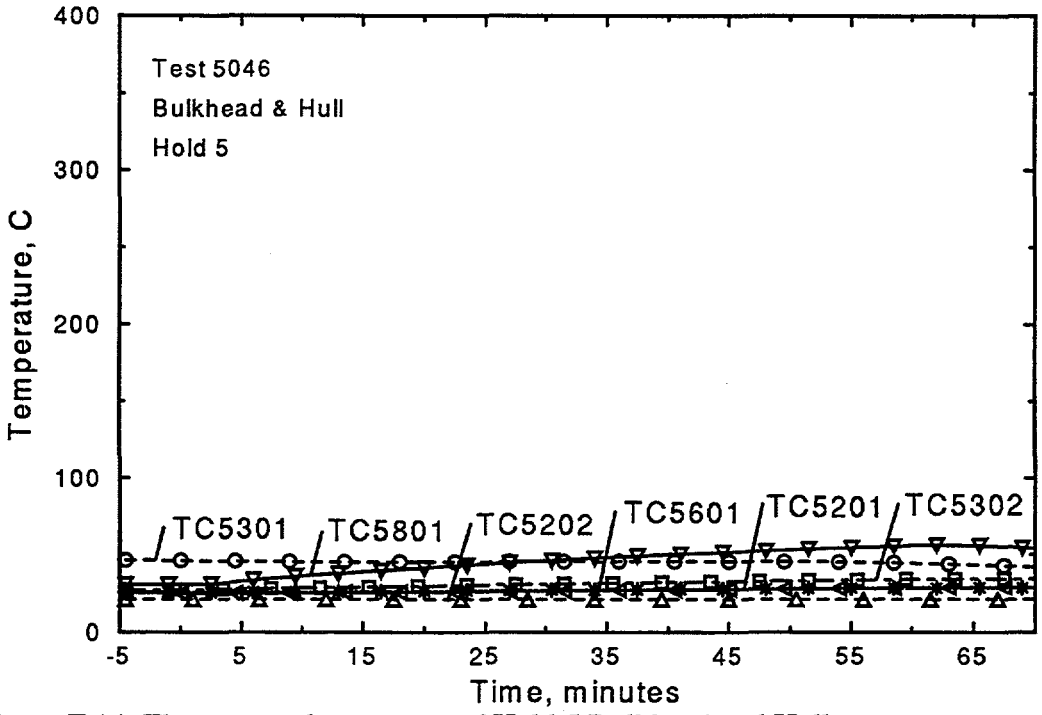

Figure F.14: Thermocouple response of Hold 5 Bulkhead and Hull

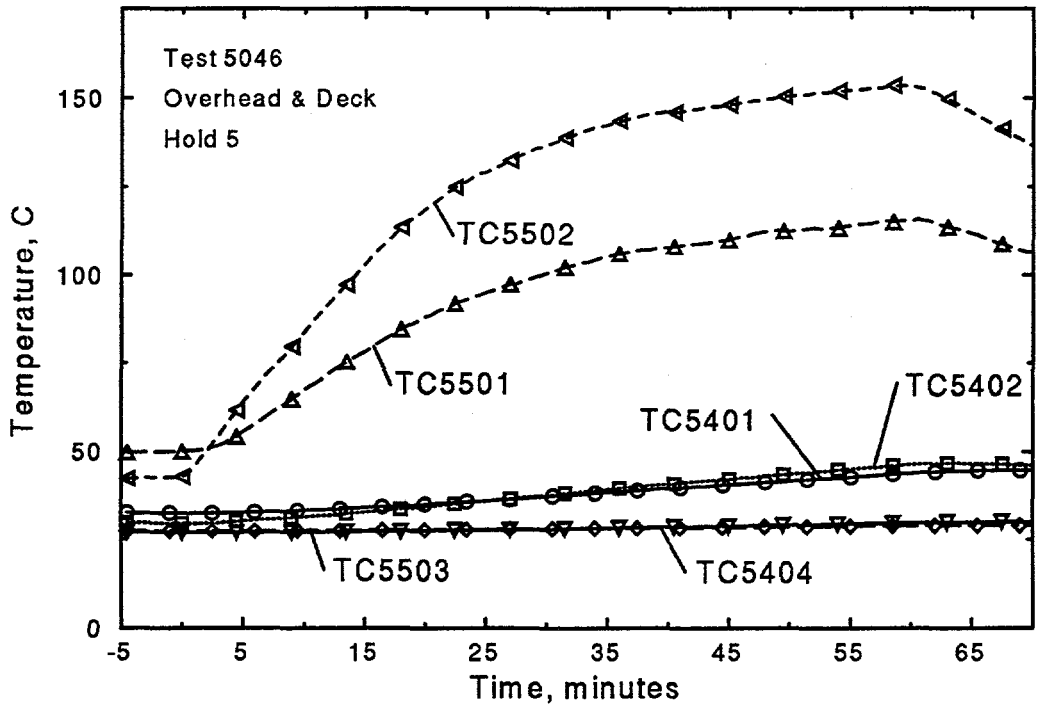

Figure F.15: Thermocouple response of Hold 5 Overhead and Deck

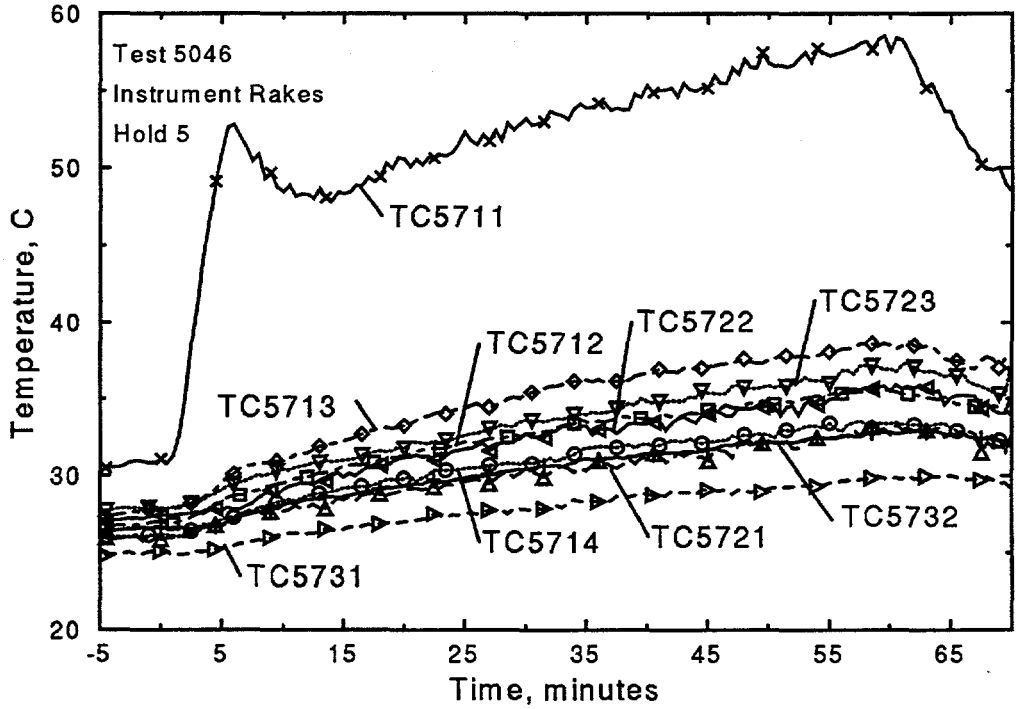

Figure F.16: Thermocouple response of Hold 5 Instrument Rakes

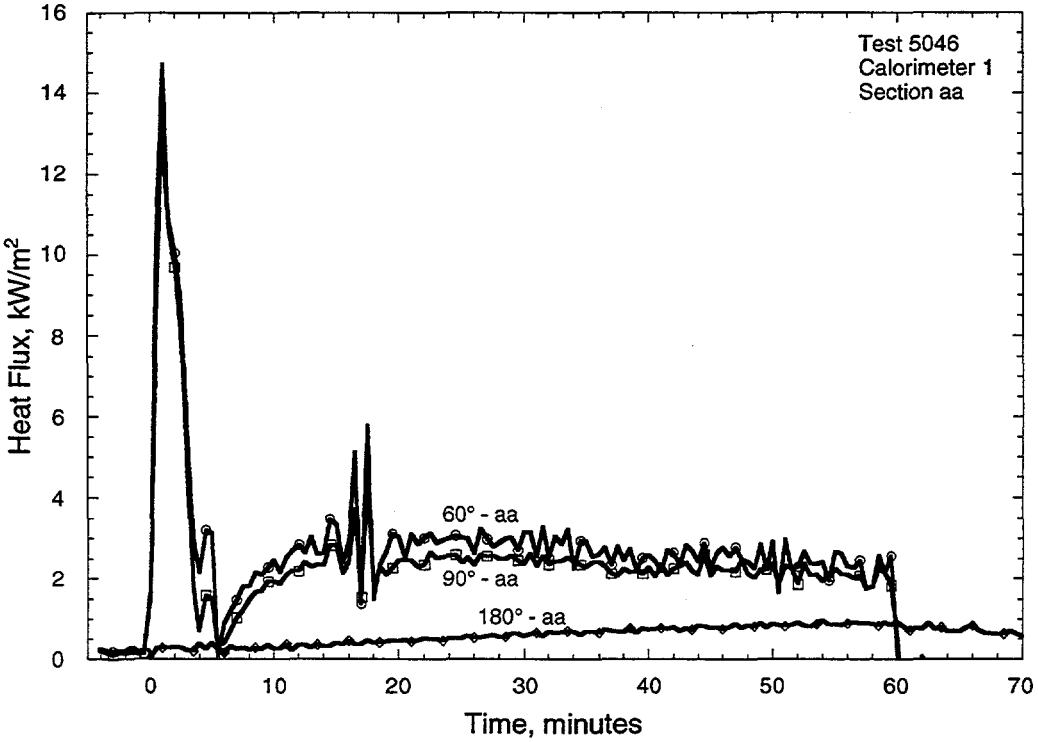

Figure F.17: Heat Flux response for Calorimeter 1, section aa

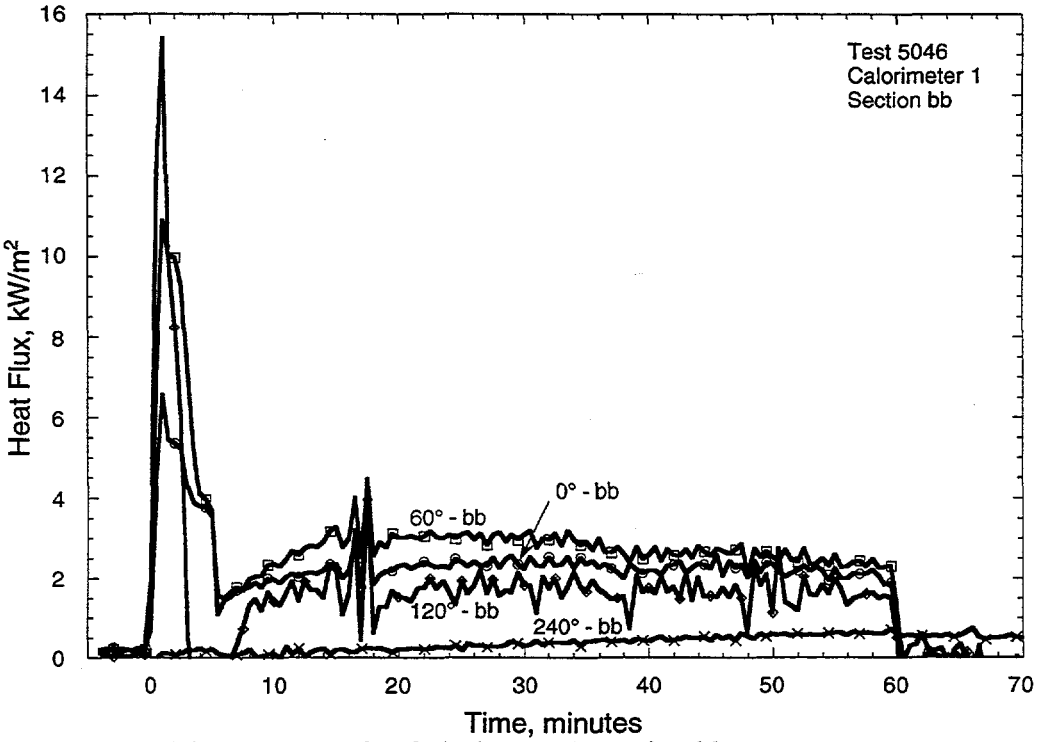

Figure F.18: Heat Flux response for Calorimeter 1, section bb

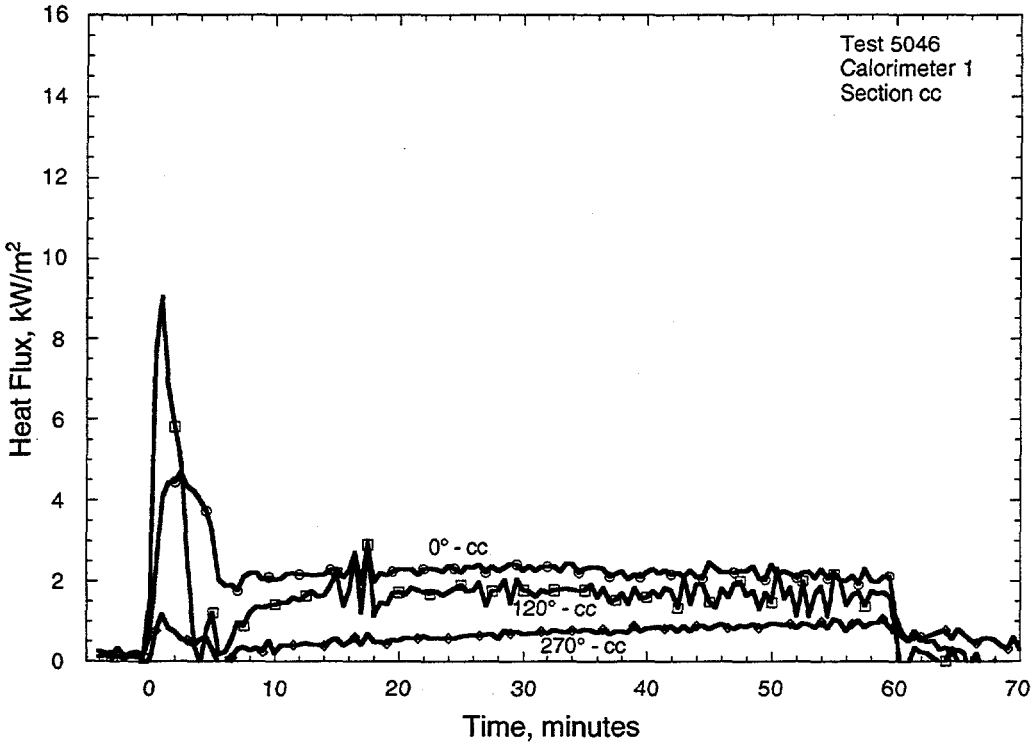

Figure F.19: Heat Flux response for Calorimeter 1, section cc

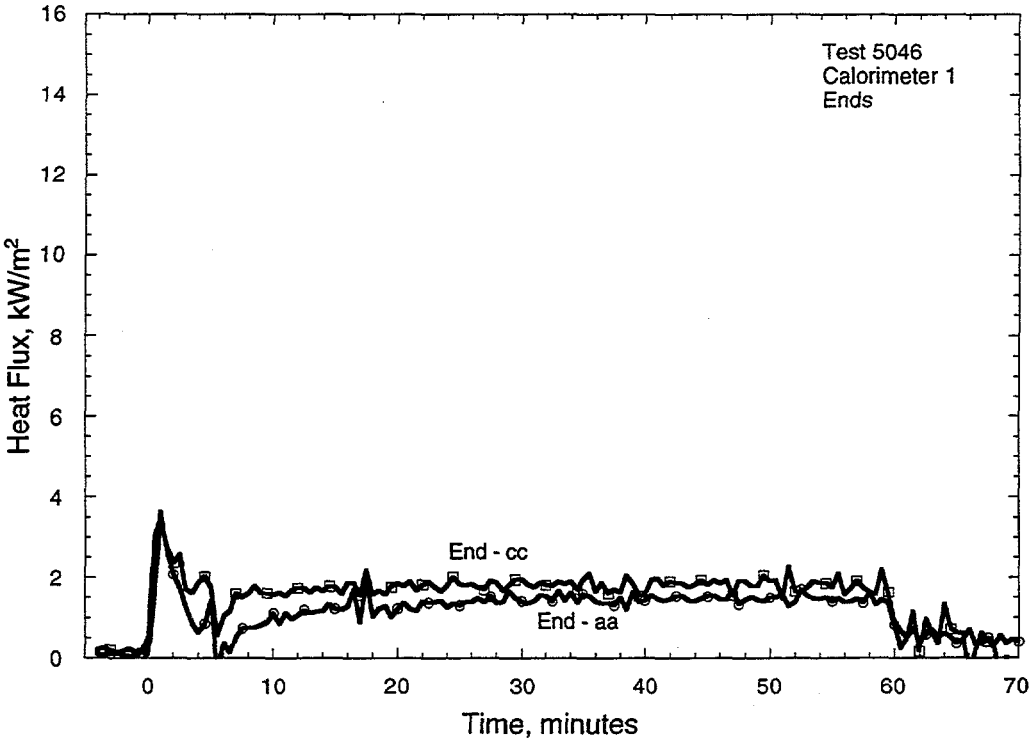

Figure F.20: Heat Flux response for Calorimeter 1, ends

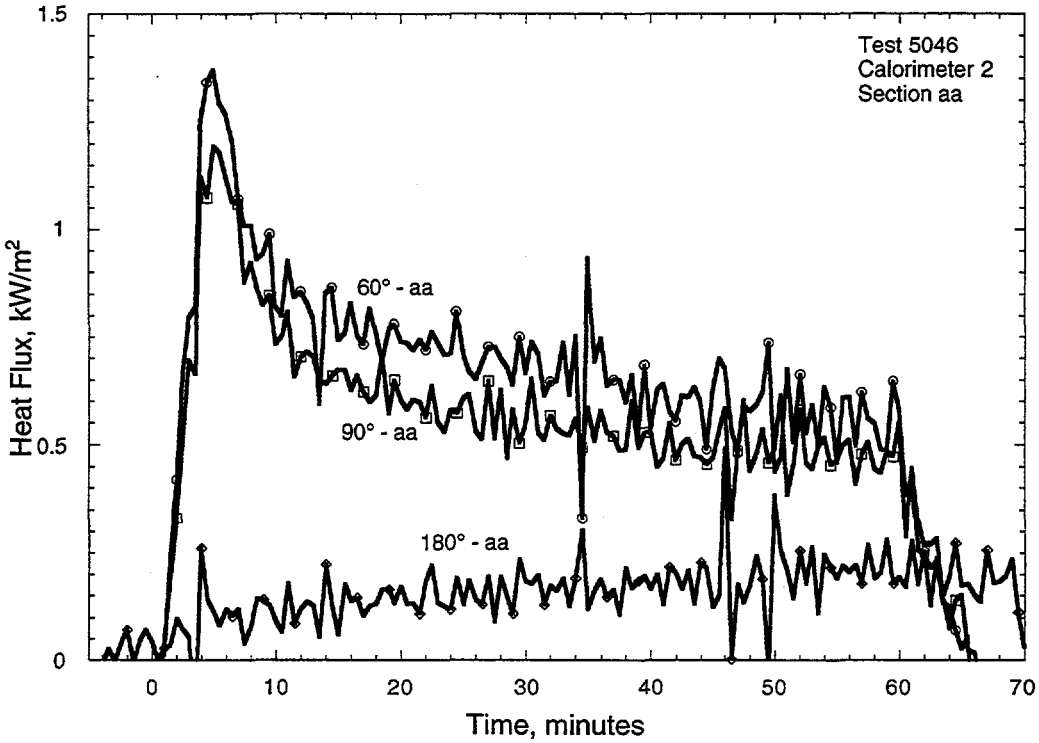

Figure F.21: Heat Flux response for Calorimeter 2, section aa

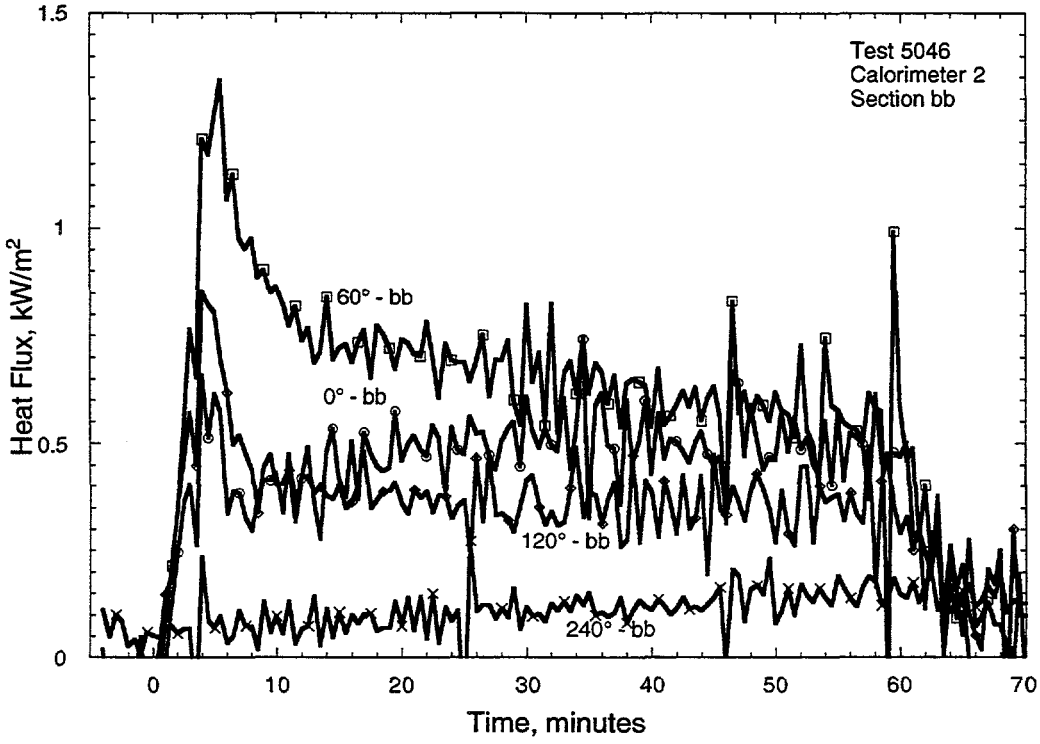

Figure F.22: Heat Flux response for Calorimeter 2, section bb

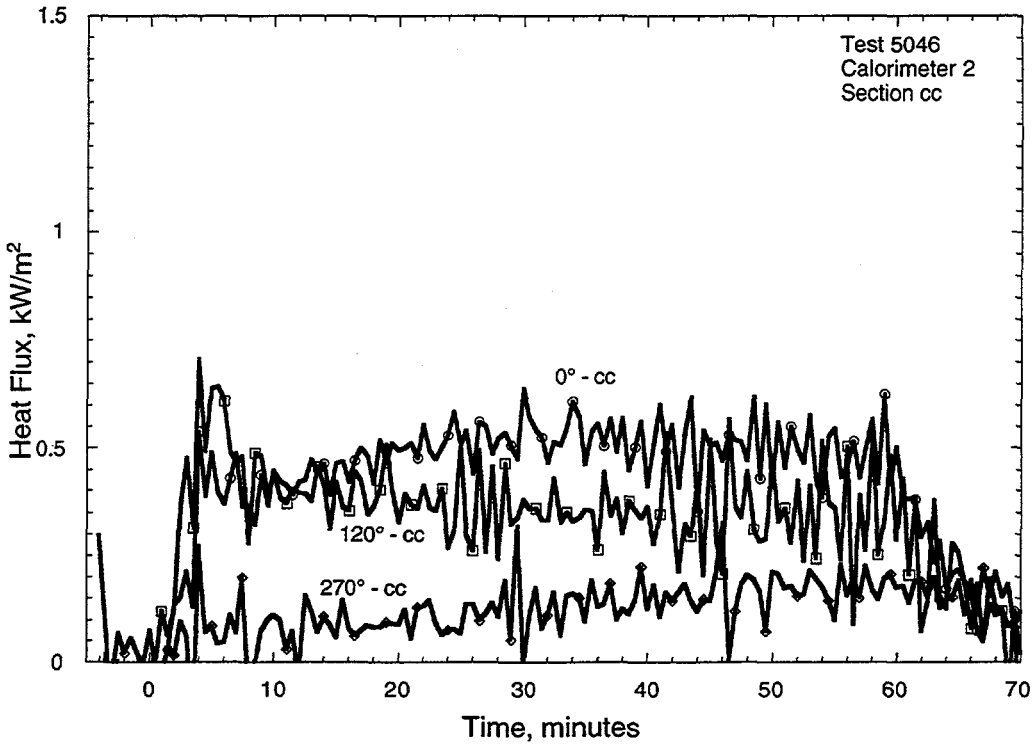

Figure F.23: Heat Flux for Calorimeter 2, section cc

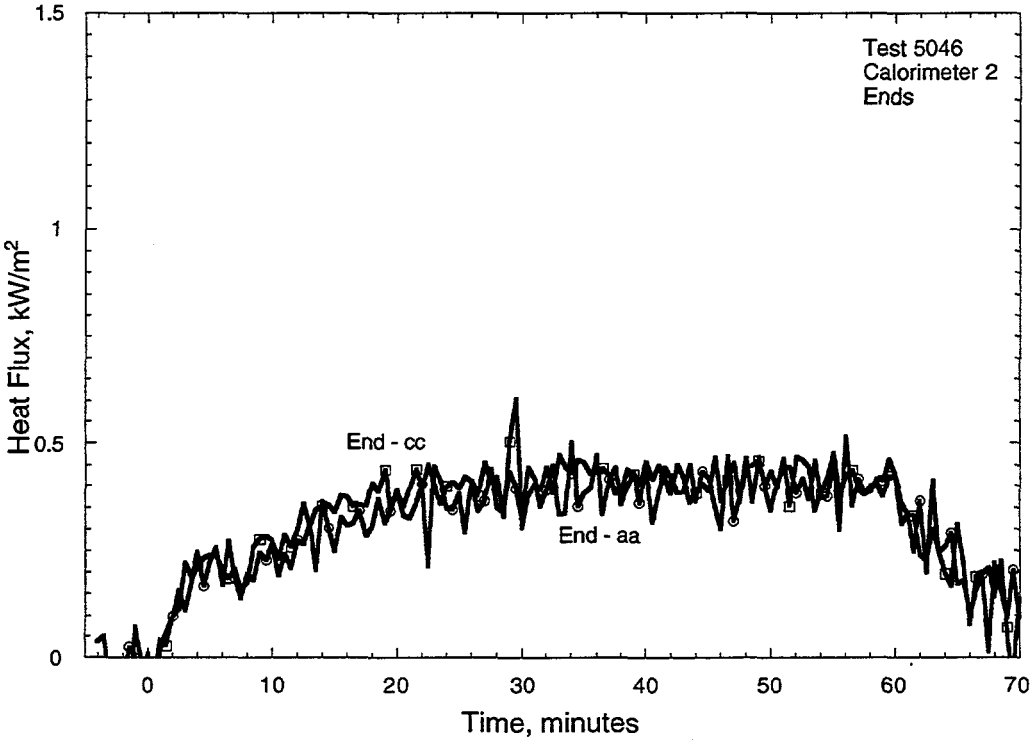

Figure F.24: Heat Flux for Calorimeter 2, ends

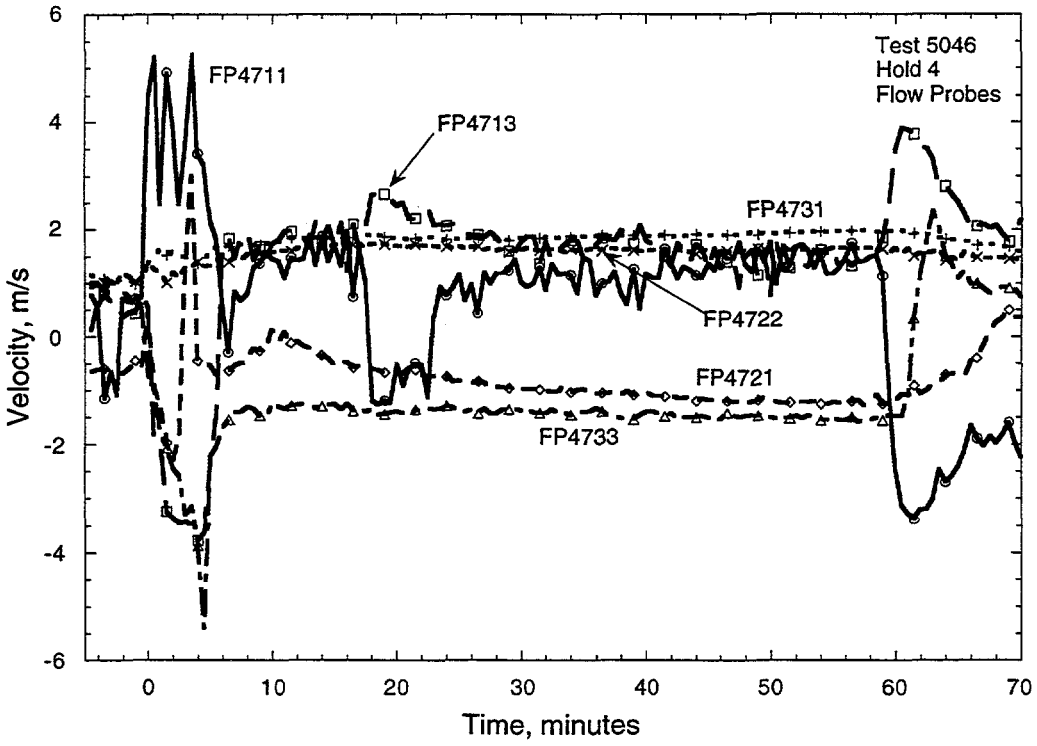

Figure F.25: Flow probes for Hold 4

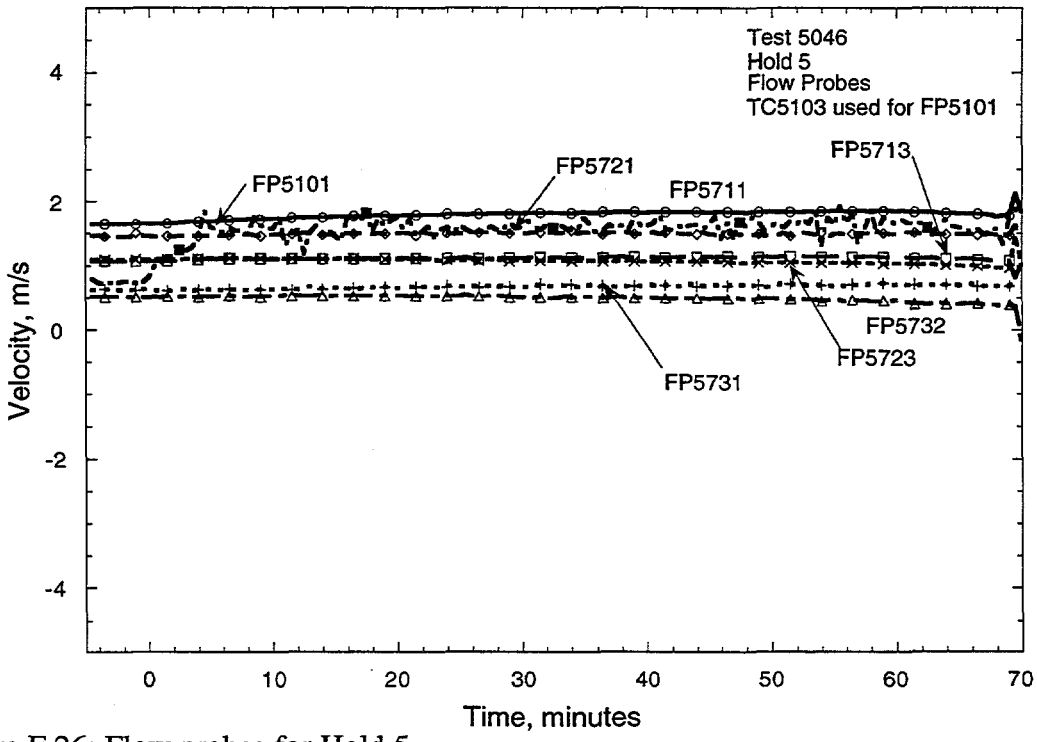

Figure F.26: Flow probes for Hold 5

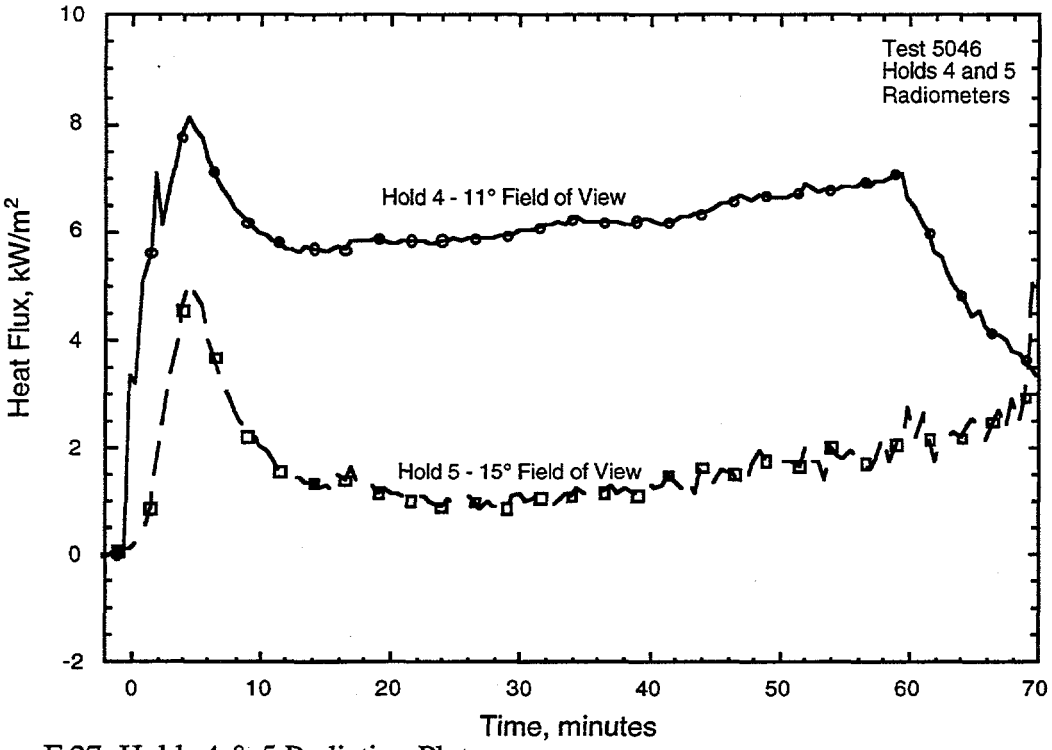

Figure F.27: Holds 4 & 5 Radiation Plot

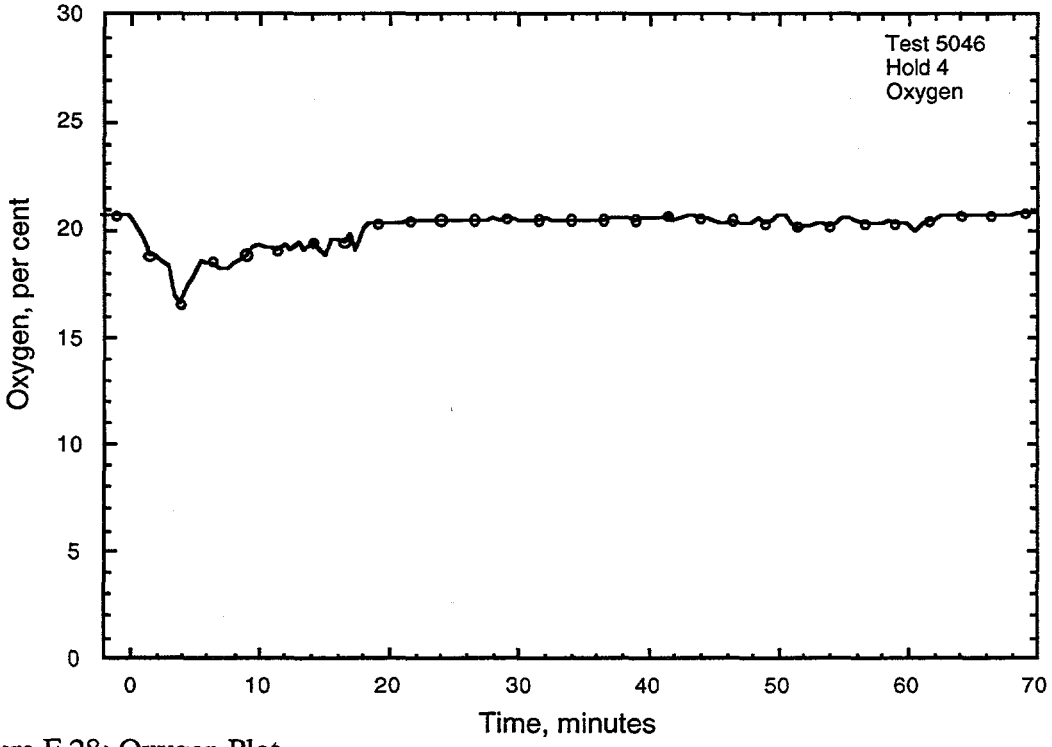

Figure F.28: Oxygen Plot

Appendix G
Test 5048
Diesel Pool Fire in Hold 4

conducted 11/14/95
3:09 PM CDT

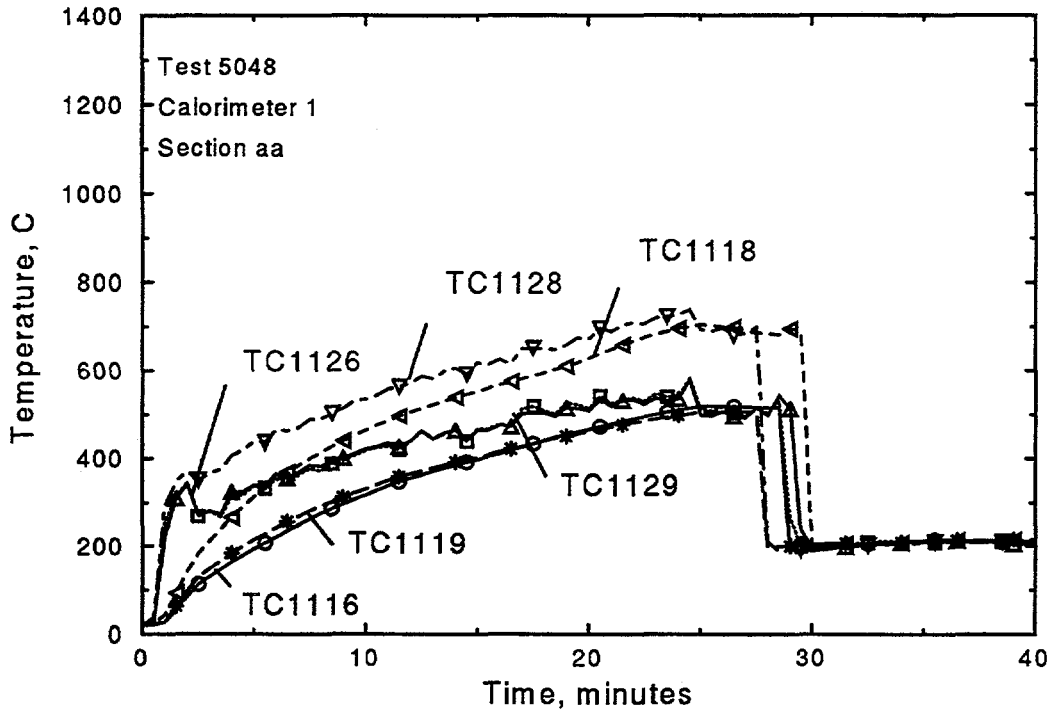

Figure F.1: Thermocouple response of Calorimeter 1, section aa

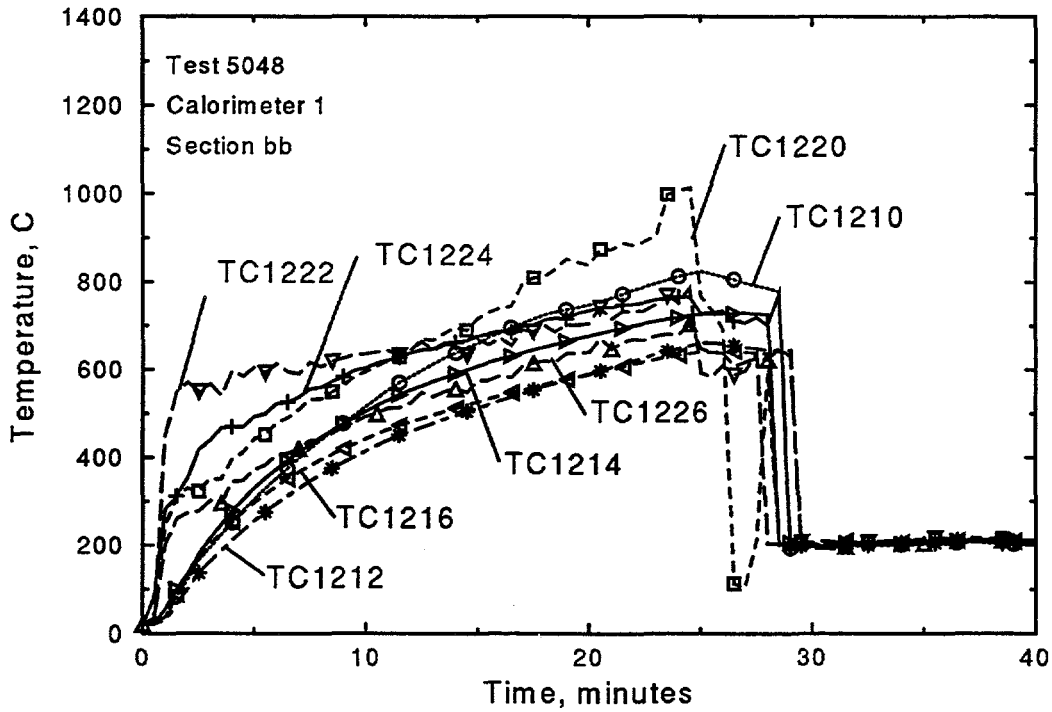

Figure G.2: Thermocouple response of Calorimeter 1, section bb

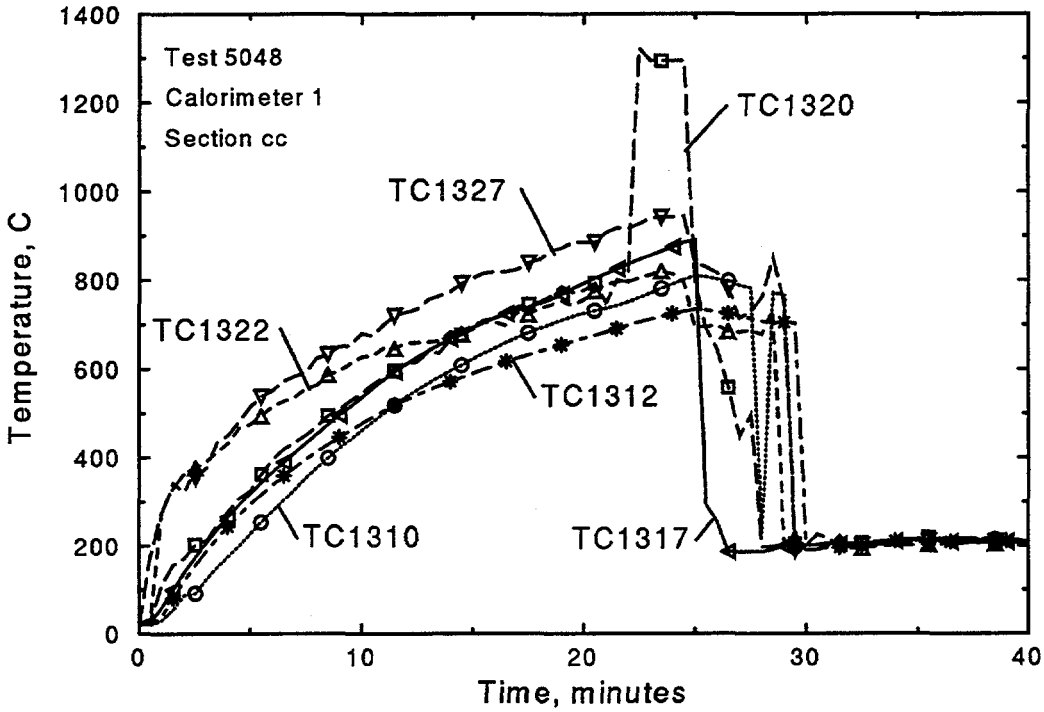

Figure G.3: Thermocouple response of Calorimeter 1, section cc

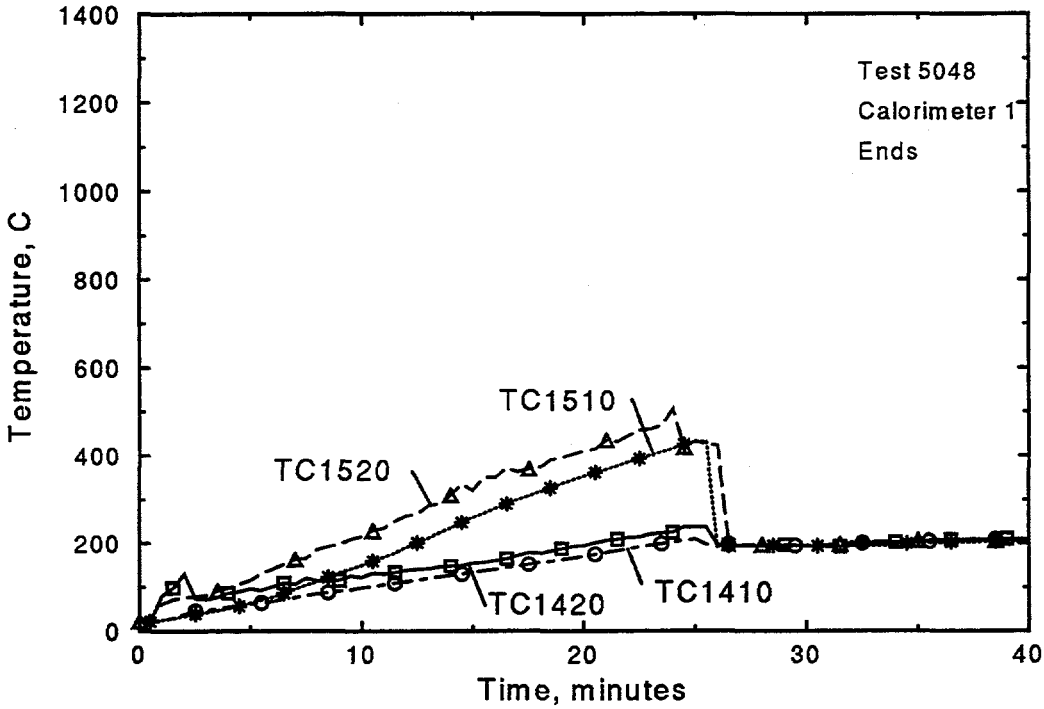

Figure G.4: Thermocouple response of Calorimeter 1, ends

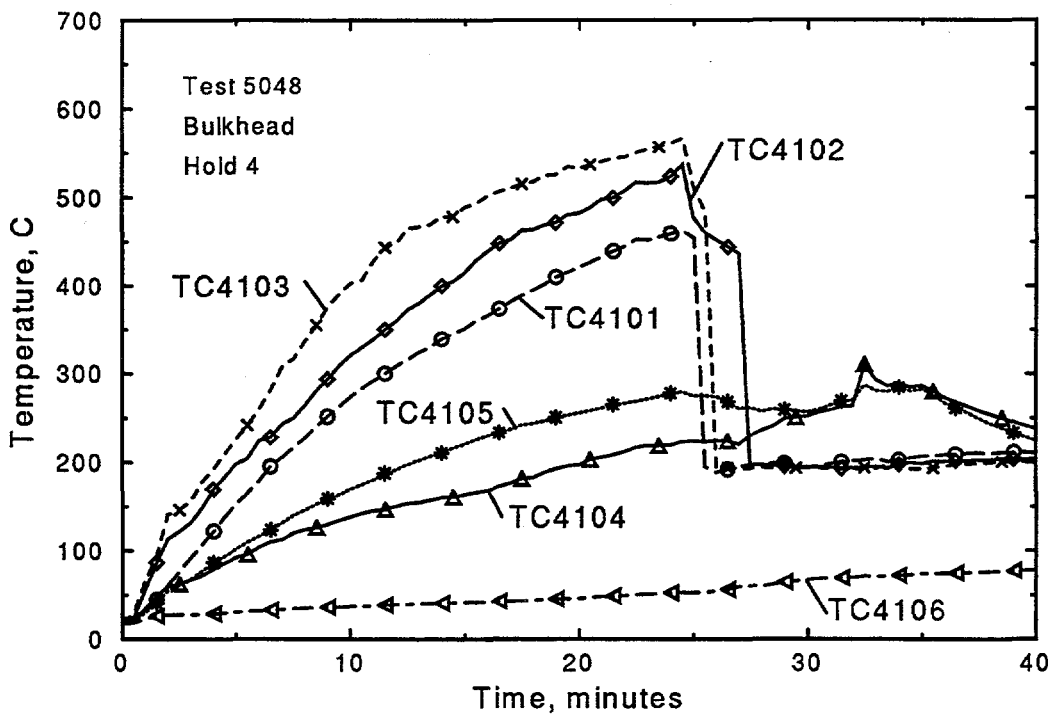

Figure G.5: Thermocouple response of Hold 4 Bulkhead

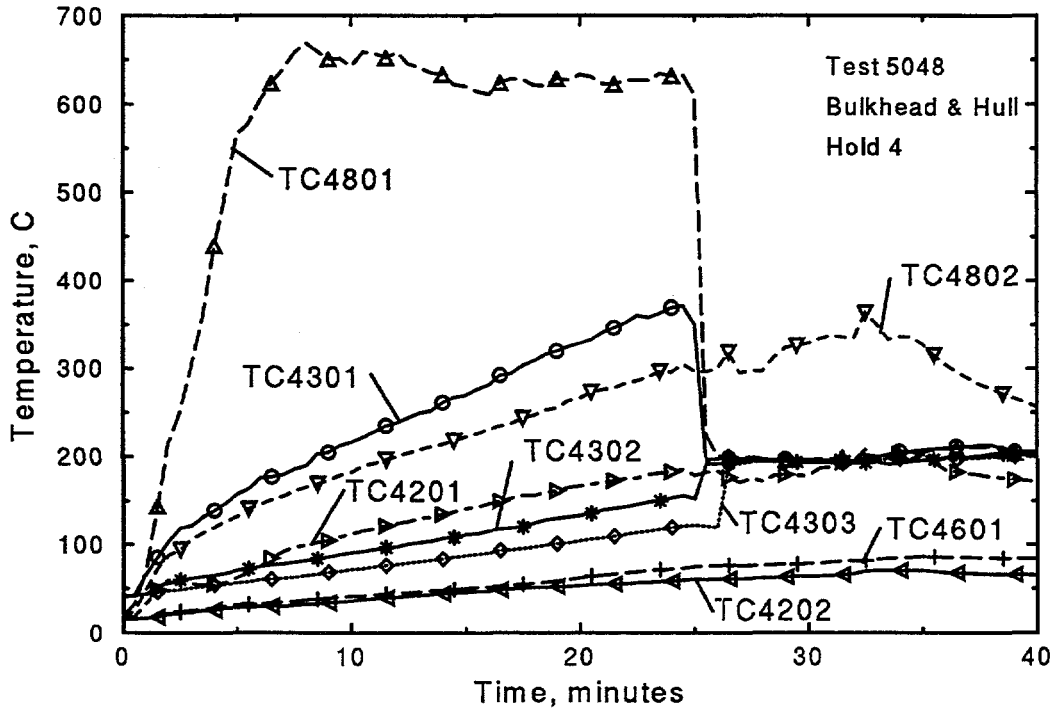

Figure G.6: Thermocouple response of Hold 4 Bulkhead and Hull

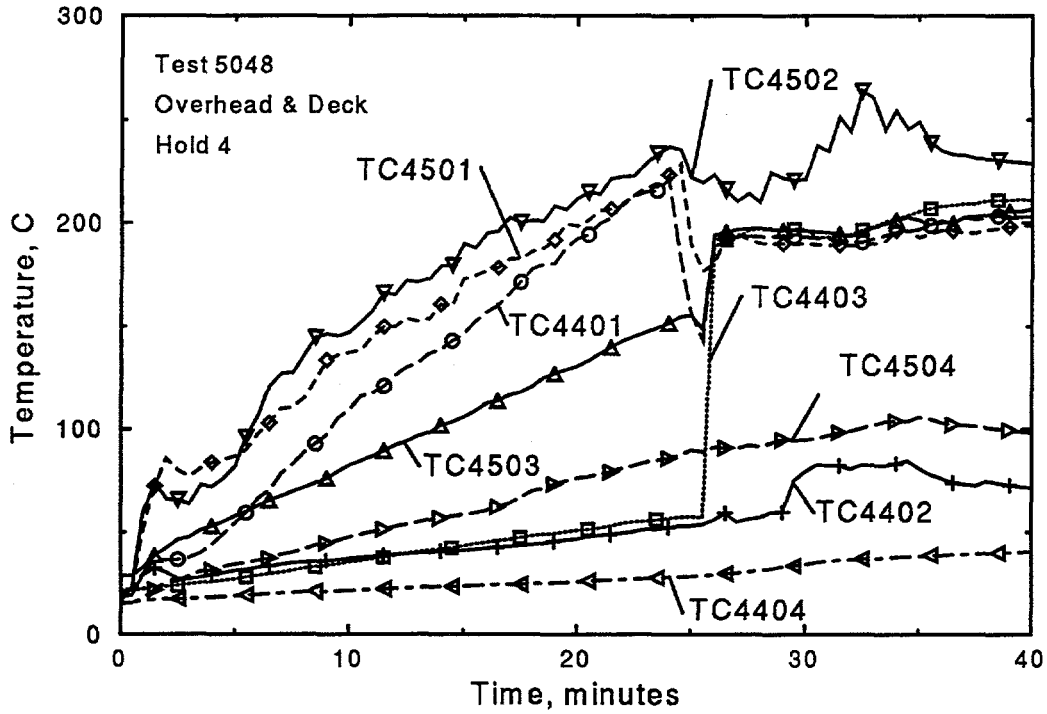

Figure G.7: Thermocouple response of Hold 4 Overhead and Deck

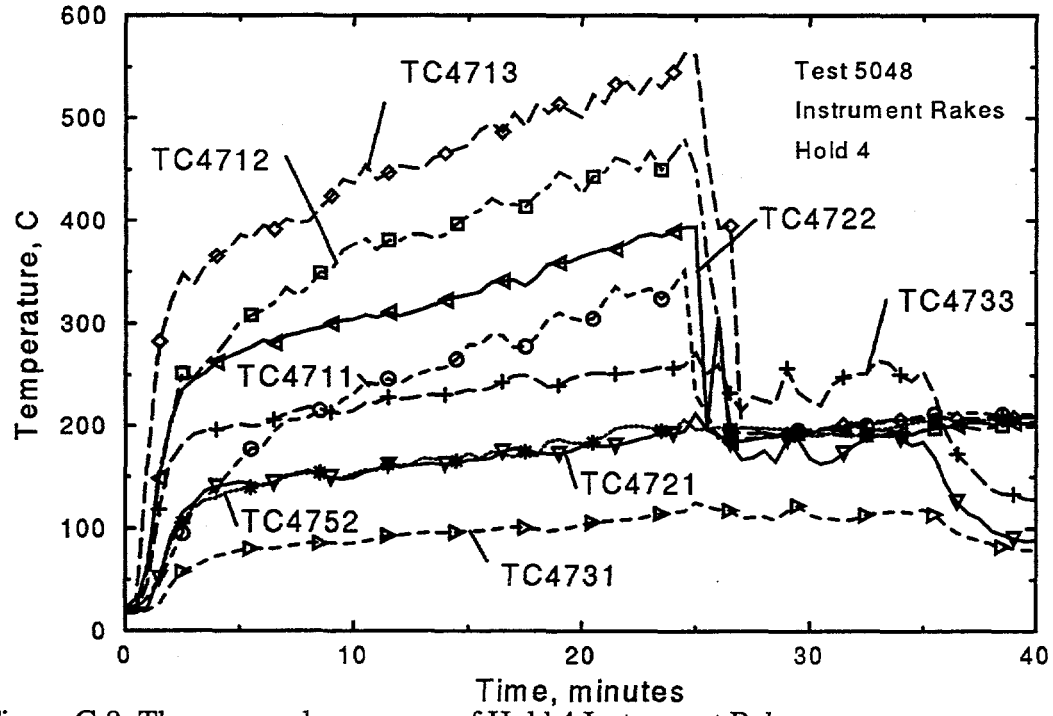

Figure G.8: Thermocouple response of Hold 4 Instrument Rakes

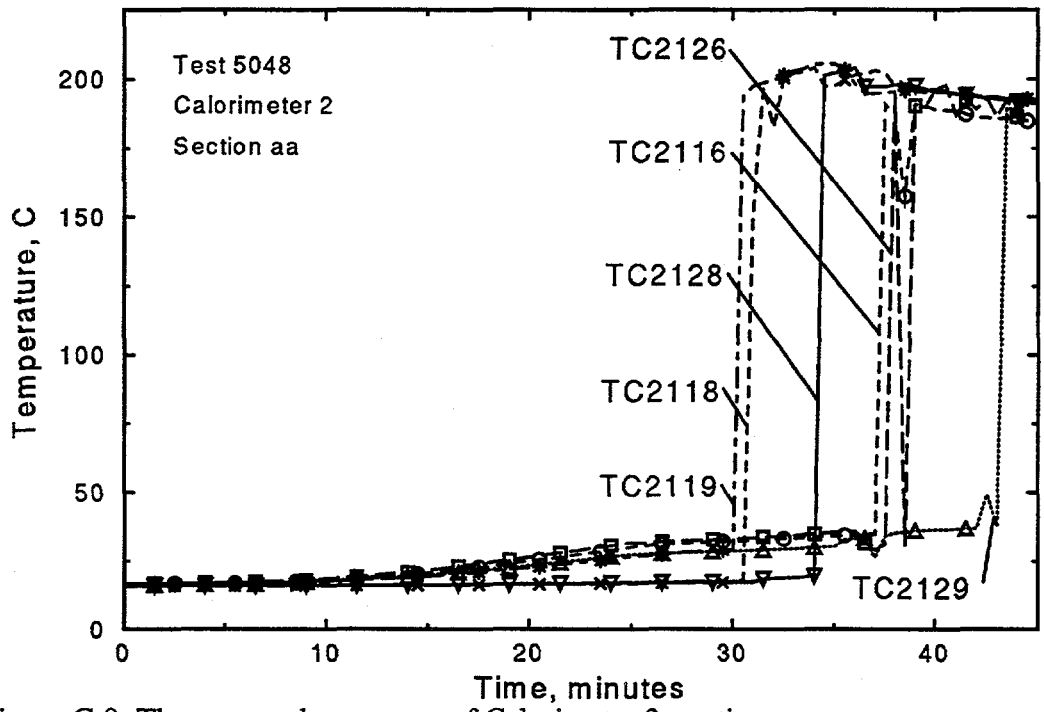

Figure G.9: Thermocouple response of Calorimeter 2, section aa

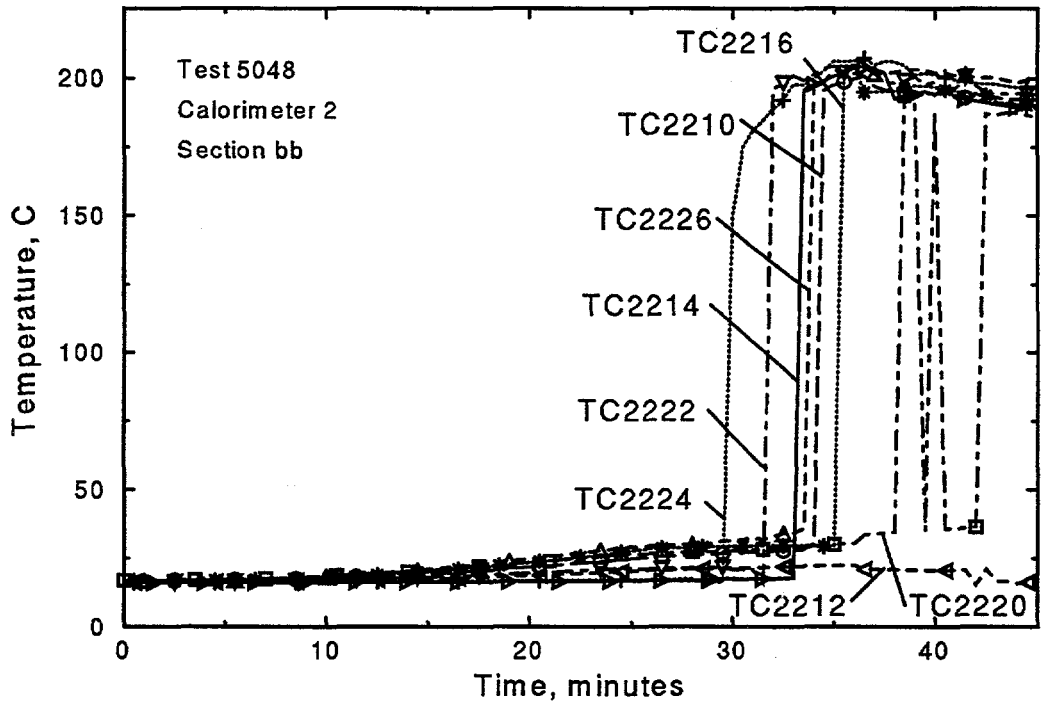

Figure G.10: Thermocouple response of Calorimeter 2, section bb

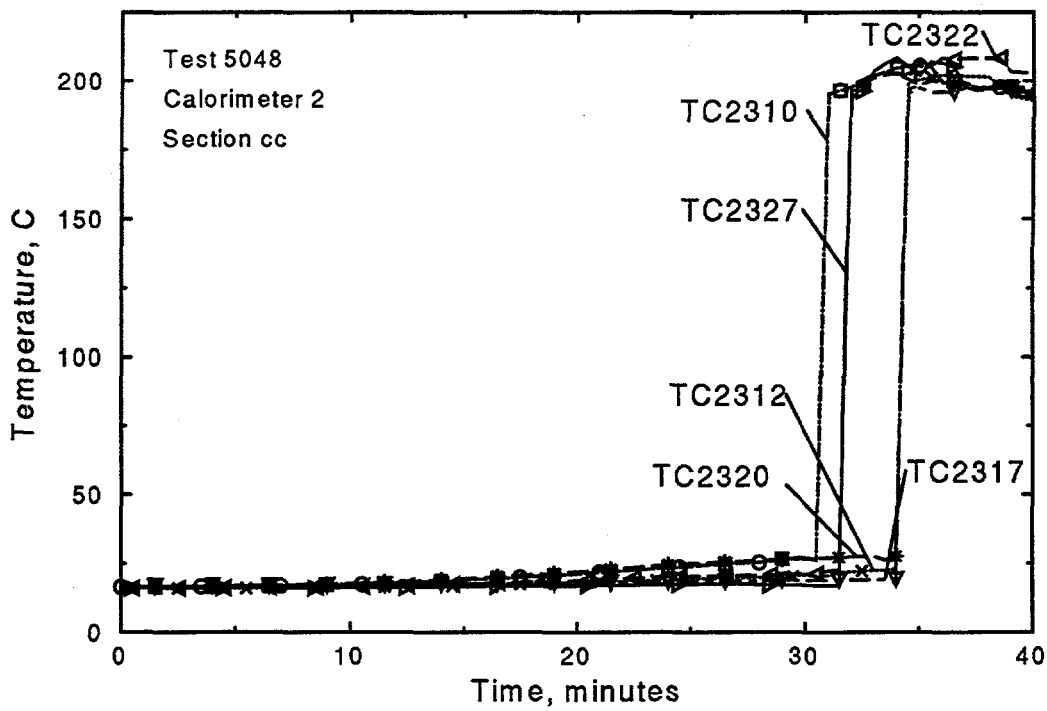

Figure G.11: Thermocouple response of Calorimeter 2, section cc

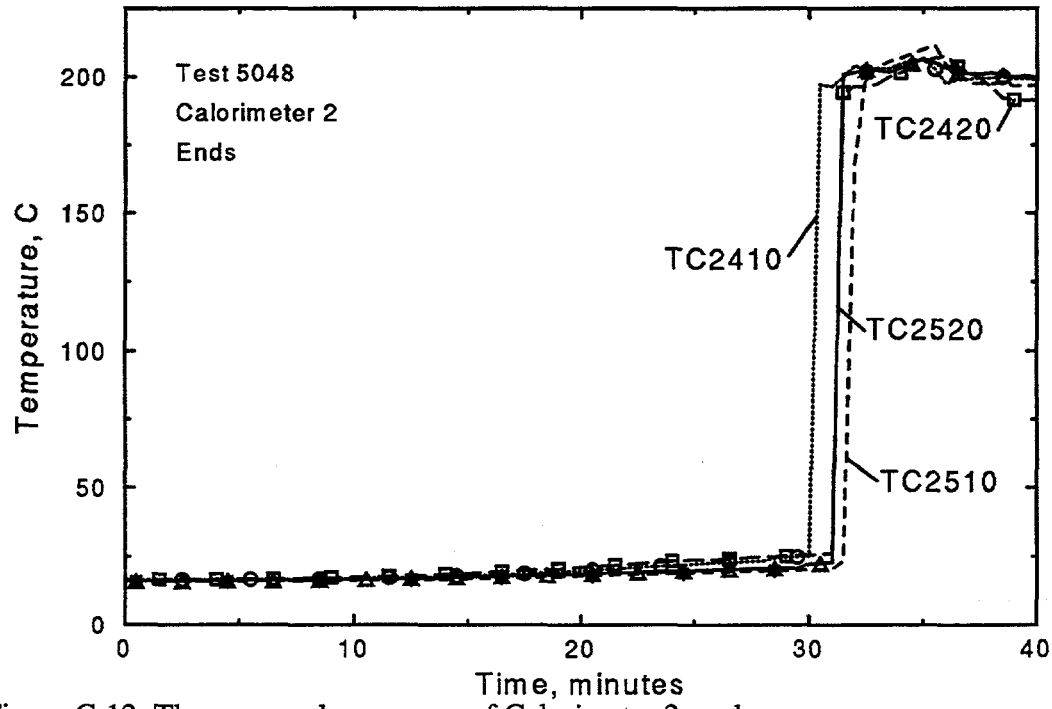

Figure G.12: Thermocouple response of Calorimeter 2, ends

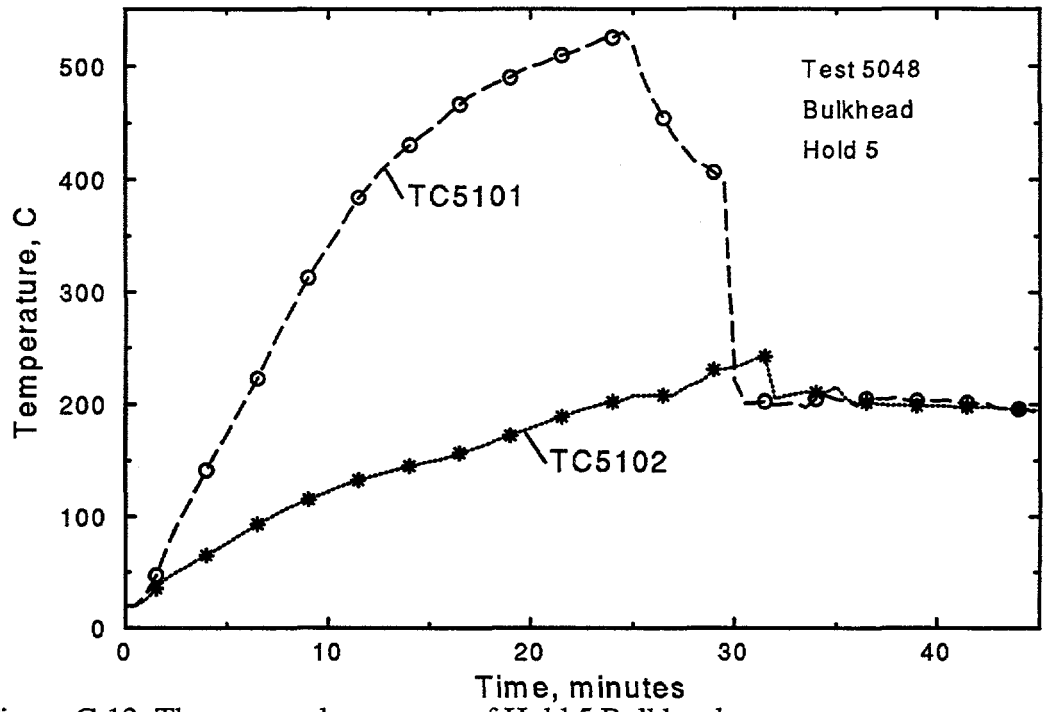

Figure G.13: Thermocouple response of Hold 5 Bulkhead

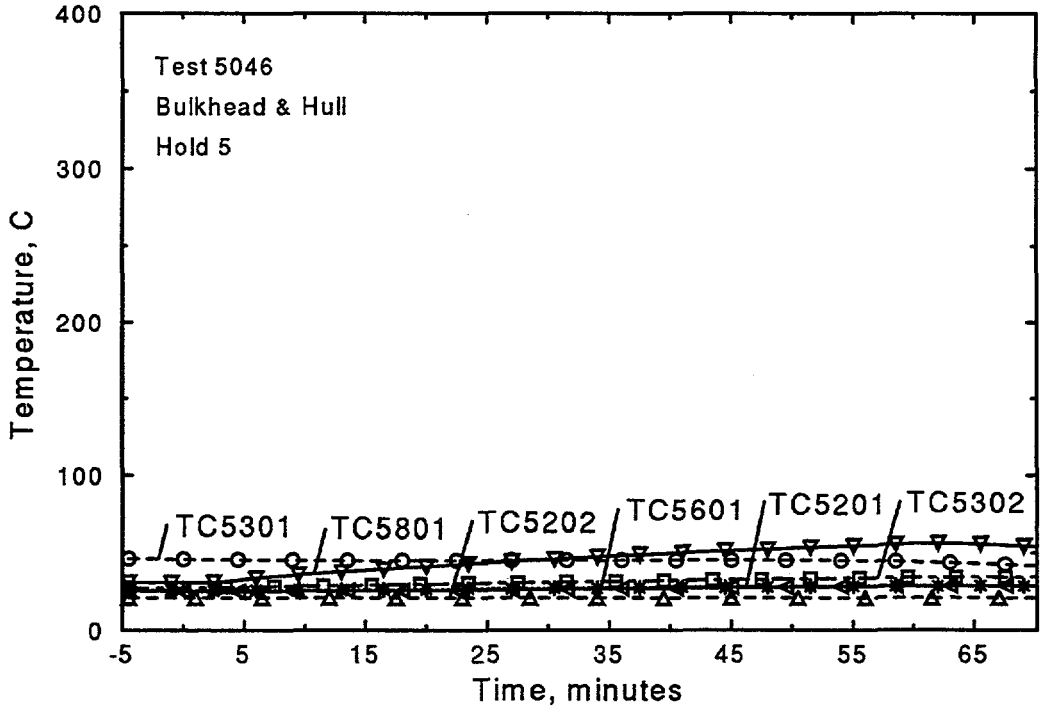

Figure G.14: Thermocouple response of Hold 5 Bulkhead and Hull

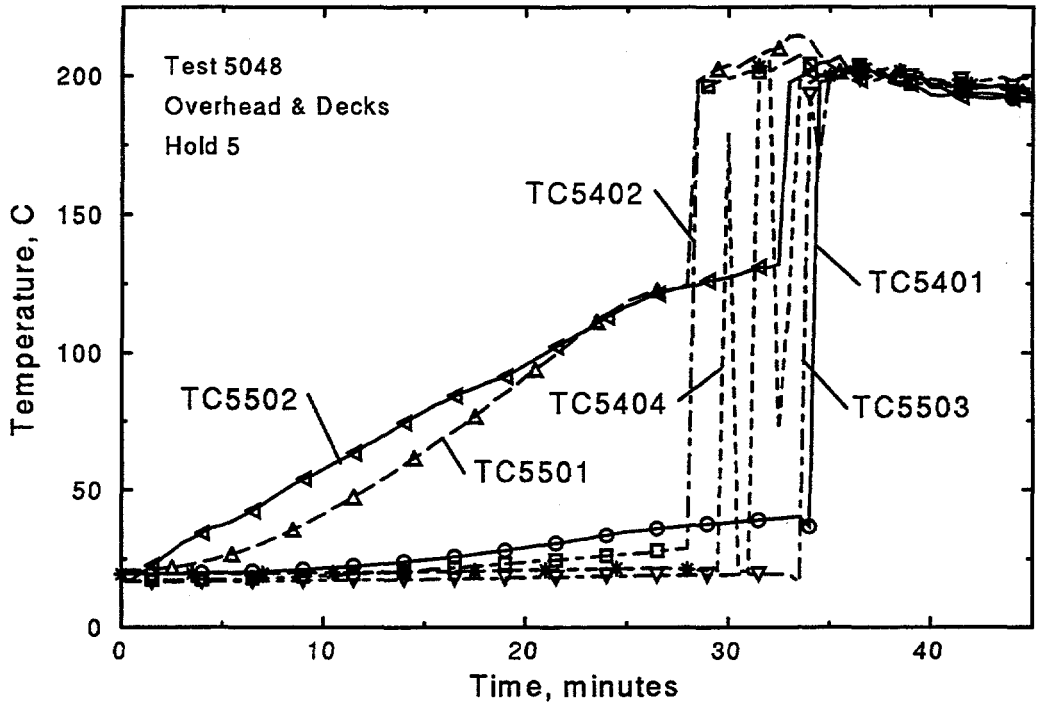

Figure G.15: Thermocouple response of Hold 5 Overhead and Deck

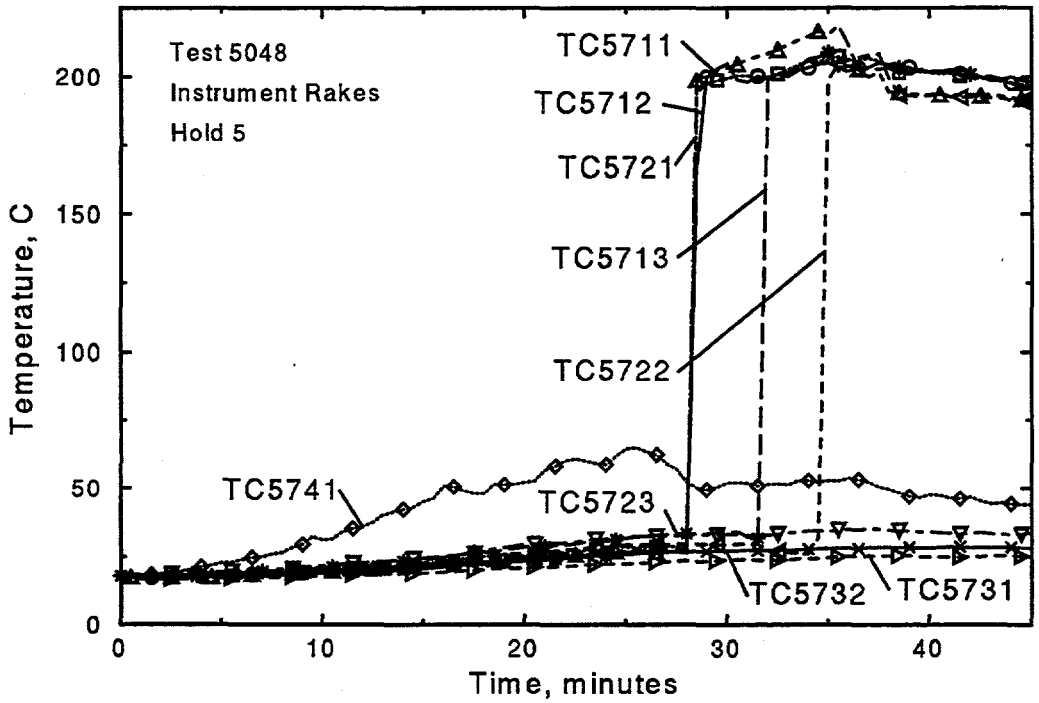

Figure G.16: Thermocouple response of Hold 5 Instrument Rakes

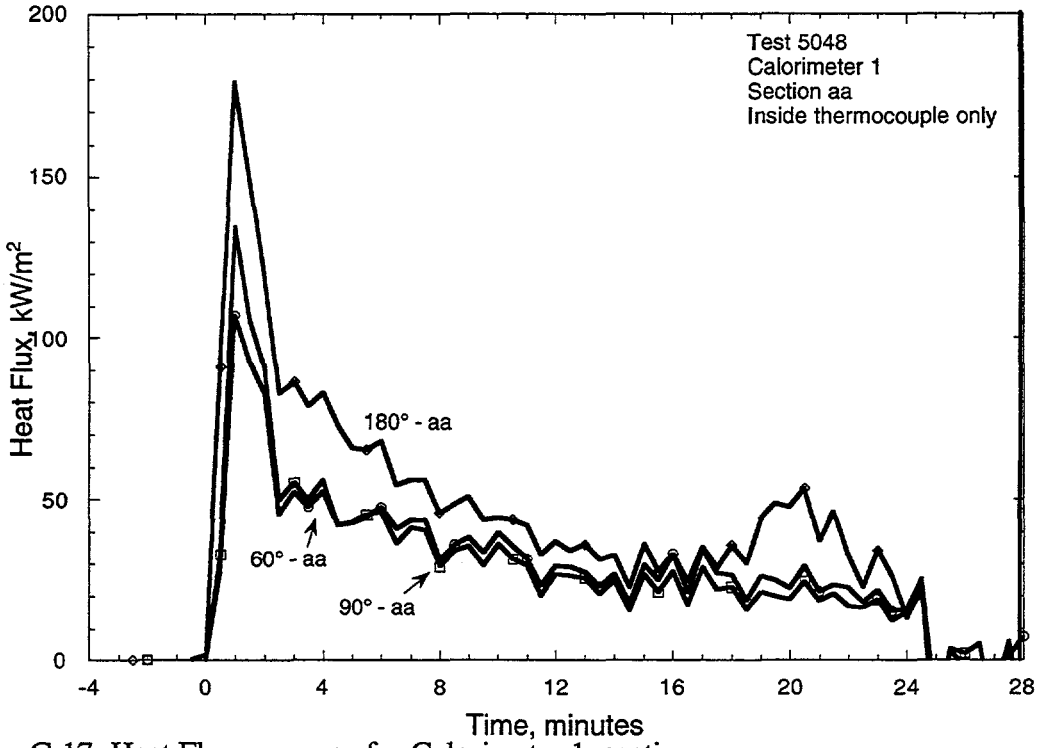

Figure G.17: Heat Flux response for Calorimeter 1, section aa

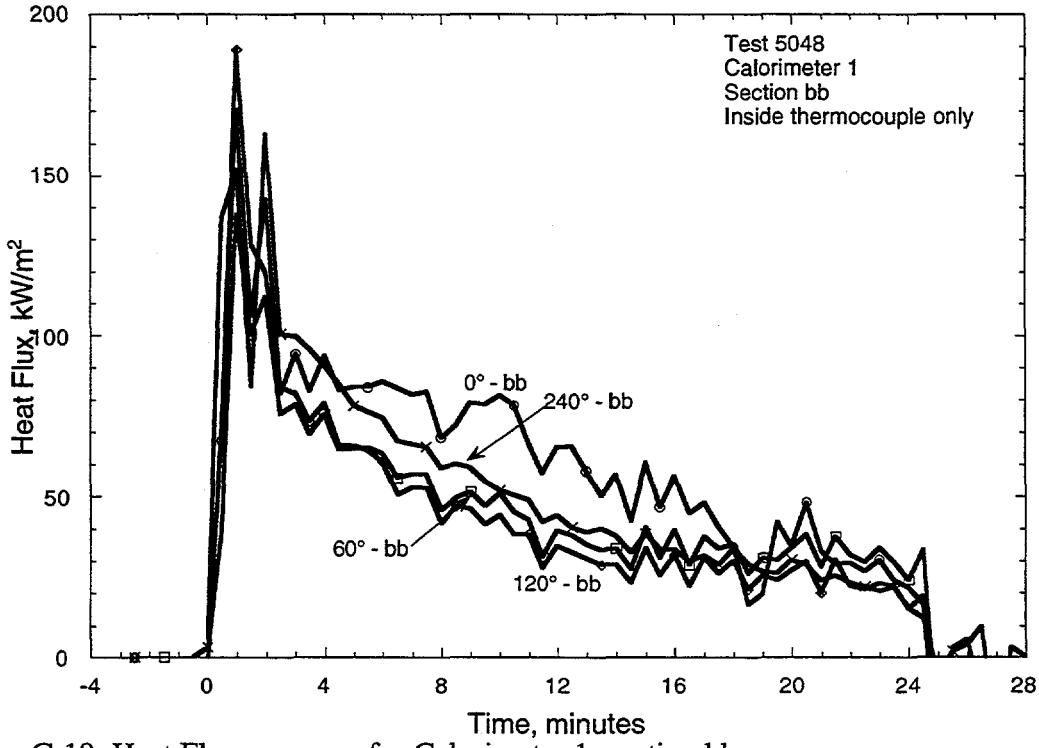

Figure G.18: Heat Flux response for Calorimeter 1, section bb

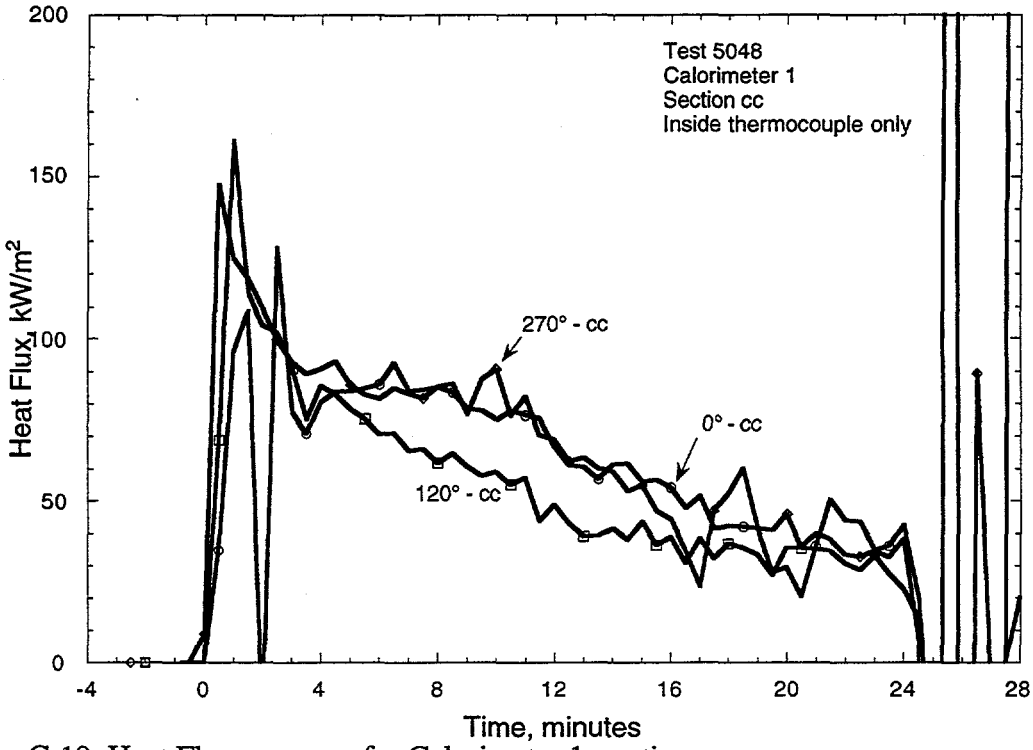

Figure G.19: Heat Flux response for Calorimeter 1, section cc

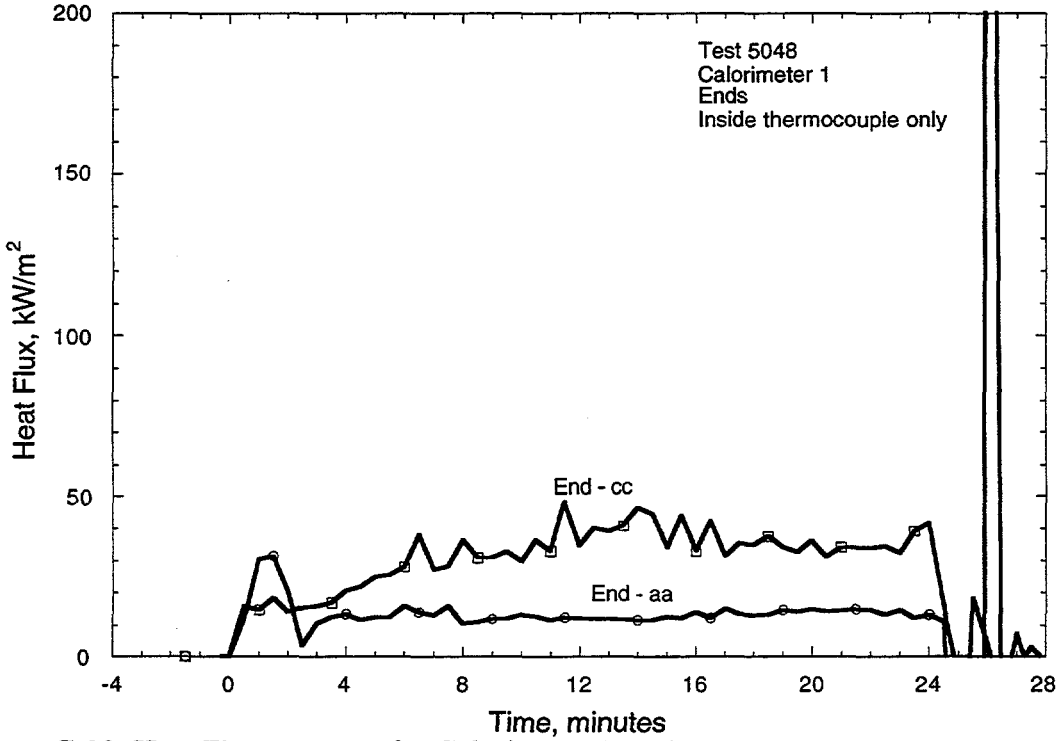

Figure G.20: Heat Flux response for Calorimeter 1, ends

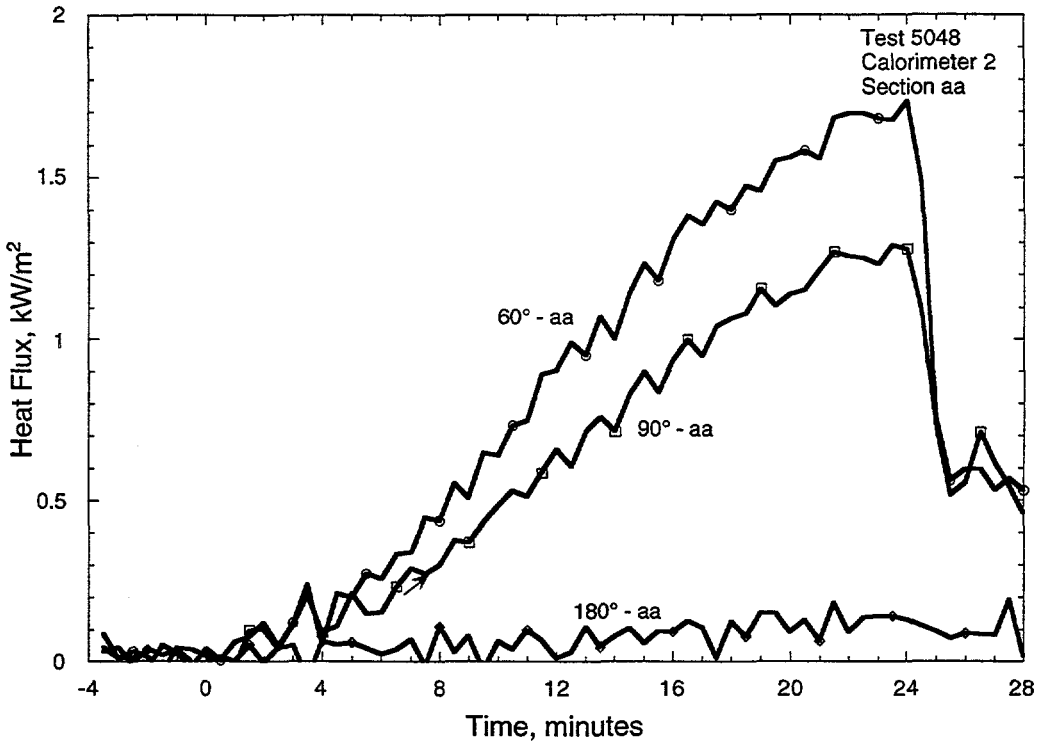

Figure G.21: Heat Flux response for Calorimeter 2, section aa

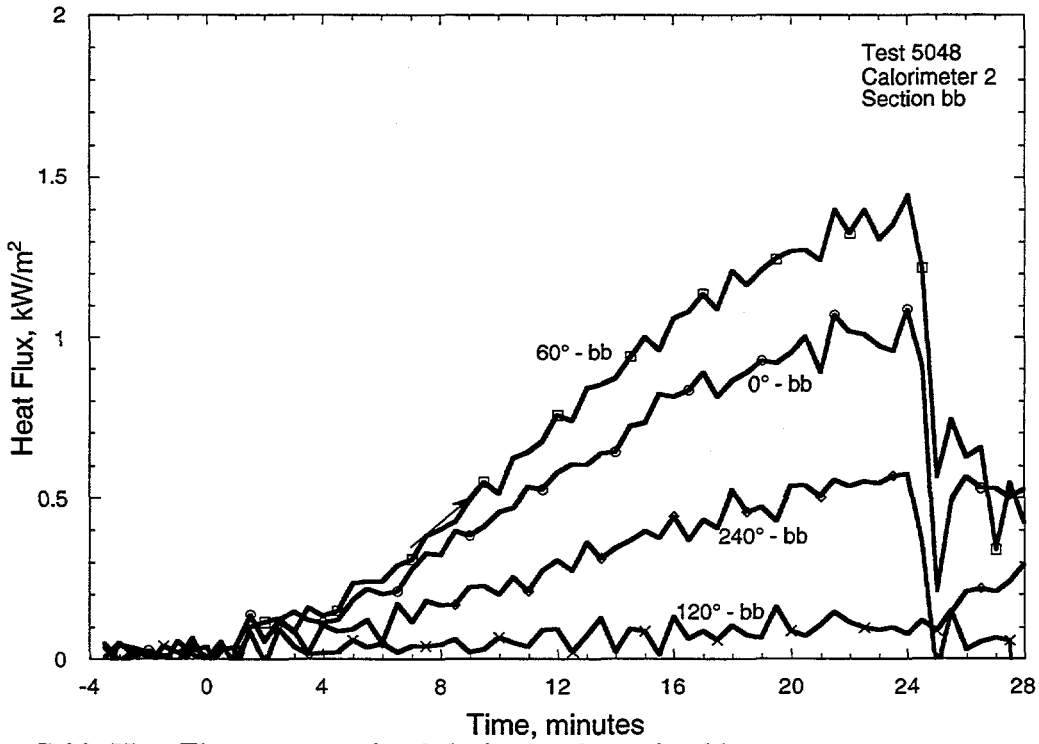

Figure G.22: Heat Flux response for Calorimeter 2, section bb

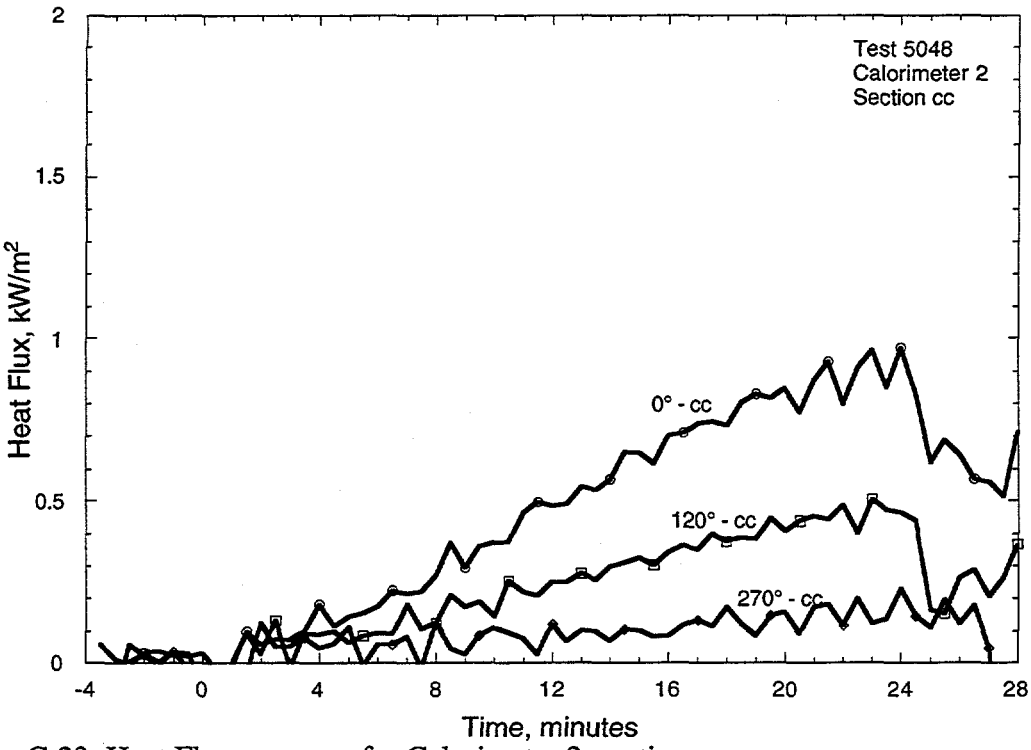

Figure G.23: Heat Flux response for Calorimeter 2, section cc

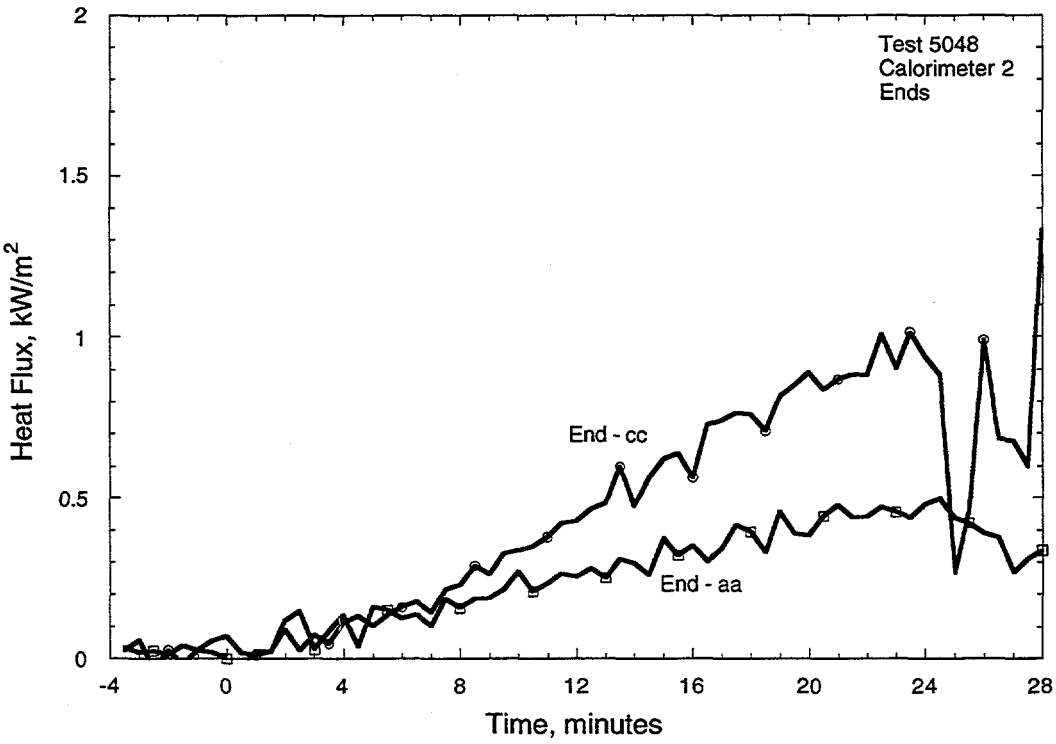

Figure G.24: Heat Flux response for Calorimeter 2, ends

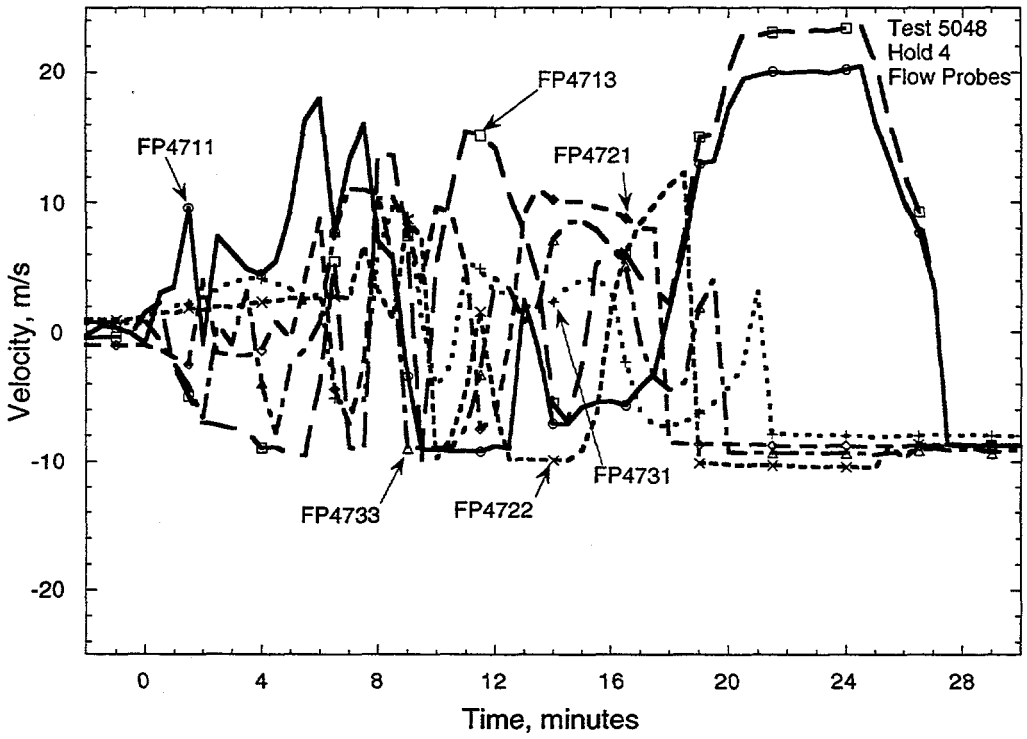

Figure G.25: Flow probes for Hold 4

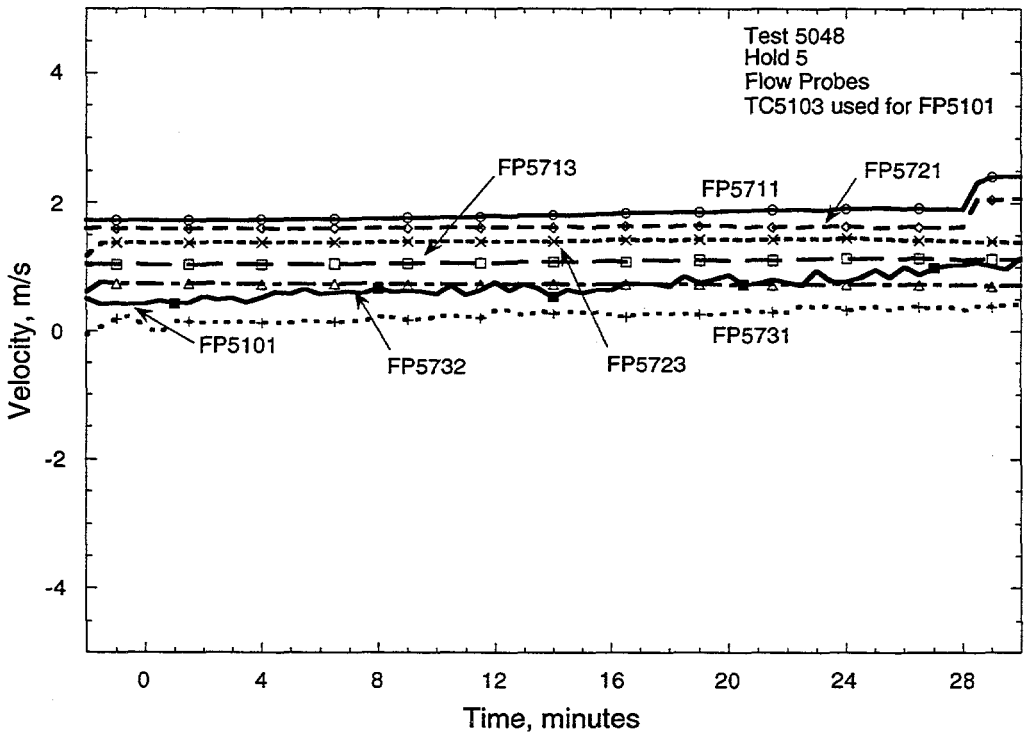

Figure G.26: Flow probes for Hold 5

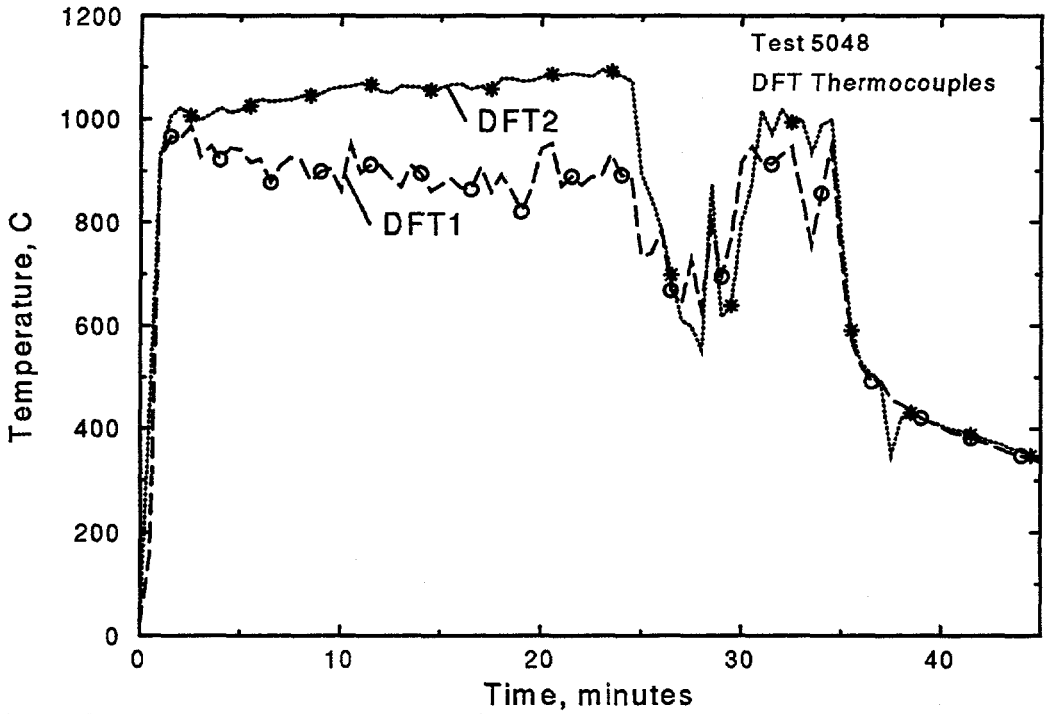

Figure G.27: Thermocouple response for DFT

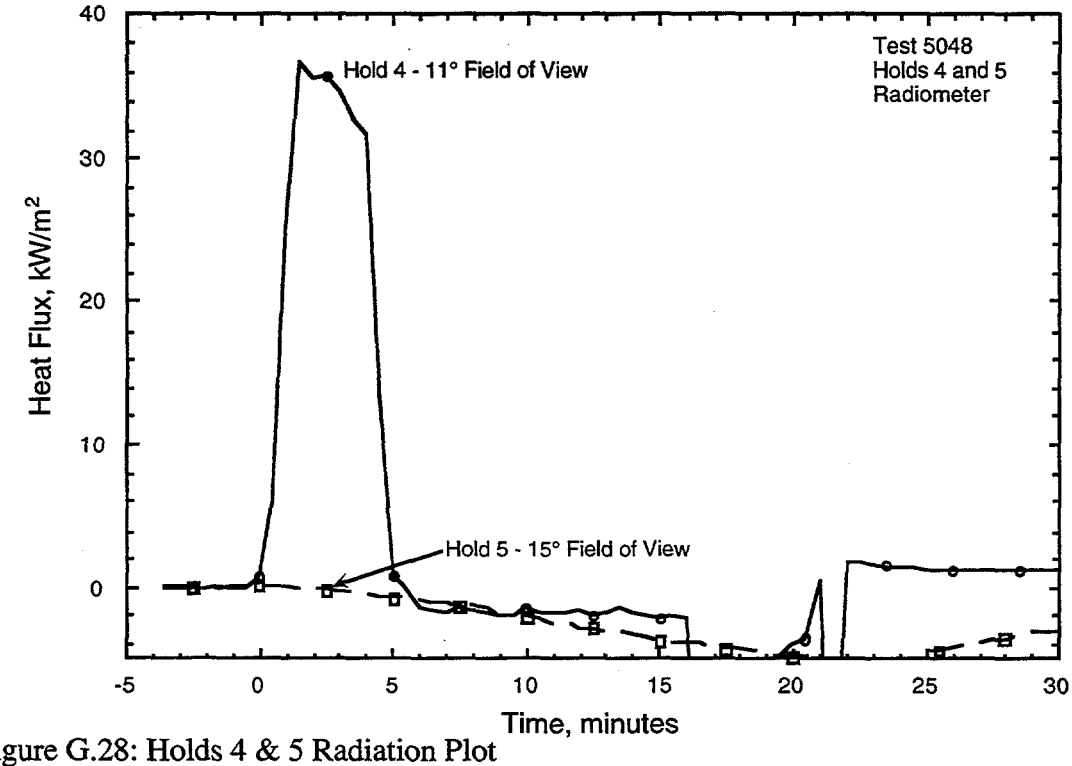

Figure G.28: Holds 4 & 5 Radiation Plot

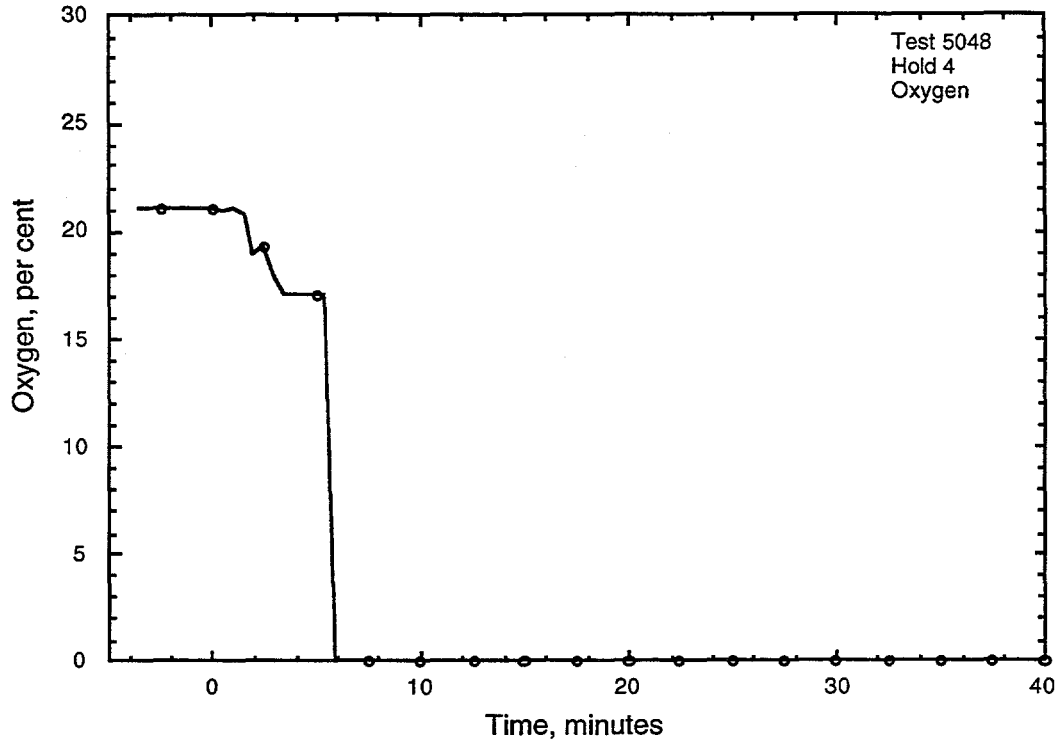

Figure G.29: Oxygen Plot

Appendix H
Test 5049
Diesel Pool Fire on Weather Deck

conducted 11/15/95
2:20 PM CDT

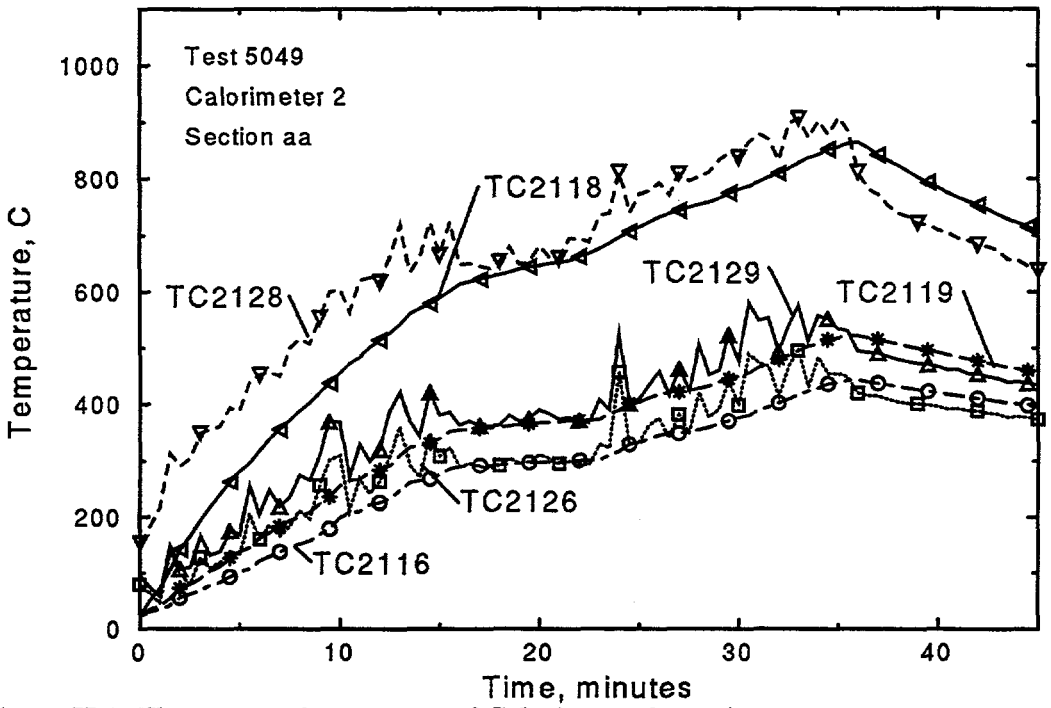

Figure H.1: Thermocouple response of Calorimeter 2, section aa

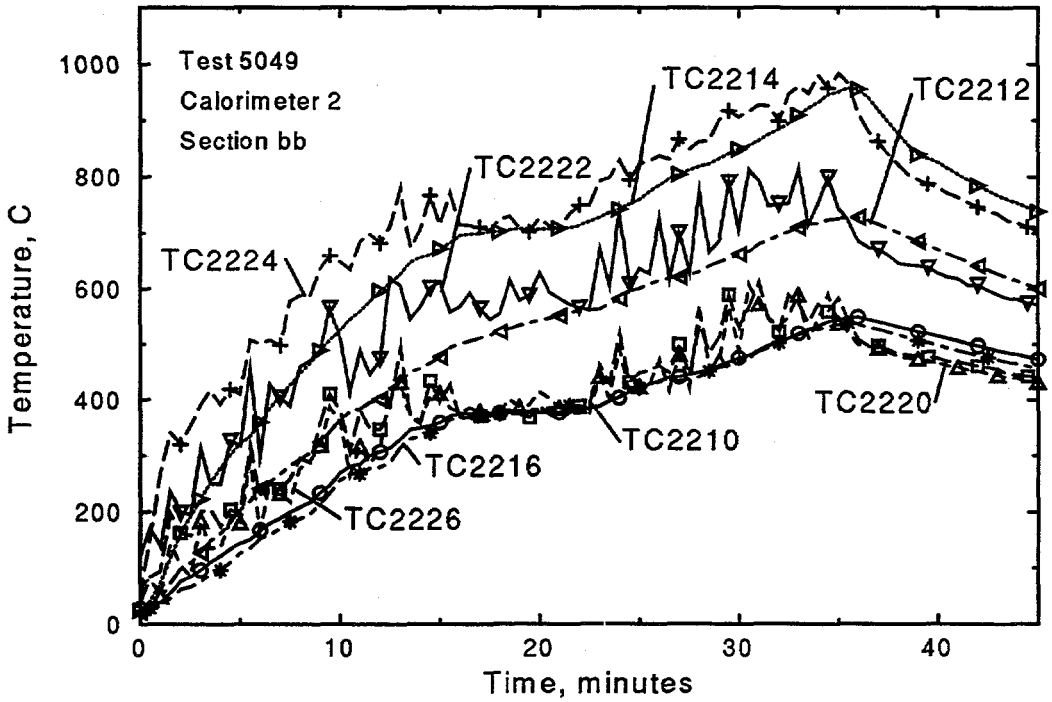

Figure H.2: Thermocouple response of Calorimeter 2, section bb

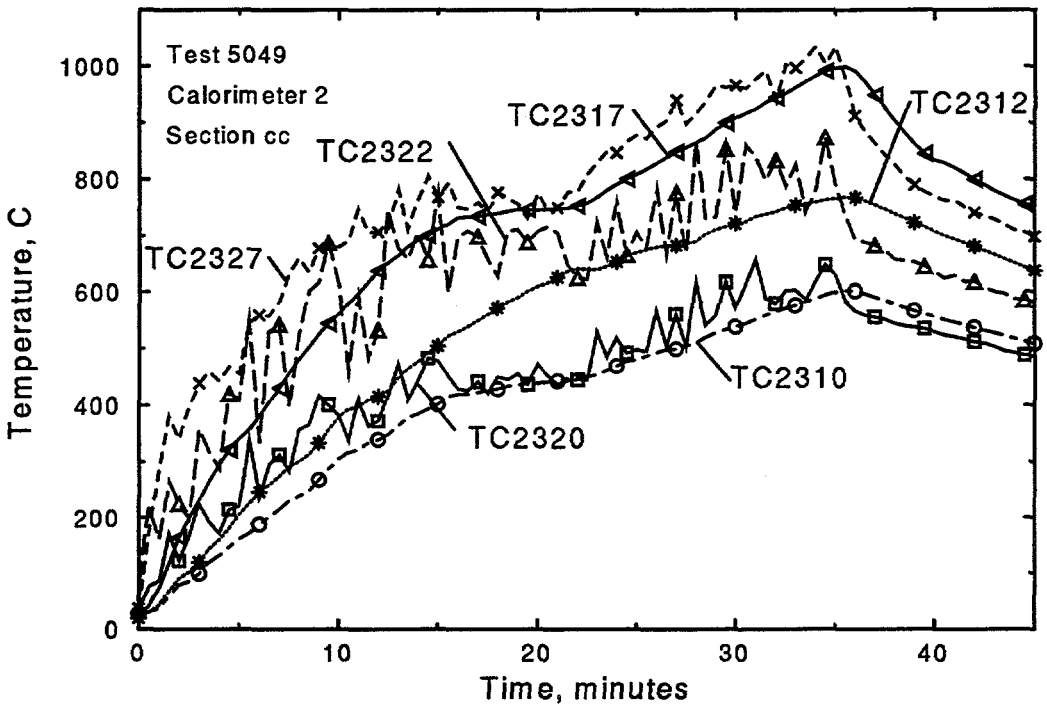

Figure H.3: Thermocouple response of Calorimeter 2, section cc

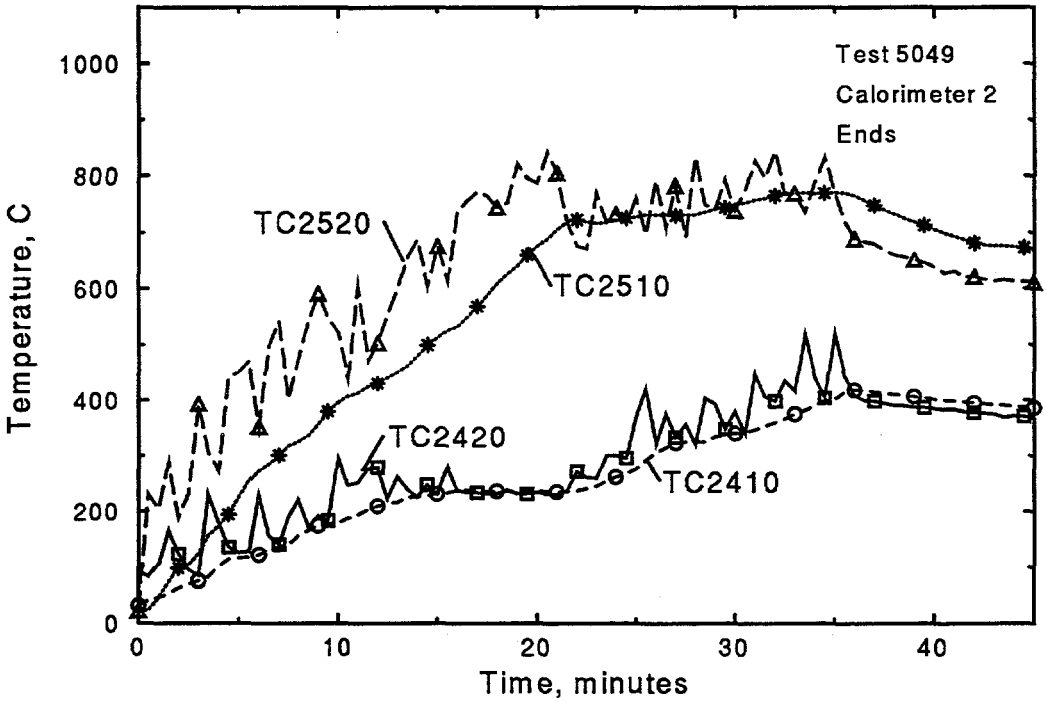

Figure H.4: Thermocouple response of Calorimeter 2, ends

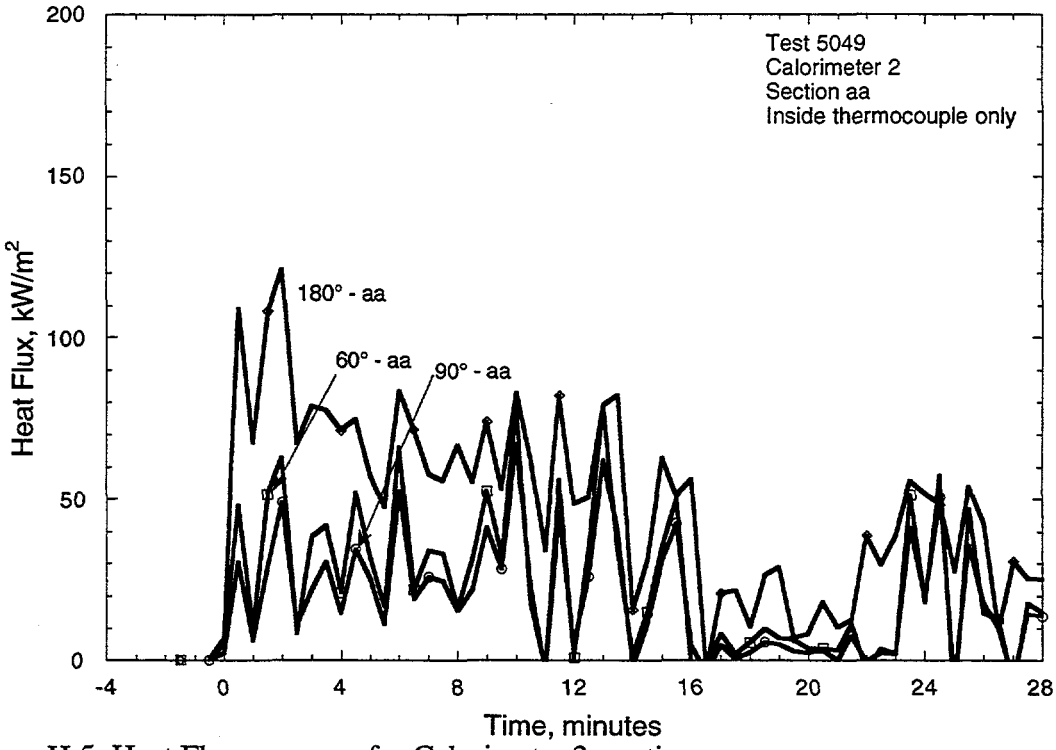

Figure H.5: Heat Flux response for Calorimeter 2, section aa

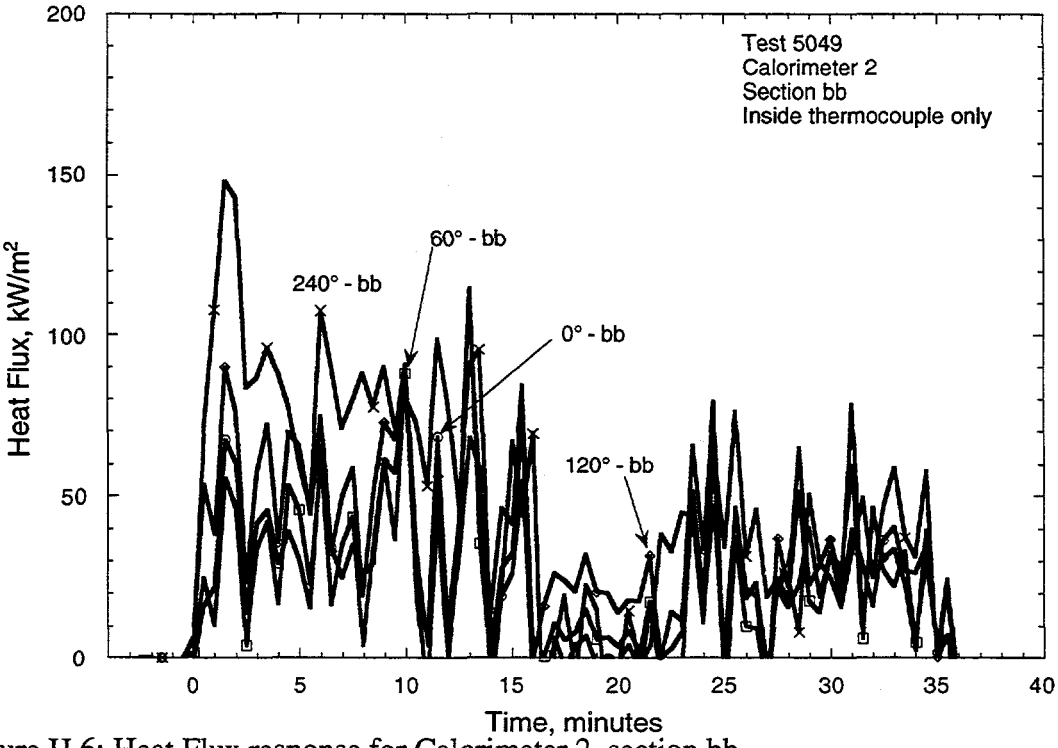

Figure H.6: Heat Flux response for Calorimeter 2, section bb

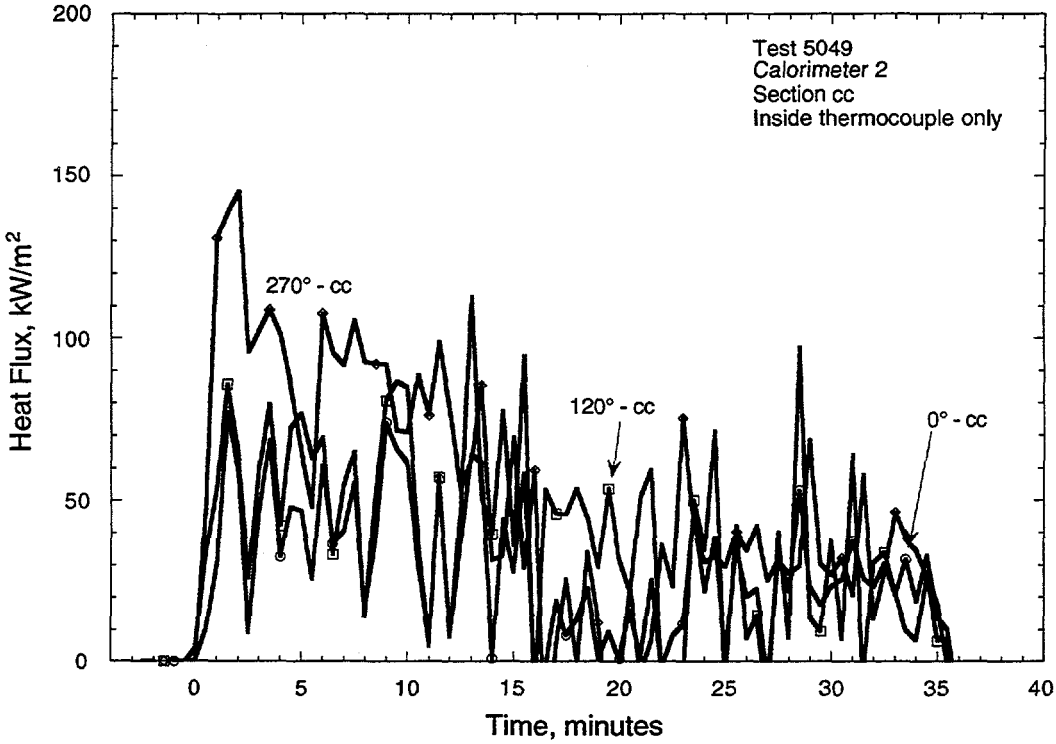

Figure H.7: Heat Flux response for Calorimeter 2, section cc

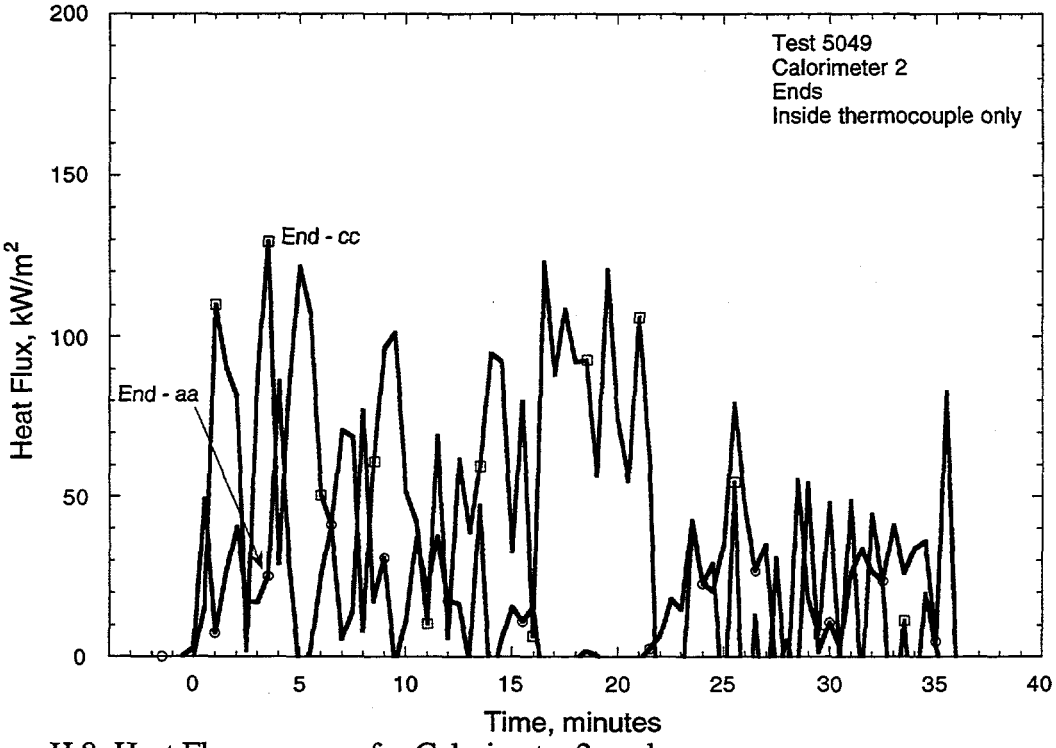

Figure H.8: Heat Flux response for Calorimeter 2, ends

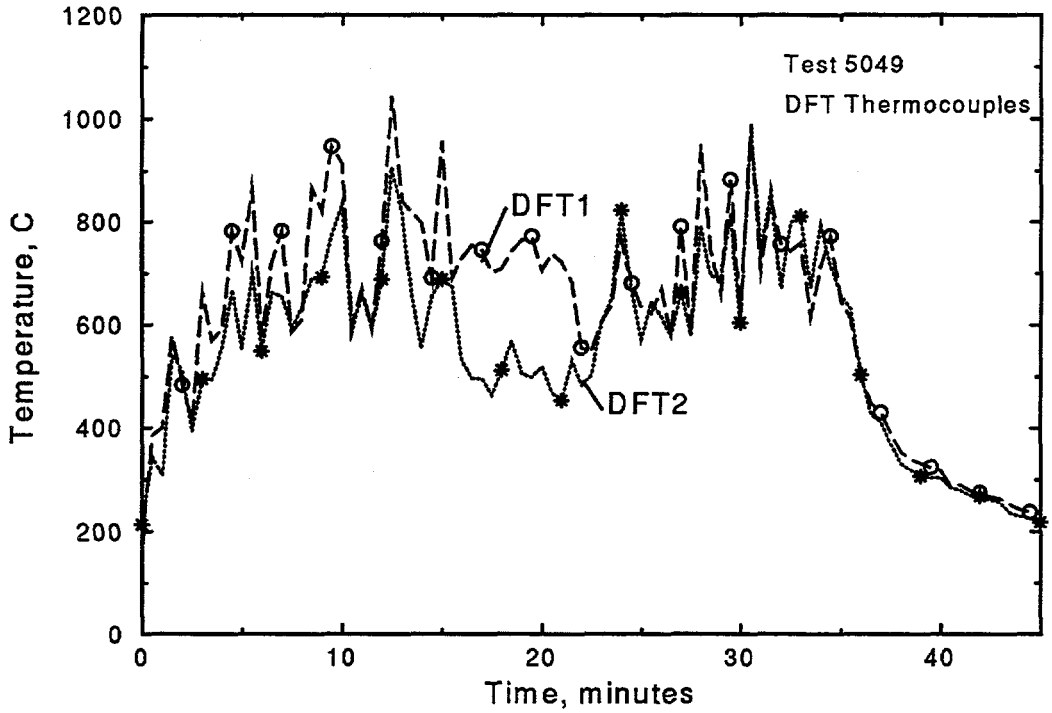

Figure H.9: Thermocouple response for DFT

DISTRIBUTION

1 Mr. Ashok Kapoor
U.S. Department of Energy
Office of Transportation, Emergency
Management, and Analytical Services
EM-70, Cloverleaf Building
19901 Germantown Road
Germantown, MD 2087-1290

2 U.S. Department of Energy
Office of Transportation, Emergency
Management, and Analytical Services
EM-76, Cloverleaf Building
19901 Germantown Road
Germantown, MD 2087-1290

Attn: Mike Keane
Rich Brancato

2 U.S. Department of Energy
Albuquerque Field Office
Mail Stop 1396
P.O. Box 5400
Albuquerque, NM 87185-1396

Attn: P. Grace
P. Dickman

5 Mr. D. E. Beene, Jr.
U.S.C.G. R & D Center
1082 Shennecossett Road
Groton, CT 06340-6096

1 CWO4 R. W. Byrd
U.S.C.G. Fire & Safety Test Det.
Bldg. S-108 MAIC
Mobile, AL 36615-1384

1 Mr. J. Graupmann
U.S.C.G. Fire & Safety Test Det.
Bldg. S-108 MAIC
Mobile, AL 36615-1384

1 Mr. E. Pfersich
Commandant G-MSO-3
2100 2nd Street SW
Washington, DC 20593

1 Mr. William Lake
U.S. Department of Energy
RW-431
Forrestal Building
1000 Independence Avenue SW
Washington, DC 20585

1 Mr. F. Armingaud
60-68 Av. du General Leclerc
B. P. No. 6
F-92265 Fontenay-aux-Roses, Cedex
France

1 Mr. B. Desnoyers
COGEMA
Service des Transports
B. P. No. 4
F-78141 Velizy Villacoublay Cedex
France

1 Richard Rawl
Wagramerstasse 5
P.O. 100
A-1400 Vienna, Austria

1 Mr. T. Schneider
Route du Panorama
F-92263 Fontenay-aux-Roses Cedex
France

1 Mr. F. Lange
Gesellshaft fur Anlagen- und
Reatorsicherheit GmbH
Schwertnerstrass 1
D-506667 Cologne
Germany

1 Mr. K. Shibata
Nucear Material Control Division
San-Kai Doh Bldg.
9-13, 1-chome, Akasaka
Minato-ku
Tokyo
Japan

1 Ms. A-M. Ericsson
AMC Konsult AB
Kammakargatan 6
S-111 40 Stockholm
Sweden

1 Mr. R. Cheshire
Transport Division
British Nuclear Fuels plc
Fleming House
Risley, Warrington
Cheshire, WA3 6AS
United Kingdom

1 Mr. M. Hussain
British Nuclear Transport Limited
Risley, Warrington
Cheshire WA3 6AS
United Kingdom

1 Mr. Clive Young
Department of Transport
Room P2/023E
2 Marsham Street
London SW1P 3EB
United Kingdom

1 Ron Pope
MS 6495
Oak Ridge National Laboratory
P.O. Box 2008
Oak Ridge, TN 37831-6495

1 Mr. N. Watabe
Nuclear Fuel Cycle Department
Central Reseach Institute of Electric
Power Industry
1646 Abiko-shi, Chiba-ken 270-11
Japan

1 Mr. Rod Fisk
Edlow International Co.
1666 Connecticut Ave. Suite 500
Washington, DC 20009

1 Mr. Robert Heid
ECO
1356 Cape St. Claire Rd.
Annapolis, MD 21401-5216

1	MS 0715	R. E. Luna, 6610
10	MS 0715	TTC Library, 6610
1	MS 0716	C. Olson, 6643
1	MS 0716	P. E. McConnell, 6643
1	MS 0717	G. F. Hohnstreiter, 6642
1	MS 0717	D. G. Ammerman, 6642
10	MS 0717	J. A. Koski, 6642
1	MS 0717	M. Arviso, 6642
1	MS 0717	J. G. Bobbe, 6642
1	MS 0718	J. L. Sprung, 6641
1	MS 0717	J. D. Pierce, 6642
1	MS 0717	J. K. Rader, 6642
1	MS 0718	H. R. Yoshimura, 6641
1	MS 0525	S. D. Wix, 1252
1	MS 0724	J. B. Woodard, 6000
1	MS 0726	J. K. Rice, 6600
2	MS 0619	Review & Approval Desk, 12690 for DOE/OSTI
5	MS 0899	Technical Library, 4414
1	MS 9111	Central Tech Files, 8940-2